ORGANISATION EUROPÉENNE POUR LA RECHERCHE NUCLÉAIRE

CERN **EUROPEAN ORGANIZATION FOR NUCLEAR RESEARCH**

2014 European School of High-Energy Physics

Garderen, the Netherlands
18 June – 1 July 2014

Proceedings

Editors: M. Mulders
G. Zanderighi

GENEVA
2016

This report is indexed in: CERN Document Server (CDS), INSPIRE, Scopus.

This report should be cited as:

Proceedings of the 2014 European School of High-Energy Physics, Garderen, the Netherlands, 18 June – 1 July 2014, edited by M. Mulders and G. Zanderighi, CERN-2015-003 (CERN, Geneva, 2016), http://dx.doi.org/10.5170/CERN-2016-003

A contribution in this report should be cited as:

[Author name(s)], in Proceedings of the 2014 European School of High-Energy Physics, Garderen, the Netherlands, 18 June – 1 July 2014, edited by M. Mulders and G. Zanderighi, CERN-2016-003 (CERN, Geneva, 2016), pp. [first page]–[last page], http://dx.doi.org/10.5170/CERN-2016-003.[first page]

Abstract

The European School of High-Energy Physics is intended to give young physicists an introduction to the theoretical aspects of recent advances in elementary particle physics. These proceedings contain lecture notes on the theory of quantum chromodynamics, Higgs physics, Flavour physics and CP violation, and Supersymmetry.

Preface

The twenty-second event in the series of the European School of High-Energy Physics took place in Garderen, the Netherlands, from 18 June to 1 July 2014. It was organized jointly by CERN, Geneva, Switzerland, and JINR, Dubna, Russia, with support from FOM and Nikhef in the Netherlands. The local organization team was chaired by Dr Olya Igonkina who was greatly assisted by Joan Berger on many practical and administrative matters. The other members of the local committee were: S. Caron, R. Fleischer, F. Linde, V. Mexner, A. Mischke, P. Pani, D. Samtleben and L. Wiggers.

A total of 100 students of 32 different nationalities attended the school, mainly from institutes in member states of CERN and/or JINR, but also a few from other regions. The participants were generally students in experimental High-Energy Physics in the final years of work towards their PhDs.

The School was hosted at the Bilderberg Hotel 't Speulderbos complex in Garderen, about 70 km from the centre of Amsterdam. According to the tradition of the school, the students shared twin rooms mixing participants of different nationalities.

A total of 32 lectures were complemented by daily discussion sessions led by six discussion leaders. The students displayed their own research work in the form of posters in an evening session in the first week, and the posters stayed on display until the end of the School. The full scientific programme was arranged in the on-site conference facilities.

A novel feature in the 2014 School was an element of outreach and media training, complementing the main scientific programme. This consisted of a course "Broadcasting your messages: Communicating clearly and concisely with non-specialist audiences" from the iOpener institute. The session was delivered by Nadia Marchant (facilitator) and Hugh Schofield (journalist and BBC correspondent in Paris). In an optional after-dinner session, students had the opportunity to act out interviews under realistic conditions based on two hypothetical scenarios. Another outreach-related activity was an entertaining after-dinner show, "HIGGS: Stand Up Physics" by Jan van den Berg.

Each discussion group subsequently carried out a collaborative project, preparing a talk on a physics-related topic at a level appropriate for a general audience. The talks were given by student representatives of each group in an evening session in the second week of the School. Feedback was provided by a jury composed of Jan van den Berg, Margriet van der Heijden, Gieljan de Vries and Ivo van Vulpen, organised by Vanessa Mexner. Many thanks are due to these people, all of whom are themselves involved in the communication of science in one way or another.

Our thanks go to the local-organization team and, in particular, to Olya Igonkina, for all of their work and assistance in preparing the School, on both scientific and practical matters, and for their presence throughout the event. Our thanks also go to the efficient and friendly hotel management and staff who assisted the School organizers and the participants in many ways.

Very great thanks are due to the lecturers and discussion leaders for their active participation in the School and for making the scientific programme so stimulating. The students, who in turn manifested their good spirits during two intense weeks, undoubtedly appreciated listening to and discussing with the teaching staff of world renown. We would like to express our appreciation to Professor Rolf Heuer, Director General of CERN, and Dr Alexander Olshevskiy representing Professor Victor Matveev, Director General of JINR, for their lectures on the scientific programmes of the two organizations and for discussing with the School participants.

In addition to the rich academic programme, the participants enjoyed numerous sports, leisure and cultural activities in and around the Bilderberg Hotel 't Speulderbos complex. Particularly noteworthy were the very nice excursions to the Dutch national park Hoge Veluwe and the Kröller-Müller museum, to Amsterdam with options to visit the Van Gogh museum or the Rijksmuseum, and to the beach and dunes near Zandvoort. Sports and leisure activities around the hotel, as well as the excursions, provided an excellent environment for informal interactions between staff and students.

We are very grateful to Kate Ross and Tatyana Donskova for their untiring efforts in the lengthy preparations for and the day-to-day operation of the School. Their continuous care of the participants and their needs during the School was highly appreciated.

The success of the School was to a large extent due to the students themselves. Their poster session was very well prepared and highly appreciated, their group projects were a great success, and throughout the School they participated actively during the lectures, in the discussion sessions and in the different activities and excursions.

<div align="right">

Nick Ellis
(On behalf of the Organizing Committee)

</div>

People in the photograph

1	Nick Ellis	39	Oskar Hartbrich	77	Miriam Heß
2	Carlos Salgado	40	Hartger Weits	78	Craig Anthony Sawyer
3	Olya Igonkina	41	Elena Giubega	79	Gabriel Palacino
4	Tamsin Nooney	42	Rute Pedro	80	Giuliano Gustavino
5	Rebecca Lane	43	Antonios Agapitos	81	Andrew Hart
6	Anders Floderus	44	Alexey Finkel	82	Irina Shakiryanova
7	Linda Finco	45	Hannah Arnold	83	Espen Bowen
8	Jan Hoss	46	Alexis Vallier	84	Tara Nanut
9	Cécile Caillol	47	Eric Laenen	85	Stephan Hageböck
10	Alex Garabedian	48	Mario Sousa	86	Lei Zhou
11	Martijn Mulders	49	Tobias Lapsien	87	Jennifer Ngadiuba
12	Deborah Pinna	50	Klaas Padeken	88	Annemarie Theulings
13	Federico Lasagni	51	Jimmy McCarthy	89	Jun Gao
14	Rafael Teixeira	52	Olga Petrova	90	Lukas Plazak
	De Lima	53	Kai Schmidt-Hoberg	91	Silvia Fracchia
15	Sara Fiorendi	54	Peter Berta	92	Mario Masciovecchio
16	Jacky Brosamer	55	Gordana Milutinovic-	93	Giulia D'Imperio
17	Ferdos Rezaei		Dumbelovic	94	Geoffrey Gilles
18	Marek Sirendi	56	Steven Schramm	95	Alexandre Aubin
19	Kurt Brendlinger	57	Callie Bertsche	96	Deborah Duchardt
20	Francis Newson	58	Alexey Aparin	97	Ilia Butorov
21	David Bertsche	59	Hans Martin Ljunggren	98	Ingrid Deigaard
22	Tatyana Donskova	60	Javier Montejo Berlingen	99	Daniel Meister
23	Andrea Festanti	61	Samuel Coquereau	100	Zuzana Barnovska
24	Cedric Delaunay	62	Milena Quittnat	101	Christine Overgaard
25	Riccardo Manzoni	63	Bob Velghe		Rasmussen
26	Alexey Gladyshev	64	Koen Oussoren	102	Elizabeth Brost
27	Kate Ross	65	Jasone Garay Garcia	103	Beata Krupa
28	Marco Mirra	66	Alessandro Calandri	104	Semen Turchikhin
29	Alessandro Morda	67	Philip Sommer	105	Maxime Levillain
30	Cristian Pisano	68	Ralph Schäfer	106	Kazuya Mochizuki
31	Kristof De Bruyn	69	Laura Franconi	107	Bartlomiej Rachwal
32	Naghmeh Mohammadi	70	Alexander Bednyakov		
33	Mikhail Mikhasenko	71	James Henderson		*students not in photograph:*
34	Marco Venturini	72	Özgur Sahin		Pierfrancesco Butti
35	Fabio Colombo	73	Walaa Kanso		Arne-Rasmus Dräger
36	Jackson Clarke	74	Jui-Fa Tsai		Mateusz Dyndal
37	Luis Pesantez	75	Yusufu Shehu		Boyana Marinova
38	Simon Spannagel	76	Christoph Hombach		Valérian Sibille

Photographs (montage)

Contents

QCD

E. Laenen
Nikhef, Amsterdam, The Netherlands
Institute for Theoretical Physics, University of Amsterdam, The Netherlands
Institute of Theoretical Physics, Utrecht University, The Netherlands

Abstract

In these lecture notes I describe the theory of QCD and its application, through
perturbation theory, at particle colliders.

1 Introduction

In particle physics, we encounter QCD nearly everywhere. The main collider of our time, the LHC,
collides protons, which are made up of quarks, antiquarks and gluons, collectively called partons. Every proton collision involves partons, which readily produce a multitude of further partons, all turning
into hadrons of one type or another. At present we are however mostly interested in *rare* final states,
faint signals involving Higgs bosons, top quarks, vector bosons, possibly new particles. Hence we
must understand very well how to separate the new from the known, to "remove the foreground", in
cosmology-speak; particle physicists call it background.

But it would do gross injustice to QCD and its dynamics to see it as merely a background engine.
It really is a beautiful theory by itself. It is the only unbroken non-abelian gauge theory we know exists
in Nature. Its Lagrangian is compact, and elegant

$$\mathcal{L}_{\text{QCD}} = -\frac{1}{4}\text{Tr}(G_{\mu\nu}G^{\mu\nu}) - \sum_{f=1}^{n_f}\overline{\psi_f}(\slashed{D} + m_f)\psi_f \,. \tag{1}$$

We shall discuss the meaning of the various symbols in this expression shortly, but one should not forget
to be amazed at the complex outcomes that this relatively simple expression generates [1]. For this reason,
QCD dynamics is very interesting to study *sui generis*. In these lecture notes I shall visit a number [2]
of aspects of QCD, as relevant in collider physics. The structure of these notes is as follows. In the
next section the fundamental degrees of freedom and symmetries of QCD are discussed. In section 3 we
discuss aspects of perturbative QCD when going to higher fixed orders. Section 4 contains an exposition
of some modern methods of calculations, focussing in particular on helicity methods. Section 5 discusses
aspects of all-order resummation, the underlying reasons and some applications. I conclude in Section
6. An appendix contains conventions and useful formulae.[3]

2 Partons and hadrons

In this section we discuss both the spectroscopic evidence for the presence of quarks and gluons in
hadrons, as well as the partonic picture relevant for high-energy collisons.

2.1 Spectroscopy and symmetries of QCD

Six types (or flavours) of quarks are presently known to exist. They are fermions and are denoted by
u, c, t and d, s, b, respectively, abbreviations of the names 'up', 'charm', 'top', and 'down', 'strange',

---

[1]Of course, for that matter, the QED Lagrangian is even simpler, and yet it governs all of atomic physics, chemistry etc.
[2]Some of the notes correspond to a forthcoming book: Field Theory in Particle Physics, by B. de Wit, E. Laenen and J.
Smith.
[3]*Caveat emptor*: though I tried to avoid them, there might be errors and inconsistencies in the equations below. In addition,
I made no effort to be exhaustive in references.

'bottom'. Three (u, c, t) have electric charge $\frac{2}{3}$ and three (d, s, b) charge $-\frac{1}{3}$ (measured in units of the elementary charge). Because quarks are not detected as separate physical particles (they are confined into hadrons), their masses are not exactly known, but can be estimated from hadron spectroscopy once the hadron composition in terms of quarks is given. The mass values thus obtained are called "constituent masses". One commonly introduces quantum numbers such as isospin or strangeness to distinguish the quark flavour, which then explains the corresponding quantum numbers of the hadronic bound states. Of course, there are also corresponding antiquarks $\bar{u}, \bar{c}, \bar{t}$ and $\bar{d}, \bar{s}, \bar{b}$, with opposite charges. The lightest-mass mesons and baryons are bound states of quarks and/or antiquarks with zero angular momentum.

For the moment let us restrict our attention to a single quark flavour, whose interactions are given by a non-abelian gauge theory. This choice is motivated by the fact that only such theories have the property that the interactions become strong at low energies, and can therefore explain confinement. We shall return to this further below. In order to let a non-abelian gauge group act on the quark field, we are forced to extend the number of fields. According to QCD, this gauge group is $\mathrm{SU}(3)$. We shall try to justify this choice for the gauge group in a little while and first consider the definition of the theory. In order that $\mathrm{SU}(3)$ can act nontrivially on the quark field $q(x)$, this field must have at least three components, so we write $q_\alpha(x) = (q_1(x), q_2(x), q_3(x))$. Hence for a given quark flavour, we have three different fields. These three varieties are called *colours* and are commonly denoted by 'red', 'green' and 'blue'. Of course, at first sight, this assumption seems to make matters worse. We started with one quark for each flavour, which cannot be observed as a free particle; now we have three times as many unobservable quarks. Actually, the problem is even more vexing. Because quarks rotate under an $\mathrm{SU}(3)$ symmetry group, one should expect a corresponding degeneracy for the observed bound states. In other words, each hadronic state should in general be degenerate and carry colour, while all other properties such as mass, electric charge and the like are independent of colour. We clearly do not observe such an exact degeneracy in Nature. Nevertheless, let us for now ignore this apparent proliferation of degrees of freedom and turn to the other ingredients of the model. Because the group $\mathrm{SU}(3)$ is eight-dimensional ($\mathrm{SU}(3)$ has eight generators), we must have eight gauge fields, denoted by $V_\mu{}^a$. Under $\mathrm{SU}(3)$ the quark fields transform in the fundamental, triplet representation, viz.

$$q(x) \rightarrow q'(x) = \exp\left(\tfrac{1}{2}\mathrm{i}\lambda_a \xi^a(x)\right) q(x) , \tag{2}$$

where $\xi^a(x)$ are the eight transformation parameters of $\mathrm{SU}(3)$, and $q(x)$ represents the three-component column vector q_α consisting of the three quark colours. The conjugate quark fields are represented by the row vector $\bar{q}_\alpha = (\bar{q}_1, \bar{q}_2, \bar{q}_3)$ and transform according to

$$\bar{q}(x) \rightarrow \bar{q}'(x) = \bar{q}(x) \exp\left(-\tfrac{1}{2}\mathrm{i}\lambda_a \xi^a(x)\right) . \tag{3}$$

The invariant Lagrangian now takes the form

$$L = -\tfrac{1}{4}(G_{\mu\nu}{}^a)^2 - \bar{q}\, \slashed{D} q - m\, \bar{q}q , \tag{4}$$

with

$$\begin{aligned} G_{\mu\nu}{}^a &= \partial_\mu V_\nu{}^a - \partial_\nu V_\mu{}^a - g f_{bc}{}^a V_\mu{}^b V_\nu{}^c , \\ D_\mu q &= \partial_\mu q - \tfrac{1}{2}\mathrm{i}g V_\mu{}^a \lambda_a q . \end{aligned} \tag{5}$$

The $\mathrm{SU}(3)$ generators $t_a = \tfrac{1}{2}i\lambda_a$ are expressed in terms of a standard set of matrices λ_a, the Gell-Mann matrices, which are generalizations of the Pauli matrices τ_a. The $\mathrm{SU}(3)$ structure constants $f_{bc}{}^a$ follow from the commutators of these generators. Note that, we choose our generators to be anti-hermitian.

For other flavours, the QCD Lagrangian takes the same form as in (4), except that the actual value for the quark-mass parameter is different. The full Lagrangian thus depends on the QCD coupling constant g and on the mass parameters m, one for each flavour (quarks of different colour but of the same

flavour should have the same mass in order to conserve the SU(3) gauge symmetry). Here we stress that the mass parameter in the Lagrangian *cannot* be identified directly with the constituent mass, which should follow from solving the full QCD field equations. Obviously, the QCD interactions leave the flavour of the quarks unchanged, and thus also strangeness and similar quantum numbers. However, with the exception of the electric charge, these quantum numbers are not conserved by the weak interactions, and quarks can change their flavour by emitting weak interaction bosons. The gluons do not carry flavour, but they do carry colour, since they transform under the SU(3) gauge group. We therefore see that the quark content of the hadrons can be probed by weak and electromagnetic interactions through deep-inelastic scattering experiments.

Of course, quarks also carry spin indices, as they are normal Dirac spinor fields, so they are quite rich in indices. One index is the spinor index, which takes four values. Then there is the colour index, denoted above by $\alpha, \beta, \ldots$, which takes three values. Finally we can assign a flavour index, which takes six values corresponding to the different flavours. As we shall discuss colour further below, let us here explore aspects of quark flavour. By construction the QCD Lagrangian is invariant under *local* SU(3). However, depending on the values for the mass parameters, there can also be a number of *global* flavour symmetries. The presence of these flavour symmetries has direct consequences for the hadronic bound states. The flavour symmetries are most relevant for the light quarks. As the mass parameters of the u and d quarks are comparable in size, the QCD Lagrangian is nearly invariant under global unitary rotations of the u and d quarks. These rotations form the group U(1) ⊗ SU(2). The invariance under U(1) is related to the conservation of baryon number (quarks carry baryon number $\frac{1}{3}$, antiquarks $-\frac{1}{3}$). The SU(2) transformations mix up and down quarks and are called isospin transformations. The breaking of isospin invariance is thus due to the fact that the u and d mass parameters are not quite equal (an additional but small breaking is caused by the electroweak interactions, which we do not consider in this chapter). The u and d mass parameters are not only nearly equal, they are also very small, which implies that the Lagrangian has in fact even more approximate flavour symmetries. To wit, for vanishing quark mass the Lagrangian is also invariant under unitary transformations of the u and d fields that contain the matrix γ_5. Such transformations are called *chiral* transformations. Because of the presence of γ_5, these transformations of the quarks will depend on their spin. We shall discuss these symmetries further below. These extra transformations involving γ_5 actually quite subtle because the chiral symmetry is realized in a so-called spontaneously broken way. The fact that the pion mass is so small (as compared to the other hadron masses) can then be explained by an approximate chiral symmetry in Nature. Obviously, we may follow the same strategy when including the s quark and consider extensions of the flavour symmetry group. Apart from the phase transformations one then encounters an SU(3) flavour group (not to be confused with the SU(3) colour group). In view of the fact that the s quark has a much higher mass, flavour SU(3) is not as good a symmetry as isospin. Symmetry breaking effects are usually of the order of 10%. Of course one may consider further extensions by including γ_5 into the tranformation rules or by including even heavier quarks. However, these extensions of the flavour symmetries tend to be less and less useful as they are affected by the large quark masses and thus no longer correspond to usefully approximate symmetries of Nature.

In order to realize the SU(3) gauge tranformations on the quark fields, we introduce three varieties of quarks, prosaically denoted by colours. However, it seems inevitable that the observed hadrons, bound states of quarks and antiquarks, will also exhibit the colour degeneracy. For instance, the pions are thought of as bound states of a u or a d quark with a $\bar{u}$ or a $\bar{d}$ antiquark. Since quarks and antiquarks come in three different colours, one has in principle *nine* types of pions of given electric charge, which must have equal mass. Altogether there should then be twenty-seven types of pions, rather then the three found in Nature!

The reason why this colour degeneracy is not observed in Nature is a rather subtle one. To explain this phenomenon, let us start by considering quarks of a single flavour, say u quarks, and construct the possible states consisting of three quarks, all at rest. Together they form a state with zero angular

momentum. Depending on the properties of the forces acting between these quarks, the three quarks may or may not cluster into a hadronic bound state. By comparing the properties of these three-quark states to those of the low-mass hadrons in Nature (in view of the centrifugal barrier one expects that states with nonzero angular momentum acquire higher masses) one may hope to unravel the systematics of quark spectroscopy and understand the nature of the forces that hold the hadrons together.

Hence, when considering the possibility of the three quarks forming a bound state, one may expect the emergence of a spin-$\frac{3}{2}$ bound state and/or one or two spin-$\frac{1}{2}$ bound states. Of course, whether or not they are actually realized as bound states depends on the properties of the interquark forces.

However, the above conclusions are invalidated as we are dealing with bound states of *identical* spin-$\frac{1}{2}$ particles. Being fermions they satisfy Pauli's exclusion principle, according to which the resulting state should be *antisymmetric* under the exchange of any two such particles. It turns out that the spin-$\frac{3}{2}$ bound state is, however, *symmetric* under the interchange of two fermions. This is easy to see for the states with $S_z = \pm\frac{3}{2}$, as they correspond to the situation where all three quark spins are aligned in the same direction. Hence a spin-$\frac{3}{2}$ bound state cannot be realized because of Pauli's exclusion principle. However, the spin-$\frac{1}{2}$ states cannot be realized either, as they are neither symmetric nor antisymmetric under the interchange of any two particles, but are of mixed symmetry (i.e., they can be (anti)symmetric under the exchange of two of the quarks, but not with respect to the third quark). Therefore, bound states of three identical spin-$\frac{1}{2}$ particles with zero angular momentum cannot exist, it would seem.

Surprisingly enough, when comparing the result of such quark model predictions to the low-mass baryons in Nature, one finds that there is in fact a bound state of three u quarks with spin-$\frac{3}{2}$, namely the Δ^{++} baryon with a mass of 1232 MeV c^{-2}, which is unstable and decays primarily into $p\,\pi^+$ with an average lifetime of 0.59×10^{-23} s. On the other hand, no spin-$\frac{1}{2}$ bound states of three u quarks are found. At this point one could of course question the quark interpretation of the Δ^{++}, were it not for the fact that this phenomenon is universal! When comparing the quark model to the data, it turns out that the baryons always correspond to bound states of quarks that are *symmetric* rather than antisymmetric under the interchange of two quarks. Therefore, one would conclude, the Pauli principle is violated in the simple quark model.

Before resolving this puzzle, let us once more exhibit this phenomenon, but now for the slightly more general case of low-mass baryons consisting of u and d quarks. Each quark in the baryon now comes in four varieties: a u quark with spin 'up' or 'down' (measured along some direction in space) or a d quark with spin 'up' or 'down'. Assuming again zero total angular momentum, there are thus $4^3 = 64$ possible spin states, twenty of which are symmetric under the interchange of two particles. These symmetric states decompose into sixteen states with both isospin and ordinary spin equal to $\frac{3}{2}$, and four states with both isospin and ordinary spin equal to $\frac{1}{2}$. The first sixteen states correspond to the baryons $\Delta^{++}(uuu)$, $\Delta^+(uud)$, $\Delta^0(udd)$ and $\Delta^-(ddd)$, which carry spin-$\frac{3}{2}$ so that each one of them appears in four possible spin states (we listed the quark content in parentheses). The latter four states correspond to the nucleons $p(uud)$ and $n(udd)$, which carry spin-$\frac{1}{2}$ and thus appear in two varieties.[4] No other states corresponding to bound states of three u or d quarks can be identified with baryons in Nature (for higher masses such bound states can be found, but those will have nonzero angular momentum).

Let us now stop exploring in detail the subtleties of the simple quark model, and turn to quantum chromodynamics. Because the quarks carry colour one can make the three-quark state antisymmetric by postulating total antisymmetry in the three colour indices. In this way the exclusion principle is preserved. This conjecture may seem rather ad hoc, and one may wonder whether there is an a priori reason for assuming antisymmetry in the colour indices. Indeed, it turns out that there is a principle behind this. When antisymmetrizing over the colour indices of a three-quark state, this state is a singlet

---

[4]As explained above, the spin-$\frac{1}{2}$ states are of mixed symmetry. However, the mixed symmetry in terms of the spin indices of the quarks can be combined with the mixed symmetry of the isospin indices in such a way that the resulting state becomes symmetric.
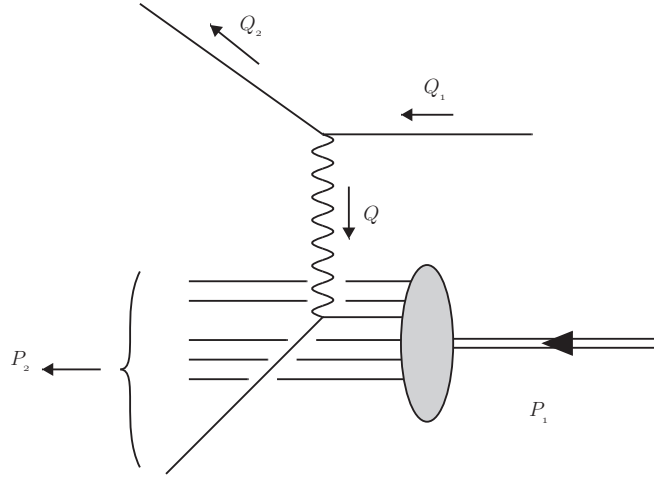
Fig. 1: Parton picture of a deep-inelastic collision process. Note that in the diagram time runs from right to left.

under the $SU(3)$ colour group. This follows from the tensor product of three triplets

$$\mathbf{3} \otimes \mathbf{3} \otimes \mathbf{3} = \mathbf{1} \oplus \mathbf{8} \oplus \mathbf{8} \oplus \mathbf{10} \,, \tag{6}$$

which yields a singlet state under colour $SU(3)$ that is fully antisymmetric.[5] Assuming that no hadrons carry colour (so that they are *invariant* under the colour gauge group) requires the three-quark states to be antisymmetric in the colour indices. By virtue of Pauli's exclusion principle, they must therefore be *symmetric* with respect to all other quantum numbers, such as spin and isospin.

The principle that hadrons should be colourless can be put to a test when considering the low-mass mesons. As we mentioned at the beginning of this section, the mesons are bound states of a quark and an antiquark. Because of the three-fold degeneracy of the quarks associated with colour, each meson should appear in nine varieties, which differ in colour, but not in electric charge and mass. However, one particular combination of these states is again colourless. This follows from the tensor product rule

$$\mathbf{3} \otimes \bar{\mathbf{3}} = \mathbf{1} \oplus \mathbf{8} \,, \tag{7}$$

according to which the nine colour states decompose into a singlet state and eight states belonging to the octet representation. Only the singlet state is realized as a physical particle, so that the colour degeneracy is avoided. This turns out to be a universal feature of all hadrons. We simply never observe the colour degrees of freedom, but only bound states of quarks that are singlets of the colour symmetry group. In other words if we assign the primary colours to $\alpha = 1, 2, 3$ then the observed hadrons must be "white". Of course, this analogy is mostly picturesque and by no means necessary.

2.2 Parton model

We mentioned above that deep-inelastic scattering reveals the presence of weakly bound point-like parton constituents inside the nucleon, which we will shortly identify as spin-$\frac{1}{2}$ fractionally charged quarks (gluons are neutral with respect to weak and electromagnetic interactions, so they are not directly involved in this process). To see this, we first examine a simple model in which the fast-moving nucleon

---

[5]The interpretation of this product rule is as before. The $3^3 = 27$ states formed by all possible products of $SU(3)$ triplet states decompose under the action of $SU(3)$ in four different representations: the singlet representation, which is completely antisymmetric, the **10** representation, which is completely symmetric, and two **8** representations, which have mixed symmetry (the $SU(3)$ representations are denoted by their dimension, unlike the representions of the rotation group, which are denoted by the value of the spin). To derive such product rules is more complicated for $SU(3)$ than for the $SU(2)$, the relevant group for spin and isospin.

consists of a finite number of particles, each carrying a certain fraction of its momentum. These constituents are so weakly bound that they may be regarded as free. For simplicity we assume also that just one parton is subject to the interaction with the photon that is exchanged in the inelastic process; the others are neutral and play the role of spectators (see Fig. 1). The charged constituent with momentum $p_\mu = \xi P_{1\mu}$ (we neglect the transverse parton momenta) and mass $m = \xi M$ ($0 < \xi < 1$) changes its momentum to $(\xi P_1 + Q)_\mu$ in the interaction with the virtual boson; the mass-shell condition requires $(\xi P_1 + Q)^2 = (\xi P_1)^2$ or $2\xi P_1 \cdot Q + Q^2 = 0$. We have then

$$\xi = -\frac{Q^2}{2P_1 \cdot Q} \equiv x \,, \tag{8}$$

where we have introduced the Bjorken scaling variable x, whose meaning is clear from (8).

Defining also the variable y by the fractional energy loss of the incoming lepton, i.e. in de target restframe by $(E' - E)/E$, one may write the differential cross section for deep-inelastic scattering (DIS), mediated by a photon, in terms of dimensionless structure functions as

$$\left(\frac{\mathrm{d}^2\sigma}{\mathrm{d}x\,\mathrm{d}y}\right)^\gamma = \frac{8\pi\alpha^2 ME}{(Q^2)^2}\left[\frac{1 + (1-y)^2}{2} 2xF_1^\gamma(x, Q^2)\right.$$

$$\left. + (1-y)\left[F_2^\gamma(x, Q^2) - 2xF_1^\gamma(x, Q^2)\right] - \frac{M}{2E}xy\,F_2^\gamma(x, Q^2)\right], \tag{9}$$

where M is the nucleon mass. The accumulated data for this process, mostly from the HERA collider at DESY, are displayed in Fig. 2. Notice that to first approximation the structure function $F_2(x, Q^2)$ only
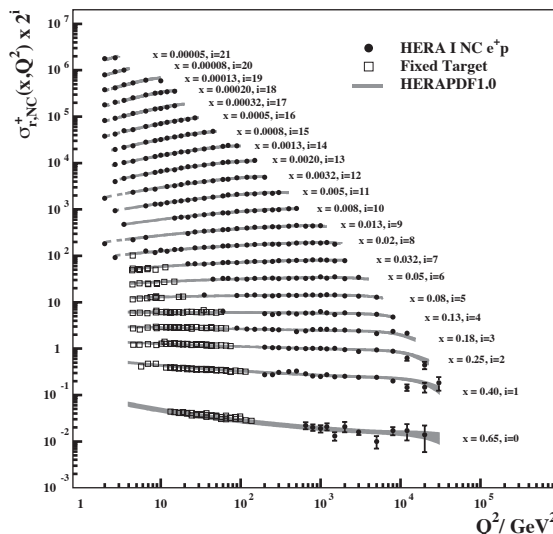

Fig. 2: The reduced cross section (corresponding to $F_2(x, Q^2)$ up to a small correction due to weak interaction effects). The data have been taken at the HERA collider [1].

depends on x, a phenomenon known as scaling. The parton model, to which we now turn, provides an explanation for this phenomenon.

After the interaction with the virtual boson has taken place, the charged constituent will move in a different direction than the spectator particles. However, during recoil it feels the influence of the binding mechanism, which forces the constituents to recombine into a new hadronic state, such as an excited nucleon or a nucleon with one or several pions (on a much longer time scale than that of the primary collision). Confinement dictates that the nature of this final-state interaction is such that the

partons cannot be produced as isolated particles, and that the binding force does not interfere with the primary interaction with the vector bosons.

Because the spectators do not participate in the primary interaction the cross section for inelastic lepton-nucleon scattering is given directly in terms of the cross section for lepton-parton scattering. Assuming that the parton is point-like and that the beam energy in the laboratory frame is large compared to the masses, one can compute, using the rules of QED

$$\left(\frac{\mathrm{d}\sigma}{\mathrm{d}y}\right)^{\gamma} = \frac{8\pi\alpha^2 ME}{(Q^2)^2} q^2 \frac{(1-y)^2 + 1}{2}\xi \, . \tag{10}$$

where the factor ξ arises because we have replaced the parton mass m by $M\xi$. Comparing (10) to (9), we conclude that the contribution from elastic parton scattering via photon exchange to the nucleon structure functions is given by

$$F_2^{\gamma}(x) = 2xF_1^{\gamma}(x) = q^2 x \delta(x - \xi) \, , \tag{11}$$

The structure functions thus satisfy the Callan-Gross relation [2]

$$F_2(x) = 2xF_1(x) \, , \tag{12}$$

which is characteristic for (massless) spin-$\frac{1}{2}$ partons Although we have now found structure functions that depend only on x, in agreement with the phenomenon of scaling discussed above, the model is clearly unrealistic as x remains restricted to a single value ξ. Therefore, to improve the situation one now assumes that the nucleon contains many partons interacting with the intermediate photon and carrying a fraction of the nucleon momentum according to a probability distribution $f(\xi)$. To be precise, $f_i(\xi)d\xi$ measures the number of partons of type i (e.g. a u-quark or a gluon) in the momentum range from ξP_1 to $(\xi + \mathrm{d}\xi)P_1$. As the nucleon may also contain anti-partons there is a corresponding distribution $\bar{f}_i(\xi)$ to measure the number of anti-partons in the same momentum range. In doing so we will keep ignoring the effect of transverse parton momenta. Furthermore we assume that the scattering on the partons is *incoherent* (i.e. quantum-mechanical interference effects between scattering reactions on different partons are ignored) so that we can simply sum and/or integrate (10) over the various (anti-)parton distributions,

$$\left(\frac{\mathrm{d}\sigma}{\mathrm{d}y}\right)^{\gamma} = \frac{8\pi\,\alpha^2 ME}{(Q^2)^2} \frac{(1-y)^2 + 1}{2} \sum_i q_i^2 \int_x^1 \mathrm{d}\xi\,\xi\,f_i(\xi) \, , \tag{13}$$

where the sum is over (anti-)-quark flavours i having fractional charge q_i (either $\frac{2}{3}$ or $-\frac{1}{3}$). Let us discuss a few more consequences of the parton model. Identifying the partons as quarks[6] we can directly derive the following parton model expression for the electromagnetic structure functions

$$\begin{aligned} x^{-1}F_2^{\gamma}(x) &= 2F_1^{\gamma}(x) \\ &= \tfrac{4}{9}[u(x) + \bar{u}(x) + c(x) + \bar{c}(x)] + \tfrac{1}{9}[d(x) + \bar{d}(x) + s(x) + \bar{s}(x)] \, . \end{aligned} \tag{14}$$

One may now also immediately state he charge sum rule

$$\begin{aligned} Q^{\mathrm{nucleon}} = \int_0^1 \mathrm{d}x \, \big[&\tfrac{2}{3}[u(x) - \bar{u}(x) + c(x) - \bar{c}(x)] \\ &- \tfrac{1}{3}[d(x) - \bar{d}(x) + s(x) - \bar{s}(x)]\big] \, , \end{aligned} \tag{15}$$

which the parton distribution functions must obey. Furthermore we note that by interchange of u and d quarks a proton becomes a neutron and vice versa (this interchange can be realized by a special isospin transformation). Therefore all neutron quark distributions follow from those of the proton: $u(x)^N = d(x)^P, d(x)^N = u(x)^P$, whereas the s- and c-distributions are equal. Henceforth we will therefore use the notation where $u(x), d(x), s(x)$ and $c(x)$ refer to the proton structure functions only. In Fig. 3
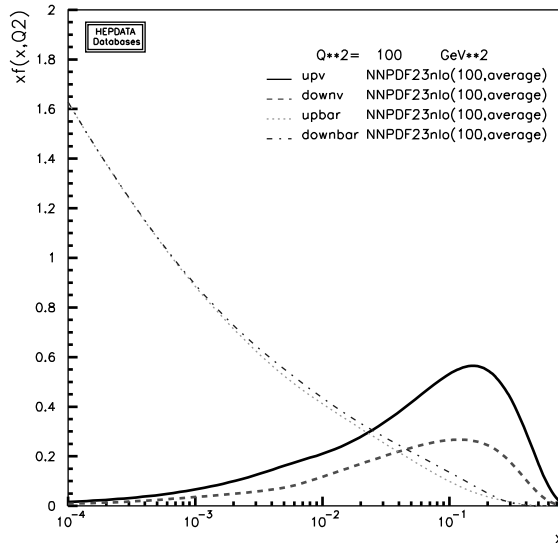
Fig. 3: The distributions of $x[u(x) - \bar{u}(x)]$ and $x[d(x) - \bar{d}(x)]$ (the valence quarks), as well as those of the anti-up $x\bar{u}(x)$ and anti-down $x\bar{d}(x)$ in the proton. The plots correspond to the NNPDF set, version 2.3 [3] for a value of $Q^2 = 100\,\mathrm{GeV}^2$ [4].

we show some examples of quark distribution functions in the proton. Unlike the quarks, the gluons are neutral under weak and electromagnetic interactions, so they are not directly observed in the deep-inelastic process. Their presence can, however, already be inferred from the naive model discussed above, because the total fraction of the nucleon momentum carried by the quarks (which is given by the areas under the curves of Fig. 3) is roughly $\frac{1}{2}$. This is an indirect indication that gluons carry the remaining nucleon momentum.

As stated above, if the nucleon is probed at large Q^2 the quarks inside will behave as free point-like objects. The QCD interactions will dissipate the momentum transfer Q^2 to other quarks, and in this process gluons will be radiated which may again interact with quarks or gluons or annihilate into quark-anti-quark pairs. This effect becomes more sizeable if the momentum transfer Q^2 is shared by many quarks and gluons, as the average momenta are then smaller so that the effective QCD coupling grows in strength. The timescale that is relevant for the final state interaction is therefore much larger than that for the primary interaction. Incorporating these quark-gluon interactions into the naive quark-parton model leads in principle to a consistent field-theoretic set-up for calculating quantum corrections in deep-inelastic scattering, and other processes.

We finally remark that the universal nature of the parton distribution functions $f_i(\xi)$ should allow us to apply the parton model also to the Drell-Yan process, in which a quark and an anti-quark inside the nucleons collide to form a lepton-anti-lepton pair. This we shall do further below in these notes.

2.3 Renormalization and asymptotic freedom

The examination of the quantum corrections in a theory can provide crucial insight into the structure of the theory, and its consistency. For example, if they break the gauge symmetries of a theory (so that these symmetries are anomalous), the theory can be inconsistent. It can also teach us about the predictive power of the theory. If the higher order corrections for some observable are so large that the very concept of perturbation theory for this case becomes doubtful, we have a crisis of the theory's predictive power

---

[6]We include u,d,s and c quarks here as they can be treated as massless quarks in most high-energy processes. Bottom and top quarks, being heavier, are often not treated as partons.

for this observable. Higher order corrections may contain ultraviolet divergences (we will discuss other divergences later). Here we discuss how one may handle them and account for them.

2.3.1 Regularization

In order to handle divergences one must first regularize the quantum field theory in such a way that the infinities become temporarily finite (would-be infinities). If done consistently, one can apply the renormalization procedure, upon which for appropiate quantities the would-be infinities cancel, so that the regularization can be removed. A number of regularization have been invented in the past, let us review some of them.

Cut-off

In this method one imposes a uniform upper limit Λ on the loop momenta

$$\int^{\Lambda} \frac{dq}{q} + \ldots = \ln \Lambda + \text{finite terms} \tag{16}$$

The would-be infinity is represented here by $\ln \Lambda$. When all would-be infinities have cancelled and only $1/\Lambda^p$ terms are left, one can remove the regulator by $\Lambda \to \infty$. The advantage of this method is that it is very intuitive, the (serious) disadvantage is that it is very cumbersome in higher orders, in particular for gauge theories. It is therefore mostly used in high energy physics for didactical purposes.

Lattice

In this method one discretizes spacetime, and defines fields to live only on the lattice points (or on the links between them). In this way momenta cannot be larger than $1/a$ where a is the lattice spacing. A major advantage of this method is that it can actually be used for computer simulation, so that the full path integral can be evaluated, without need to expand it in perturbation theory. Among the drawbacks are difficulties in maintaining continuum symmetries on the lattice. It is however a widely used method, mostly for lower energy observables, such as hadron masses and decay constants.

Dimensional regularization

This is the regularization that is most powerful in perturbative quantum field theory, and therefore also most widely used. It consists of the temporary extension of the number of dimensions in spacetime, or conversely, momentum space, from 4 to $4 + \varepsilon$

$$\int d^4 x \mathcal{L}(x) \to \int d^{4+\varepsilon} \mathcal{L}(x) \tag{17}$$

How does this method regularize ultraviolet diverences[7]? A careful dimensional analysis shows that (i) momentum space propagators continue to look like $1/(q^2 + m^2)$, and (ii) gauge couplings now get dimension $-\varepsilon/2$. Then a one-loop integral is extended as follows

$$\int d^4 q \frac{1}{q^4} \to \int d^{4+\varepsilon} q \frac{1}{q^4} \tag{18}$$

In $n = 4 + \varepsilon$ dimensional polar coordinates this may be written as (introducing a lower limit Q on the q integral)

$$\int d\Omega_{3+\varepsilon} \int_Q^{\infty} dq q^{3+\varepsilon} \frac{1}{q^4} \tag{19}$$

These d dimensional integrals can be carried out to yield

$$\frac{2\pi^{2+\varepsilon/2}}{\Gamma(2 + \varepsilon/2)} \frac{-1}{\varepsilon} Q^{\varepsilon} \tag{20}$$

---

[7]A more careful treatment of dimensional regularization, including the conditions on the complex parameter ε can be found in [5].

The Euler gamma function $\Gamma(2 + \varepsilon/2)$ makes a frequent appearance in this regularization method. The would-be infinity is $1/\varepsilon$. Removing the regulator would correspond to taking the limit $\varepsilon \to 0$.

2.3.2 Renormalization

Now that we know how to regularize a quantum field theory we are ready to understand conceptually the renormalization procedure. At its heart is the question how to have a predictive theory when higher-order corrections contribute an infinite amount to various Green functions.

Let us first form a physical picture for the case of the QED lagrangian

$$\mathcal{L}_{\text{QED}} = -\tfrac{1}{4}\big(\partial_\mu A_\nu - \partial_\nu A_\mu\big)^2 - \bar{\psi}\,\slashed{\partial}\psi - m\,\bar{\psi}\psi + \text{ie}\,A_\mu\bar{\psi}\gamma^\mu\psi\,, \tag{21}$$

with A_μ representation the photon field, ψ the electron field, and e the electric charge. For QCD the conceptual points are the same, if a bit more complicated. At lowest order, and after gauge-fixing, the lagrangian provides an electron 2-point function (leading to the electron propagator), a photon 2-point function (leading to the photon propagator), and a photon-electron 3-point function (leading to the QED interaction vertex), see Fig. 4. Let us now look at some of their one-loop correction when the
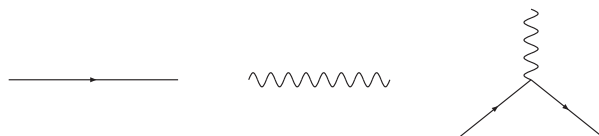

Fig. 4: Lowest order Green's functions provided by lagrangian

loop-momentum q becomes very large. In Fig. 5 we indicate how these corrections may be viewed. Be-
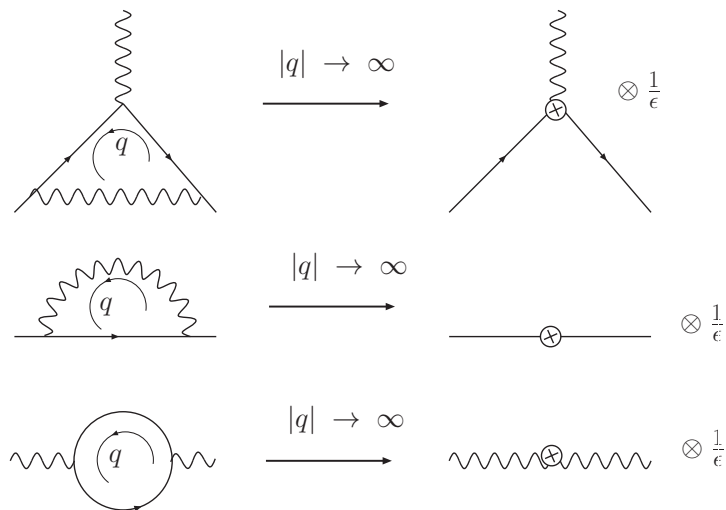

Fig. 5: One-loop corrections to lowest order Green's functions and their UV limit.

cause the loop momentum becomes so large, the loop reduces to a very local effect, of would-be infinite strength. It should be noticed that the result is simply a would-be infinite coefficient times the lowest order Green function. This is an important result. For example in Fig. 6 we see that the UV limit of the box graph, while leading to local 4-photon vertex which does *not* occur in the lagrangian, is also *not* would-be infinite. This suggests that we can absorb in this case the $1/\varepsilon$'s into the couplings and field normalizations of the lagrangian, without need to introduced new types of interactions. Quantum Electrodynamics is in fact a renormalizable theory. This means that it is sufficient to renormalize e, m, ψ, A_μ
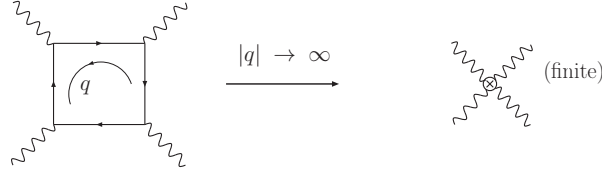
QCD

Fig. 6: UV limit of QED box graph

to absorb/cancel all would-be infinities for any Green function in QED. Let us see how this absorption works, using dimensional regularization.

First, let us recall that in dimensional regularization the dimension of the gauge coupling is no longer zero, but rather

$$[e] = \frac{2-d}{2} = -\frac{\varepsilon}{2} \tag{22}$$

To keep count of such dimensionalities, and to be able to define a dimensionless coupling, we introduce a mass scale μ, whose value is intrinsically arbitrary, such that

$$e = e(\mu)\mu^{-\varepsilon/2} \tag{23}$$

We now *renormalize* e by a factor Z_e that contains would-be infinities

$$e = e_R(\mu)\mu^{-\varepsilon/2} Z_e\left(\frac{1}{\varepsilon}, e_R(\mu)\right) = \left(1 + e_R(\mu)^2 \frac{1}{\varepsilon} z_e^{(1)} + e_R(\mu)^4 \left[\frac{1}{\varepsilon^2} z_e^{(2)} + \frac{1}{\varepsilon} z_e^{(1,1)}\right] + \dots\right) \tag{24}$$

The renormalized coupling $e_R(\mu)$ is finite, and is can be directly related to an actual physical quantity like the fine-structure constant. How this works when what is supposed to be a number actually depends on μ we will see below.

We have not yet specified the constants $z_e^{(1)}, z_e^{(2)}, z_e^{(1,1)}$ etc. Let us now consider an observable O which we have computed to 1-loop, using the QED Feynman rules

$$O = e\,C + e^3\left[A\frac{1}{\varepsilon}(Q^2)^{-\varepsilon/2} + B\right] \tag{25}$$

where Q is the typical energy scale of the observable. We now renormalize the coupling according to (24) and obtain, to order $e_R(\mu)^3$ and obtain

$$O = \mu^{-\varepsilon/2}\left\{e_R(\mu)\,C + e_R(\mu)^3\left[A\frac{1}{\varepsilon}\left(\frac{Q^2}{\mu^2}\right)^{-\varepsilon/2} + C\frac{1}{\varepsilon}z_e^{(1)} + B\right]\right\} \tag{26}$$

We can now choose $z_e^{(1)} = -A/C$. Then the poles in ε will cancel, and we can expand the result in ε

$$O = \left\{e_R(\mu)\,C + e_R(\mu)^3\left[A\ln\left(\frac{Q^2}{\mu^2}\right) + B\right].\right\} \tag{27}$$

One might think that it is not so hard to cancel divergences if one can simply choose to do so by picking $z_e^{(1)} = -A/C$. The remarkable fact, and the essence of the renormalizability of a theory, is however that this same choice works for all cases. One would always, for QED, find the same answer for $z_e^{(1)}$. Similarly for $Z_\psi\left(\frac{1}{\varepsilon}, e_R(\mu)\right), Z_\alpha\left(\frac{1}{\varepsilon}, e_R(\mu)\right), Z_m\left(\frac{1}{\varepsilon}, e_R(\mu)\right)$. To find their coefficients in the $e_R(\mu)$ expansion one can take some relatively simple observables, and compute them once and for all.

Based on the example just discussed it should not be too great a surprise to learn that the generic structure of the observable, after renormalization, is

$$O(Q, \mu) = e_R(\mu)^2\,[O_1] + \tag{28}$$

$$e_R(\mu)^4 \left[O_{10} + O_{11} \ln \left(\frac{Q^2}{\mu^2} \right) \right] + \tag{29}$$

$$e_R(\mu)^6 \left[O_{20} + O_{21} \ln \left(\frac{Q^2}{\mu^2} \right) + O_{20} \ln^2 \left(\frac{Q^2}{\mu^2} \right) \right] + \ldots \tag{30}$$

where the O_{ij} are various constants. We note that (i) $O(Q,\mu)$ is finite, and (ii) it depends on the determined scale μ both directly, via the logaritms, and implicitly, via the renormalized coupling $e_R(\mu)$. The last point is problematic: if we have consistently cancelled the divergences only for O to depend on an arbitrary scale it seems we have not gained much predictive power. However, the μ dependence is precisely such that for Eq. (28)

$$\mu \frac{d}{d\mu} O(Q,\mu) = \mathcal{O}(e_R^8(\mu)) \tag{31}$$

i.e. one order beyond the one calculated. Should one add another order to the result in (28) the residual dependence on μ would be $\mathcal{O}(e_R^{10}(\mu))$ and therefore progressively less, and the prediction ever more precise. Some uncertainty will however remain, and it is customary to estimate it by varying μ/Q from 2 to $1/2$.

2.3.3 Running coupling, β function

What is the origin of this conspirational μ dependence? It is in fact the renormalization procedure itself. In the problem sets it was shown that from the relation (24) one can derive (by acting with $d/d\ln\mu$ on both side) a first order differential equation for the μ dependence of the finite renormalized coupling

$$\mu \frac{d}{d\mu} e_R(\mu) = \beta_0 e_R(\mu)^3 + \beta_1 e_R(\mu)^5 + \ldots \equiv \beta(e_R(\mu)) \tag{32}$$

known as the β function equation, or sometimes also as the renormalization group equation for the running coupling.

The β-function equation plays an important role in the Standard Model. It should be clear that its occurrence is generic. Because each coupling in the Standard Model requires renormalization, each will have its own β-function. The β functions are only known in form of a perturbative expansion, as in Eq. (32). For non-abelian gauge theory no less than the first four terms are known (five for the case of SU(3) [6]!). The first term

$$\beta_0 = -\frac{11C_A - 4T_F N_F}{12\pi} \tag{33}$$

was calculated in the early 70's. The 2004 Nobel Prize was awarded for this calculation, in particular for the interpretation for the fact that the term is *negative*, about which more below. From eq. (32) we can already see that if the function has negative coefficents, as non-abelian gauge theories such as QCD do, the coupling decreases for a positive increment in the scale μ, i.e. when $\mu \to \mu + d\mu$, leading to asymptotic freedom in the ultraviolet, and strong binding at low scales μ.

2.3.4 Symmetries of QCD

Before diving further into the perturbative aspects of QCD, let us devote now a bit of space to considering the fundamental symmetries of QCD. We discussed some of this already qualitatively in section 2.1, here we discuss these from a field-theoretical point of view. The defining symmetry of QCD is the local SU(3) symmetry, under which the quark transform as

$$\psi(x) \to \psi'(x) = U(x)\,\psi(x), \qquad U = \exp(\xi^a t_a), \tag{34}$$

where the matrices t_a are called the *generators* of the group defined in the representation appropriate to ψ, and the ξ^a constitute a set of linearly independent *real* parameters in terms of which the group

elements can be described. The number of generators is obviously equal to the number of independent parameters ξ^a and therefore to the dimension of the group, but is not necessarily related to the dimension of the matrices U and $t_a{}^8$. Hence, U is a square matrix whose dimension is equal to the number of components in ψ (3 in the case of QCD). The covariant derivative should be such that when acting on a field that already transforms covariantly, the result will transform covariantly also

$$D_\mu \psi(x) \to (D_\mu \psi(x))' = U(x) \, D_\mu \psi(x). \tag{35}$$

To this end one introduces a (set of) gauge field(s)

$$D_\mu \psi \equiv \partial_\mu \psi - W_\mu \, \psi, \qquad W_\mu = W_\mu^a \, t_a \,, \tag{36}$$

so that also W_μ is matrices, and the number of gauge fields equals the number of generators (8 in the case of SU(3)). With the property (35) it is easy to construct non-abelian gauge theory. The rule (35) holds if W_μ transforms as

$$W_\mu \to W_\mu' = U W_\mu U^{-1} + (\partial_\mu U) U^{-1} \,, \tag{37}$$

i.e. inhomogeneously (the second term does not contain W_μ), and non-covariantly (the second term depends on the derivative of $U(x)$). With the covariant derivative one can also construct the field strength tensor

$$G_{\mu\nu} = -[D_\mu, D_\nu] = \partial_\mu W_\nu - \partial_\nu W_\mu - [W_\mu, W_\nu], \tag{38}$$

The field strength transforms covariantly and homogenously

$$G_{\mu\nu} \to G_{\mu\nu}' = U G_{\mu\nu} U^{-1} \,. \tag{39}$$

Finally, the QCD coupling constant can be introduced by replacing

$$W_\mu^a \to g \, W_\mu^a \,, \qquad G_{\mu\nu}^a \to g \, G_{\mu\nu}^a \,. \tag{40}$$

With this we can write down the QCD Lagrangian for one quark flavour, with mass m

$$\begin{aligned}\mathcal{L} &= \mathcal{L}_W + \mathcal{L}_\psi \\ &= \tfrac{1}{4} \mathrm{Tr}\, [G_{\mu\nu} \, G^{\mu\nu}] - \bar\psi \, \slashed{D} \psi - m \, \bar\psi \, \psi \,. \end{aligned} \tag{41}$$

Thanks to the rules in (34,35) and (39), it is straightforward to check its local SU(3) invariance

We now turn to a global symmetry of the QCD Lagrangian, that is relevant because there is more than one quark flavour. The full QCD Lagrangian reads

$$\mathcal{L}_{\mathrm{QCD}} = -\frac{1}{4} \mathrm{Tr}(G_{\mu\nu} G^{\mu\nu}) - \sum_{f=1}^{n_f} \overline{\psi_f}(\slashed{D} + m_f)\psi_f \,. \tag{42}$$

Besides having local symmetry, this Lagrangian has an interesting global symmetry if the masses of the quarks may be neglected. We can use the chiral projector $P_L = (1 + \gamma_5)/2$ and $P_R = (1 - \gamma_5)/2$ (it is easy to check that they are idempotent, that $P_L P_R = P_R P_L = 0$ and that they and sum to 1) to define left- and righthanded quarks

$$\psi_L = P_L \psi, \qquad \psi_R = P_R \psi \,. \tag{43}$$

In these terms, the fermion sector of (42) reads

$$\sum_{f=1}^{n_f} \overline{\psi_f}(\slashed{D} + m_f)\psi_f = \sum_{f=1}^{n_f} (\overline{\psi_{L,f}} \slashed{D} \psi_{L,f} + \overline{\psi_{R,f}} \slashed{D} \psi_{R,f}) \sum_{f=1}^{n_f} m_f(\overline{\psi_{L,f}} \psi_{R,f} + \overline{\psi_{R,f}} \psi_{L,f}) \,. \tag{44}$$

---

[8]For instance, for the three SU(2) generators one can choose 2,3,... dimensional matrices, corresponding to (iso)spin $\frac{1}{2}, 1, \ldots$.

When setting $m_f = 0$ one notes that the left- and righthanded quarks have no interactions. We may in fact mix them independently

$$\psi_{L,i} \to \psi'_{L,i} = U_{L,ij}\psi_{L,j}, \qquad \psi_{R,i} \to \psi'_{R,i} = U_{R,ij}\psi_{R,j}, \tag{45}$$

with U_L and U_R independent unitarity matrices. The dimension of these matrices is equal to the number of quark flavours that is (approximately) massless. This is a good a approximation for the up and down quarks, in general still reasonable for the strange quark, but for the heavy quarks not anymore. Note that the chiral symmetry $U_L \otimes U_R$ is a global symmetry, we do not make an effort to make this symmetry local. It relates many properties of pions and kaons.

But this symmetry becomes especially interesting when one accounts for the fact that the QCD nonperturbative vacuum should have the structure

$$\sum_f \langle \overline{\psi_{L,f}} \psi_{R,f} \rangle + (L \leftrightarrow R). \tag{46}$$

In words, in the QCD groundstate left- and righthanded projections of quark flavours are coupled, so that this chiral symmetry is spontaneously broken. By Goldstone's theorem, the spectrum of QCD (the set of actually realized particles) should feature massless spinless bosons. They must however be odd under parity, so that they are in fact pseudoscalar bosons. The obvious candidates for these would be the pions and kaons of the pseudoscalar meson octet. The reason is that the groundstate (46) is still invariant when choosing $U_L = U_R$ (so-called vector rotations), but when transforming left- and righthanded quarks differently, a γ_5 remains, which implies that the goldstone bosons behaves as $\overline{\psi}\gamma_5\psi$, i.e. as pseudoscalar mesons.

Though it still an unsolved problem how to compute the non-perturbative QCD spectrum fully analytically from the Lagrangian (42), one may set up an effective theory, Chiral Perturbation Theory (χPT), for pions (and kaons) valid for low energy scattering. However, in these notes we shall not go further into this interesting subject.

2.4 Evidence for colour

Because the QCD colour quantum number is so central to its understanding and functioning, it would be interesting to verify it. This is not straightforward, as we discussed, since colour is confined (hadrons are "white"), so that its existence can only be inferred. Let's see how this might be done. Consider the total cross section for the production of a fermion-antifermion pair $f\bar{f}$ in an electron-positron collision, to lowest order in the electromagnetic coupling. The fermion has e.m. charge $Q_f e$ and mass m, and we approximate the electron to be massless. The answer is in fact quite simple

$$\sigma_f(s) = \frac{4\pi\alpha^2 Q_f^2}{3s}\beta\left(1 + \frac{2m_f^2}{s}\right)\theta(s - 4m_f^2) \tag{47}$$

where s is the center-of-mass energy squared. Note that we have attached a label f to the mass the type of fermion f. The factor involving the electric charges also depends on the fermion "flavour". Thus, for an electron, muon and tau $Q_f = -1$, for up, charm, and top quarks $Q_f = 2/3$, while for down, strange and bottom quarks $Q_f = -1/3$. The factor $\beta = \sqrt{1 - 4m_f^2/s}$ is a phase space volume factor; when s is just a little bit larger than $4m^2$ β is close to zero, i.e. near threshold the cross section is small. Far above threshold $\beta \sim 1$. The theta function ensures that the cross section is only non-zero is the center of mass energy is large enough to produce the quark pair.

How might we use this result? If the produced fermions are electrons, muons or taus we can directly confront the result with data, and agreement is in fact very good. There is a more interesting use

of the formula in Eq. (47). Consider the inclusive *quark* cross section

$$\sigma_{had}(s) = \sum_{f=u,d,s,c,...} \frac{4\pi\alpha^2 Q_f^2}{3s}\beta\left(1+\frac{2m_f^2}{s}\right)\theta(s-4m_f^2)N_c \tag{48}$$

The extra factor N_c at the end accounts for the fact that quarks come in $N_c = 3$ colours. We may interpret this in fact as a prediction for the inclusive *hadron* cross section, because the quark final state must, before they reach any detector, make a transition to a hadronic final state, see the illustration in Fig. 7. In Fig. 8 we see the confrontation of this result with data, and that the agreement is very good,
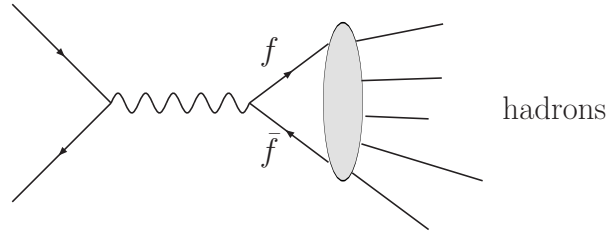

Fig. 7: $e^+e^- \to$ hadrons; the blob represents the "hadronization" process. Note that time runs from left to right in this diagram.

except that we did not anticipate the huge peak near $\sqrt{s} \simeq 90$GeV. That is because we did not include in our calculation of $\sigma_f(s)$ in eq. (47) a second diagram in which not a photon (as in Fig. 7) but a Z-boson of mass $M_Z \simeq 90$GeV mediates the scattering. Had we done so, we would have more terms in final answer for $\sigma(s)$ in Eq. (47), with the factor $1/s$ replaced $1/(s - M_Z^2 + \Gamma_Z^2)$, where Γ_Z is the Z-boson decay width (about 2 GeV). The good agreement also implies that the effect of higher order corrections to $\sigma(s)$ should be small, and indeed they turn out to be so, after calculation. We can now define an
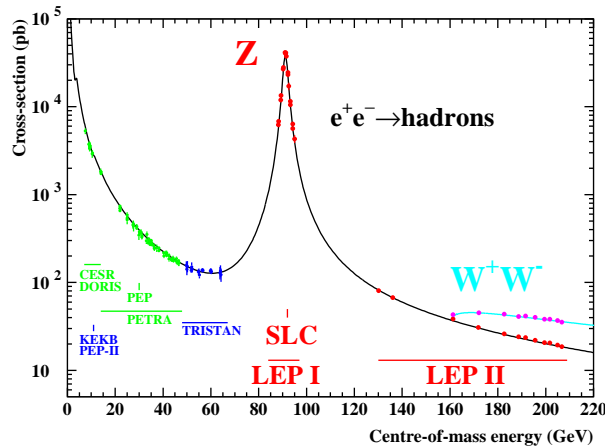
Fig. 8: Total cross section for e^+e^- to fermions.

observable traditionally called R

$$R(s) = \frac{\sigma(e^+e^- \to \text{ hadrons})}{\sigma(e^+e^- \to \mu^+\mu^-)} \tag{49}$$

The benefit of defining such a ratio is that a many common factors cancel in the theoretical prediction, and that many experimental uncertainties cancel in the experimental measurement. We have then

$$R(s) = \frac{\sum_{f=u,d,s,c,...} \sigma(e^+e^- \to f\bar{f})}{\sigma(e^+e^- \to \mu^+\mu^-)} \tag{50}$$

For large center-of-mass energy $\sqrt{s}$ we can derive from (48) that

$$R(s) \stackrel{s \to \infty}{\longrightarrow} N_c \sum_{f=u,d,s,c,\dots} Q_f^2 \theta(s - 4m_f^2) \tag{51}$$

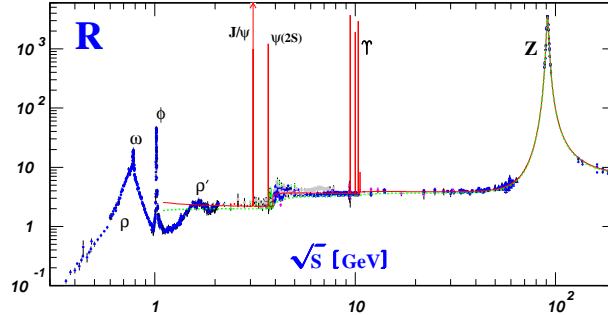In Fig. 9 we confront this result with experiment. We can draw the conclusions that (i) there is again

Fig. 9: R-ratio vs. center of mass energy

fairly good agreement between prediction and measurement; (ii) we see the effects of new quark flavour f being "turned on" as the energy increases beyond $2m_f$ ($m_c \simeq 1.5$ GeV, $m_b \simeq 5$ GeV); (iii) the larger step at charm than at bottom (proportional to $Q_c^2 = 4/9$ and $Q_b^2 = 1/9$, respectively) is well-predicted; (iv) the value of $R(s)$, say beyond the bottom quark threshold

$$R(s) = N_c \sum_{f=u,d,s,c,b} Q_f^2 \theta(s - 4m_f^2) = 3 \left(\tfrac{4}{9} + \tfrac{1}{9} + \tfrac{1}{9} + \tfrac{4}{9} + \tfrac{1}{9} \right) = \tfrac{11}{3} \tag{52}$$

agrees with experiment, and indicated that quarks come indeed in 3 colours.

3 Higher orders

In this section we discuss a number of key aspects relevant for computing higher-order effects in QCD. These are crucial to present-day applications of QCD for collider physics, so we provide a fair amount of detail.

3.1 Parton distribution functions (PDFs)

Before discussing how to compute higher-order partonic cross sections, let us discuss the quantities that form the interface of these to the hadronic cross sections: parton distribution functions. A recent, excellent review can be found in [7]. We already encountered the PDFs in section 2.2 in the context of the parton model, where they were functions of the momentum fraction variable ("x") only. However, in the context of higher-order calculations they play a central role in the cancellation of initial state collinear divergences, and in that process also acquire (logarithmic) factorization scale dependence. It should be clear that, being the interface between hadronic and partonic cross sections, they play a crucial role at the hadron colliders such as the HERA, Tevatron and LHC, and the quality of theoretical predictions is directly tied to knowing the PDFs well. Thus, we need to understand how to determine the PDFs and their uncertainties. To be precise, 11 of them: 5 quark, 5 anti-quark and 1 gluon PDF, which we denote by $\phi_{i/P}(\xi, \mu_F)$, the number of partons of type i in the proton with momentum fraction ξ, at factorization scale μ_F.

Key to this determination is their universality: the QCD factorization theorems [8] ensure that it is same set PDFs that occurs in all well-defined partonic cross sections to any fixed order. Therefore, one may choose (with care) a set of observables (e.g. DIS structure functions, certain hadron collider cross

sections) to infer the PDFs from. Since each is described as a combination of PDFs and partonic cross sections we have the set of equations

$$[O_n + \Delta O_n]^{\text{exp}} = \sum_{i=1}^{11} \phi_{i/P} \otimes [\hat{\sigma}_{n,i} \pm \delta\hat{\sigma}_{n,i}]^{\text{theory}} \, , \tag{53}$$

where also the experimental and theoretical uncertainties are indicated. From this set of equations the PDFs may be inferred. Notice that if the calculations on the rhs are all of order $N^k LO$, then the PDFs inferred are also labelled $N^k LO$, even though there are intrinsically non-perturbative functions. The $N^k LO$ PDFs can then be consistently used for other $N^k LO$ (and of course also for lower k) calculations.

The determination of the PDFs is not a trivial matter, and is performed by various groups, each taking different approachs. The groups are known by acronyms of various lengths: MSTW, CTEQ, NNPDF, GJR, HERAPDF, ABKM, etc. Below we shall discuss briefly some features and results of some of these approaches.

First, a brief aside on the formal aspects of a PDF. Although they cannot yet be computed from first principles, it is possible to give a precise definition of PDFs in terms of operators. In essence, it is the expectation value of a parton counting operator (think of $a^\dagger a$ for a harmonic oscillator in quantum mechanics) in a proton state. For the quark case it is

$$\phi_{q/P}(\xi, \mu) = \frac{1}{4\pi} \int_{-\infty}^{+\infty} dy^- e^{-ip^+ y^-} \langle p|\bar{q}(0, y^-, 0_T)\gamma^+ q(0, 0, 0_T)|p\rangle \, . \tag{54}$$

We have introduced here also lightcone notation for 4-vectors

$$p^\pm = \frac{p^0 \pm p^3}{\sqrt{2}}, \qquad p \cdot q = -p^+ q^- - p^- q^+ + p_T \cdot q_T \, . \tag{55}$$

so that $\gamma^+ = (\gamma^0 + \gamma^3)/\sqrt{2}$ in (54). The benefit of having a definition such as (54) is that one can compute now higher-order corrections to the operator, renormalize it, and then have a renormalization group equation for it. This is in fact then precisely the DGLAP equation. Note this can all be done in QCD perturbation theory. For the purposes of such calculations one can replace the proton states with parton states. Of course, the non-perturbative aspect comes in when evaluating the operator in a proton state. The DGLAP evolution equation reads

$$\mu \frac{d}{d\mu} \phi_{i/P}(\xi, \mu) = \sum_j \int_\xi^1 \frac{dz}{z} P_{ij}(z, \alpha_s(\mu)) \phi_{j/P}\left(\frac{\xi}{z}, \mu\right) \, , \tag{56}$$

where the P_{ij} are the Altarelli-Parisi splitting functions, which act here as evolution kernels. With evolution is meant the change in form of the function as the energy scale μ evolves. They are now known to NNLO (3-loop) [9, 10]. The logic is thus not unlike that of the running coupling, but now we have "running functions".

Returning now to how to extract the actual functional form of the PDFs from the equation (53), we see how the DGLAP equation is very useful. The data, on the lhs of (53), are taken at various energy scales. The theoretical description can for each observable be computed at the same energy scale because the scale evolution of the PDFs is known, so that meaningful comparison can be made.

The selection of observables to be used in eq. (53) must be done with care. Different observables should be sensitive in different ways to the various PDFs, so that a reliable extraction of a PDF is possible for each parton type. For instance, in DIS the most important partonic subprocess is $\gamma^* q \to q + X$ (where the off-shell photon is exchanged with the initial electron), so that associated observables are particularly sensitive to light quark PDFs. A nice overview of the main processes involved can be found in table 1, taken from Reference [11], which lists the processes that are included in a typical present-day

Process	Subprocess	Partons	x range
$\ell^{\pm}\{p,n\} \to \ell^{\pm} X$	$\gamma^* q \to q$	$q, \bar{q}, g$	$x \gtrsim 0.01$
$\ell^{\pm} n/p \to \ell^{\pm} X$	$\gamma^* d/u \to d/u$	d/u	$x \gtrsim 0.01$
$pp \to \mu^+ \mu^- X$	$u\bar{u}, d\bar{d} \to \gamma^*$	$\bar{q}$	$0.015 \lesssim x \lesssim 0.35$
$pn/pp \to \mu^+ \mu^- X$	$(u\bar{d})/(u\bar{u}) \to \gamma^*$	$\bar{d}/\bar{u}$	$0.015 \lesssim x \lesssim 0.35$
$\nu(\bar{\nu}) N \to \mu^-(\mu^+) X$	$W^* q \to q'$	$q, \bar{q}$	$0.01 \lesssim x \lesssim 0.5$
$\nu N \to \mu^- \mu^+ X$	$W^* s \to c$	s	$0.01 \lesssim x \lesssim 0.2$
$\bar{\nu} N \to \mu^+ \mu^- X$	$W^* \bar{s} \to \bar{c}$	$\bar{s}$	$0.01 \lesssim x \lesssim 0.2$
$e^{\pm} p \to e^{\pm} X$	$\gamma^* q \to q$	$g, q, \bar{q}$	$0.0001 \lesssim x \lesssim 0.1$
$e^+ p \to \bar{\nu} X$	$W^+ \{d, s\} \to \{u, c\}$	d, s	$x \gtrsim 0.01$
$e^{\pm} p \to e^{\pm} c\bar{c} X$	$\gamma^* c \to c, \gamma^* g \to c\bar{c}$	c, g	$0.0001 \lesssim x \lesssim 0.01$
$e^{\pm} p \to \text{jet} + X$	$\gamma^* g \to q\bar{q}$	g	$0.01 \lesssim x \lesssim 0.1$
$p\bar{p} \to \text{jet} + X$	$gg, qg, qq \to 2j$	g, q	$0.01 \lesssim x \lesssim 0.5$
$p\bar{p} \to (W^{\pm} \to \ell^{\pm} \nu) X$	$ud \to W, \bar{u}\bar{d} \to W$	$u, d, \bar{u}, \bar{d}$	$x \gtrsim 0.05$
$p\bar{p} \to (Z \to \ell^+ \ell^-) X$	$uu, dd \to Z$	d	$x \gtrsim 0.05$

Table 1: The main processes, their dominant subprocesses and the parton types they mostly affect, and the relevant x range. that are included in the MSTW 2008 global PDF analysis. They are partitioned into fixed-target experiments, HERA and the Tevatron.

global fit (MSTW08), and the PDFs they constrain. A priori, the space of functions is too large to be constrained through a global fit implied by solving eq. (53) for the PDFs using a finite amount of data, so some assumptions must be made. The various groups differ in their approaches to this issue to varying degrees, and, related to this, also in their determination of the errors of the extracted PDFs.

A few constraints are taken along. First, charm and bottom PDF's can be determined from the light flavour ones, assuming that such heavy quark arise from gluon splittings in the proton. This can be done in different ways, known as variable flavour number schemes, see also [7] for further comments and references. Also, the already mentioned charge and momentum sum rules must be obeyed precisely.

The most common approach is to take a physically motivated form for the PDFs at a low fixed scale Q_0 such as

$$\phi_{i/P}(x, Q_0^2 = x^{\alpha_i}(1-x)^{\beta_i} g_i(x) , \tag{57}$$

with the choice of function $g_i(x)$ differing per group (polynomials, exponentials etc). The form at other scales is found by solving the DGLAP evolution equation (56). Typically about 20-30 parameters are then to be fitted using χ^2 as goodness-of-fit

$$\chi^2 = \sum_{i,j=1}^{N_{data}} (D_i - T_i) \left(V^{-1}\right)_{ij} (D_j - T_j) , \tag{58}$$

where D_i, T_i are data and theoretical prediction, respectively, and V is the experimental covariance matrix. The uncertainties are determined by varying the parameters such that per variation along certain directions in parameter space (determined by the Hessian matrix) the χ^2 increased by a fixed amount. In this way, one generates a best-fit PDF set and a collection of one-sigma error sets, from which then uncertainties for physical observables may be determined.

Another approach is to use, instead of the fixed forms in (57), an approach that does not include theoretical bias at the outset, using neural networks. The number of free (architecture) parameters in this case is of order 200-300 and very redundant, but that's ok. The probability distribution in the space of function is modelled by a Monte Carlo sample of replica's, so that averages and standard deviations can be easily computed using sums over replicas.

Both approaches agree quite well, and differences are very instructive. A comparison of various recent sets for the LHC at 8 TeV is shown in Fig. 10 Clearly, the topic of PDF determination is highly
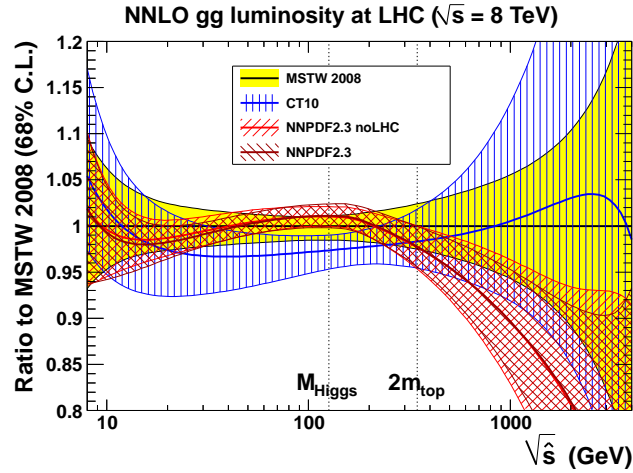

Fig. 10: Comparison of gluon-gluon luminosity functions for various PDFsets, relative to the MSTW08 set. Taken from [7].

important, and progress continues as data accumulate and understanding of subtle bias effects improves. A recent review [12] describes the state of affairs at the start of LHC run 2.

3.2 e^+e^- collisions and event shapes

Before continuing with aspects of QCD at hadron colliders, let us first have a look at issues in QCD at e^+e^- colliders, such as the former LEP collider at CERN. Such colliders are, in a sense, the cleanest place to study QCD, due to the pointline, non-strongly interacting initial state particles. We already saw how the number of colours, and the masses of heavy quarks can be seen in in R-ratio. However, the R-ratio involves the total cross section, and is not sensitive to the particular shape or structure of the final state.

There are other observables or variables that can be, and were, measured, experimentally. and are also theoretically consistent (that is, they are infrared-safe, which we discuss in section 3), and are sensitive to the geometry or structure of the final state. These *event shape* observables describe properties of final state configurations differently from the total cross section in e^+e^- collisions (they have also been generalized to other collision types).

A well-known example of such an infrared safe event shape is the maximum directed momentum, or thrust T, in e^+e^- collisions. The thrust of an event is defined by

$$T = \max_{\hat{n}} \frac{\sum_i |\vec{p_i} \cdot \vec{\hat{n}}|}{\sum_i |\vec{p_i}|}, \tag{59}$$

where the p_i are the momenta of the particles and the unit three-vector $\vec{\hat{n}}$ is varied until a maximum value of T is obtained. It varies between $T = \frac{1}{2}$ for a spherical energy flow and $T = 1$ for a pencil-like linear energy flow of two very narrow, back-to-back jets. Let us illustrate this discussion by the calculation of the thrust distribution for the reaction

$$e^+(k_1) + e^-(k_2) \to \gamma(q) \to q(p_1) + \bar{q}(p_2) + g(p_3). \tag{60}$$

The Feynman diagrams are shown in Fig. 11. The kinematical situation is that of an off-shell photon decaying into three massless partons, which allows us to use Dalitz plot variables to describe the final
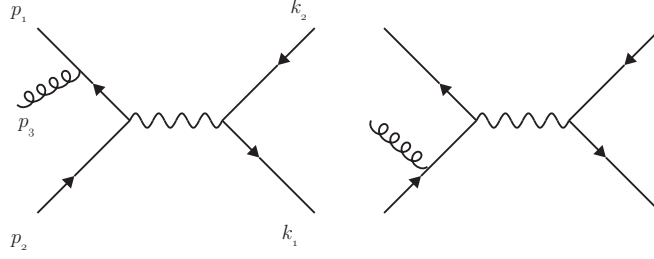
Fig. 11: Feynman diagrams for $e^+e^- \to \gamma \to q\bar{q}g$ at lowest order in the QCD coupling

state. The Dalitz plot for a decay into 3-particle final state is a scatterplot of events in a plane spanned by two of the final particle energies. The reason for plotting events this way is that the phase space measure is "flat" in those variables, so that any clustering of events represents an intermediate resonance in the decay.

Let us then choose two energies to specify the allowed region in a Dalitz plot, or, more conveniently and equivalently, choose invariant mass variables. Hence, using the particle name to represent its four momentum, we introduce $s_{13} = -(p_1 + p_3)^2$, $s_{23} = -(p_2 + p_3)^2$ and $s_{12} = -(p_1 + p_2)^2$. Since the three final particles are coplanar, the whole kinematics is specified by s_{13}, s_{23} and 3 angular variables. One angular variable θ specifies the polar angle between the beam axis and a line in the three-particle plane. Another azimuthal angular variable ϕ specifies the orientation of the plane will respect to this line and finally there is an overall azimuthal angle χ. The phase space for the final three particles therefore becomes

$$\frac{1}{(2\pi)^5} \int \frac{d^3 p_1}{2E_1} \int \frac{d^3 p_2}{2E_2} \int \frac{d^3 p_3}{2E_3} = \frac{1}{(2\pi)^5} \int \frac{1}{32 q^2} ds_{13} ds_{23} d\phi d\sin\theta d\chi \,. \tag{61}$$

The expression for the cross-section after squaring the matrix element for $e^+e^- \to q\bar{q}g$ and integrating over ϕ and χ turns out to be

$$\frac{d^3\sigma}{ds_{13} ds_{23} d\sin\theta} = \frac{\alpha_e^2}{8} \frac{\alpha_s}{q^2} \left(x_1{}^2 + x_2{}^2\right) \left(2 + \cos^2\theta\right) \frac{1}{s_{13} s_{23}} \,, \tag{62}$$

where the variables $x_i = E_i/E$, with $E = \sqrt{q^2}/2$, are related to the invariant mass variables by $s_{13} = q^2(1 - x_2), s_{23} = q^2(1 - x_1), s_{12} = q^2(1 - x_3)$. Note that $x_1 + x_2 + x_3 = 2$. From (62) we see that the angular distribution of the normal to the plane with respect to the beam line is given by $2 + \cos^2\theta$. A final integration over $\sin\theta$ yields the two equivalent expressions.

$$\sigma_T^{-1} \frac{d^2\sigma}{ds_{13} ds_{23}} = \frac{2}{3\pi} \alpha_s \frac{x_1^2 + x_2^2}{s_{13} s_{23}} \,, \tag{63}$$

or

$$\sigma_T^{-1} \frac{d^2\sigma}{dx_1 dx_2} = \frac{2}{3\pi} \alpha_s \frac{x_1^2 + x_2^2}{(1 - x_1)(1 - x_2)} \,, \tag{64}$$

where we have divided both sides of the equation by $\sigma_T = \frac{4}{3}\pi\alpha_e^2/s$, the $e^+e^- \to \mu^+\mu^-$ cross section. These distributions diverge for small invariant masses, or, equivalently as the scaled energies $x_{1,2}$ of the quark and antiquark go to one. It is not very difficult to show that the thrust variable T for the present case is equal to $\max(x_1, x_2, x_3)$ for each event, with $\frac{2}{3} \leq T \leq 1$. For fixed T the allowed region in x_1, x_2 is then shown in Fig. 12. The lines EF, FD and DE are the lines $x_1 = 1$, $x_2 = 1$ and $x_3 = 1$, respectively. The figure shows the subdivision of the final phase space into three regions depending on which particle has the largest x value. Consider first the case $T = x_2$. Then we have

$$\sigma_T^{-1} \frac{d\sigma}{dT} = \frac{2\alpha_s}{3\pi} \int dx_1 dx_2 \delta(T - x_2)\theta(T - x_1)\theta(T - x_3)$$
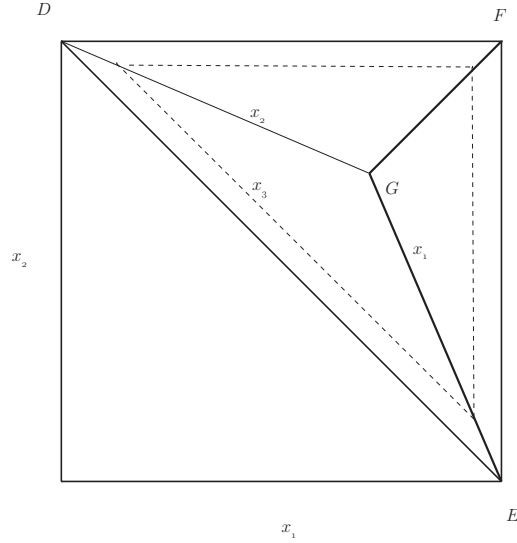
Fig. 12: Contributing regions in $x_{1,2}$ for a given value of thrust T. On the line DE $x_3 = 1$ (recall that $x_1 + x_2 + x_3 = 2$). At the point G all three x_i are equal to $2/3$. In each of the three triangles that join at G one of the three x_i is largest, as indicated. On the dashed line the value of T is constant.

$$
\times \frac{x_1^2 + x_2^2}{(1 - x_1)(1 - x_2)}
$$

$$
= \frac{2\alpha_s}{3\pi} \int_{2(1-T)}^{T} dx \frac{T^2 + x^2}{(1 - T)(1 - x)}
$$

$$
= \frac{2\alpha_s}{3\pi} \left\{ \frac{1 + T^2}{1 - T} \ln \frac{2T - 1}{1 - T} + \frac{3T^2 - 14T + 8}{2(1 - T)} \right\}, \tag{65}
$$

with an identical result for $T = x_1$. The $T = x_3$ case is slightly different, and corresponds to integrating over the dashed line parallel to DE in Fig. 12. On this line we have that $x_1 = 2 - T - x_2$, while x_2 ranges from $2(1 - T)$ to T. One then finds

$$
\sigma_T^{-1} \frac{d\sigma}{dT} = \frac{4\alpha_s}{3\pi} \left\{ \frac{1 + (1 - T)^2}{T} \ln \frac{2T - 1}{1 - T} + 2 - 3T \right\}. \tag{66}
$$

Clearly there is different, interesting dependence on T for the various cases.

Note that the thrust distributions for the quark and antiquark are singular as $T \to 1$, signifying the appearance of soft and/or collinear singularities, where either the gluon is very soft, or the (anti-)quark-gluon splitting is essentially collinear (in the $T = x_3$ case (66) the distribution is singular but integrable). In these infared and collinear regions of phase space non-perturbative effects must start playing a role in order to cure this apparent problem in perturbative QCD.

The different expressions for the thrust dependence for different regions in Fig. 12 allow us to make an interesting observation. Since the integral of the gluon T distribution in (66) is integrable at $T = 1$, we can integrate it from $T = 2/3$ to $T = 1$ to find the probability that the gluon is the most energetic particle. This yields

$$
\sigma_T^{-1} \int_{2/3}^{1} \frac{d\sigma}{dT} dT = 0.61 \frac{\alpha_s}{\pi}. \tag{67}
$$

We can reasonably [9] assume that α_s is a function of q^2, the center-of-mass energy squared, so that the

---

[9] A higher-order calculation of the thrust distribution [13–16], which requires renormalization of the QCD coupling, confirms this.

total probability that the gluon is the most energetic particle decreases with increasing q^2. The probability that the quark or the antiquark is the most energetic particle is then given by $(1 - 0.61\alpha_s/\pi)$.

The total thrust distribution is twice the result (65) (accounting for the cases $T = x_1$ and $T = x_2$) added to the result (66), which yields

$$\sigma_T^{-1}\frac{d\sigma}{dT} = \frac{2\alpha_s}{3\pi}\left[\frac{2(3T^2 - 3T + 2)}{T(1 - T)}\ln\frac{2T - 1}{1 - T} - \frac{3(3T - 2)(2 - T)}{1 - T}\right]. \tag{68}$$

Because the integrand is integrable at $T = 1$ we can also compute the average value of $(1 - T)$ from this formula

$$\langle 1 - T\rangle \equiv \sigma_T^{-1}\int dT\frac{d\sigma}{dT}(1 - T) = 1.05\frac{\alpha_s(q^2)}{\pi}. \tag{69}$$

We see that this average value of $(1 - T)$ decreases with increasing q^2.

A comparison of higher-order calculations for thrust with data is shown in Fig. 13, showing the good quality of (but also the need for) the NNLO approximation.

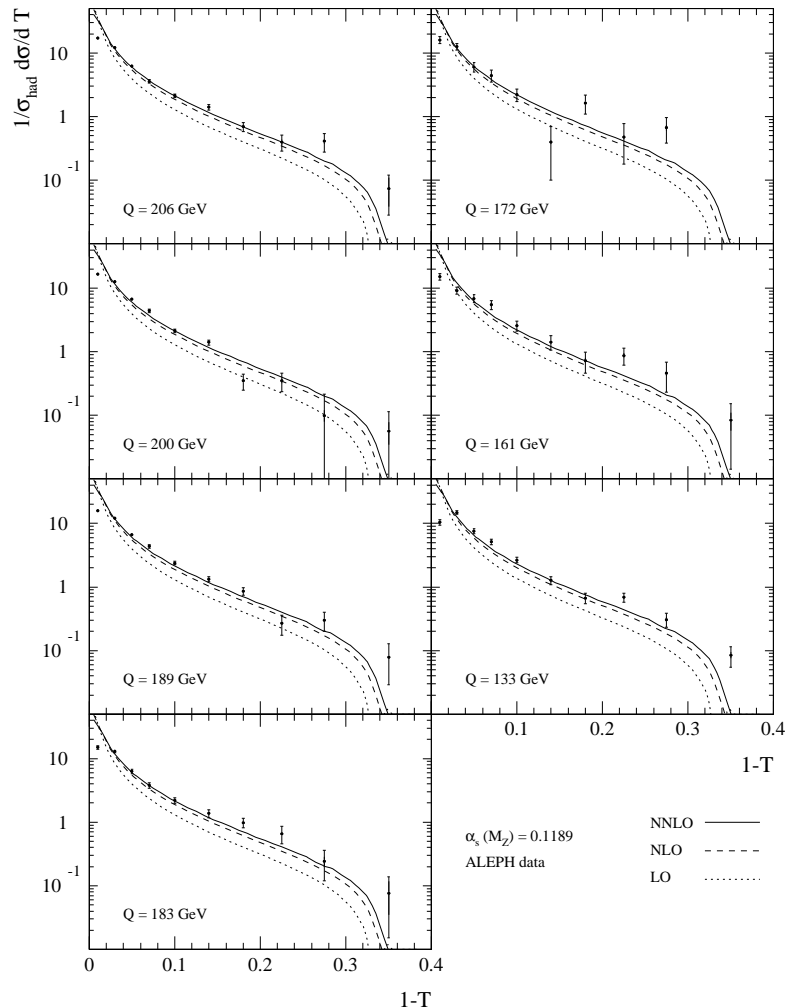**Fig. 13:** A comparison of thrust data from the ALEPH collaboration, with LO, NLO and NNLO calculations for various LEP cm energies. Figure taken from [17].

This concludes our rather detailed look at event-shape variables, where we already saw the appearance of infrared and collinear singularities. We now turn to a more detailed discussion of these, as this is a central issue in the application of perturbative QCD for colliders.

3.3 More on e^+e^- cross sections, IR divergences, KLN theorem

The ratio $R = \sigma(e^+e^- \to \text{hadrons})/\sigma(e^+e^- \to \mu^+\mu^-)$ was already discussed in section 2.4 when discussing evidence for colour. In order to compute higher-order QCD corrections to this ratio, i.e. to the e^+e^- total cross section, we must deal with infrared and collinear divergences (often collectively called "infrared"). This can be seen if one would integrate the expression (68) over T; it would produce a divergence due to the $1/(1 - T)$ behaviour.

The Kinoshita-Lee-Nauenberg theorem [18, 19] (KLN) now states that, when summing over all contributions to the observable at that order (i.e. also the loop-corrections) the divergences cancel if the sum is over a sufficiently degenerate set of states.

This is a very powerful result, so let us discuss it a bit further. One of the crucial aspects of massless particles is indeed that one is dealing with degenerate states. For instance, in quantum electrodynamics, it is not meaningful to distinguish between a single electron and an electron accompanied by any number of zero-momentum photons, as the corresponding states carry the same electric charge, energy and momentum. An (infinite) degeneracy of states implies that a naive application of perturbation theory may run into difficulties, a phenomenon that is, for instance, also known from applications in quantum mechanics. According to the Kinoshita-Lee-Nauenberg (KLN) theorem [18, 19] the divergences that are in principle present in partial transition probabilites, must cancel when averaging over a suitable set of degenerate states. This theorem encompasses in fact the older Bloch-Nordsieck [20] theorem.

Observables sufficiently inclusive to allow a sum over a sufficiently large ensemble of degenerate states for the KLN cancellations to occur, are known as *infrared safe*. How large an ensemble should be depends on the experimental process that one is considering. Of course in electron-positron annihilation at high energies, the *total* cross section (where one sums over *all* possible finite states) certainly constitutes an infrared safe quantity, so reliable predictions in perturbative QCD should be possible.

Let us, then, examine the first three terms in the perturbation series for R [21], in the limit of zero fermion mass (owing to the KLN theorem the quark mass could be suppressed without encountering infrared divergences)

$$
\begin{aligned}
R(t) \;=\; & \left(\textstyle\sum_f Q_f^2\right) \left\{ 1 + \frac{\alpha_s(t)}{4\pi} 3 C_2(R) \right. \\
& + \left(\frac{\alpha_s(t)}{4\pi}\right)^2 \left[-\tfrac{1}{2} C_2^2(R) + \left(\tfrac{123}{2} - 44\zeta(3)\right) C_2(G)\,C_2(R) \right. \\
& \left. \left. + n_{\mathrm{f}} \left(-22 + 16\zeta(3)\right) C_2^2(R)\, \tfrac{3}{8} \right] \right\},
\end{aligned}
\tag{70}
$$

where $\left(\sum_f Q_f^2\right)$ denotes the square of the electric charges of the fermions and $C_2(G), C_2(R)$ are colour factors of SU(3), As before, t represents the logarithm of the ratio of two energy scales, one being the total center-of-mass energy q^2 of the incoming electron-positron pair and the other some reference scale. Obviously, the running coupling constant should be evaluated to the same order as the cross section. Through $\alpha_s(t)$ this result thus depends on the number of quark flavours n_{f}.

The Riemann zeta function invariably appears in higher-loop calculations. It is defined by $\zeta(z) = \sum_{n=0}^{\infty} 1/n^z$. The specific value encountered above is $\zeta(3) \approx 1.2020569$. Using these values, the numerical coefficients for SU(3) with $n_{\mathrm{f}} = 5$ quark flavours yield

$$
R(t) = \left(\textstyle\sum_f Q_f^2\right) \left(1 + \frac{\alpha_s(t)}{\pi} + 1.409\left(\frac{\alpha_s(t)}{\pi}\right)^2 \right) .
\tag{71}
$$

We see that the coefficient in front of the $(\alpha_s(t)/\pi)^2$ is not too large, and the perturbative description is well-behaved. As is clear from Fig. 9 the result above should be used with great caution in the vicinity of

heavy flavour thresholds, because bound states appear in $R(t)$, which are not describable in finite order perturbation theory.

Let us next discuss two important, technical but generic issues that arise in the derivation of results such as (71) in the context of dimensional regularization. The first concerns the integration over phase space. Because the quantities that one calculates are infrared safe, infrared divergences must cancel at the end of the calculation. This requires one to determine the full cross section in n dimensions and take the limit $n \to 4$ only at the end. In particular, also the phase-space integrals should be evaluated in n dimensions. The second issue is that that the mass shell for massless particles poses problems in perturbative calculations. On-shell massless particles may split into perfectly collinear massless particles which then remain on their mass shells. This makes the mass shell ill-defined, and singularities appear, as we will see below. Moreover, there is a conceptual problem in that on-shell massless particles should correspond to asymptotic states. But in a confined theory such as QCD the massless partons do not correspond to *physical* states, which consist of massive hadrons. For infrared safe observables this is in fact not fatal to predictive power, but for calculations this is at least at an intermediate level a cumbersome feature. We now discuss these two aspects in turn.

In n dimensions the two-particle phase-space integral is defined by

$$I^{(n)}(s, m_3^2, m_4^2) = \int \frac{\mathrm{d}^{n-1} p_3}{(2\pi)^{n-1} 2\omega_3} \frac{\mathrm{d}^{n-1} p_4}{(2\pi)^{n-1} 2\omega_4} (2\pi)^n \, \delta^{(n)}(p_1 + p_2 - p_3 - p_4) \,, \tag{72}$$

where $s = -(p_1 + p_2)^2$ and $\omega_{3,4} = (\mathbf{p}_{3,4}^2 + m_{3,4}^2)^{1/2}$. We choose the centre-of-mass frame and decompose the full integral in one over the $n - 2$ angular variables (which we leave unperformed) and one over the length of the $(n-1)$-dimensional momentum vector $\mathbf{p}_3 = -\mathbf{p}_4$, which contains a delta function, and which we do perform. It yields

$$I^{(n)}(s, m_3^2, m_4^2) = \frac{1}{8\pi\sqrt{s}} \left[\frac{\lambda(s, m_3^2, m_4^2)}{16\pi^2 s} \right]^{\frac{n-3}{2}} \int \mathrm{d}\Omega_{CM} \,, \tag{73}$$

where $\lambda(x, y, z) = x^2 + y^2 + z^2 - 2xy - 2xz - 2yz$. As usual this expression must be combined with the square of the invariant amplitude to yield a cross section or decay rate. Assuming that the invariant amplitude depends only on the deflection angle θ_{CM} between $\mathbf{p}_1$ and $\mathbf{p}_3$, we can integrate over the remaining $n - 3$ angles, using the formula

$$\int \mathrm{d}\Omega_{CM} = \frac{2\pi^{-1+\frac{1}{2}n}}{\Gamma(\frac{1}{2}n - 1)} \int_0^\pi \mathrm{d}\theta_{CM} \left[\sin\theta_{CM} \right]^{n-3} \,, \tag{74}$$

where the integral on the left-hand side runs over all $n - 2$ angles, while the integral on the right-hand side contains only the deflection angle. Typically one needs the integral for $m_4 = 0$, reflecting emission of a massless particle. Replacing m_3 by m and introducing the variables $x = m^2/s$ and $y = \frac{1}{2}(1 + \cos\theta)$ the combined result for the phase-space integral reads

$$I^{(n)}(s, m^2, 0) = \frac{1}{8\pi} \left(\frac{m^2}{4\pi} \right)^{-2+\frac{1}{2}n} \frac{x^{2-\frac{1}{2}n}(1-x)^{n-3}}{\Gamma(\frac{1}{2}n - 1)} \int_0^1 \mathrm{d}y \, [y(1-y)]^{-2+\frac{1}{2}n} \,, \tag{75}$$

which has the correct dimension of a mass to the power $n - 4$. For $n > 2$ this expression is free of singularities. Corresponding expressions can be derived for multi-particle phase-space integrals. Formulae like (75) are obviously needed for calculating decay rates and cross sections in arbitrary dimension, the squared invariant amplitudes for which are then functions of y. The y-integral can be evaluated by using the relation

$$\int_0^1 \mathrm{d}y \, y^{p-1}(1-y)^{q-1} = B(p, q) = \frac{\Gamma(p)\Gamma(q)}{\Gamma(p+q)} \,, \tag{76}$$

where $B(p, q)$ is the Euler beta-function. Depending on the invariant amplitude of the process, infrared divergences can then appear as poles in the Gamma function, just as for virtual corrections.

The second issue involves the definition of the mass shell for massless particles in dimensional regularization. To this end we let us turn to the evaluation of a typical one-loop self-energy diagram This
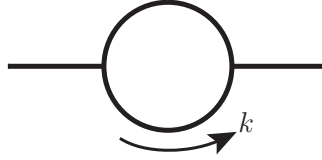

Fig. 14: A typical one-loop self-energy diagram

involves an integral of the type

$$I(k^2, m_1^2, m_2^2) = \frac{1}{(2\pi)^n} \int \frac{\mathrm{d}^n q}{\left((q + \frac{1}{2}k)^2 + m_1^2\right)\left((q - \frac{1}{2}k)^2 + m_2^2\right)}. \tag{77}$$

We imagine k to be the momentum of a massless particle that is off-shell and put $m_1 = m_2 = 0$. Using Feynman parameters one obtains

$$I(k^2, 0, 0) = \frac{\mathrm{i}}{16\pi^2} \Gamma(2 - \tfrac{1}{2}n)\left(\frac{k^2}{4\pi}\right)^{-2+\frac{1}{2}n} \int_0^1 \mathrm{d}x \, [x(1-x)]^{-2+\frac{1}{2}n}. \tag{78}$$

The x integral can be evaluated using (76) and becomes $(\Gamma(\tfrac{1}{2}n - 1))^2/\Gamma(n - 2)$, so that

$$I(k^2, 0, 0) = \frac{\mathrm{i}}{16\pi^2} \frac{\Gamma(2 - \tfrac{1}{2}n)\Gamma(\tfrac{1}{2}n - 1)^2}{\Gamma(n - 2)} \left(\frac{k^2}{4\pi}\right)^{-2+\frac{1}{2}n}. \tag{79}$$

This expression exhibits poles for both large and small values of n, signaling ultraviolet and infrared singularities respectively. The last factor in (79) shows that the result is in fact ambiguous when approaching the mass shell, $k^2 \to 0$. When considering infrared divergences one assumes $n > 4$ so that the integral is in fact zero on the mass shell. Hence, one can omit self-energy loop corrections for massless external particles. In fact, their zero contribution can be shown to be due to a perfect cancellation between a UV divergence and a collinear divergence. However, one must still include the UV counterterms on the external lines. The sum of the two is then in fact the collinear divergence, which in turn will cancel in a calculation of infrared safe quantities.

3.4 Jets

Besides event shapes there is another important class of infrared safe observables that uses the notion of a jet. In high-energy e^+e^- collisions the photon couples directly to a quark-antiquark pair, and the latter are then produced back-to-back in the e^+e^- cm frame, with high momentum. As the quarks begin to fly apart they undergo the complicated fragmentation or hadronization process that leads to colourless hadronic final states. One could therefore expect the final hadrons to follow the line of flight of the quarks to produce two streams of back-to-back particles, as depicted in Fig. 15. The angular distribution of the quarks is $1 + \cos^2\theta$, where θ is the polar angle between a quark and the beam direction. The angular distribution of the hadrons should then have roughly the same dependence on $\cos\theta$. Indeed this is the case.

In the context of considering the effect of higher orders, one may ask how this angular distribution is changed by the emission of an additional gluon. Remember that the contribution due to gluon emission contains soft and collinear divergences, to be cancelled via the KLN theorem. Intuitively, one would
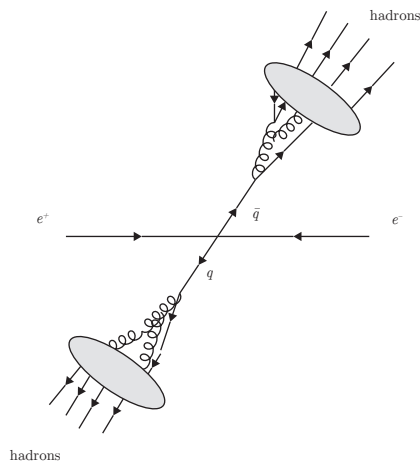
Fig. 15: Two jets of hadrons arising from quark-antiquark production in an e^+e^- collision. The blobs represent the hadronization process.

think that one does not need to integrate over *all* possible gluon emission energies and angles; if we only integrate the gluon emission rate over a small angle close to the quark or antiquark direction the collinear divergence should already cancel with the divergence contained in the virtual contribution, leaving a contribution depending on the size of the angular range. Also, if we allow a (very) soft gluon to be emitted and add this contribution to that from the virtual contribution we expect that the infrared divergences will cancel too. The result will then still depend on one angle and one energy. One could therefore define a two-jet event as one where almost all of the energy, namely $(1-\epsilon)\sqrt{s}$, is contained in two small cones of semi-angle δ, where ϵ and δ are fixed, and can be reasonably large, as shown in Fig. 16. An explicit calculation of the corrections to the (anti)quark angular distribution shows that the
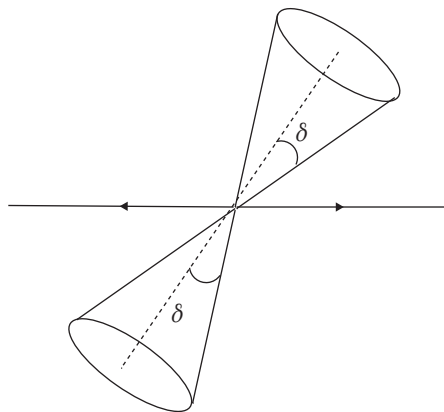
Fig. 16: Two jets defined by an opening angle δ

angular distribution is still proportional to $1 + \cos^2\theta$ but the coefficient in front is modified by the factor

$$1 - \frac{\alpha_s(q^2)C_2(R)}{\pi}\left[(4\ln 2\epsilon + 3)\ln\delta + \pi^2/3 - 5/2 + 0(\epsilon) + 0(\delta)\right]. \tag{80}$$

As one would expect, if one would take the limit ϵ and $\delta \to 0$ divergences the divergences show up again in this factor, so one must be careful to choose ϵ or δ small but large enough that the α_s correction in (80) is still relatively small. In this way, due to Sterman and Weinberg [22], the jet angular distribution is well-defined and has been successfully compared with experiment.

One may now generalize the definition of a jet such that singularities still cancel, but that their definitions are more easily implemented in both experimental measurements and theoretical calculations, the latter in the form of a Monte Carlo program. To this end one constructs an iterative algorithm for combining the measured hadrons (or computed partons) into jets. The starting point of such an algorithm is a list of particles (hadrons or partons) with their energies and angles. For example, in one algorithm, for all particle pairs i and j one then calculates the quantity $y_{ij} = 2E_iE_j(1 - \cos\theta_{ij})/s$. All y_{ij}'s are now compared with a chosen value y_{cut}. For each y_{ij} that is smaller than y_{cut} the two momenta of particles i and j are combined according some chosen prescription, for instance "add the four-momenta". Particles i and j are then removed from the list, but their combination is returned to the list as a new 'pseudoparticle'. The procedure is repeated until no two (pseudo)particles have an y_{ij} that is smaller than y_{cut}. This subdivides the experimentally measured or theoretically simulated events into a number of clustered jets, of which one can study the properties. One should be aware however that not all algorithms are infrared safe for all collider types.

This concludes our discussion of higher orders for collider processes with quarks and gluons only in the final state. We now turn to the case where there are strongly interacting particles in the initial state as well.

3.5   The Drell-Yan process

The Drell-Yan process [23] is, and has been, an important reaction in particle physics. It involves the production of a lepton-antilepton pair in proton-(anti)proton collisions,

$$p + \bar{p}/p \to l + \bar{l} + X$$

where X denotes the rest of the final state. Leptons are relatively easy to detect and through this reaction a number of important discoveries such as of the J/Ψ and the Υ mesons (and therefore of the charm and bottom quarks), and of the W and Z vector bosons were made. From a theoretical point of view, its QCD corrections are prototypical for any high-energy cross section with initial state hadrons, and it is from this perspective that we shall discuss these corrections here. For simplicity we will only examine the QCD corrections to the single differential cross section in the lepton pair invariant mass Q, i.e. $d\sigma/dQ^2$. Therefore the process is inclusive in all the hadron final states, which renders the KLN theorem for the QCD corrections in principle operative (as we will see, only for the final state). To calculate the corrections we consider the reaction at the partonic level, where the lowest order approximation only involves only quark-antiquark annihilation into a virtual photon, which then couples to the lepton-antilepton pair. The total cross section for quark-antiquark annihilation in the reaction $q(p_1) + \bar{q}(p_2) \to l(q_1) + \bar{l}(q_2)$ can be computed as

$$\sigma_{q\bar{q}}^{(0)}(\hat{s}) = \frac{1}{4N_c^2}\frac{1}{2\hat{s}}\int\frac{d^3q_1}{(2\pi)^32\omega_1}\int\frac{d^3q_2}{(2\pi)^32\omega_2}(2\pi)^4\delta(p_1+p_2-q_1-q_2)\sum|\mathcal{M}|^2\,, \qquad (81)$$

where $\hat{s} = -(p_1+p_2)^2 = -(q_1+q_2)^2 = Q^2$, the sum is over all initial and final spin and colour indices, and initial state spins and colours are averaged over.

We remind the reader that the hadronic cross section follows by convoluting this result with partonic densities in the incoming hadrons, as in sections 2.2 and 3.1. We write $\hat{s} = \xi_1\xi_2 s$, where $\xi_{1,2}$ are parton momentum fractions and s is the collider cm energy squared. Also we introduce the variable $\tau = Q^2/s$ so that

$$\frac{d\sigma_{pp}^{(0)}(\tau)}{dQ^2} = \sum_{i,j}\int_{\xi_{1,\min}}^1 d\xi_1\int_{\xi_{2,\min}}^1 d\xi_2\, f_{i/p}(\xi_1)f_{j/p}(\xi_2)\frac{d\sigma_{ij}^{(0)}(\xi_1,\xi_2)}{dQ^2}\,, \qquad (82)$$

where the f's are the parton distribution functions for the quarks and antiquarks in the proton and antiproton. The sum runs over all quarks and antiquarks in both the proton and antiproton, while $\xi_{1,\min} = \tau$, and $\xi_{2,\min} = \tau/\xi_1$. We return to this formula towards the end of this section.

The only Feynman diagram to compute is the one photon exchange diagram for which the square of the amplitude yields

$$\sum |\mathcal{M}|^2 = e^4 Q_f^2 \text{Tr}(\gamma_\mu \slashed{p}_1 \gamma_\nu \slashed{p}_2) \text{Tr}(\gamma_\mu \slashed{q}_2 \gamma_\nu \slashed{q}_1) \frac{1}{\hat{s}^2} \,. \tag{83}$$

The charge of quark flavour f is $Q_f e$, and the final trace is over the unit N_c-dimensional matrix labelled by the colour indices. It is not difficult to work out (83). Moreover the integration over the lepton trace in (81) can be done by applying the so-called Lenard identity (here given in n dimensions)

$$\int \mathrm{d}^n q_1 \, \delta(q_1^2) \int \mathrm{d}^n q_2 \, \delta(q_2^2) \, \delta^n(q - q_1 - q_2) \, q_1^\mu q_2^\nu =$$
$$\left(\frac{-q^2}{4}\right)^{(n-4)/2} \frac{\pi^{(n-1)/2}}{\Gamma((n+1)/2)} \frac{1}{32} (q^2 \eta^{\mu\nu} + 2 q^\mu q^\nu) \,. \tag{84}$$

The final result, in 4 dimensions,

$$\sigma_{q\bar{q}}^{(0)}(\hat{s}) = \frac{4\pi\alpha^2}{3 N_c \hat{s}} \,, \tag{85}$$

is only a function of $\hat{s}$. The differential cross section with respect to $Q^2 = -(q_1 + q_2)^2$ can now be derived using

$$\frac{d\sigma_{q\bar{q}}^{(0)}(Q^2)}{dQ^2} = \left[\frac{4\pi\alpha^2}{3 N_c (Q^2)^2}\right] \delta\left(1 - \frac{Q^2}{\hat{s}}\right) \,. \tag{86}$$

Indeed, as a check

$$\sigma_{q\bar{q}}^{(0)}(\hat{s}) = \int \frac{d\sigma_{q\bar{q}}^{(0)}(Q^2)}{dQ^2} dQ^2 = \frac{4\pi\alpha^2}{3 N_c} \int \frac{dQ^2}{(Q^2)^2} \delta\left(1 - \frac{Q^2}{\hat{s}}\right) = \frac{4\pi\alpha^2}{3 N_c \hat{s}} \,. \tag{87}$$

Note that (86) is no longer a function but a distribution as it is proportional to a δ-function with argument proportional to $\hat{s} - Q^2$. Therefore as far as the lowest order formula is concerned we can write either $d\sigma_{q\bar{q}}^{(0)}/dQ^2$ or $d\sigma_{q\bar{q}}^{(0)}/d\hat{s}$. The expression in square brackets in (86) we will refer to as $\sigma_\gamma^{(0)}$.

For the calculation of the QCD corrections we would prefer not to include the part of the diagram where the photon decays into leptons, which is common to all diagrams to any order in QCD perturbation theory. One can account for that by computing the ratio K of the squared amplitude for the process $q(p_1) + \bar{q}(p_2) \to \gamma^*(q)$ ($q^2 = -Q^2$) and the $q(p_1) + \bar{q}(p_2) \to l\bar{l}(q)$ at lowest order as follows

$$\sigma^{(0)}(l\bar{l}) = K \sigma^{(0)}(\gamma^*) \,. \tag{88}$$

The factor K can be computed in dimensional regularization. It is valid to all orders in perturbative QCD, because it only involves the electroweak final state. We shall not give the expression here, but thanks to (88) we can now suffice with computing the cross section for γ^* production.

Let us now evaluate the next order corrections to (82). We consider the quark-antiquark channel and calculate the processes involving the virtual corrections to the Born reaction, and the counterterm contributions. In Fig. 17 we show these, and also contributions to the quark-gluon channel, which are typically smaller. The Feynman diagrams must be evaluated in n-dimensions and a colour matrix must be added at the quark gluon vertex. We split the correction as follows

$$\frac{d\sigma_{q\bar{q}}^{(1)}}{dQ^2} = \frac{d\sigma_{q\bar{q}}^{(1)}}{dQ^2}\bigg|_{\text{virtual}} + \frac{d\sigma_{q\bar{q}}^{(1)}}{dQ^2}\bigg|_{\text{real}} \,. \tag{89}$$

Incidentally, we use n-dimensional regularization also for infrared divergences, and consider the quark and anti-quark to be massless and on-shell. To see how this affects the loop integrals, let present the
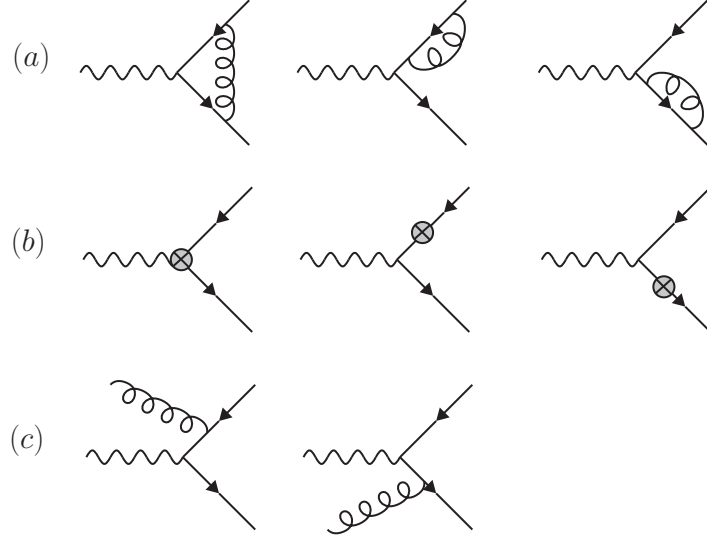
QCD

Fig. 17: The Feynman diagrams for the first order QCD corrections to the partonic Drell-Yan reaction in the quark-antiquark collisions producing an off-shell photon. Shown are (a) loop contributions (b) counterterm contributions, and (c) radiative graphs. The leptons into which the photon decays are not shown. Time runs from right to left in this figure.

result for $J(t,0,0)$, the scalar vertex function, where $t = -Q^2$. It occurs in the first diagram in Fig. 17a and is defined by

$$J(t,0,0) = \frac{1}{(2\pi)^n} \int \frac{d^n q}{((p+q)^2)((p'+q)^2)(q^2)} \,, \tag{90}$$

where $p^2 = p'^2 = 0$. The integral may be computed using standard methods in dimensional regularization. The result is

$$J(t,0,0) = i(4\pi)^{-\frac{n}{2}} \left(\frac{-t}{\mu^2}\right)^{\frac{n-6}{2}} (\mu^2)^{\frac{n-6}{2}} \frac{\Gamma(3-n/2)\Gamma^2(n/2-1)}{\Gamma(n-3)} \times \frac{4}{(n-4)^2} \,, \tag{91}$$

where we have inserted a mass scale μ to make the integral have the correct dimension in n space-time dimensions. Notice that the last factor shows a double pole in $n-4$, arising from the overlap of an infrared and a collinear singularity, when the virtual gluon both becomes soft and collinear to either the incoming quark or anti-quark. Also a two-denominator integral occurs when including numerator factors in the leftmost graph of Fig. 17a. It reads

$$I(k^2,0,0) = \frac{1}{(2\pi)^n} \int \frac{d^n q}{((q+\frac{1}{2}k)^2)((q-\frac{1}{2}k)^2)} \,, \tag{92}$$

with $k^2 = Q^2$, and the result of doing the integral is

$$I(-t,0,0) = i(4\pi)^{-\frac{n}{2}} \left(\frac{-t}{\mu^2}\right)^{\frac{n-4}{2}} (\mu^2)^{n/2-2} \frac{\Gamma(3-n/2)\Gamma^2(n/2-1)}{\Gamma(n-2)} \times \frac{2}{4-n} \,. \tag{93}$$

Again it features a pole in $n-4$. Note that it is not always obvious from superficial inspection to see whether a $1/(n-4)$ pole has an ultraviolet, infrared or collinear origin. However, in general, a UV divergence occurs after the n-dimensional integral over the loop momentum, while the IR and collinear singularities arise from the integrations over the Feynman parameters. The full result for the vertex graph in Fig. 17a including numerator factors, reads, after substituting $n = 4 + \varepsilon$

$$\Lambda(p',p) = e^3 \gamma_\mu i(4\pi)^{-2} \left(\frac{-t}{4\pi\mu^2}\right)^{\varepsilon/2} (\mu^2)^{\varepsilon/2} \frac{\Gamma(1-\varepsilon/2)\Gamma^2(1+\varepsilon/2)}{\Gamma(2+\varepsilon)}$$

$$\times \left[\frac{8}{\varepsilon^2} + \frac{2}{\varepsilon} + 1 \right] . \tag{94}$$

Besides the vertex graph we should also consider other virtual contributions, namely the one-loop gluon self-energy corrections to the incoming on-shell quark and anti-quark, as well as contributions from counterterms. However, none of these contribute to the present calculation. To see this, consider first the self-energy contribution for an on-shell massless fermion

$$\Sigma(p) = -\mathrm{i}p\!\!\!/ - g^2 \int \frac{d^n q}{(2\pi)^n} \frac{(-\mathrm{i}p\!\!\!/)(-\mathrm{i}p\!\!\!/ - \mathrm{i}q\!\!\!/)(-\mathrm{i}p\!\!\!/)}{(p+q)^2 q^2} . \tag{95}$$

Using $p^2 = 0$ this reduces to

$$\Sigma(p) = -\mathrm{i}p\!\!\!/ - \mathrm{i}p\!\!\!/ g^2 \int \frac{d^n q}{(2\pi)^n} \frac{2p \cdot q}{(p+q)^2 q^2} . \tag{96}$$

Writing

$$2p.q = (q+p)^2 - q^2 , \tag{97}$$

we see that the $\mathcal{O}(g^2)$ correction vanishes, by the rules of dimensional regularization, in which scaleless loop integrals may be consistently set to zero.

Besides the loop diagrams also the $\mathcal{O}(\alpha_s)$ counterterms in the Lagrangian must be included in the virtual contributions, shown in Fig. 17b. This is so even when a loop graph itself is zero, such as for the quark and antiquark self energy corrections. There are in fact three counterterm diagrams in the Lagrangian, indicated in Fig. 17b. The quark colours, when including initial quark colour averaging, here merely lead to a common factor $C_2(R)/N_c$ for all three contributions. The counterterm contributions for the self energy corrections must be included with a factor $1/2$ due to the need to normalize the scattering amplitude using the residue at the pole. When one does this, the counterterm contributions cancel agains each other.

So, remarkably, in the end only the triangle diagram contributes to the virtual contribution, and we have the result

$$\begin{aligned}
\frac{d\sigma_{q\bar{q}}^{(1)}}{d\hat{s}}\Big|_{\text{virtual}} &= \sigma_\gamma^{(0)} Q_f^2 \frac{1}{2\pi} C_2(R) \left(\frac{4\pi\mu^2}{\hat{s}} \right)^{-\varepsilon/2} \frac{\Gamma(1+\varepsilon/2)}{\Gamma(1+\varepsilon)} \\
&\quad \times \left[-\frac{8}{\varepsilon^2} + \frac{6}{\varepsilon} - 8 + \frac{2\pi^2}{3} + O(\varepsilon) \right] \delta(1-x) ,
\end{aligned} \tag{98}$$

where $x = \hat{s}/s$. We have used the expansion $\Re(-1)^{\varepsilon/2} = \Re \exp(\varepsilon \mathrm{i}\pi/2) \simeq 1 - \pi^2 \varepsilon^2/8$. (We dropped the imaginary part $\varepsilon \mathrm{i}\pi/2$ since we only need the real part of the virtual contributions in the interference with the Born diagram.) The other π^2 terms in (98) follow from expansion of the Gamma functions

$$\Gamma(1-\varepsilon/2)\Gamma(1+\varepsilon/2) = 1 + \frac{\pi^2}{6}\frac{\varepsilon^2}{4} + O(\varepsilon^3) . \tag{99}$$

Next we must consider the real gluon bremsstrahlung graphs which as far as the partonic channel is concerned contribute to the two-to-two body scattering cross section for $q(p_1) + \bar{q}(p_2) \to \gamma(q) + g(k)$. Now since $\hat{s} = -(p_1 + p_2)^2$ is the square of the total centre-of-mass energy and $Q^2 = -q^2 = (q_1 + q_2)^2$ is the invariant mass of the dilepton pair then $\hat{s} \neq Q^2$. It is convenient to rewrite the Mandelstam invariants in terms of the two variables $x = Q^2/s$ and $y = (1 + \cos\theta)/2$. This yields the relations $s = Q^2/x$, $\hat{t} = -Q^2(1-x)(1-y)/x$, and $\hat{u} = -Q^2(1-x)y/x$. In this bremsstrahlung correction we will have contributions from the region $x = Q^2/s < 1$, whereas the virtual and counterterm diagrams only contribute at $x = 1$.

30

Let us introduce a convenient shorthand notation for an l-particle n-dimensional phase-space measure

$$\int_{\text{PS}l} dq_1 \cdots dq_l = (2\pi)^{n+l(1-n)} \int \frac{d^{n-1}q_1}{2q_1^0} \cdots \frac{d^{n-1}q_l}{2q_l^0} \, \delta^{(n)}(P - \sum_i^l q_i) \,, \tag{100}$$

where we have left the masses of each particle unspecified. We need to evaluate

$$\frac{d\sigma_{q\bar{q}}^{(1)}}{dQ^2}|_{\text{real}} = \frac{1}{8N_c^2\hat{s}} \int_{\text{PS3}} dk dq_1 dq_2 \delta^{(n)}(p_1 + p_2 - k - q_1 - q_2) \sum |\mathcal{M}|^2 \,, \tag{101}$$

where $\mathcal{M}$ is the matrix element of the two-to-three body reaction $q(p_1) + \bar{q}(p_2) \to l(q_1) + \bar{l}(q_2) + g(k)$. The three-body phase-space integral can be factorized into two two-body phase-space integrals by inserting

$$1 = \int \frac{dQ^2}{2\pi} \int d^n q \delta^{(n)}(q - q_1 - q_2)(2\pi)\delta(q^2 - Q^2) \,, \tag{102}$$

into the integral. Then we write the integral over dq as a $n-1$ dimensional integral using $\delta(q^2 - Q^2)$. If we use the notation $p = p_1 + p_2$ then the integrals can be written as

$$\frac{d\sigma_{q\bar{q}}^{(1)}}{dQ^2}|_{\text{real}} = \frac{1}{16\pi N_c^2\hat{s}} \int_{\text{PS2}} dk dq \int_{\text{PS2}} dq_1 dq_2 \sum |\mathcal{M}|^2 \,, \tag{103}$$

where the first phase space-integral has a δ-function $\delta^{(n)}(p - q - k)$ and the second one $\delta^{(n)}(q - q_1 - q_2)$. This enables us again to factor off the decay of the γ^* into the lepton-antilepton pair, leading to the equation (88) but now also for the real emission contribution.

The square of the partonic matrix element summed over all initial and final spins and polarizations can then be written in terms of the Mandelstam invariants for the reaction $q(p_1) + \bar{q}(p_2) \to \gamma(q) + g(k)$. These we will call $s = -(p_1+p_2)^2$, $t = -(p_1-k)^2$, and $u = -(p_2-k)^2$, which satisfy $s+t+u = -Q^2$ Note that a term involving a new mass scale μ will be required because the QCD coupling constant g has mass dimension $(4-n)/2$ in n-dimensions. There is no need to write an n-dimensional generalization for the QED coupling constant so we can keep e in four dimensions. The answer in terms of $n = 4 + \varepsilon$ reads

$$\begin{aligned}
\frac{d\sigma_{q\bar{q}}^{(1)}}{d\hat{s}}|_{\text{real}} &= \sigma_\gamma^{(0)} Q_f^2 \frac{1}{2\pi} C_2(R) \Big(\frac{4\pi\mu^2}{\hat{s}}\Big)^{-\varepsilon/2} \frac{\Gamma(1+\varepsilon/2)}{\Gamma(1+\varepsilon)} \frac{4}{\varepsilon} \\
&\quad \times \Big[2x^{1-\varepsilon/2}(1-x)^{-1+\varepsilon} + x^{-\varepsilon/2}(1-x)^{1+\varepsilon} \Big] \,.
\end{aligned} \tag{104}$$

A collinear pole in ε resulting from the angular integral is now explicit. If we integrate over the variable x, which we must to form the hadronic cross section, a second pole will appear from the region $x \to 1$. That is the infrared pole. After integration there are therefore double pole terms from overlapping divergences and single pole terms from the either soft or the collinear singularities. Using the KLN theorem to cancel these pole terms against the contributions from the virtual graphs, which only exist for $x = 1$ would be convenient, especially before doing the integration over x. So, we would need a way of combining the contributions from the virtual and bremsstrahlung graphs as functions of x.

One way to do this is to split off a small piece in (104) between $x = 1 - \delta$ and $x = 1$ and call this the "soft" bremsstrahlung piece. In this small range near unity one can substitute $x = 1$ whenever this is allowed and simply do the x integral yielding terms in $\ln\delta$ as well as poles in ε. These pieces can then be added to the contributions from the virtual graphs. The remaining "hard" bremsstrahlung integral over the range 0 to $1 - \delta$ is finite, and can be take in $n = 4$ dimensions., Integration will then yield a term involving $\ln\delta$ which should cancel with the corresponding $\ln\delta$ term in the virtual graphs. This method is called the phase-space slicing method.

We will employ another method. We would like a relation that expresses the double pole terms immediately in terms of $\delta(1-x)$. Such a relation does exist but in the sense of distributions, namely when multiplied by a smooth function $F(x)$ and integrated between 0 and 1 (like the δ-function itself). Assume the function $F(x)$ has a Taylor expansion near $x = 1$ so we can write $F(x) = F(1) + F(x) - F(1)$, where the difference between the last two terms is proportional to the finite derivative of $F(x)$ at $x = 1$. Let us consider therefore

$$\int_0^1 dx \, \frac{F(x)}{(1-x)^{1-\varepsilon}} = F(1) \int_0^1 dx \, \frac{1}{(1-x)^{1-\varepsilon}} + \int_0^1 dx \, \frac{F(x) - F(1)}{(1-x)^{1-\varepsilon}} . \tag{105}$$

The first integral yields $F(1)\varepsilon^{-1}$. We can rewrite this again as an integral over dx with the argument $\delta(1-x)$. In the second integral we can expand the denominator so it yields

$$\int_0^1 dx \, \frac{F(x) - F(1)}{(1-x)^{1-\varepsilon}} = \int_0^1 dx \, \frac{F(x) - F(1)}{(1-x)}$$
$$+ \varepsilon \int_0^1 dx \, [F(x) - F(1)] \frac{\ln(1-x)}{(1-x)} + O(\varepsilon^2) , \tag{106}$$

near $\varepsilon = 0$. Therefore we have the identity

$$\int_0^1 dx \, \frac{F(x)}{(1-x)^{1-\varepsilon}} = \frac{1}{\varepsilon} \int_0^1 dx \, F(x)\delta(1-x) + \int_0^1 dx \, \frac{F(x) - F(1)}{1 - x}$$
$$+ \varepsilon \int_0^1 dx [\, F(x) - F(1)] \frac{\ln(1-x)}{1 - x} + O(\varepsilon^2) . \tag{107}$$

This we will write in shorthand notation as

$$\frac{1}{(1-x)^{1-\varepsilon}} = \frac{1}{\varepsilon}\delta(1 - x) + \left[\frac{1}{1 - x} \right]_+ + \varepsilon \left[\frac{\ln(1-x)}{1 - x} \right]_+ + O(\varepsilon^2) , \tag{108}$$

where on the right hand side we see so-called "plus" distributions. Note that this result is exact for a lower integration limit $x = 0$. If the lower limit is not zero then there are additional finite terms involving logarithms of this lower limit.

Our final result for the gluon radiation graphs therefore follows by expanding the terms in the square bracket in (104) in powers of ε and using (108). We find

$$\frac{d\sigma_{q\bar{q}}^{(1)}}{d\hat{s}}\Big|_{\text{real}} = \sigma_\gamma^{(0)} Q_f^2 \frac{1}{2\pi} \left(\frac{4\pi\mu^2}{\hat{s}} \right)^{-\varepsilon/2} \frac{\Gamma(1 + \varepsilon/2)}{\Gamma(1 + \varepsilon)} \left[\frac{8}{\varepsilon^2}\delta(1 - x) \right.$$
$$+ \frac{4}{\varepsilon}(1 + x^2) \left[\frac{1}{1 - x} \right]_+ + 4(1 + x^2) \left[\frac{\ln 1 - x}{1 - x} \right]_+$$
$$\left. - 2(1 + x^2) \frac{\ln x}{1 - x} + O(\varepsilon) \right] . \tag{109}$$

Now we have isolated the term in $\delta(1 - x)$ containing the double pole we see that it cancels the corresponding term from the virtual graphs in (98). These are the overlap terms containing both soft and collinear divergences and they cancel as expected from the KLN theorem. The single pole term in ε however cannot possibly cancel against a virtual contribution, as it is not purely a $\delta(1 - x)$ term. Therefore we are left with an uncancelled collinear singularity.

Finally we can finally sum (98) and (109) and find

$$\frac{d\sigma_{q\bar{q}}^{(1)}}{d\hat{s}} = \sigma_\gamma^{(0)} Q_f^2 \frac{1}{2\pi} C_2(R) \left(\frac{4\pi\mu^2}{\hat{s}} \right)^{-\varepsilon/2} \frac{\Gamma(1 + \varepsilon/2)}{\Gamma(1 + \varepsilon)}$$

$$\times \left\{ \frac{4}{\varepsilon}\left((1+x^2)\left[\frac{1}{1-x}\right]_+ + \frac{3}{2}\delta(1-x)\right) + 4(1+x^2)\left[\frac{\ln(1-x)}{1-x}\right]_+ \right.$$
$$\left. -2(1+x^2)\frac{\ln x}{1-x} + (4\zeta(2)-8)\delta(1-x) + O(\varepsilon) \right\}, \tag{110}$$

with $\zeta(2) = \pi^2/6$. The remaining pole term in ε implies that the KLN theorem is inoperable when there are collinear singularities in the initial partonic state. How are we then going to make sense of this result?

First, let us observe that if one expands all functions in (110) in ε one finds

$$\frac{d\sigma_{q\bar{q}}^{(1)}}{d\hat{s}} = \sigma_\gamma^{(0)} Q_f^2 \frac{1}{2\pi} C_2(R) 2\left(\frac{2}{\varepsilon} - \ln 4\pi + \gamma_E\right)\left((1+x^2)\left[\frac{1}{1-x}\right]_+\right.$$
$$\left. + \frac{3}{2}\delta(1-x)\right) + \mathcal{O}(\varepsilon^0)$$
$$= \sigma_\gamma^{(0)} Q_f^2 \frac{1}{2\pi} C_2(R) 2\left(\frac{2}{\varepsilon} - \ln 4\pi + \gamma_E\right)\left[\frac{1+x^2}{1-x}\right]_+ + \mathcal{O}(\varepsilon^0). \tag{111}$$

Next, we realize that this expression should be substituted into the convolution (82). At this point one may, in a sense, *renormalize* (or rather: *factorize*) the parton distributions in (82) as

$$f_{q/A}(\xi) = \int_0^1 dz \int_0^1 dy\, f_{q/A}(y, \mu_F)\Phi_{qq}^{-1}(z, \mu_F)\delta(\xi - zy), \tag{112}$$

with μ_F the factorization scale, introduced in the previous section, and Φ_{qq} a transition function. This fucntion is analogous to the Z-factors for UV renormalization in section 2.3.2.

To first order, the above relation can be written as

$$f_{q/A}(\xi) = f_{q/A}(\xi, \mu_F) - \int_\xi^1 \frac{dz}{z} f_{q/A}\left(\frac{\xi}{z}, \mu_F\right)$$
$$\times \left\{ \frac{\alpha_s(\mu)C_2(R)}{2\pi} \frac{1}{\varepsilon}\left(\frac{4\pi\mu^2}{\mu_F^2}\right)^{-\varepsilon/2}\left[\frac{1+z^2}{1-z}\right]_+ \right\}. \tag{113}$$

Collecting terms we see indeed, as we announced, the collinear singularities cancel after renormalization of the parton distribution by the transition functions, leaving a finite remainder. The final result is

$$\frac{d\sigma_{q\bar{q}}^{(1)}}{d\hat{s}} = \sigma_\gamma^{(0)} Q_f^2 \frac{1}{2\pi} C_2(R)$$
$$\times \left\{ 2\ln\left(\frac{Q^2}{\mu_F^2}\right)\left[\frac{1+z^2}{1-z}\right]_+ + 4(1+x^2)\left[\frac{\ln(1-x)}{1-x}\right]_+ \right.$$
$$\left. -2(1+x^2)\frac{\ln x}{1-x} + (4\zeta(2)-8)\delta(1-x) \right\}. \tag{114}$$

This result we can now insert into (82), use NLO PDF's and predict the Drell-Yan cross section.

3.6 Factorization

The fact that the initial state divergences cancel through a renormalization/factorization of the PDFs, as in (112) is a one-loop manifestation of the QCD factorization theorem [8]. This is the full QCD generalization of the parton model formula, and states that for IR safe cross sections, the initital state collinear divergences can be consistently removed in this way. The consistency lies in the fact that this factorization does not depend on the process, i.e. that it is *always the same set* of Φ_{ij} functions, computed to the appropriate order. This aspect is the one that preserves predictive power: indeed if we

devote certain set of observables to infer the PDF's, as we discussed extensively in section 3.1, we can use these for any other reaction and predict the outcome. To cover the details of the factorization proof for the inclusive Drell-Yan cross section would take us too far. However, it is worthwhile to point out that factorization proofs for other observables (differential cross sections, cross sections near phase space edges, or with vetoed phase space regions) are an active and important area of research [24, 25].

4 Modern methods

In this section I discuss a number of modern methods in the application of perturbative QCD, focussing mostly on spinor helicity techniques, and the essence of the recent "NLO revolution". For lack of space I shall not discuss the enormous strides made in Monte Carlo methods and applications in recent years.

4.1 Spinor methods, recursion relations

At high center-of-mass energies, final states produced in particle colliders usually contain many more than two particles. Calculations of such processes are long and complicated because one must write down the individual amplitudes for the Feynman graphs and then square the result, which involves all the cross products between them. In this section we describe methods to shorten these calculations by using clever choices for external line polarizations and simplifications owing to the masslessness of the particles. We also note that at high energies most of the final state particles can be considered massless, so that in order to represent fermions we may make use of a chiral spinor basis because at large momenta chirality and helicity are related. In that case many external helicities configurations are in fact simply not allowed by parity invariance. There are moreover many relations among the amplitudes so the number of amplitudes to compute is not overly large. An interesting thing to note is that by specifying all external line quantum numbers, the expression for each helicity amplitude is simply a complex number. This can then obviate the need for analytically spin-summing over the absolute value squared of the invariant amplitudes, and allow this task to be handled by a computer, reducing the amount of laborious computation further.

Let us see how the use of spinors of definite chirality or helicity can significantly simplify the calculation of Feynman diagrams with massless fermions and gauge bosons. We will also use the freedom of gauge choice for external gauge fields to maximal advantage. I try to give a reasonably explicit and self-contained presentation of these helicity spinor methods. We shall need the Dirac gamma matrices γ^μ, γ^5 and the charge conjugation matrix C in the Weyl basis:

$$\gamma^k = \begin{pmatrix} 0 & \sigma_k \\ \sigma_k & 0 \end{pmatrix}, \quad k = 1, 2, 3; \qquad \gamma^0 = \begin{pmatrix} 0 & \mathbb{1} \\ -\mathbb{1} & 0 \end{pmatrix},$$

$$\gamma^5 = \gamma_5 = -\mathrm{i}\gamma^0\gamma^1\gamma^2\gamma^3 = \begin{pmatrix} \mathbb{1} & 0 \\ 0 & -\mathbb{1} \end{pmatrix}, C = \mathrm{i}\gamma^1\gamma^3 = \begin{pmatrix} \sigma_2 & 0 \\ 0 & \sigma_2 \end{pmatrix}. \tag{115}$$

The explicit form of the u and v spinors in this basis is

$$u(\boldsymbol{P}, \xi) = \frac{\mathrm{e}^{\mathrm{i}\pi/4}}{\sqrt{2(m + \omega(\boldsymbol{P}))}} \begin{pmatrix} \left[(m + \omega(\boldsymbol{P}))\mathbb{1} - \boldsymbol{P} \cdot \boldsymbol{\sigma}\right]\xi \\ -\mathrm{i}\left[(m + \omega(\boldsymbol{P}))\mathbb{1} + \boldsymbol{P} \cdot \boldsymbol{\sigma}\right]\xi \end{pmatrix},$$

$$v(\boldsymbol{P}, \bar{\xi}) = \frac{\mathrm{e}^{\mathrm{i}\pi/4}}{\sqrt{2(m + \omega(\boldsymbol{P}))}} \begin{pmatrix} -\left[(m + \omega(\boldsymbol{P}))\mathbb{1} - \boldsymbol{P} \cdot \boldsymbol{\sigma}\right]\bar{\xi} \\ -\mathrm{i}\left[(m + \omega(\boldsymbol{P}))\mathbb{1} + \boldsymbol{P} \cdot \boldsymbol{\sigma}\right]\bar{\xi} \end{pmatrix}, \tag{116}$$

with $\bar{\xi} = \mathrm{i}\sigma_2\xi^*$. The momentum $P^\mu = \omega(\boldsymbol{P}), \boldsymbol{P}$ is the on-shell momentum of the fermion, and the charge conjugation matrix is used to define the charge conjugate spinor

$$\psi^{\mathrm{c}} \equiv C^{-1}\bar{\psi}^{\mathrm{T}}. \tag{117}$$

Having this explicit form will allow us to derive a number of useful identities which make calculations with massless particle must more efficient. The following identity,

$$\left[(m + \omega(\boldsymbol{P}))\mathbb{1} \pm \boldsymbol{P} \cdot \boldsymbol{\sigma}\right]^2 = 2\big(m + \omega(\boldsymbol{P})\big)\left[\omega(\boldsymbol{P})\,\mathbb{1} \pm \boldsymbol{P} \cdot \boldsymbol{\sigma}\right] \tag{118}$$

suggests that there is a more systematic way to write these spinors. To see this let us define σ_μ and $\bar{\sigma}_\mu$ as four-vector arrays of 2×2 hermitian matrices,

$$\sigma_\mu = (-\mathbb{1}, \boldsymbol{\sigma}), \quad \bar{\sigma}_\mu = (-\mathbb{1}, -\boldsymbol{\sigma}), \quad (P \cdot \sigma)(P \cdot \bar{\sigma}) = -P^2 = m^2\,. \tag{119}$$

In terms of these matrices one has the identities

$$(\mathrm{i}\slashed{P} \pm m) = \begin{pmatrix} \pm m\mathbb{1} & \mathrm{i}P \cdot \sigma \\ -\mathrm{i}P \cdot \bar{\sigma} & \pm m\mathbb{1} \end{pmatrix},$$

$$-P^\mu \sigma_\mu = \omega(\boldsymbol{P})\,\mathbb{1} - \boldsymbol{P} \cdot \boldsymbol{\sigma}\,,$$

$$-P^\mu \bar{\sigma}_\mu = \omega(\boldsymbol{P})\,\mathbb{1} + \boldsymbol{P} \cdot \boldsymbol{\sigma}\,. \tag{120}$$

Observe that $-P \cdot \sigma$ and $-P \cdot \bar{\sigma}$ are hermitian positive definite matrices with eigenvalues equal to $\omega(\boldsymbol{P}) \pm |\boldsymbol{P}|$.

Let us now consider the case of massless spinors. In that case the matrices $-P \cdot \sigma$ and $-P \cdot \bar{\sigma}$ have one zero eigenvalue and become equal to $2\,\omega(\boldsymbol{P})$ times a projection operator, as follows from (118). Indeed, the massless limit of (116) equals

$$u(\boldsymbol{P}, \xi) = \frac{e^{\mathrm{i}\pi/4}}{\sqrt{2\omega(\boldsymbol{P})}} \begin{pmatrix} (-P \cdot \sigma)\,\xi \\ -\mathrm{i}(-P \cdot \bar{\sigma})\,\xi \end{pmatrix},$$

$$v(\boldsymbol{P}, \bar{\xi}) = \frac{e^{\mathrm{i}\pi/4}}{\sqrt{2\omega(\boldsymbol{P})}} \begin{pmatrix} -(-P \cdot \sigma)\,\bar{\xi} \\ -\mathrm{i}(-P \cdot \bar{\sigma})\,\bar{\xi} \end{pmatrix}. \tag{121}$$

Before proceeding, let us introduce the light-cone basis for a generic massless momentum p^μ. In this basis the components p^0 and p^3 are replaced by

$$p^+ = \frac{p^0 + p^3}{\sqrt{2}}, \qquad p^- = \frac{p^0 - p^3}{\sqrt{2}}, \tag{122}$$

where the two remaining components are denoted by the two-component vector $p_\perp = (p^1, p^2)$. In this basis

$$p^2 = -2\,p^+p^- + {p_\perp}^2\,. \tag{123}$$

The advantage of this basis is clear when considering a massless particle moving along the 3-axis. In the standard basis the momentum four-vector has two non-zero components, namely p^0 and p^3, but in the light-cone basis there is only one non-vanishing component (i.e. either p^+ or p^-), which helps with the calculations as we will see below.

The positive frequency solution is degenerate and can be further classified using the chirality projectors $P_\mathrm{L} = (1 + \gamma_5)/2$ and $P_\mathrm{R} = (1 - \gamma_5)/2$, which project onto the upper and lower two components of the spinor, respectively. Thus we have the left- and right-handed solutions

$$u_\mathrm{L}(\boldsymbol{P}, \xi) = \frac{e^{\mathrm{i}\pi/4}}{\sqrt{2\omega(\boldsymbol{P})}} \begin{pmatrix} (-P \cdot \sigma)\,\xi \\ 0 \end{pmatrix}, \qquad u_R(\boldsymbol{P}, \xi) = \frac{e^{-\mathrm{i}\pi/4}}{\sqrt{2\omega(\boldsymbol{P})}} \begin{pmatrix} 0 \\ (-P \cdot \bar{\sigma})\,\xi \end{pmatrix}, \tag{124}$$

and likewise for the spinors v_L and v_R. We can specify further the two-component spinors ξ. We note that $-P \cdot \sigma$ and $-P \cdot \bar{\sigma}$ project onto negative and positive helicity eigenstates, respectively. For instance, from

$$(-P \cdot \sigma)\xi = (|\vec{P}| - \vec{P} \cdot \vec{\sigma})\xi \,, \tag{125}$$

we see that the right hand side is only non-zero for ξ a negative helicity, ξ_-. Because $-P \cdot \sigma$ and $-P \cdot \bar{\sigma}$ are projectors, we can, without loss of generality, choose a convenient basis for the $\xi_\pm$ spinors independent of momentum. We choose ξ_- (ξ_+) such that, in the frame where $\vec{P}$ is along the z-axis, u_L (u_R) has j_3 eigenvalue $-\frac{1}{2}$ ($+\frac{1}{2}$), in correspondence with the helicity-chirality relation $2h = -\gamma_5$. We thus choose

$$\xi_- = \begin{pmatrix} 0 \\ 1 \end{pmatrix}, \qquad \xi_+ = \begin{pmatrix} 1 \\ 0 \end{pmatrix} \,. \tag{126}$$

In this case we have for $u_L(P, \xi)$ and $u_R(P, \xi)$

$$u_L(\boldsymbol{P}, \xi) = \frac{e^{\mathrm{i}\pi/4}}{\sqrt{2P^0}} \begin{pmatrix} -P_T^* \\ \sqrt{2}P^+ \\ 0 \\ 0 \end{pmatrix}, \qquad u_R(\boldsymbol{P}, \xi) = \frac{e^{-\mathrm{i}\pi/4}}{\sqrt{2P^0}} \begin{pmatrix} 0 \\ 0 \\ \sqrt{2}P^+ \\ P_T \end{pmatrix} \,. \tag{127}$$

For the rest of this section we change from chirality to helicity labels, and allow for a change in normalization

$$u_L \equiv \frac{1}{c_-} u_- \,, \quad u_R \equiv \frac{1}{c_+} u_+ \,. \tag{128}$$

Once can show that in order to have $u_\pm(P)^\dagger u_\pm(P) = 2P^0$ one must, up to phases, choose $c_- = 2^{1/4}\sqrt{P^0/P^+}$ and $c_+ = 2^{1/4}\sqrt{P^0/P^-}$. We choose the phases of $u_\pm$ now such that

$$u_-(\boldsymbol{P}, \xi) = 2^{1/4} \begin{pmatrix} -\sqrt{P^-}e^{-\mathrm{i}\phi_p} \\ \sqrt{P^+} \\ 0 \\ 0 \end{pmatrix}, \qquad u_+(\boldsymbol{P}, \xi) = 2^{1/4} \begin{pmatrix} 0 \\ 0 \\ \sqrt{P^+} \\ \sqrt{P^-}e^{\mathrm{i}\phi_p} \end{pmatrix} \,. \tag{129}$$

where the phase ϕ_p is defined through

$$P_T = e^{\mathrm{i}\phi_p}\sqrt{2P^+P^-} \,. \tag{130}$$

Having constructed quite explicit forms for helicity spinors we now use them to derive useful computational rules. Arguments of spinors we now indicate with lower-case four-momenta. To begin, we define *spinor products* together with bra-ket notation, as follows

$$\mathrm{i}\overline{u_-}(k)u_+(p) \equiv \langle k-|p+\rangle \equiv \langle kp \rangle \,, \tag{131}$$

and

$$\mathrm{i}\overline{u_+}(k)u_-(p) \equiv \langle k+|p-\rangle \equiv [kp] \,. \tag{132}$$

One may show that

$$\langle kp \rangle = (e^{\mathrm{i}\phi_k}\sqrt{2k^-p^+} - e^{\mathrm{i}\phi_p}\sqrt{2k^+p^-}) \,, \tag{133}$$

and

$$[kp] = \langle kp \rangle = (e^{-\mathrm{i}\phi_k}\sqrt{2k^-p^+} - e^{-\mathrm{i}\phi_p}\sqrt{2k^+p^-}) \,, \tag{134}$$

so that

$$\langle kp \rangle = -\langle pk \rangle, \quad [kp] = -[pk], \quad \langle kp \rangle^* = [kp] \,, \tag{135}$$

and

$$\langle kp \rangle[kp] = -2k \cdot p \,. \tag{136}$$

The real benefits of working with helicity spinors come to the fore when also the polarization vectors $\varepsilon^\mu(k, \lambda)$ of massless spin-1 particles with momentum k and helicity λ are expressed in terms of them. To see how this works, we first choose the frame in which the on-shell massless gauge boson momentum has only a $+$ component. In this frame only the ε^1 and ε^2 components are meaningful, corresponding to the two helicity states of the massless vector field. For the chosen frame the third component of the spin is identical to the helicity, and the transversality condition $k \cdot \varepsilon(k) = 0$ becomes

$$k^+ \varepsilon^-(k, \lambda) = 0 \,, \tag{137}$$

which implies that $\varepsilon^0 = \varepsilon^3$. From this explicit solution one observes that $(\varepsilon_\mu(k, +))^*$ has negative helicity. Our normalization is such that

$$(\varepsilon_\mu(k, +))^* = \varepsilon_\mu(k, -) \,. \tag{138}$$

and

$$\varepsilon(k, +) \cdot \varepsilon(k, -) = -1 \,. \tag{139}$$

We will also use the notation

$$\varepsilon^\mu(k, \pm) = \varepsilon_\pm^\mu(k) \,. \tag{140}$$

Let us now demonstrate that we may write the polarization vector indeed in terms of spinors of fixed helicity, as follows

$$\varepsilon_+^\mu(k, p) = A_+ \overline{u_+}(k, +) \gamma^\mu u(p, +) \equiv -\mathrm{i} A_+ \langle k+ | \gamma^\mu | p+ \rangle \,, \tag{141}$$

and similarly for negative helicity. Note the extra momentum p, called the *reference momentum*, of the second u spinor. It is in fact arbitrary, with $p^2 = 0$, we will discuss it further below. From the explicit form of the helicity spinors in (129) and the form of the solutions one may derive

$$A_+ = \frac{-\mathrm{i}}{\sqrt{2}\langle kp \rangle} \,, \quad A_- = \frac{-\mathrm{i}}{\sqrt{2}[kp]} \,. \tag{142}$$

Recall that any multiple of k^μ may be added to the expressions for the photon polarizations without changing the amplitude, as this is just a gauge transformation.

From the explicit form of the u and v spinors (129), one can prove the following series of identities

$$\langle k+ | p+ \rangle = 0 \,, \tag{143}$$
$$\langle k+ | \gamma^\mu | p- \rangle = \langle k+ | \gamma_5 | p+ \rangle = 0 \,, \tag{144}$$
$$\langle k+ | \gamma^\mu | k+ \rangle = 2k^\mu \,, \tag{145}$$
$$\langle k+ | \gamma^\mu | p+ \rangle = \langle p- | \gamma^\mu | k- \rangle \,, \tag{146}$$

and similarly with all helicities reversed. These identities are remarkably useful in practical calculations with helicity spinors. Another very important property for this is Fierz reordering, with which one may "recouple" the spinors. Consider the following expression

$$\langle 1+ | \gamma^\mu | 2+ \rangle \langle 3- | \gamma_\mu | 4- \rangle \,, \tag{147}$$

where we have abbreviated $|k_1+\rangle = |1+\rangle$ etc. This is in fact the most general form for such a contraction of spinor products. Let us define the following complete set of 16 matrices

$$O_I = \{1, \gamma_5, \gamma^\mu, \mathrm{i}\gamma^\mu \gamma_5, \sigma^{\mu\nu}\} \,, \tag{148}$$

with the orthogonality property

$$\frac{1}{4} \mathrm{Tr}\,[O_I O_J] = \delta_{IJ} \,, \quad I = 1 \ldots 5 \,. \tag{149}$$

We can insert this relation into (147), which may then be written as

$$\frac{1}{4}\sum_I \langle 1+|\gamma^\mu O_I \gamma_\mu|4-\rangle\langle 3-|O_I|2+\rangle\,. \tag{150}$$

Because of the chirality properties of the bra's and kets, only the two diagonal O_I yield a non-zero result, 1 and γ_5, and they moreover yield the same result. Hence the Fierz recoupling identity reads simply

$$\langle 1+|\gamma^\mu|2+\rangle\langle 3-|\gamma_\mu|4-\rangle = 2\langle 1+|4-\rangle\langle 3-|2+\rangle\,, \tag{151}$$

where e.g. $\langle 1+|$ has been recoupled to $|4-\rangle$ in the spinor product. With this identity we can now check the normalization of the polarization vectors and find

$$\varepsilon^+(k,p)\cdot\varepsilon^-(k,p) = -A_+ A_- \langle k+|\gamma^\mu|p+\rangle\langle k-|\gamma_\mu|p-\rangle = 1\,, \tag{152}$$

and similarly that $\varepsilon_\pm(k,p)\cdot\varepsilon_\pm(k,p) = 0$. The identities involving the sum over spin polarizations read in terms of helicity spinors

$$\not{k} = |k+\rangle\langle k+| + |k-\rangle\langle k-|\,. \tag{153}$$

One can derive the completeness relation for the polarization vectors in the representation (141)

$$\sum_{\lambda=\pm} \varepsilon_\lambda^\mu(k,p)\,(\varepsilon_\lambda^\nu(k,p))^* = \eta^{\mu\nu} - \frac{p^\mu k^\nu + p^\nu k^\mu}{p\cdot k}\,, \tag{154}$$

and that a change in reference momentum amounts to a different gauge choice

$$\varepsilon_+^\mu(k,p) - \varepsilon_+^\mu(k,q) = \frac{\sqrt{2}\langle pq\rangle}{\langle kp\rangle\langle kq\rangle}k^\mu\,. \tag{155}$$

We have now sufficient ingredients to demonstrate the efficiency of using helicity spinors in computing invariant amplitudes for a few examples. For each amplitude we shall discuss the result for various sets of helicities for the external particles. We shall also take each external particle as massless so that helicity is a conserved quantum number. For convenience we choose momenta of the external particles outgoing, and express possible anti-fermion spinors in terms of u spinors using $v_+ = u_-$ and $v_- = u_+$.

The reaction $e^+e^- \to \mu^+\mu^-$

We first consider the reaction

$$e^-(k_1) + e^+(k_2) \to \mu^-(k_3) + \mu^+(k_4)\,, \tag{156}$$

mediated via a photon. The invariant amplitude may be represented as

$$\mathcal{M}(1^{\lambda_1}, 2^{\lambda_2}, 3^{\lambda_3}, 4^{\lambda_4})\,, \tag{157}$$

where we have indicated only the label of each external line momentum, and the associated helicity. Using the rules derived in this section we have

$$\mathcal{M}(1^+, 2^-, 3^+, 4^-) = (ie)^2 \langle 2-|\gamma^\mu|1-\rangle \frac{-i}{s_{12}}\langle 3+|\gamma_\mu|4+\rangle\,, \tag{158}$$

where we used the notation $s_{ij} = -(k_i + k_j)^2$. Using the Fierz identity (151) and the shorthand notation of (131) and (132) this can be written as

$$\mathcal{M}(1^+, 2^-, 3^+, 4^-) = 2ie^2 \frac{[24]\langle 31\rangle}{\langle 12\rangle[12]}\,. \tag{159}$$

QCD

Using momentum conservation this may be further rewritten as

$$\mathcal{M}(1^+, 2^-, 3^+, 4^-) = 2\mathrm{i}e^2 \frac{[13]^2}{[12][34]} . \tag{160}$$

It may be readily verified that

$$\mathcal{M}(1^-, 2^+, 3^-, 4^+) = 2\mathrm{i}e^2 \frac{\langle 13 \rangle^2}{\langle 12 \rangle \langle 34 \rangle} . \tag{161}$$

The expressions in (160) and (161) are quite compact, and can be transformed into each other by either a parity transformation or a charge conjugation. For any other helicity configuration the amplitude actually vanishes.

The reaction $\mathrm{e}^+\mathrm{e}^- \rightarrow \mu^+\mu^-\gamma$

In this second example we study the production of a muon pair together with a photon in electron positron annihilation

$$e^-(k_1) + e^+(k_2) \rightarrow \mu^-(k_3) + \mu^+(k_4) + \gamma(k_5) \tag{162}$$

The photon can be radiated off any of the four external fermion lines, leading to the four diagrams shown in Fig. 18. Let us list another useful identity, not difficult to prove, for a positive helicity massless vector
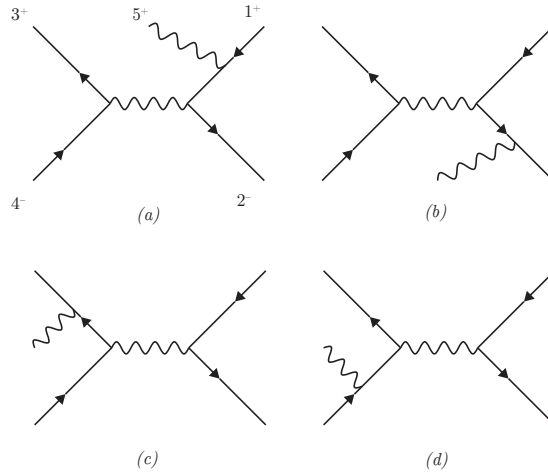

Fig. 18: Feynman diagrams contributing a particular helicity amplitude, indicated in diagram (a), for $\mathrm{e}^+\mathrm{e}^- \rightarrow \mu^+\mu^-\gamma$ at lowest order. All momenta are outgoing, and time runs from right to left.

boson with polarization $\varepsilon_+^\mu(k,p)$ emitted from a fermion by

$$\not{\varepsilon}_+(k,p) = \frac{\mathrm{i}\sqrt{2}}{\langle kp \rangle} \left(|p+\rangle\langle k+| + |k-\rangle\langle p-| \right) . \tag{163}$$

For the negative helicity case one has, in analogy

$$\not{\varepsilon}_-(k,p) = \frac{-\mathrm{i}\sqrt{2}}{[kp]} \left(|k+\rangle\langle p+| + |p-\rangle\langle k-| \right) . \tag{164}$$

The invariant amplitude reads

$$\mathcal{M}(1^{\lambda_1}, 2^{\lambda_2}, 3^{\lambda_3}, 4^{\lambda_4}, 5^{\lambda_5}) . \tag{165}$$

Given that each external line can have two helicity values, it might seem that this process allows thirty-two different independent helicity amplitudes. However, helicity conservation and invariance under charge conjugation and parity transformation ensure that there is in fact only one independent amplitude. We thus consider the helicity amplitude

$$\mathcal{M}(1^+, 2^-, 3^+, 4^-, 5^+),\tag{166}$$

and choose as k_4 as reference momentum for the outgoing photon. Diagram (a) then reads

$$\mathcal{M}_a(1^+, 2^-, 3^+, 4^-, 5^+) = (ie)^3 \langle 2 - |\gamma^\mu \frac{-i(\slashed{1} + \slashed{5})}{-s_{15}} \slashed{\epsilon}_+(k_5, k_4)|1-\rangle \times \frac{-i}{s_{34}} \langle 3 + |\gamma_\mu|4+\rangle .\tag{167}$$

Using the results in eqs. (163) and (164) we find

$$\mathcal{M}_a(1^+, 2^-, 3^+, 4^-, 5^+) = -2\sqrt{2}e^3 \frac{\langle 24\rangle^2 [23]}{\langle 15\rangle\langle 45\rangle\langle 34\rangle[34]} .\tag{168}$$

For diagram (b) we find similarly

$$\mathcal{M}_b(1^+, 2^-, 3^+, 4^-, 5^+) = 2\sqrt{2}e^3 \frac{\langle 24\rangle^2 [13]}{\langle 25\rangle\langle 45\rangle\langle 34\rangle[34]} ,\tag{169}$$

while for (c) we have

$$\mathcal{M}_c(1^+, 2^-, 3^+, 4^-, 5^+) = 2\sqrt{2}e^3 \frac{\langle 24\rangle^2}{\langle 12\rangle\langle 35\rangle\langle 45\rangle} .\tag{170}$$

Notice that with our choice of reference momentum we have

$$\mathcal{M}_d(1^+, 2^-, 3^+, 4^-, 5^+) = 0 .\tag{171}$$

Adding up the contributions we find

$$\mathcal{M}(1^+, 2^-, 3^+, 4^-, 5^+) = 2\sqrt{2}e^3 \frac{\langle 24\rangle^2}{\langle 12\rangle} \left(\frac{[34]}{\langle 15\rangle\langle 45\rangle[12]} + \frac{1}{\langle 35\rangle\langle 45\rangle} \right) .\tag{172}$$

Again this is a nice, compact result, a complex number fully expressed in terms of helicity spinors.

Without further proof we can list what is perhaps the most famous result in tree-level QCD amplitudes calculations [26]: the so-called maximal helicity violating (MHV) amplitudes (aka. Parke-Taylor amplitudes) for n-gluon scattering. One may first organize the full tree-level invariant amplitude in the colour quantum number as

$$M_n(p_i, \lambda_i, a_i) = g^{n-2} \sum_{\sigma \in S_n/Z_n} \left(T_{\sigma(a_1)} \ldots T_{\sigma(a_n)} \right) A_n \left(\sigma(p_1^{\lambda_1}), \ldots, \sigma(p_n^{\lambda_n}) \right) .\tag{173}$$

where the sum is over all permutations σ modulo the cyclic ones. The amplitudes A_n are called "colour-ordered". Such amplitudes [27–29] are considerably easier to calculate. First, if all gluons have the same helicity, say $+$, then the amplitude is zero. The same holds if one of them has helicity $-$. With two helicities $-$, we have the MHV amplitude. The stunningly simple expression (a result of millions of Feynman diagrams if n is large enough) for the colour-ordered amplitude reads

$$A_n(1^+, \ldots, i^-, \ldots, j^-, \ldots n^+) = i \frac{\langle ij\rangle^4}{\langle 12\rangle\langle 23\rangle \ldots \langle n-1, n\rangle\langle n1\rangle} .\tag{174}$$

When flipping all $-$ to $+$ and vice versa, all one has to do is replace the angled brackets by squared ones.

Helicity spinor methods are now a standard tool in the computation of QCD scattering amplitudes for the LHC. It is worth mentioning that among the very interesting developments in QCD in recent years has been the realization of recursion relations among these amplitudes [30, 31], after new insights where gained after phrasing them in terms of so-called twistors [32, 33]. Such recursion relations, besides the still very powerful, and often faster [34, 35], earlier ones by Berends and Gield [28] have been important in extending analytical and numerical computational power to high-multiplicity amplitudes.
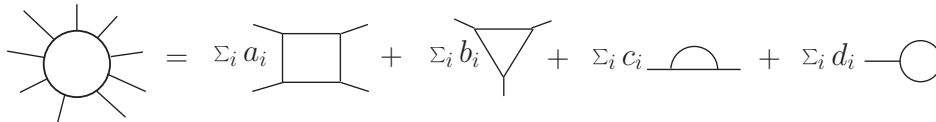
Fig. 19: Expansion of n-leg one-loop amplitude in sum of tadpoles, bubbles, triangles and boxes.

4.2 The NLO revolution

I will here briefly touch upon recent ideas that have spurred what is sometimes referred to as the NLO revolution. An extensive and clear review by some of the instigators is Ref. [36]. For many years the bottleneck in computing NLO cross sections for many external lines were the one-loop diagrams for the virtual part of the cross section. They become increasingly hard to calculate when the number of external lines grows from 4 to 5, 6 etc. Because of similar arguments just mentioned for the case of high-multiplicity tree-level amplitudes one can restrict oneself to a smaller set of diagrams having a particular colour order. The objects to compute have, besides the denominator factors due to the propagators in the loop, a numerator containing dot products among external momenta, polarization vectors, and the loop momentum. Hence, the integral over the loop momentum has possibly a number of loop momenta in the numerator, with open Lorentz- indices.

Such tensor integrals can be reduced to scalar integrals in a well-defined procedure [37]. New stable and efficient reduction techniques for tensor integrals have been proposed in Refs. [38, 39], and have found much use.

One may also express external vectors in terms of a basis set of four. In this procedure also denominators are cancelled, reducing the n-point function to lower-point ones. This leads to an expansion of the amplitude in terms of scalar functions down from n-point ones. Furthermore, up to (here irrelevant) $\mathcal{O}(\epsilon)$ terms, five- and higher point functions can be expressed in terms of four-point functions and lower [40–42]. The price to pay is that for these lower point functions the external momenta are not subsets but rather combinations of the original, massless external momenta. These combinations then are not massless. The upshot is that one has, schematically

$$A_n^{\mathrm{one-loop}} = \sum_{j \in B} c_j \mathcal{I}_j \tag{175}$$

where B is a basis set that consists of a certain set of box-, triangle and bubble integrals with or without massive external legs [43], and the c_j are rational functions of dot products of external momenta and polarization vectors, see Fig. 19. With a generic representation (175) in hand, the task of calculating $A_n^{\mathrm{one-loop}}$ is then mapped to the task of find the coefficients c_j.

For this one may use unitarity methods [44]. In Eq. (175) the elements of the basis set on the *right hand side* may have branchcuts in the invariants on which the logarithms and dilogarithms in the $\mathcal{I}_j$ depend. For instance, a particular integral may have terms of the type $\ln(-s_{ij}/\mu^2)$, with $s_{ij} = p_{ij}^2 = (p_i + p_j)^2 = 2p_i \cdot p_j$, which clearly has a branchcut in the s_{ij} variable.

On the other hand, one can also examine a particular discontinuity across a particular branch cut for a particular invariant, or channel, for *the left-hand side* in Eq. (175), which is done by cutting the amplitude and replacing cut propagators in the loop by delta functions.

$$\frac{1}{p^2 + i\epsilon} \to -i2\pi\, \delta(p^2) \tag{176}$$

This amounts to taking the imaginary part. From the comparison of both sides the coefficients c_j can then be determined. Essentially, one thus determines the function $A_n^{\mathrm{one-loop}}$ from its poles and cuts. This
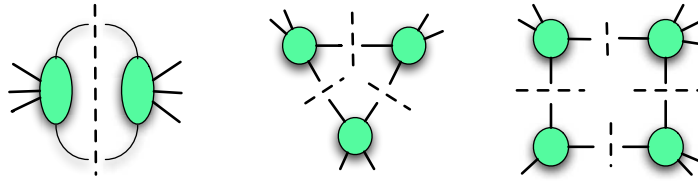
Fig. 20: Generalized unitarity

is vastly more efficient than computing every term fully by itself, and is the key insight that spurred the NLO revolution.

However, there are important subtleties. Using four-dimensional momenta in the cuts leaves an ambiguity in the form of a rational function. Using a $n = 4 + \varepsilon$ version of the unitary method [45, 46] avoids this, but this is somewhat more cumbersome to use. A number of other methods have been devised to fix this ambiguity, such as using recursion relations [30, 31], or using D-dimensional unitarity [47, 48]. Particularly fruitful is the use of complex kinematics, which allows non-vanishing, non-trivial three-point amplitudes. This allows taking multiple cuts of a box integral, such as in Fig. 20, which goes under the name "generalized unitarity". By so doing, one may determine the coefficients c_j purely algebraically [49], since the four delta-functions fix the loop momentum.

An effective way of solving Eq. (175) was proposed in Ref. [50], and is known as the OPP method. Writing the equivalent of Eq. (175) at the *integrand* level, the coefficients of the box etc integral can then be extracted by choosing different values of the loop momentum, and perform the inversion numerically.

Furthermore, numerical [51, 52] and semi-numerical [53] techniques for loop integrals have progressed to the level where much work is taken care of for the user through programs like Blackhat [54], Cuttools [55], or Rocket [56] and MCFM [57]. The level of automation, including the matching to parton showers, has now been stepped up tremendously, with the POWHEG Box [58] and aMC@NLO-MadGraph5 [59] framework. They have brought NLO calculations now to the general user.

As this snaphot of the NLO revolution suggests, the area of NLO calculations was a very lively marketplace of ideas and methods. Although it is still a bustling place, attention is now shifting to exporting the revolution to NNLO.

4.3   Aspects of NNLO

Here I will not say much, as this falls out of the scope of the lectures. Many of the conceptual issues in earlier sections play a role here as well. The accounting of singularities in a flexible way is much harder at this order. An equation as (175) does not yet fully exist for this order, though impressive progress is being made [60]. Nevertheless, results were obtained first already many years ago for DIS [61], Drell-Yan [62] and some time later for Higgs production [63–65]. Recently the latter was even computed to NNNLO using powerful and clever methods involving threshold expansions [66].

Essential for any NNLO calculation for hadron colliders are the NNLO (3-loop) Altarelli-Parisi splitting functions. These were calculated some time ago [9, 10] thanks also to the powers of the computer algebra program FORM [67, 68].

For top quark pair production [69] the first full two-to-two QCD process calculated to NNLO was completed recently (more about this below). Many other results are now appearing (see e.g. [70] for NNLO results on jet cross sections), the review of which would take us too far afield, and would anyway be out of date in very short order.

This concludes our discussions of finite order QCD methods and results. Let us now turn to aspects of QCD resummation, and all-order results.

5 All orders

"Resummation" is shorthand for all-order summation of classes of potentially large terms in quantum field perturbation theory. To review status and progress in a field defined so generally is an impossibly wide scope, and I will restrict myself to certain types in QCD, related of course to observables at high-energy hadron colliders.

Let us first form an impression of what resummation is and what it does. Let $d\sigma$ be a (differential) cross section with the schematic perturbative expansion

$$d\sigma = 1 + \alpha_s(L^2 + L + 1) + \alpha_s^2(L^4 + L^3 + L^2 + L + 1) + \dots \tag{177}$$

where α_s is the coupling, also serving as expansion parameter, L is some logarithm that is potentially large. In our discussion we focus on gauge theories, and on the case with at most two extra powers of L per order, as Eq. (177) illustrates. An extra order corresponds to an extra emission of a gauge boson, the two ("Sudakov") logs resulting from the situation where the emission is simultaneously soft and collinear to the parent particle direction.

Denoting $L = \ln A$, we can next ask what A is. In fact, A will in general depend on the cross section at hand. For example, for a thrust (T) distribution $A = 1 - T$, while for $d\sigma(p\bar{p} \to Z + X)/dp_T^Z$ $A = M_Z/p_T^Z$. It should be pointed out already here that A is not *necessarily* constructed out of measured variables but can also be a function of unobservable partonic momenta that are to be integrated over. E.g. for inclusive heavy quark production A could be $1 - 4m^2/(x_1 x_2 S)$ in hadron collisions with energy $\sqrt{S}$, where x_1, x_2 are partonic momentum fractions. When L is numerically large so that even for small α_s, the convergent behaviour of the series is endangered, resummation of the problematic terms into an analytic form might provide a remedy, and thereby extend the theory's predictive power to the range of large L. In general the resummed form of $d\sigma$ may be written schematically as

$$d\sigma_{res} = C(\alpha_s) \exp\left[L g_1(\alpha_s L) + g_2(\alpha_s L) + \alpha_s g_3(\alpha_s L) + \dots\right] + R(\alpha_s) \tag{178}$$

where $g_{1,2,\dots}$ are computable functions. The series $C(\alpha_s)$ multiplies the exponential, and $R(\alpha_s)$ denotes the remainder.

The key aspect of resummation is finding the functions g_i. With only g_1 one has leading logarithmic resummation (LL), with also g_2 NLL etc. For NNLL resummation the matching function C must also be known to next order in α_s.

5.1 Resummation basics, eikonal approximation, webs

Well-developed arguments exist for the exponentiation properties of the Drell-Yan cross section near threshold [71, 72]. Some are based on identifying further evolutions equations [71, 73] based on refactorizations of the cross section into different regions only sensitive to either collinear, soft or hard corrections. This has been made into a formidable systematic programme based on effective field theory [74–77].

The connection between refactorization and resummation is already illustrated by perturbative renormalization, in which the general relation of unrenormalized and renormalized Green functions of fields ϕ_i carrying momenta p_i is

$$G_{\text{un}}(p_i, M, g_0) = \prod_i Z_i^{1/2}(\mu/M, g(\mu)) \, G_{\text{ren}}(p_i, \mu, g(\mu)) \,. \tag{179}$$

M is an ultraviolet cutoff, and $g(\mu)$ and g_0 are the renormalized and bare couplings respectively. The independence of G_{un} from μ and G_{ren} from M may be used to derive renormalization group equations,

$$\mu \frac{d \ln G_{\text{ren}}}{d\mu} = -\sum_i \gamma_i(g(\mu)) \,, \tag{180}$$
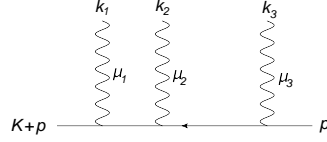
Fig. 21: Soft photon emission from an energetic line

in which the anomalous dimensions $\gamma_i = (1/2)(\mu d/d\mu) \ln Z_i$ appear as constants in the separation of variables, free of explicit dependence on either μ or M. The solution to (180)

$$G_{\mathrm{ren}}(p_i, 1, g(M)) = G_{\mathrm{ren}}(p_i, M/\mu_0, g(\mu_0)) \exp\left[-\sum_i \int_{\mu_0}^{M} \frac{d\mu}{\mu} \gamma_i(g(\mu))\right], \qquad (181)$$

is clearly an exponential. While in this example the factorization involves separation of UV modes from finite energy ones, for the resummation we discuss in this section one (re)factorizes collinear modes from soft-, anticollinear and hard modes. In a manner similar to this example differential equations may be set up whose solution, in terms of appropiate exponentials of (double) integrals over anomalous dimensions, is the resummed cross section [73].

To see the appearance of exponentials in a different way we can observe that in the refactorization approach the soft or eikonal part of the observable is isolated in a well-defined way. One may then use the property that moments of the eikonal DY cross section exponentiate at the level of integrands [72,78–80], with exponents consisting of so-called *webs*. These are selections of cut diagrams under criteria defined by graphical topology (irreducibility under cuts of the eikonal lines) and with possibly modified colour weights. Each web is a cut diagram, and can be integrated over the momentum k that it contributes to the final state.

To see how webs work, let us first consider the abelian case[10]. Webs are phrased in terms of eikonal Feynman rules. In order to derive these one may consider a single hard massless external line of final on-shell momentum p, originating from some unspecified hard interaction described by $\mathcal{M}_0(p)$. The hard line may emit a number n of soft photons with momenta k_i, as depicted in Fig. 21, where k_1 is emitted closest to the hard interaction. We shall take the emitting particle to be a scalar (the argument for fermions is very similar). For this case the hard interaction is dressed according to

$$\mathcal{M}^{\mu_1 \cdots \mu_n}(p, k_i) = \mathcal{M}_0(p) \frac{1}{(p + K_1)^2} (2p + K_1 + K_2)^{\mu_1} \cdots \frac{1}{(p + K_n)^2} (2p + K_n)^{\mu_n}, \qquad (182)$$

where we have introduced the partial momentum sums $K_i = \sum_{m=i}^{n} k_m$.

The eikonal approximation in this case can simply be defined as the leading-power contribution to the amplitude when the photon momenta $k_i^{\mu_i} \to 0$, $\forall i$, in both numerator and denominator. In this limit, eq. (182) becomes

$$\mathcal{M}^{\mu_1 \cdots \mu_n}(p, k_i) = \mathcal{M}_0(p) \frac{p^{\mu_1} \cdots p^{\mu_n}}{(p \cdot K_1) \dots (p \cdot K_n)}. \qquad (183)$$

The eikonal factor is insensitive to the spin of the emitting particles. One may also notice that the eikonal factor does not depend on the energy of the emitter, since it is invariant under rescalings of the hard momentum p^{μ}: at leading power in the soft momenta, one is effectively neglecting the recoil of the hard particle against soft radiation.

The eikonal factor can be further simplified by employing Bose symmetry. Indeed for the physical quantity depending on the amplitude $\mathcal{M}^{\mu_1 \cdots \mu_n}(p, k_i)$, one must sum over all diagrams corresponding to

---

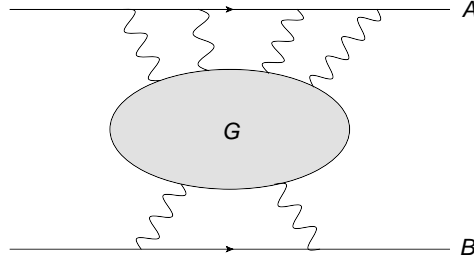[10]This text is derived from section 2 in [81].

Fig. 22: A process involving two eikonal lines A and B, interacting through the exchange of soft gluons forming diagram G.

permutations of the emitted photons along the hard line. Having done this, the eikonal factor multiplying $\mathcal{M}_0(p)$ on the *r.h.s.* of (183) will be replaced by the symmetrized expression

$$E^{\mu_1\cdots\mu_n}(p, k_i) = \frac{1}{n!} p^{\mu_1}\ldots p^{\mu_n} \sum_\pi \frac{1}{p\cdot k_{\pi_1}} \frac{1}{p\cdot(k_{\pi_1}+k_{\pi_2})}\cdots\frac{1}{p\cdot(k_{\pi_1}+\ldots+k_{\pi_n})}, \quad (184)$$

where the sum is over all permutations of the photon momenta, and k_{π_i} is the ith momentum in a given permutation. There are $n!$ permutations, and each gives the same contribution to any physical observable. This becomes manifest using the *eikonal identity*

$$\sum_\pi \frac{1}{p\cdot k_{\pi_1}} \frac{1}{p\cdot(k_{\pi_1}+k_{\pi_2})}\cdots\frac{1}{p\cdot(k_{\pi_1}+\ldots k_{\pi_n})} = \prod_i \frac{1}{p\cdot k_i}. \quad (185)$$

Using (185), the eikonal factor $E^{\mu_1\cdots\mu_n}(p, k_i)$ arising from n soft emissions on an external hard line becomes simply

$$E^{\mu_1\cdots\mu_n}(p, k_i) = \prod_i \frac{p^{\mu_i}}{p\cdot k_i}, \quad (186)$$

which is manifestly Bose symmetric and invariant under rescalings of the momenta $\{p_i\}$. In practice, each eikonal emission can then be expressed by the effective Feynman rule

$$= \frac{p^\mu}{p\cdot k} \quad (187)$$

These Feynman rules can be obtained by replacing the hard external line with a Wilson line along the classical trajectory of the charged particle. In abelian quantum field theories this is given by the expression

$$\Phi_\beta(0, \infty) = \exp\left[ie \int_0^\infty d\lambda\, \beta\cdot A(\lambda\beta)\right], \quad (188)$$

where β is the dimensionless four-velocity corresponding to the momentum p. (For non-abelian gauge theory the gauge field is a matrix $A_\mu = A_\mu^a T_a$ with T_a matrices that represent the generators of the group. Because the exponent is an integral over a matrix-valued function, the exponential is a path-ordered expression.) This expresses the fact that soft emissions affect the hard particle only by dressing it with a gauge phase. Having constructed the effective Feynman rules, one may proceed to demonstrate the exponentiation of soft photon corrections as follows. As an example, we consider graphs of the form shown in Fig. 22, at a fixed order in the perturbative expansion. Fig. 22 consists of two eikonal lines, labelled A and B, each of which emits a number of soft photons. One may envisage lines A and B

as emerging from a hard interaction, and one may consider the graph G either as a contribution to an amplitude, or to a squared amplitude (in which case some of the propagators in G will be cut).

Diagram G can be taken as consisting only of soft photons and fermion loops. Photons originating from one of the two eikonal lines must land on the other one, or on a fermion loop inside G. Indeed, a photon cannot land on the same eikonal line, as in that case the diagram is proportional to $p^\mu p_\mu = 0$.

Using eikonal Feynman rules, one finds that graphs of the form of Fig. 22 contribute to the corresponding (squared) amplitude a factor

$$\mathcal{F}_{AB} = \sum_G \left[\prod_i \frac{p_A^{\mu_i}}{p_A \cdot k_i} \right] \left[\prod_j \frac{p_B^{\nu_j}}{p_B \cdot l_j} \right] G_{\mu_1 \ldots \mu_n; \nu_1 \ldots \nu_m}(k_i, l_j), \tag{189}$$

where k_i, l_j are the momenta of the photons emitted from lines A and B respectively, with $i = 1, \ldots, n$ and $j = 1, \ldots, m$.

Given that we have already summed over permutations in order to obtain the eikonal Feynman rules, each diagram G can be uniquely specified by the set of connected subdiagrams it contains, as indicated schematically in Fig. 23, where each possible connected subdiagram $G_c^{(i)}$ occurs N_i times. According to the standard rules of perturbation theory, diagram G has a symmetry factor corresponding to the number of permutations of internal lines which leave the diagram invariant. This symmetry factor is given by

$$S_G = \prod_i S_i^{N_i} (N_i)!, \tag{190}$$

where S_i is the symmetry factor associated with each connected subdiagram $G_c^{(i)}$, and the factorials account for permutations of identical connected subdiagrams, which must be divided out. Contracting Lorentz indices as in (189), the eikonal factor $\mathcal{F}_{AB}$ may be written as

$$\mathcal{F}_{AB} = \sum_{\{N_i\}} \prod_i \frac{1}{N_i!} \left[\mathcal{F}_c^{(i)} \right]^{N_i}, \tag{191}$$

where

$$\mathcal{F}_c^{(i)} = \frac{1}{S_i} \left(\prod_q \frac{p_A^{\mu_q}}{p_A \cdot k_q} \right) \left(\prod_r \frac{p_B^{\nu_r}}{p_B \cdot l_r} \right) G_{\mu_1 \ldots \mu_{n_q}; \nu_1 \ldots \nu_{m_r}}^{(i)}(k_q, l_r), \tag{192}$$

is the expression for each connected subdiagram, including the appropriate symmetry factor. Recognising (191) as an exponential series, it follows that

$$\mathcal{F}_{AB} = \exp \left[\sum_i \mathcal{F}_c^{(i)} \right]. \tag{193}$$

We conclude that soft photon corrections exponentiate in the eikonal approximation, and the exponent is given by the sum of all connected subdiagrams. Having seen the abelian case, the non-abelian case for the eikonal cross section is not all that much more difficult, though we shall not treat it here.

Following arguments similar to that for the abelian case [79] [78, 80, 82–84] one may in fact arrive at the result that the eikonal cross section is a sum over eikonal diagrams D

$$\sigma^{(\mathrm{eik})} = \exp \left[\sum_W \sum_{D, D'} \mathcal{F}(D) R_{DD'}^{(W)} C(D') \right], \tag{194}$$

where a mixing matrix R connects the momentum space parts of the diagrams $\mathcal{F}(D)$ and their colour factors $C(D)$ in an interesting way. A very recent, pedagogical review of this and other aspects of webs can be found in [85].
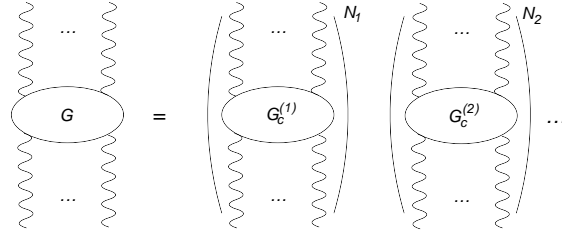
Fig. 23: Decomposition of a soft photon graph into connected subdiagrams $G_c^{(i)}$, each of which occurs N_i times.

The functions g_i that constitute the resummation are usually not only defined by the eikonal cross section. Hard collinear modes in the higher-order corrections can be resummed in different ways, through so-called jet functions. These are in fact also universal, so that by now constructing a resummed cross section is often a matter of putting the right set of all-order functions together. Some automation of this has already been undertaken [86, 87] and is at present being worked on further by various groups.

5.2 Some applications in threshold resummation: heavy quark production, Higgs production

The very general arguments in the previous section can be applied to transverse momentum resummation and threshold resummation. Here we focus on the latter. An illuminating study of the effects of threshold resummation was given in Ref. [88]. One can representing the partonic resummed cross section in moment space as

$$\sigma_{DY}(N, Q^2) = H(Q) \exp\left[G_{DY}(N, Q)\right] \tag{195}$$
$$G_{DY} = 2\ln N g_1(2\lambda) + g_2(2\lambda) + \alpha_s g_3(2\lambda) + \ldots \tag{196}$$
$$\lambda = \beta_0 \alpha_s \ln N, \tag{197}$$

which was already more schematically given in (178), and where

$$g_1(\lambda) = \frac{C_F}{\beta_0 \lambda} \left[\lambda + (1 - \lambda)\ln(1 - \lambda)\right]. \tag{198}$$

In Fig. 24 [88] convergence properties for both the exponent and the resummed cross section are shown (for toy PDF's) when increasing the logarithmic accuracy of the exponent, and of the hadronic K factor. One observes good convergence as the logarithmic accuracy of the resummation is increased. For the inverse Mellin transform, required to compute the hadronic cross section in momentum space, one may use the so-called minimal prescription [89].

Very similar to Drell-Yan is Higgs production, in the large top mass limit where there is essentially a pointlike gluon-gluon-Higgs coupling. A recent N^3LL threshold resummed result [90] is shown in Fig. 25.

We conclude this section with the already mentioned NNLO top quark cross section results, matched to a NNLL threshold resummed calculation for this observable [91]. For the resummed part an added complication is the accounting for colour, as all four external particles are coloured. This issue was solved in Refs. [73, 92, 93], we shall not go into the technical aspects of this. The result of the very impressive, and important calculation [69] is shown in Fig. 26

6 Conclusions

In these lectures I have discussed many aspects of QCD, from the conceptual to the practical, that are relevant for understanding and appreciating its role in the physics of particle colliders. These aspects are often quite technical in nature, and no doubt I have done poor justice to them in the limited space
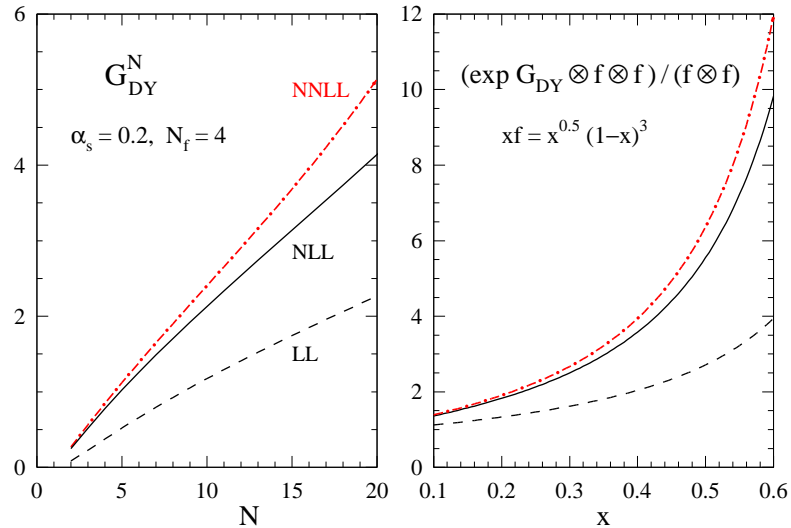
Fig. 24: Convergence behavior of Drell-Yan partonic and hadronic cross section [88]
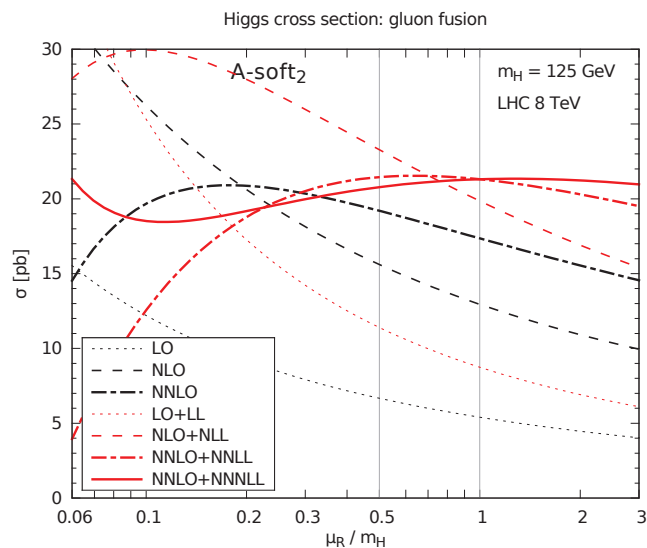
Fig. 25: A recent result [90] for the N^3LL cross section for Higgs production. One observes the notably less dependence of the result on the renormalization scale μ_R.

available. Nevertheless, some attention must be given to these, in order to assess the strengths and weaknesses of theoretical results. This is of crucial importance when confronting these results with data. With the focus of theory and measurement turning towards precision, having paid this attention should be all the more valuable.

Nevertheless I hope that readers are not blinded by the technicalities, but are able to sharpen their intuition regarding how QCD behaves a bit further. Both technical understanding and intuition will be fruitful in the theory-experiment collaborations, joint workshops etc in which they may find themselves at times, and upon which much of the success of the LHC research programme depends.
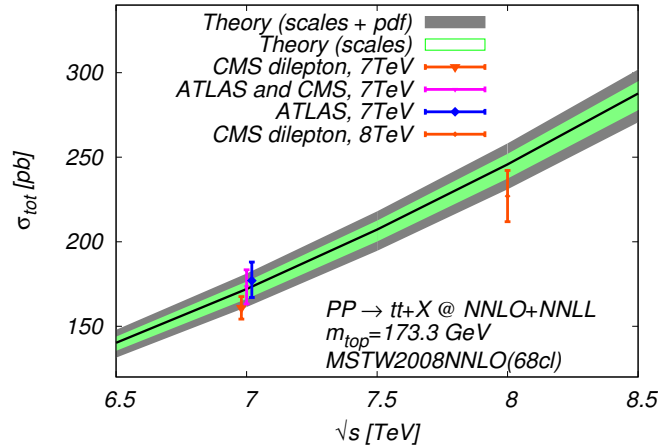
Fig. 26: Theoretical prediction for the LHC as a function of the collider c.m. energy, compared to available measurement from ATLAS and/or CMS at 7 and 8 TeV.

Appendices

A   Conventions and useful formulae

Units

We use here $\hbar = 1$ and $c = 1$. Energy can be converted to inverse distance and vice versa by the relation $1 = 197.3\text{MeV fm}$, with 1 fm ("fermi" or "femtometer") equal to 10^{-15}m, and $c = 2.998 \cdot 10^8$ m/s.

Cross sections are expressed in nanobarns (nb), picobarns (pb) etc, where $1\,\text{b} = 10^{-24} cm^2$.

The metric tensor we use in this course is

$$\eta^{\mu\nu} = \text{diag}(-1, 1, 1, 1) \tag{A.1}$$

Cross sections and decay rates

The cross section for the scattering of two incoming massless particles with momenta k_1 and k_2 to n particles with momenta $\{p_i\}$ is given by

$$\sigma = \frac{1}{2s} \overline{\sum_{spins}} \int |\mathcal{M}|^2 \, dPS(n) \tag{A.2}$$

where the bar indicates initial spin averaging and

$$dPS(n) = \prod_{j=1}^{n} \frac{d^3 p_j}{(2\pi)^3 \, 2E_j} \times (2\pi)^4 \delta \left(k_1 + k_2 - \sum_i^n p_i \right) \tag{A.3}$$

If there are j identical particles among the n, there is an extra factor $1/j!$. For the case $n = 2$, in the center of momentum frame, and with both outgoing particles having equal mass m

$$dPS(2) = \frac{1}{16\pi} \sqrt{1 - \frac{4m^2}{s}} \, d\cos\theta \,, \tag{A.4}$$

where θ is the polar angle of one of the outgoing particles with respect to the collision axis.

The width for the decay of a particle with mass Q and 4-momentum k to n particles with 4-momenta $\{p_i\}$ reads

$$\Gamma = \frac{1}{2Q} \overline{\sum}_{\text{spins,(colours..)}} \int |\mathcal{M}|^2 \, dPS(n) \,. \tag{A.5}$$

If there are j identical particles among the n, there is an extra factor $1/j!$. For the case $n = 2$, in the center of momentum frame

$$dPS(2) = \frac{1}{16\pi Q^2} \sqrt{\lambda(Q^2, m_1^2, m_2^2)} d\cos\theta \,, \tag{A.6}$$

where θ is the polar angle of one of the outgoing particles with respect to some arbitrary axis, and $\lambda(x, y, z) = x^2 + y^2 + z^2 - 2xy - 2xz - 2yz$.

Dirac algebra

Dirac equation in x-space:
$$(\slashed{\partial} + m)\psi(x) = 0 \tag{A.7}$$

Dirac equation in momentum space for u and v spinors:

$$(i\slashed{p} + m)\, u(p, s) = 0, \qquad (i\slashed{p} - m)\, v(p, s) = 0 \tag{A.8}$$

$$\{\gamma^\mu, \gamma^\nu\} = 2\eta^{\mu\nu} \tag{A.9}$$

where on the right hand side the 4 by 4 unit matrix in spinor space is implied. An often-used identity based on this is
$$\slashed{p}\slashed{p} = p^2 \,. \tag{A.10}$$

Other useful relations:

$$\gamma^0 = -i \begin{pmatrix} 1 & 0 \\ 0 & -1 \end{pmatrix}, \qquad \vec{\gamma} = -i \begin{pmatrix} 0 & \vec{\sigma} \\ -\vec{\sigma} & 0 \end{pmatrix}, \tag{A.11}$$

$$(\gamma^\mu)^\dagger = \gamma^0 \gamma^\mu \gamma^0 \,, \tag{A.12}$$

$$\gamma_5 = i\gamma_0\gamma_1\gamma_2\gamma_3 \,, \tag{A.13}$$

$$\gamma_5 = \begin{pmatrix} 0 & 1 \\ 1 & 0 \end{pmatrix}, \tag{A.14}$$

$$\{\gamma_5, \gamma^\mu\} = 0 \,, \tag{A.15}$$

$$\gamma^\mu \slashed{a} \gamma_\mu = -2\slashed{a}, \quad \gamma^\mu \slashed{a}\slashed{b}\gamma_\mu = 4a\cdot b, \quad \gamma^\mu \slashed{a}\slashed{b}\slashed{c}\gamma_\mu = -2\slashed{c}\slashed{b}\slashed{a}\,, \tag{A.16}$$

$$\text{Tr}(\gamma^\mu) = \text{Tr}(\gamma_5) = 0\,, \quad \text{Tr}(\gamma^\mu\gamma^\nu\gamma^\rho) = 0\,,$$
$$\text{Tr}(\gamma_5\gamma_\mu) = \text{Tr}(\gamma_5\gamma_\mu\gamma_\nu) = \text{Tr}(\gamma_5\gamma_\mu\gamma_\nu\gamma_\rho) = 0\,, \tag{A.17}$$

$$\text{Tr}(\gamma^\mu\gamma^\nu) = 4\,\eta^{\mu\nu}, \quad \text{Tr}(\gamma^\mu\gamma^\nu\gamma^\rho\gamma^\sigma) = 4\left(\eta^{\mu\nu}\eta^{\rho\sigma} - \eta^{\mu\rho}\eta^{\nu\sigma} + \eta^{\mu\sigma}\eta^{\nu\rho}\right), \tag{A.18}$$

$$\text{Tr}(\gamma_\mu\gamma_\nu\gamma_\rho\gamma_\sigma\gamma_5) = -4i\epsilon_{\mu\nu\rho\sigma}\,, \quad \epsilon_{0123} = +1\,. \tag{A.19}$$

Conjugate spinor:
$$\bar{\psi} = i\psi^\dagger\gamma^0 \,. \tag{A.20}$$

With this definition the term
$$\bar{\psi}\psi \tag{A.21}$$

is hermitean, since γ^0 is anti-hermitean. The chiral (left- and righthanded) projections of a fermion are defined by

$$
\begin{aligned}
\psi_L &= \left(\frac{1+\gamma_5}{2}\right)\psi\,, \\
\psi_R &= \left(\frac{1-\gamma_5}{2}\right)\psi\,.
\end{aligned}
\tag{A.22}
$$

A parity transform on a spinor is defined by

$$
P : \psi(x) \to \gamma_0\psi(\tilde{x})\,,
\tag{A.23}
$$

with $\tilde{x} = (x^0, -\vec{x})$. Complex-conjugation of general spinor-trace:

$$
(\bar{u}(p)\gamma_{\mu_1}\cdots\gamma_{\mu_n}u(p'))^* = (-)^n \left(\bar{u}(p')\gamma_{\mu_n}\cdots\gamma_{\mu_1}u(p)\right),
\tag{A.24}
$$

$$
(\bar{u}(p)\gamma_{\mu_1}\cdots\gamma_{\mu_n}\gamma_5 u(p'))^* = -(-)^n \left(\bar{u}(p')\gamma_5\gamma_{\mu_n}\cdots\gamma_{\mu_1}u(p)\right).
\tag{A.25}
$$

Unitary groups and their Lie algebras

The U(1) Lie algebra has only 1 generator t, which we choose hermitean. Acting on a d-dimensional vector t may be represented as the d-dimensional unit matrix. The group elements are then

$$
\exp\left(i\alpha\,t\right).
\tag{A.26}
$$

The SU(2) Lie algebra has 3 generators t_i, $i = 1, 2, 3$. If we choose the t_i hermitean, then in the fundamental representation $t_i^{(F)} = \sigma_i/2$, with σ_i the Pauli matrices

$$
\sigma_1 = \begin{pmatrix} 0 & 1 \\ 1 & 0 \end{pmatrix} \quad \sigma_2 = \begin{pmatrix} 0 & -i \\ i & 0 \end{pmatrix} \quad \sigma_3 = \begin{pmatrix} 1 & 0 \\ 0 & -1 \end{pmatrix}.
\tag{A.27}
$$

The group elements are

$$
U = \exp\left(i\xi^i\,t_i\right).
\tag{A.28}
$$

Note that for the fundamental representation

$$
\sigma_2 U \sigma_2 = U^* = (U^\dagger)^T.
\tag{A.29}
$$

Note that the SU(2) Lie-algebra is isomorphic to the SO(3) Lie-algebra, whose generators $t_i = -iS_i$ read, in the fundamental representation:

$$
S_1 = \begin{pmatrix} 0 & 0 & 0 \\ 0 & 0 & 1 \\ 0 & -1 & 0 \end{pmatrix} \quad S_2 = \begin{pmatrix} 0 & 0 & -1 \\ 0 & 0 & 0 \\ 1 & 0 & 0 \end{pmatrix} \quad S_3 = \begin{pmatrix} 0 & 1 & 0 \\ -1 & 0 & 0 \\ 0 & 0 & 0 \end{pmatrix}.
\tag{A.30}
$$

The SU(3) Lie algebra has 8 generators t_i, $i = 1,\ldots 8$, which are not needed explicitly. Lie algebra generators in general obey the commutation relations

$$
[t_i, t_j] = i\,f_{ijk}\,t_k\,,
\tag{A.31}
$$

with the f_{ijk} the structure constants for the given group. The kj matrix element of the generator $t_i^{(A)}$ in the adjoint representation is defined as

$$
\left[t_i^{(A)}\right]_{kj} = i\,f_{ijk}\,.
\tag{A.32}
$$

Note that we can always choose anti-hermitean generators t' by multiplying the hermitean versions t by i. In that case the group elements for SU(2) e.g. are

$$\exp\left(\xi^i\, t'_i\right).$$ (A.33)

Representations of SU(2), etc. groups are often indicated by $\underline{2}, \ldots$ indicating the size of the matrices of that representation. Trivial or singlet representation are then indicated with $\underline{1}$.

Some other group theory factors (the so-called Casimir factors):

$$\begin{aligned} \text{SU}(2): & \quad C_A &= & \quad 2, \quad C_F = \frac{3}{4}, \\ \text{SU}(3): & \quad C_A &= & \quad 3, \quad C_F = \frac{4}{3}. \end{aligned}$$

For the fundamental representation of $SU(N)$ we have

$$\text{Tr}\left[t_i^{(F)} t_j^{(F)}\right] = \frac{1}{2}\delta_{ij}.$$ (A.34)

Standard Model quantities

The amount of electric charge (in units of e) Q, the hypercharge Y and the third component of weak isospin t_3 are related by

$$Y = 2(Q - t_3).$$ (A.35)

In the Standard Model the generator of the U(1) of hypercharge is conventionally written as

$$\frac{1}{2}Y,$$ (A.36)

and is then represented on d-dimensional vectors as $1/2$ times the hypercharge eigenvalue times the unit matrix.

The gauge couplings associated with the $\text{SU}_{I_W}(2)$ and $\text{U}_Y(1)$ gauge groups are traditionally denoted g and g' respectively. In terms of these couplings the unit of electric charge is

$$e = \frac{g\,g'}{\sqrt{g^2 + g'^2}} = g\,\sin\theta_W = g'\,\cos\theta_W,$$ (A.37)

with $\sin^2\theta_W \simeq 0.226$.

The gauge fields are mixed as follows:

$$\begin{aligned} B_\mu &= \cos\theta_W A_\mu - \sin\theta_W Z_\mu, \quad W_\mu^3 = \cos\theta_W Z_\mu + \sin\theta_W A_\mu, \end{aligned}$$ (A.38)

$$W_\mu^1 - iW_\mu^2 = \sqrt{2}W_\mu^+, \quad W_\mu^1 + iW_\mu^2 = \sqrt{2}W_\mu^-.$$ (A.39)

The Fermi constant is defined by

$$G_F = \frac{g^2}{4\sqrt{2}m_W^2} = \frac{1}{\sqrt{2}v^2} \simeq 1.2 \times 10^{-5}\,\text{GeV}^2.$$ (A.40)

Vector boson masses in GeV:

$$m_Z = \frac{gv}{2\cos\theta_W} = 91.1876 \pm 0.0021, \quad m_W = \frac{gv}{2} = 80.385 \pm 0.015.$$ (A.41)

The photon and gluon are massless.

Heavy quark masses in GeV:

$$m_c = 1.5, \quad m_b = 5, \quad m_t = 175. \tag{A.42}$$

u, d, s are massless.

Lepton masses in GeV:

$$m_\tau = 1.7, \quad m_\mu = 0.105, \quad m_e = 0.0005. \tag{A.43}$$

QCD scale in GeV:

$$\Lambda_{QCD} \simeq 0.2. \tag{A.44}$$

Assorted Feynman rules

All momenta in vertex Feynman rules are incoming here.

– Fermion propagator

$$\frac{1}{i(2\pi)^4} \frac{(-i\not{p} + m)_{\beta\alpha}}{p^2 + m^2 - i\epsilon} \tag{A.45}$$

– Electron-electron photon vertex
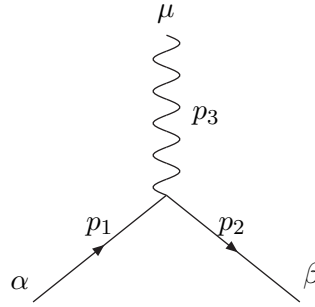
$$i(2\pi)^4 \delta(p_1 + p_2 + p_3)(-ie)\, \gamma^\mu_{\beta\alpha} \tag{A.46}$$

where the three momentum vectors (not drawn) are pointing to the vertex.

– Outgoing fermion: $\overline{u}(p,s)$ Row spinor

– Outgoing anti-fermion: $v(p,s)$ Column spinor

– Incoming fermion: $u(p,s)$ Column spinor

– Incoming antifermion: $\overline{v}(p,s)$ Row spinor

– Outgoing vector boson: $\epsilon^*_\mu(k,\lambda)$

– Incoming vector boson: $\epsilon_\mu(k,\lambda)$

In Feynman diagrams, always start where the charge vector top of the fermion lines *ends* (i.e. start with a row spinor), and work your way back against the charge flow.

Integrate over internal momenta: $\int d^4 k_i$

Completeness relations for spin sums over polarization spinors and polarization vectors, associated with external particles

$$\sum_s u_\alpha(p,s)\overline{u}_\beta(p,s) = (-i\not{p} + m)_{\alpha\beta}\,, \tag{A.47}$$

$$\sum_s v_\alpha(p,s)\overline{v}_\beta(p,s) = (-i\not{p} - m)_{\alpha\beta}\,, \tag{A.48}$$

with m the fermion mass, α, β are spinor indices.

For photons the sum over the two physical polarizations gives

$$\sum_\lambda \epsilon^\mu(k,\lambda)\epsilon^{*\,\nu}(k,\lambda) = \eta^{\mu\nu} - \frac{k^\mu \bar{k}^\nu + k^\nu \bar{k}^\mu}{k \cdot \bar{k}}\,, \tag{A.49}$$

where the sum is over the physical spin only, and we define

$$k^\mu = (k^0, \vec{k}), \qquad \bar{k}^\mu = (-k^0, \vec{k})\,. \tag{A.50}$$

The photon propagator is (κ is the gauge parameter here)

$$\Delta_{\mu\nu}(k) = \frac{1}{i(2\pi)^4}\frac{1}{k^2 - i\epsilon}\left(\eta_{\mu\nu} - \left(1 - \frac{1}{\kappa^2}\right)\frac{k_\mu k_\nu}{k^2}\right)\,. \tag{A.51}$$

The scalar field propagator is simply

$$\Delta(p) = \frac{1}{i(2\pi)^4}\frac{1}{p^2 + m^2 - i\epsilon}\,. \tag{A.52}$$

For massive vector bosons the sum over the three physical polarizations gives

$$\sum_\lambda \epsilon^\mu(k,\lambda)\epsilon^{*\,\nu}(k,\lambda) = \eta^{\mu\nu} + \frac{k^\mu k^\nu}{M^2}\,. \tag{A.53}$$

Loop integrals

$$\frac{1}{A_1 A_2} = \int_0^1 dx_1 \int_0^1 dx_2 \frac{\delta(1 - x_1 - x_2)}{[x_1 A_1 + x_2 A_2]^2}\,. \tag{A.54}$$

The result for the integral

$$I(n,\alpha) = \int d^n q \frac{1}{(q^2 + m^2 - i\epsilon)^\alpha} \tag{A.55}$$

is

$$I(n,\alpha) = i\pi^{n/2}\frac{\Gamma(\alpha - (n/2))}{\Gamma(\alpha)}\left(m^2\right)^{(n/2)-\alpha}\,. \tag{A.56}$$

The Euler gamma function $\Gamma(z)$ has the following relevant properties:

$$\Gamma(z+1) = z\Gamma(z), \quad \Gamma(1) = 1\,, \tag{A.57}$$

$$\ln\Gamma(1+z) \simeq -z\gamma_E + \mathcal{O}(z^2), \quad \gamma_E = 0.577\ldots \tag{A.58}$$

References

[1] H1 and ZEUS Collaboration, F. D. Aaron *et al.*, "Combined Measurement and QCD Analysis of the Inclusive e^+p Scattering Cross Sections at HERA," *JHEP* **1001** (2010) 109, `0911.0884`.

[2] J. Callan, C. G. and D. J. Gross, "High-energy electroproduction and the constitution of the electric current," *Phys. Rev. Lett.* **22** (1969) 156–159.

[3] R. D. Ball, V. Bertone, S. Carrazza, C. S. Deans, L. Del Debbio, *et al.*, "Parton distributions with LHC data," *Nucl.Phys.* **B867** (2013) 244–289, `1207.1303`.

[4] "The durham hepdata project,".

[5] B. De Wit and J. Smith, *Field Theory in Particle Physics Volume 1*. North-Holland, Amsterdam, Netherlands, 1986.

[6] P. A. Baikov, K. G. Chetyrkin, and J. H. KÃijhn, "Five-Loop Running of the QCD coupling constant," `1606.08659`.

[7] S. Forte and G. Watt, "Progress in the Determination of the Partonic Structure of the Proton," *Ann.Rev.Nucl.Part.Sci.* **63** (2013) 291–328, `1301.6754`.

[8] J. C. Collins, D. E. Soper, and G. Sterman, "Factorization of hard processes in qcd,". in *Perturbative Quantum Chromodynamics*, A.H. Mueller ed., World Scientific, Singapore, 1989.

[9] S. Moch, J. A. M. Vermaseren, and A. Vogt, "The three-loop splitting functions in qcd: The non-singlet case," *Nucl. Phys.* **B688** (2004) 101–134, `hep-ph/0403192`.

[10] A. Vogt, S. Moch, and J. A. M. Vermaseren, "The three-loop splitting functions in qcd: The singlet case," *Nucl. Phys.* **B691** (2004) 129–181, `hep-ph/0404111`.

[11] A. D. Martin, W. J. Stirling, R. S. Thorne, and G. Watt, "Parton distributions for the LHC," *Eur. Phys. J.* **C63** (2009) 189–285, `0901.0002`.

[12] J. Rojo, A. Accardi, R. D. Ball, A. Cooper-Sarkar, A. de Roeck, *et al.*, "The PDF4LHC report on PDFs and LHC data: Results from Run I and preparation for Run II," `1507.00556`.

[13] K. Fabricius, I. Schmitt, G. Kramer, and G. Schierholz, "Higher order perturbative qcd calculation of jet cross- sections in e+ e- annihilation," *Zeit. Phys.* **C11** (1981) 315.

[14] G. K. J. F. Vermaseren, J. A. M. and S. J. Oldham, "Perturbative QCD calculation of jet cross-sections in e^+e^- annihilation," *Nucl.Phys.* **B187** (1981) 301.

[15] Z. Kunszt, "Comment on the $\mathcal{O}(\alpha_S^2)$ corrections to jet production in e^+e^- annihilation," *Phys. Lett.* **B99** (1981) 429.

[16] R. K. Ellis, D. A. Ross, and A. E. Terrano, "The perturbative calculation of jet structure in e+ e- annihilation," *Nucl. Phys.* **B178** (1981) 421.

[17] A. Gehrmann-De Ridder, T. Gehrmann, E. W. N. Glover, and G. Heinrich, "NNLO corrections to event shapes in e^+e^- annihilation," *JHEP* **12** (2007) 094, `0711.4711`.

[18] T. Kinoshita, "Mass singularities of Feynman amplitudes," *J. Math. Phys.* **3** (1962) 650–677.

[19] T. D. Lee and M. Nauenberg, "Degenerate Systems and Mass Singularities," *Phys. Rev.* **133** (1964) B1549–B1562.

[20] F. Bloch and A. Nordsieck, "Note on the Radiation Field of the electron," *Phys. Rev.* **52** (1937) 54–59.

[21] C. K. G. K. J. H. Baikov, P. A. and J. Rittinger, "Adler function, sum rules and Crewther relation of order $O(\alpha_s^4)$: the singlet case," *Phys. Lett.* **B714** (2012) 62–65, `1206.1288`.

[22] G. F. Sterman and S. Weinberg, "Jets from quantum chromodynamics," *Phys. Rev. Lett.* **39** (1977) 1436.

[23] S. D. Drell and T.-M. Yan, "Partons and their applications at high-energies," *Annals Phys.* **66** (1971) 578.

[24] J. R. Forshaw, M. H. Seymour, and A. Siodmok, "On the Breaking of Collinear Factorization in

QCD," *JHEP* **11** (2012) 066, 1206.6363.

[25] S. Catani, D. de Florian, and G. Rodrigo, "Factorization violation in the multiparton collinear limit," *PoS* **LL2012** (2012) 035, 1211.7274.

[26] S. J. Parke and T. R. Taylor, "An amplitude for n gluon scattering," *Phys. Rev. Lett.* **56** (1986) 2459.

[27] F. A. Berends, W. T. Giele, and H. Kuijf, "Exact expressions for processes involving a vector boson and up to five partons," *Nucl. Phys.* **B321** (1989) 39.

[28] F. A. Berends and W. T. Giele, "Recursive calculations for processes with n gluons," *Nucl. Phys.* **B306** (1988) 759.

[29] M. L. Mangano, "The Color Structure of Gluon Emission," *Nucl. Phys.* **B309** (1988) 461.

[30] R. Britto, F. Cachazo, and B. Feng, "New recursion relations for tree amplitudes of gluons," *Nucl. Phys.* **B715** (2005) 499–522, hep-th/0412308.

[31] R. Britto, F. Cachazo, B. Feng, and E. Witten, "Direct proof of tree-level recursion relation in Yang- Mills theory," *Phys. Rev. Lett.* **94** (2005) 181602, hep-th/0501052.

[32] E. Witten, "Perturbative gauge theory as a string theory in twistor space," *hep-th/0312171* (2003) hep-th/0312171.

[33] F. Cachazo, P. Svrcek, and E. Witten, "Mhv vertices and tree amplitudes in gauge theory," *JHEP* **09** (2004) 006, hep-th/0403047.

[34] C. Duhr, S. Hoche, and F. Maltoni, "Color-dressed recursive relations for multi-parton amplitudes," *JHEP* **08** (2006) 062, hep-ph/0607057.

[35] M. Dinsdale, M. Ternick, and S. Weinzierl, "A comparison of efficient methods for the computation of Born gluon amplitudes," *JHEP* **03** (2006) 056, hep-ph/0602204.

[36] Z. Bern, L. J. Dixon, and D. A. Kosower, "On-Shell Methods in Perturbative QCD," *Annals Phys.* **322** (2007) 1587–1634, 0704.2798.

[37] G. Passarino and M. J. G. Veltman, "One Loop Corrections for e+ e- Annihilation Into mu+ mu- in the Weinberg Model," *Nucl. Phys.* **B160** (1979) 151.

[38] A. Denner and S. Dittmaier, "Reduction schemes for one-loop tensor integrals," *Nucl. Phys.* **B734** (2006) 62–115, hep-ph/0509141.

[39] T. Binoth, J. P. Guillet, G. Heinrich, E. Pilon, and C. Schubert, "An algebraic / numerical formalism for one-loop multi-leg amplitudes," *JHEP* **10** (2005) 015, hep-ph/0504267.

[40] W. L. van Neerven and J. A. M. Vermaseren, "Large loop integrals," *Phys. Lett.* **B137** (1984) 241.

[41] Z. Bern, L. J. Dixon, and D. A. Kosower, "Dimensionally regulated one loop integrals," *Phys. Lett.* **B302** (1993) 299–308, hep-ph/9212308.

[42] Z. Bern, L. J. Dixon, and D. A. Kosower, "Dimensionally regulated pentagon integrals," *Nucl. Phys.* **B412** (1994) 751–816, hep-ph/9306240.

[43] R. K. Ellis and G. Zanderighi, "Scalar one-loop integrals for QCD," *JHEP* **02** (2008) 002, 0712.1851.

[44] Z. Bern, L. J. Dixon, D. C. Dunbar, and D. A. Kosower, "One loop n point gauge theory amplitudes, unitarity and collinear limits," *Nucl. Phys.* **B425** (1994) 217–260, hep-ph/9403226.

[45] Z. Bern, L. J. Dixon, D. C. Dunbar, and D. A. Kosower, "One-loop self-dual and N = 4 superYang-Mills," *Phys. Lett.* **B394** (1997) 105–115, hep-th/9611127.

[46] Z. Bern and A. G. Morgan, "Massive loop amplitudes from unitarity," *Nucl. Phys.* **B467** (1996) 479–509, hep-ph/9511336.

[47] C. Anastasiou, R. Britto, B. Feng, Z. Kunszt, and P. Mastrolia, "Unitarity cuts and reduction to master integrals in d dimensions for one-loop amplitudes," *JHEP* **03** (2007) 111, hep-ph/0612277.

[48] A. Brandhuber, S. McNamara, B. J. Spence, and G. Travaglini, "Loop amplitudes in pure

Yang-Mills from generalised unitarity," *JHEP* **10** (2005) 011, `hep-th/0506068`.

[49] R. Britto, F. Cachazo, and B. Feng, "Generalized unitarity and one-loop amplitudes in N = 4 super-Yang-Mills," *Nucl. Phys.* **B725** (2005) 275–305, `hep-th/0412103`.

[50] G. Ossola, C. G. Papadopoulos, and R. Pittau, "Reducing full one-loop amplitudes to scalar integrals at the integrand level," *Nucl. Phys.* **B763** (2007) 147–169, `hep-ph/0609007`.

[51] Z. Nagy and D. E. Soper, "Numerical integration of one-loop Feynman diagrams for N- photon amplitudes," *Phys. Rev.* **D74** (2006) 093006, `hep-ph/0610028`.

[52] C. Anastasiou, S. Beerli, and A. Daleo, "Evaluating multi-loop Feynman diagrams with infrared and threshold singularities numerically," *JHEP* **05** (2007) 071, `hep-ph/0703282`.

[53] R. K. Ellis, W. T. Giele, and G. Zanderighi, "Semi-numerical evaluation of one-loop corrections," *Phys. Rev.* **D73** (2006) 014027, `hep-ph/0508308`.

[54] C. F. Berger *et al.*, "One-Loop Calculations with BlackHat," `0807.3705`.

[55] G. Ossola, C. G. Papadopoulos, and R. Pittau, "CutTools: a program implementing the OPP reduction method to compute one-loop amplitudes," *JHEP* **03** (2008) 042, `0711.3596`.

[56] W. T. Giele and G. Zanderighi, "On the Numerical Evaluation of One-Loop Amplitudes: the Gluonic Case," `0805.2152`.

[57] J. M. Campbell and R. K. Ellis, "Radiative corrections to Z b anti-b production," *Phys. Rev.* **D62** (2000) 114012, `hep-ph/0006304`.

[58] S. Alioli, P. Nason, C. Oleari, and E. Re, "A general framework for implementing NLO calculations in shower Monte Carlo programs: the POWHEG BOX," *JHEP* **06** (2010) 043, `1002.2581`.

[59] J. Alwall, R. Frederix, S. Frixione, V. Hirschi, F. Maltoni, *et al.*, "The automated computation of tree-level and next-to-leading order differential cross sections, and their matching to parton shower simulations," *JHEP* **1407** (2014) 079, `1405.0301`.

[60] H. Johansson, D. A. Kosower, and K. J. Larsen, "An Overview of Maximal Unitarity at Two Loops," *PoS* **LL2012** (2012) 066, `1212.2132`.

[61] E. B. Zijlstra and W. L. van Neerven, "Order alpha-s**2 qcd corrections to the deep inelastic proton structure functions f2 and f(l)," *Nucl. Phys.* **B383** (1992) 525–574.

[62] R. Hamberg, W. L. van Neerven, and T. Matsuura, "A complete calculation of the order alpha-s**2 correction to the drell-yan k factor," *Nucl. Phys.* **B359** (1991) 343–405.

[63] C. Anastasiou and K. Melnikov, "Higgs boson production at hadron colliders in nnlo qcd," *Nucl. Phys.* **B646** (2002) 220–256, `hep-ph/0207004`.

[64] R. V. Harlander and W. B. Kilgore, "Next-to-next-to-leading order higgs production at hadron colliders," *Phys. Rev. Lett.* **88** (2002) 201801, `hep-ph/0201206`.

[65] V. Ravindran, J. Smith, and W. L. van Neerven, "Two-loop corrections to higgs boson production," *Nucl. Phys.* **B704** (2005) 332–348, `hep-ph/0408315`.

[66] C. Anastasiou, C. Duhr, F. Dulat, F. Herzog, and B. Mistlberger, "Higgs boson gluon-fusion production in N3LO QCD," `1503.06056`.

[67] J. A. M. Vermaseren, "The FORM project," *Nucl.Phys.Proc.Suppl.* **183** (2008) 19–24, `0806.4080`.

[68] U. T. V. J. A. M. Kuipers, J. and J. Vollinga, "FORM version 4.0," *Comput.Phys.Commun.* **184** (2013) 1453–1467, `1203.6543`.

[69] M. Czakon, P. Fiedler, and A. Mitov, "The total top quark pair production cross-section at hadron colliders through $\mathcal{O}(\alpha_S^4)$," *Phys.Rev.Lett.* **110** (2013) 252004, `1303.6254`.

[70] A. Gehrmann-De Ridder, T. Gehrmann, E. Glover, and J. Pires, "Second order QCD corrections to jet production at hadron colliders: the all-gluon contribution," *Phys.Rev.Lett.* **110** (2013), no. 16, 162003, `1301.7310`.

[71] G. Sterman, "Summation of large corrections to short distance hadronic cross-sections," *Nucl.*

Phys. **B281** (1987) 310.

[72] S. Catani and L. Trentadue, "Resummation of the QCD Perturbative Series for Hard Processes," *Nucl. Phys.* **B327** (1989) 323.

[73] H. Contopanagos, E. Laenen, and G. Sterman, "Sudakov factorization and resummation," *Nucl. Phys.* **B484** (1997) 303–330, `hep-ph/9604313`.

[74] C. W. Bauer, S. Fleming, D. Pirjol, and I. W. Stewart, "An effective field theory for collinear and soft gluons: Heavy to light decays," *Phys. Rev.* **D63** (2001) 114020, `hep-ph/0011336`.

[75] C. W. Bauer, D. Pirjol, and I. W. Stewart, "Soft-Collinear Factorization in Effective Field Theory," *Phys. Rev.* **D65** (2002) 054022, `hep-ph/0109045`.

[76] M. Beneke, A. P. Chapovsky, M. Diehl, and T. Feldmann, "Soft-collinear effective theory and heavy-to-light currents beyond leading power," *Nucl. Phys.* **B643** (2002) 431–476, `hep-ph/0206152`.

[77] T. Becher, A. Broggio, and A. Ferroglia, "Introduction to Soft-Collinear Effective Theory," `1410.1892`.

[78] G. Sterman, "Infrared divergences in perturbative qcd. (talk),". In *Tallahassee 1981, Proceedings, Perturbative Quantum Chromodynamics*, 22-40.

[79] J. G. M. Gatheral, "Exponentiation of eikonal cross-sections in nonabelian gauge theories," *Phys. Lett.* **B133** (1983) 90.

[80] J. Frenkel and J. C. Taylor, "Nonabelian eikonal exponentiation," *Nucl. Phys.* **B246** (1984) 231.

[81] E. Laenen, L. Magnea, G. Stavenga, and C. D. White, "Next-to-eikonal corrections to soft gluon radiation: a diagrammatic approach," *JHEP* **01** (2011) 141, `1010.1860`.

[82] E. Laenen, G. Stavenga, and C. D. White, "Path integral approach to eikonal and next-to-eikonal exponentiation," `0811.2067`.

[83] E. Gardi, E. Laenen, G. Stavenga, and C. D. White, "Webs in multiparton scattering using the replica trick," *JHEP* **11** (2010) 155, `1008.0098`.

[84] A. Mitov, G. Sterman, and I. Sung, "Diagrammatic Exponentiation for Products of Wilson Lines," *Phys. Rev.* **D82** (2010) 096010, `1008.0099`.

[85] C. White, "An Introduction to Webs," `1507.02167`.

[86] A. Banfi, G. P. Salam, and G. Zanderighi, "Principles of general final-state resummation and automated implementation," *JHEP* **03** (2005) 073, `hep-ph/0407286`.

[87] T. Becher, R. Frederix, M. Neubert, and L. Rothen, "Automated NNLL + NLO resummation for jet-veto cross sections," *Eur.Phys.J.* **C75** (2015), no. 4, 154, `1412.8408`.

[88] A. Vogt, "Next-to-next-to-leading logarithmic threshold resummation for deep-inelastic scattering and the drell-yan process," *Phys. Lett.* **B497** (2001) 228–234, `hep-ph/0010146`.

[89] S. Catani, M. L. Mangano, P. Nason, and L. Trentadue, "The resummation of soft gluons in hadronic collisions," *Nucl. Phys.* **B478** (1996) 273–310, `hep-ph/9604351`.

[90] M. Bonvini and S. Marzani, "Resummed Higgs cross section at N^{3}LL," *JHEP* **1409** (2014) 007, `1405.3654`.

[91] M. Czakon, A. Mitov, and G. F. Sterman, "Threshold Resummation for Top-Pair Hadroproduction to Next-to-Next-to-Leading Log," *Phys.Rev.* **D80** (2009) 074017, `0907.1790`.

[92] N. Kidonakis and G. F. Sterman, "Resummation for QCD hard scattering," *Nucl. Phys.* **B505** (1997) 321–348, `hep-ph/9705234`.

[93] R. Bonciani, S. Catani, M. L. Mangano, and P. Nason, "NLL resummation of the heavy-quark hadroproduction cross- section," *Nucl. Phys.* **B529** (1998) 424–450, `hep-ph/9801375`. [Erratum-ibid.B803:234,2008].

Higgs Physics

A. Pomarol
Dept. de Física, Universitat Autònoma de Barcelona, Barcelona, Spain

Abstract
With the discovery of the Higgs, we have access to a plethora of new physical processes that allow us to further test the SM and beyond. We show a convenient way to parametrize these physics using an effective theory for Higgs couplings, discussing the importance of the basis selection, predictions from a SM effective field theory, and possible ways to measure these couplings with special attention to the high-energy regime. Predictions from the MSSM and MCHM, with the comparison with data, are also provided.

1 Motivation

The 4th of July of 2012 marked a milestone in particle physics, as CERN announced the discovery of a new particle whose properties were in accordance with the sought-after Higgs boson [1]. Since then, we have been accumulating more and more data and measuring more decay channels, increasing the significance of the discovery while keeping at the same time a good agreement with the predictions from the Standard Model (SM) Higgs [2, 3]. To appreciate this agreement, it is convenient to plot the experimental fit to Higgs couplings in the coupling–mass plane, as shown in Fig. 1 by courtesy of CMS [2]. Were this new particle not the SM Higgs, we would have expected its couplings to lay on any point of this plane, and therefore differing significantly from the SM predictions. As an example, let us consider a scalar coming from a weak-doublet not being (the main) responsible for electroweak symmetry breaking (EWSB). This scalar could have couplings to fermions as large as $O(1)$, but very small couplings to Z/W. These predictions are shown in red in Fig. 1. Data clearly disfavours this type of scalars as compared with the SM Higgs whose predictions lay on a straight line. We can then say today that the SM Higgs is significantly supported by the experimental data, leaving most competitors far behind.

Having discovered the Higgs, we have now experimental access to new processes that will help us to test the SM and beyond. There is a fundamental aspect that makes Higgs physics very special: the Higgs is the only particle of the SM that its lightness ($m_h \sim 125$ GeV $\ll M_P$) is not expected on theoretical grounds, requiring the presence of new physics beyond the SM (BSM) at the TeV. This is referred as the hierarchy problem. This makes the Higgs boson one of the most sensitive SM particle to BSM effects, and therefore the measurement of its properties one of the best ways to indirectly discover new physics and help to discriminate between different BSMs. As an example, two of the most well-motivated BSM scenarios, the minimal supersymmetric SM and the composite Higgs, predict, as we will see below, sizeable corrections to the Higgs couplings. In few words, natural theories explaining the lightness of the Higgs demand the Higgs to be SM-like only in a first approximation, predicting departures from the SM predictions to be seen in the near future.

2 Effective Higgs couplings

To characterize the most interesting Higgs processes, it is convenient to parametrize, in the most general way possible, the couplings of the Higgs to the SM particles. For this purpose we will write an effective theory for the Higgs couplings, $\mathcal{L}_h$. We will define $\mathcal{L}_h$ in position-space, as it makes it simpler to eliminate redundancies. Our only approximation at this point will be to assume that the momenta q in the Higgs form-factors are smaller than a heavy scale Λ associated with the BSM physical scale, $q/\Lambda \ll 1$. This is equivalent to say that we can make an expansion in derivatives D_μ/Λ in $\mathcal{L}_h$. We leave for later the implications when an expansion of SM fields over Λ can be also carried out. We assume that the interactions preserve $SU(3)_c \times U(1)_{EM}$, with the Higgs defined as a neutral CP-even scalar field.
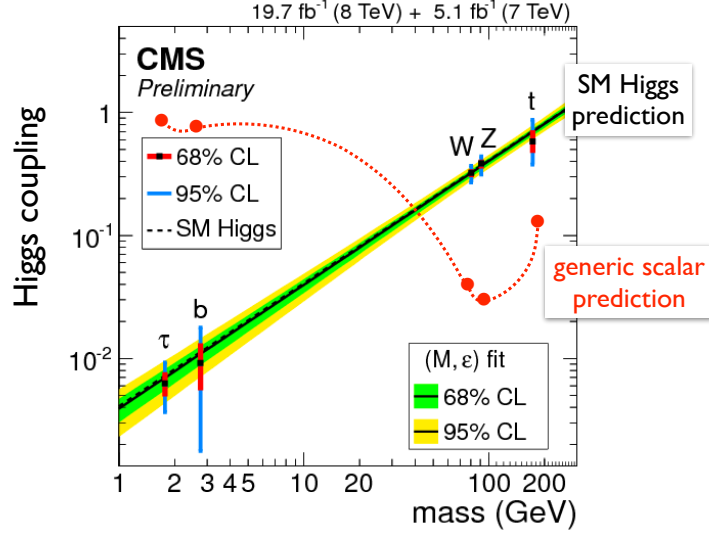
Fig. 1: Fit of the Higgs couplings, g^h_{ff} and $\sqrt{g^h_{VV}/2v}$, and predictions from the SM [2]. A generic scalar would have couplings to the SM particles laying in any point of this plane, as the example shown in red. The experimental data clearly favors a SM Higgs.

We split the Higgs couplings in two sets. One set that consists of what we call *primary* Higgs couplings and the other set containing the rest. These primaries, as we will explain later, play an important role, both theoretically and phenomenologically. We then write

$$\mathcal{L}_h = \mathcal{L}_h^{\text{primary}} + \Delta\mathcal{L}_h. \tag{1}$$

We will only keep interactions up to order $O(h^3)$, $O(h\partial^2 V^2)$ and $O(hVf^2)$ since they are the most relevant for Higgs phenomenology (adding more derivatives will be suppressed by inverse powers of Λ, and adding more fields makes the interactions harder to be observed at colliders since they will be further suppressed by phase space). Then, for CP-conserving couplings, we have *without loss of generality* [1]

$$
\begin{aligned}
\mathcal{L}_h^{\text{primary}} &= g^h_{VV}\, h\left[W^{+\mu}W^-_\mu + \frac{1}{2c^2_{\theta_W}}Z^\mu Z_\mu\right] + \frac{1}{6}\,g_{3h}\,h^3 + g^h_{ff}\,\left(h\bar{f}_L f_R + h.c.\right)\\
&+ \kappa_{GG}\frac{h}{2v}G^{A\mu\nu}G^A_{\mu\nu} + \kappa_{\gamma\gamma}\frac{h}{2v}A^{\mu\nu}A_{\mu\nu} + \kappa_{Z\gamma}\frac{h}{v}A^{\mu\nu}Z_{\mu\nu},
\end{aligned}\tag{2}
$$

and

$$
\begin{aligned}
\Delta\mathcal{L}_h &= \delta g^h_{ZZ}\,h\frac{Z^\mu Z_\mu}{2c^2_{\theta_W}} + g^h_{Zff}\,\frac{h}{2v}\left(Z_\mu J^\mu_N + h.c.\right) + g^h_{Wff'}\,\frac{h}{v}\left(W^+_\mu J^\mu_C + h.c.\right)\\
&+ \kappa_{WW}\frac{h}{v}W^{+\mu\nu}W^-_{\mu\nu} + \kappa_{ZZ}\frac{h}{2v}Z^{\mu\nu}Z_{\mu\nu},
\end{aligned}\tag{3}
$$

where $J^\mu_N = \bar{f}\gamma^\mu f$ (for $f = f_L, f_R$) and $J^\mu_C = \bar{f}\gamma^\mu f'$ are respectively the neutral and charged currents. Flavour indices are implicit. We also defined $c_{\theta_W} \equiv \cos\theta_W$ where θ_W is the weak-angle, and $G^A_{\mu\nu} \equiv \partial_\mu G^A_\nu - \partial_\nu G^A_\mu$ for gluons, and similarly for the photon, A_μ, the Z_μ and W^+_μ. We can use field redefinitions to rewrite the couplings in Eq. (2) and Eq. (3) in a different way. For example, some linear combinations of the contact-interactions $hV_\mu J^\mu$ could be written as interactions of the type $hV_\mu\partial_\nu F^{\mu\nu}$ [4] by the redefinition $V_\mu \to (1 + \alpha h)V_\mu$, with an appropriate α, in the full Lagrangian (and using integration by parts). Nevertheless, we consider that Eq. (2) and Eq. (3) are the most convenient

---

[1]From here and on, all Higgs-coupling coefficients are defined real.

way to write the Higgs couplings. Our parametrization of Higgs couplings gives priority to operators with the largest number of fields (as opposed to operators with more derivatives), as this is important when estimating the size of the couplings or looking for the dominant effects in the high-energy regime, as we will show later.

For CP-violating couplings we have

$$
\mathcal{L}_h^{\text{primary}} = \delta\tilde{g}_{hff}\left(ih\bar{f}_L f_R + h.c.\right) + \widetilde{\kappa}_{GG}\frac{h}{2v}G^{A\,\mu\nu}\widetilde{G}^A_{\mu\nu} + \widetilde{\kappa}_{\gamma\gamma}\frac{h}{2v}A^{\mu\nu}\widetilde{A}_{\mu\nu} + \widetilde{\kappa}_{Z\gamma}\frac{h}{v}A^{\mu\nu}\widetilde{Z}_{\mu\nu}\,, \quad (4)
$$

$$
\Delta\mathcal{L}_h = \tilde{g}^h_{Zff}\frac{h}{2v}\left(iZ_\mu J_N^\mu + h.c.\right) + \tilde{g}^h_{Wff'}\frac{h}{v}\left(iW_\mu^+ J_C^\mu + h.c.\right)
$$
$$
+ \widetilde{\kappa}_{WW}\frac{h}{v}W^{+\,\mu\nu}\widetilde{W}^-_{\mu\nu} + \widetilde{\kappa}_{ZZ}\frac{h}{2v}Z^{\mu\nu}\widetilde{Z}_{\mu\nu}\,, \quad (5)
$$

where $\widetilde{G}^{A\,\mu\nu} = \epsilon^{\mu\nu\rho\sigma}G^A_{\rho\sigma}/2$ and similarly for other gauge bosons.

It is important to understand the implications of global symmetries in the Higgs couplings. In particular, if the Higgs couplings are induced from BSMs that respect a custodial SU(2) symmetry [5] only weakly broken by the gauging of U(1)$_Y$ and fermions masses, and responsible for $m_W^2 = m_Z^2 c_{\theta_W}^2$ at tree-level, we have the relations [6] [2]

$$
\kappa_{WW} = c_{\theta_W}^2 \kappa_{ZZ} + s_{2\theta_W}\kappa_{Z\gamma} + s_{\theta_W}^2 \kappa_{\gamma\gamma}\,, \quad (6)
$$
$$
c_{\theta_W}g^h_{Zff} = \sqrt{2}\,T_{3f}\,g^h_{Wff'}V^\dagger_{\text{CKM}} - Y_f\,\delta g^h_{ZZ}/m_W \quad \text{for } f = \text{up-type fermion}\,,
$$
$$
c_{\theta_W}g^h_{Zf'f'} = \sqrt{2}\,T_{3f'}\,V^\dagger_{\text{CKM}}g^h_{Wff'} - Y_{f'}\,\delta g^h_{ZZ}/m_W \quad \text{for } f' = \text{down-type fermion}\,, \quad (7)
$$

where T_{3f} and Y_f are respectively the 3-component isospin and hypercharge of the fermion f, with $Q_f = T_{3f} + Y_f$ the electric charge, and V_{CKM} the CKM quark-mixing matrix [7]. Eq. (6) was first derived in [8]. A left-right parity P_{LR} [9] can further restrict the coefficients [6]:

$$
\kappa_{Z\gamma} = \frac{c_{2\theta_W}}{s_{2\theta_W}}\kappa_{\gamma\gamma}\,. \quad (8)
$$

Similar expressions are derived for the CP-violating counterparts.

We can also have a reduction of Higgs couplings due to dynamical reasons. For example, in BSMs with a strongly-interacting Higgs, we can neglect $\kappa_{ZZ,WW}$ in comparison with g^h_{VV} and δg^h_{ZZ}, as the formers are associated to interactions that contain more derivatives and therefore are expected to be smaller in our D_μ/Λ expansion (see later a power counting for these couplings). Also in "universal" BSMs (as those in which the BSM states only couple to SM bosons and not to fermions) we only have three relevant contact-interactions $hV_\mu J^\mu$:

$$
g^h_{ZJ_3}\frac{h}{v}Z_\mu J_3^\mu\,, \quad g^h_{ZJ_Y}\frac{h}{v}Z_\mu J_Y^\mu\,, \quad g^h_{WJ}\frac{h}{v}\left(W_\mu^+ J_W^\mu + h.c.\right)\,, \quad (9)
$$

where J_3^μ, J_Y^μ and J_W^μ are respectively the 3-component isospin, hypercharge and charged SM currents [7]. Demanding also custodial invariance, we obtain

$$
g^h_{ZJ_3} = \frac{g^h_{WJ}}{c_{\theta_W}}\,, \quad g^h_{ZJ_Y} = -\frac{\delta g^h_{ZZ}}{c_{\theta_W}m_W}\,, \quad (10)
$$

that is equivalent to

$$
g^h_{Wff'} = g^h_{WJ}V_{\text{CKM}}\,, \quad g^h_{Zff} = T_{3f}\frac{\sqrt{2}g^h_{WJ}}{c_{\theta_W}} - Y_f\frac{\delta g^h_{ZZ}}{c_{\theta_W}m_W}\,. \quad (11)
$$

Eq. (11), together with Eq. (6), show that universality and custodial symmetry reduce Eq. (3) to only 3 independent Higgs couplings, that we can take to be δg^h_{ZZ}, κ_{ZZ} and g^h_{WJ}. This is in accordance with [8].

---

[2]The terms proportional to Y_f arise from the operator $\partial_\mu h Z_\nu g'B^{\mu\nu}$ that, after field redefinitions, can be rewritten as interactions in Eq. (2) and Eq. (3). One has to have this in mind when estimating the size of the coefficients.

3 The SM predictions for Higgs couplings

In the SM the Higgs sector is given by

$$\mathcal{L}_h^{\text{SM}} = |D_\mu H|^2 - (y_u \bar{Q}_L \widetilde{H} u_R + y_d \bar{Q}_L H d_R + y_e \bar{L}_L H e_R + h.c.) + \mu^2 |H|^2 - \lambda |H|^4, \qquad (12)$$

where the complex Higgs field H is a $\mathbf{2_{1/2}}$ of SU(2)$_L \times$U(1)$_Y$, $\widetilde{H} = i\sigma^2 H^*$, and

$$Q_L = \begin{pmatrix} u_L \\ d_L \end{pmatrix}, \quad L_L = \begin{pmatrix} \nu_L \\ e_L \end{pmatrix}. \qquad (13)$$

When the Higgs gets a vacuum expectation value (VEV), $\langle H \rangle = (0 \; v/\sqrt{2})^T$, where $v \simeq 246$ GeV, the gauge bosons W/Z and fermions get a mass proportional to their coupling to the Higgs field. Out of the 4 degrees of freedom in H, 3 corresponds to the would-be Nambu-Golstone bosons that become the longitudinal component of the W and Z, and the 4th is the Higgs particle h. In the SM all couplings of the Higgs are predicted as a function of particle masses. We have, at tree-level, that the only nonzero couplings are

$$g_{ff}^h = -\frac{g m_f}{2 m_W}, \quad g_{VV}^h = g m_W, \quad g_{3h} = -\frac{3 g m_h^2}{2 m_W}, \qquad (14)$$

that lead to the straight line of Fig. 1. The rest of the Higgs couplings arise at the loop level; κ_{GG} is mainly induced by the top loop, while $\kappa_{\gamma\gamma}$ and $\kappa_{Z\gamma}$ are generated by W and top loops, as can be found for example in [10].

4 Higgs couplings in an Effective Field Theory approach to the SM

Let us consider BSMs characterized by a mass-scale Λ much larger than the electroweak scale m_W, such that, after integrating out the BSM sector, we can make an expansion not only in derivatives D_μ over Λ, as we did in previous sections, but also an expansion of SM fields over Λ. In this way we can obtain an Effective Field Theory (EFT) made of local operators: [3]

$$\mathcal{L}_{\text{EFT}} = \frac{\Lambda^4}{g_*^2} \mathcal{L} \left(\frac{D_\mu}{\Lambda}, \; \frac{g_* H}{\Lambda}, \; \frac{g_* f_{L,R}}{\Lambda^{3/2}}, \; \frac{g F_{\mu\nu}}{\Lambda^2} \right) \simeq \mathcal{L}_4 + \mathcal{L}_6 + \cdots. \qquad (15)$$

Here $\mathcal{L}_d$ denotes the term in the expansion made of local operators of dimension d, while g_* denotes a generic coupling, and g and $F_{\mu\nu}$ represent respectively the SM gauge couplings and field-strengths. The Lagrangian in Eq. (15) is based on dimensional analysis and the dependence on the coupling g_* is easily obtained when the Planck constant $\hbar$ is put back in place. Indeed, working with units $\hbar \neq 1$, the couplings have dimensions $[g_*] = [\hbar]^{-1/2}$, while $[H] = L^{-1} \cdot [\hbar]^{1/2}$ and the Lagrangian mass-terms $[\Lambda] = L^{-1}$. This dictates the dimensionless expansion-parameters to be $g_* H / \Lambda$ and D_μ / Λ, and that terms in the Lagrangian that contains n fields must carry $n - 2$ couplings to have the right dimensions. This counting is therefore valid even if g_* is not small. Although we are using a generic coupling and mass-scale, g_* and Λ, it is clear that this ought not to be always the case. For example, for a strongly-interacting light Higgs (SILH) [4] only the couplings of the Higgs to the strong BSM sector are large ($g_* \gg 1$ for the Higgs), while SM fermions are assumed to have small couplings ($g_* \sim \sqrt{y_f}$ for fermions).

The Lagrangian terms of $\mathcal{L}_4$ redefine the SM (and have no physical impact), while $\mathcal{L}_6$ encodes the dominant BSM effects. Therefore the study of the physical implications of $\mathcal{L}_6$ in the physics of the SM is of great importance. There are different bases used in the literature for the set of independent $d = 6$ operators in $\mathcal{L}_6$. Although physics is independent of the choice of basis, it is clear that some bases are better suited than others in order to extract the relevant information, *e.g.*, for Higgs physics.

---

[3] This EFT also contains operators of dimension five, $\mathcal{L}_5$, but these induce neutrino masses and therefore their coefficients must be very small (or their suppression scale Λ very large). For this reason we neglect them here since they cannot play any role for Higgs physics at the TeV.

The first complete and non-redundant basis of dimension-6 operators was given in [11]. The virtue of that basis is that it is constructed with the maximum number of operators made of fields instead of using derivatives, following our approach for Eq. (2) and Eq. (3). As we mentioned, this can be useful when estimating the size of the coefficients (see section below) or looking for the dominant effects at high-energies. Nevertheless, from a model-building point of view, it can be more advantageous to define bases that capture in few operators the impact of the most interesting BSM scenarios. With this philosophy, the SILH basis was constructed in [4], and generalised to a complete $\mathcal{L}_6$ basis in [8,9]. In this basis "universal" BSMs are encoded in few operators made only of SM bosons. This has the virtue of, for example, having a more direct connection between operator coefficients and the S and T parameters [12] that characterize the main electroweak effects of these BSMs. This simplicity is not present in the basis of [11] in which the equivalent of the S and T parameters involve vertex corrections [13] and then a less direct connection with the operator coefficients. Another useful basis is given in [14] with the interesting property of having a one-to-one correspondence between operators and the most relevant physical interactions measured at experiments.

In all the above mentioned bases it is possible to separate the operators into the following two groups: those that could (in principle) be induced *at tree-level* from integrating out heavy states with spin ≤ 1 in renormalizable weakly-interacting BSMs, and those operators that can only be induced *at the one-loop level* from these BSMs [9,15]. This property is, however, not respected for bases constructed with the operators of [16] where *tree* and *loop* operators are mixed.

The coefficients of $\mathcal{L}_6$, referred as Wilson coefficients, are generated at the scale Λ where they are generated after integrating out the BSM heavy states. The renormalization group evolution (RGE) from Λ down to the electroweak scale, where they are supposed to be measured, can give important corrections to the Wilson coefficients and mix them [9,17,18]. For example, in supersymmetric theories or composite Higgs models, where the Wilson coefficients can be determined (see below), the RGE give us the leading-log corrections to the predictions for the Higgs couplings at low-energy that can be significant in certain cases [9].

The full set of physical implications of $\mathcal{L}_6$ was given in [13], where it was shown that not all type of interactions can be obtained from $\mathcal{L}_6$ and, of the possible ones, not all of them are independent. The set of independent couplings that are, at present, the experimentally best tested ones, were called *primary* couplings. The ones of the Higgs are presented below.

4.1 Primary Higgs couplings

Among all dimension-6 operators present in $\mathcal{L}_6$, there are few of them that contribute *only* to Higgs couplings and not to other couplings (such as Vff) [9]. These are the set of independent dimension-6 operators constructed with $|H|^2$. The CP-conserving ones are [4]

$$
|H|^2 \bar{Q}_L \widetilde{H} u_R + h.c. , \quad |H|^2 \bar{Q}_L H d_R + h.c. , \quad |H|^2 \bar{L}_L H e_R + h.c. ,
$$
$$
|H|^2 |D_\mu H|^2 , \; |H|^6 , \; |H|^2 G^{A\,\mu\nu} G^A_{\mu\nu} , \; |H|^2 B^{\mu\nu} B_{\mu\nu} , \; |H|^2 W^{a\,\mu\nu} W^a_{\mu\nu} , \tag{16}
$$

where W^a_μ, B_μ are the SU(2)$_L \times$U(1)$_Y$ gauge bosons. To see that, indeed, the above operators can *only* be probed by measuring Higgs couplings, we just have to put the Higgs field in the EWSB vacuum, $|H|^2 \to v^2/2$, and realize that the resulting terms are operators already present in the SM, *i.e.*, their only effect is a redefinition of the SM parameters.

The set of Higgs couplings that can be independently generated from Eq. (16) are the primary Higgs couplings [13]. Their measurements provide new probes to new physics only accessible by Higgs physics. The number of primary Higgs couplings must obviously coincide with the number of Wilson coefficients associated with the operators of Eq. (16) (for the CP-conserving case). We have chosen as primary Higgs couplings those in Eq. (2), as all of them can be independently generated from the

---

[4] Notice that the operator $|H|^2 f \overleftrightarrow{\slashed{D}} f$ can always be eliminated from the Lagrangian by field redefinitions.

operators of Eq. (16). We must be aware however that the correspondence is not one-to-one [9, 19]. There is a certain freedom to choose the set of primary Higgs couplings. For example, instead of $\kappa_{\gamma\gamma}$ and $\kappa_{Z\gamma}$, we could have taken $\kappa_{ZZ,WW}$, as these latter can also receive independent contributions from Eq. (16). The reason to choose Eq. (2) as primary Higgs couplings it is just experimental: they are the set of primary Higgs couplings best measured at the LHC.

Similarly, the CP-violating dimension-6 operators constructed with $|H|^2$ are

$$i|H|^2\bar{Q}_L\widetilde{H}u_R + h.c. , \quad i|H|^2\bar{Q}_L H d_R + h.c. , \quad i|H|^2\bar{L}_L H e_R + h.c. ,$$
$$|H|^2 G^{A\,\mu\nu}\widetilde{G}^A_{\mu\nu} , \quad |H|^2 B^{\mu\nu}\widetilde{B}_{\mu\nu} , \quad |H|^2 W^{a\,\mu\nu}\widetilde{W}^a_{\mu\nu} , \tag{17}$$

that can independently generate the set of primary Higgs couplings of Eq. (4). Again, all these operators for $|H|^2 \to v^2/2$ generate SM terms (that redefine SM parameters) and therefore their physical effects can only be seen in Higgs physics.

The primary Higgs couplings can enter at the quantum level in other non-Higgs observables. For example, the CP-violating Higgs couplings can contribute at the loop-level to the neutron and electron electric dipole moment (EDM). The fact that we have excellent bounds on these EDMs, place indirect bounds on these Higgs couplings. We must be aware however that these bounds are model-dependent, as there can be, in principle, other BSM effects entering in the EDMs.

4.2 Beyond the primaries

The rest of CP-conserving Higgs couplings, beyond the primaries, are those of Eq. (3) at the order we mentioned before. They can in principle be generated from operators in $\mathcal{L}_6$. [5] Nevertheless, it can be proven [9, 19] that contributions from $\mathcal{L}_6$ to Eq. (3) are not independent from contributions to primary Higgs couplings and other electroweak couplings. Therefore they can, in principle, be constrained by other experimental measurements. As an example, consider the operator $H^\dagger D_\mu H \bar{e}_R \gamma^\mu e_R$. This gives a contribution to the Higgs coupling g^h_{Zff}, but it also contributes to the coupling $Z\bar{e}_R e_R$ that has been very-well measured at LEP, putting strong bounds on possible BSM effects.

The explicit relations between the $\mathcal{L}_6$-contributions to Eq. (3) and to other couplings were explicitly calculated in [13, 14, 19] assuming family universality. Here we give these relations for the general case (derived at the tree-level) [6]:

$$\delta g^h_{ZZ} = 2g t^2_{\theta_W} m_W \left(c^2_{\theta_W} \delta g^Z_1 - \delta\kappa_\gamma \right) ,$$
$$g^h_{Zff} = 2\delta g^Z_{ff} - 2\delta g^Z_1 (g^Z_{ff} c_{2\theta_W} + g^\gamma_{ff} s_{2\theta_W}) + 2\delta\kappa_\gamma Y_f \frac{e s_{\theta_W}}{c^3_{\theta_W}} , \quad g^h_{Wff'} = 2\delta g^W_{ff'} - 2\delta g^Z_1 g^W_{ff'} c^2_{\theta_W} , \tag{18}$$

$$\kappa_{ZZ} = \frac{1}{c^2_{\theta_W}}\delta\kappa_\gamma + 2\frac{c_{2\theta_W}}{s_{2\theta_W}}\kappa_{Z\gamma} + \kappa_{\gamma\gamma} , \qquad\qquad \kappa_{WW} = \delta\kappa_\gamma + \kappa_{Z\gamma} + \kappa_{\gamma\gamma} , \tag{19}$$

with

$$\delta g^W_{ff'} = \frac{c_{\theta_W}}{\sqrt{2}} \left(\delta g^Z_{ff} V_{\text{CKM}} - V_{\text{CKM}} \delta g^Z_{f'f'} \right) \text{ for } f = f_L , \tag{20}$$

and where

$$g^\gamma_{ff} = e Q_f , \quad g^Z_{ff} = \frac{g}{c_{\theta_W}} \left(T_{3f} - Q_f s^2_{\theta_W} \right) , \quad g^W_{ff'} = \frac{g}{\sqrt{2}} V_{\text{CKM}}, 0 \text{ resp. for } f = f_L, f_R , \tag{21}$$

are the γ, Z and W couplings to fermions in the SM. Flavor indices are again implicit. We have also defined by δg^Z_{ff} ($\delta g^W_{ff'}$) the BSM corrections to the Z (W) couplings to fermions:

$$\Delta\mathcal{L}^V_{ff} = \frac{\delta g^Z_{ff}}{2} \left(Z_\mu J^\mu_N + h.c. \right) + \delta g^W_{ff'} \left(W^+_\mu J^\mu_C + h.c. \right) , \tag{22}$$

---

[5] At $O(hFff)$ we also have dipole-type interactions that can arise from $\mathcal{L}_6$. Their Wilson coefficients are however expected to be suppressed by SM Yukawa-couplings (otherwise could largely contribute at the loop level to the SM fermion masses). These couplings are related to fermion EDMs as can be found in [13].

while δg_1^Z is the correction to the ZWW coupling and $\delta\kappa_\gamma$ parametrizes BSM contributions to the EDM of the W, following the notation of [16] for anomalous triple gauge couplings (TGC):

$$\Delta\mathcal{L}_{3V} = igc_{\theta_W}\delta g_1^Z \left[Z^\mu \left(W^{+\,\nu}W_{\mu\nu}^- - h.c.\right) + Z^{\mu\nu}W_\mu^+ W_\nu^- \right] + ie\delta\kappa_\gamma \left[(A^{\mu\nu} - t_{\theta_W}Z^{\mu\nu})W_\mu^+ W_\nu^- \right] . \tag{23}$$

Following [13], we have chosen to work in the mass-eigenstate basis within a parametrization in which kinetic terms and masses do not receive corrections and then take the SM values. All BSM effects are in couplings. We think this is the most convenient parametrization of BSM effects due to the straightforward connection between couplings and physical processes, that in most of the cases is a one-to-one correspondence. The SM input parameters can be taken to be $\alpha_{\rm EM}$, m_Z and m_W that, in our parametrization, do not have BSM corrections, as opposed to G_F that receive corrections from 4-fermion interactions. We remark again that the predictions Eq. (18) and Eq. (19) are derived at the tree-level and only apply to BSM effects coming from $\mathcal{L}_6$. There are also SM contributions to these couplings at the loop level, that can be as important as new-physics contributions, and must be incorporated accordingly.

Eq. (18) and Eq. (19) are important results. They show that all Higgs couplings of Eq. (3) can be written as a function of BSM effects to two primary Higgs couplings ($\kappa_{\gamma\gamma}$, $\kappa_{Z\gamma}$), Z/W couplings to SM fermions (δg_{ff}^Z, $\delta g_{f_R f_R'}^W$), and two TGC (δg_1^Z, $\delta\kappa_\gamma$). Experimental bounds on $\kappa_{\gamma\gamma,Z\gamma}$ are already at the per-cent level [19], while Z/W couplings have also been experimentally contrained, mostly from LEP and SLC [20, 21] (with Tevatron providing an accurate measurement of the W-mass). One finds that bounds on δg_{ff}^Z are quite strong, at the per mille-level in most of the cases, but bounds on δg_1^Z and $\delta\kappa_\gamma$ are much weaker [22]. Therefore, at present, we can already derive, using Eq. (18) and Eq. (19), relevant model-independent bounds on the Higgs couplings of Eq. (3) [19].

In the case of custodial-invariant universal BSMs, Eq. (18) reduces to

$$\delta g_{ZZ}^h = 2gt_{\theta_W}^2 m_W \left(c_{\theta_W}^2 \delta g_1^Z - \delta\kappa_\gamma + \widehat{S} \right) ,$$

$$g_{Zff}^h = -2T_{3f}\,\delta g_1^Z gc_{\theta_W} - Y_f \frac{\delta g_{ZZ}^h}{c_{\theta_W} m_W} , \qquad\qquad g_{Wff'}^h = -2\delta g_1^Z g_{ff'}^W c_{\theta_W}^2 , \tag{24}$$

where $\widehat{S}$ is, up to a normalization constant [23], the S-parameter [12]. As expected, Eq. (24) and Eq. (18) fulfill Eq. (6) and Eq. (11), and g_{Zff}^h is fully determined by the custodial symmetry as a function of $g_{Wff'}^h$ and δg_{ZZ}^h.

The CP-violating non-primary Higgs couplings, Eq. (5), are also not independent but related to other couplings. We have

$$\tilde{g}_{Zff}^h = 2\delta\tilde{g}_{ff}^Z , \qquad\qquad \tilde{g}_{Wff'}^h = 2\delta\tilde{g}_{ff'}^W ,$$

$$\widetilde{\kappa}_{ZZ} = \frac{1}{c_{\theta_W}^2}\delta\widetilde{\kappa}_\gamma + 2\frac{c_{2\theta_W}}{s_{2\theta_W}}\widetilde{\kappa}_{Z\gamma} + \widetilde{\kappa}_{\gamma\gamma} , \qquad\qquad \widetilde{\kappa}_{WW} = \delta\widetilde{\kappa}_\gamma + \widetilde{\kappa}_{Z\gamma} + \widetilde{\kappa}_{\gamma\gamma} , \tag{25}$$

where

$$\delta\tilde{g}_{ff'}^W = \frac{c_{\theta_W}}{\sqrt{2}}\left(\delta\tilde{g}_{ff}^Z V_{\rm CKM} - V_{\rm CKM}\delta\tilde{g}_{f'f'}^Z \right) \text{ for } f = f_L , \tag{26}$$

with $\delta\tilde{g}_{ff}^Z$ and $\delta\tilde{g}_{ff'}^W$ defined as

$$\Delta\tilde{\mathcal{L}}_{ff}^V = \frac{\delta\tilde{g}_{ff}^Z}{2}\left(iZ_\mu J_N^\mu - h.c. \right) + \delta\tilde{g}_{ff'}^W \left(iW_\mu^+ J_C^\mu - h.c. \right) , \tag{27}$$

and $\widetilde{\kappa}_\gamma$ being the CP-violating TGC:

$$\Delta\mathcal{L}_{3\widetilde{V}} = ie\delta\widetilde{\kappa}_\gamma \left[(\widetilde{A}^{\mu\nu} - t_{\theta_W}\widetilde{Z}^{\mu\nu})W_\mu^+ W_\nu^- \right] . \tag{28}$$

The predictions Eq. (18), Eq. (19) and Eq. (25) rely on the (quite plausible) hypothesis that the leading SM deviations arise from $\mathcal{L}_6$. Finding experimental evidence for deviations from these predictions, would mean that nature does not fulfil this hypothesis: either because there are light BSM states ($\Lambda \lesssim m_h$), the composite-scale of the Higgs is low ($\Lambda \sim g_* v$), that is equivalent to say that h cannot be identified within the SM doublet, or that there are other sources of EWSB independent of $\langle H \rangle$ [24].

4.3 Power counting for Higgs couplings

It can be useful to estimate the size of the contributions to the effective Higgs couplings arising from generic BSMs. As it is clear from the expansion in Eq. (15), the coefficients in Eq. (2) and Eq. (3) can have different dependence with g_*. The Higgs couplings that can receive the largest power of g_* are g_{3h} and g_{ff}^h where

$$\delta g_{3h} \sim \frac{g_*^4 v^3}{\Lambda^2} \ , \ \delta g_{ff}^h \sim \frac{g_*^3 v^2}{\Lambda^2} \ . \tag{29}$$

For $g_* \gg 1$, Eq. (29) can give $O(1)$ corrections to g_{3h} and g_{ff}^h, even after demanding $g_*^2 v^2 / \Lambda^2 \ll 1$ necessary to make the expansion Eq. (15) valid. Nevertheless, in theories where the Higgs mass is protected by a symmetry, as it happens in theories that solve the hierarchy problem such as supersymmetry or composite Higgs models, the contributions to g_{3h} are also expected to be protected and then proportional to $m_h^2/v^2 \sim \lambda$. Also it is natural to expect that chirality protects terms proportional to $\bar{f}_L f_R$, at least by a Yukawa coupling $y_f \sim m_f/v$, otherwise corrections to fermion masses would be too large. For this reason, it is more natural to assume that the corrections to these Higgs couplings are of order

$$\delta g_{3h} \sim \lambda v \frac{g_*^2 v^2}{\Lambda^2} \ , \ \delta g_{ff}^h \sim y_f \frac{g_*^2 v^2}{\Lambda^2} \ , \tag{30}$$

that potentially give relative corrections of $O(g_*^2 v^2/\Lambda^2)$. At the same order, we also have

$$\delta g_{VV}^h \sim g^2 v \frac{g_*^2 v^2}{\Lambda^2} \ , \tag{31}$$

and

$$\delta g_{ff}^Z, \delta g_1^Z \sim g \frac{g_*^2 v^2}{\Lambda^2} \ . \tag{32}$$

Finally, couplings coming from a derivative (or field-strength) expansion, the κ_i, are expected to scale as

$$\kappa_i \sim \frac{g^2 v^2}{\Lambda^2} \ . \tag{33}$$

Nevertheless, in renormalizable BSMs these coefficients can only be induced at the loop-level and therefore expected to be

$$\kappa_i \sim \frac{g_*^2}{16\pi^2} \frac{g^2 v^2}{\Lambda^2} \ . \tag{34}$$

Indeed, it can be shown [4, 9] that the κ_i cannot be generated *at tree-level* from integrating out scalars, fermions and vector bosons in renormalizable theories.

The above estimates are useful to determine which are the most sizeable BSM corrections to the Higgs couplings. For example, in theories in which the Higgs is strongly coupled, the largest corrections are those of Eq. (30) and Eq. (31) that depend quadratically in the strong coupling $g_* \gg 1$ [4]. If also the SM fermions are strongly-coupled, Eq. (32) can also give similar size corrections. It is also important to remark that even for theories in which the field expansion in Eq. (15) is not valid (*e.g.*, when $g_* v \sim \Lambda$), the power counting for Higgs couplings given here is expected to be correct. In particular, the above estimates are in accordance with the NDA analysis of [25] proposed for QCD.
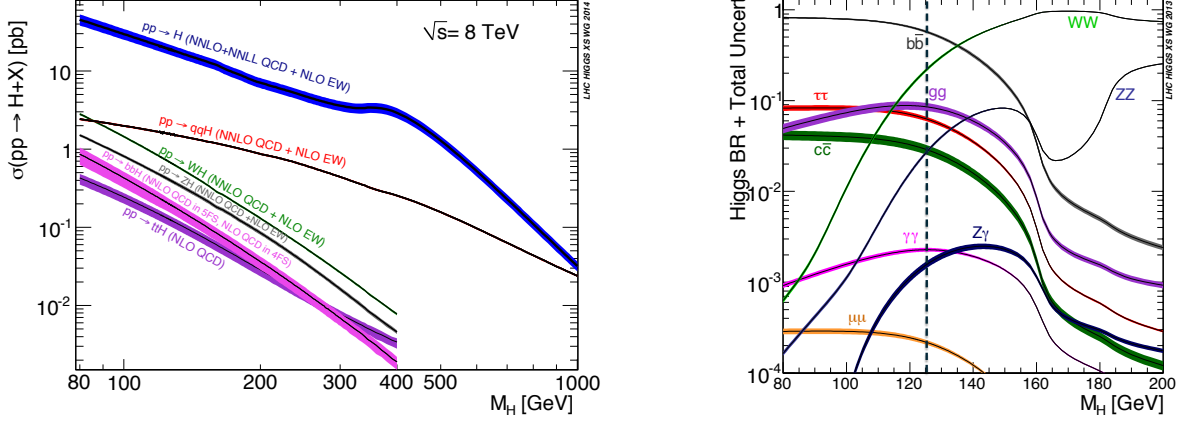
Fig. 2: Predictions for the main Higgs production cross-sections and Higgs BR in the SM [26].

For the non-primary Higgs couplings we have the estimates

$$\frac{\delta g_{ZZ}^h}{g^2 v}, \frac{g_{Zff}^h}{g}, \frac{g_{Wff'}^h}{g} \sim \frac{g_*^2 v^2}{\Lambda^2} \quad \text{and} \quad \kappa_{ZZ}, \kappa_{WW} \sim \frac{g^2 v^2}{\Lambda^2}, \tag{35}$$

in agreement with the relations in Eq. (18). Similar estimates follow for CP-violating Higgs couplings.

5   Experimental determination of the effective Higgs couplings

The primary Higgs couplings can be determined by searching for the Higgs through the different production mechanisms and decays. The main Higgs production mechanisms at the LHC are

$$
\begin{aligned}
\text{Gluon fusion:} \quad & GG \to h, \\
Vh\text{-associated production:} \quad & q\bar{q} \to Vh, \\
\text{Vector boson fusion (VBF):} \quad & qq \to qqVV^* \to qqh, \\
htt\text{-associated production:} \quad & GG \to t\bar{t}h,
\end{aligned}
\tag{36}
$$

while the most important Higgs branching ratios (BR) are

$$BR(h \to b\bar{b}), \ BR(h \to \tau\bar{\tau}), \ BR(h \to Vf\bar{f}), \ BR(h \to \gamma\gamma), \ BR(h \to Z\gamma). \tag{37}$$

The predictions for a SM Higgs are given in Fig. 2. The Higgs mass can be mainly determined from the Higgs decay to $\gamma\gamma$ and Zff that allows to obtain

$$
\begin{aligned}
m_h &= 125.03 \, {}^{+0.26}_{-0.27} \, (stat.) \, {}^{+0.13}_{-0.15} \, (syst.) \ \text{GeV} \quad \text{from CMS}, \\
m_h &= 125.36 \pm 0.37 \, (stat.) \pm 0.18 \, (syst.) \ \text{GeV} \quad \text{from ATLAS}.
\end{aligned}
\tag{38}
$$

At the LHC one can combine the different Higgs production mechanisms and BR of Eq. (36) and Eq. (37) to determine 7 primary Higgs couplings: g_{ff}^h ($f = t, b, \tau$), g_{VV}^h, κ_{GG}, $\kappa_{\gamma\gamma}$ and $\kappa_{Z\gamma}$. [6] The CMS fit of six of the primary Higgs couplings is shown in Fig. 3, where other Higgs couplings have been set to zero. [7] The fit shows a good agreement with the SM predictions and no sing of new-physics. The implications of these measurements in particular BSMs will be discussed in the next section. The

---

[6] We note that g_{tt}^h and g_{VV}^h also affect $BR(h \to \gamma\gamma/Z\gamma)$ and $\sigma(GG \to h)$ at the one-loop level [4].

[7] The ATLAS results are not shown here since the fit is performed only for few primaries at each time instead of a global fit to all of them [3]. For a combination of ATLAS and CMS data see, for example, [28, 29].
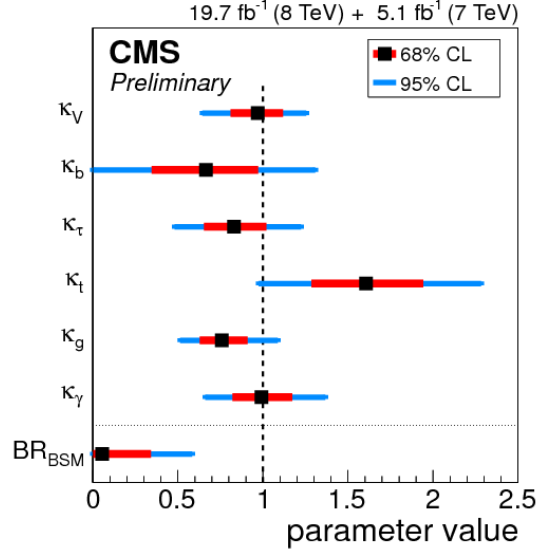
Fig. 3: Fit of 6 primary Higgs couplings from CMS [2]. Notation: $\kappa_V \equiv g_{VV}^h/g_{VV}^{h\,\mathrm{SM}}$, $\kappa_f \equiv g_{ff}^h/g_{ff}^{h\,\mathrm{SM}}$, $\kappa_g \equiv \kappa_{GG}/\kappa_{GG}^{\mathrm{SM}}$ and $\kappa_\gamma \equiv \kappa_{\gamma\gamma}/\kappa_{\gamma\gamma}^{\mathrm{SM}}$; loop effects in κ_{GG} and $\kappa_{\gamma\gamma}$ are not included [2].

primary coupling $\kappa_{Z\gamma}$ has not been included in the fit of Fig. 3, but one can use the experimental bound $BR(h \to Z\gamma)/BR(h \to Z\gamma)_{\mathrm{SM}} \lesssim 10$ [27] to derive the constraint $-0.01 \lesssim \kappa_{Z\gamma} \lesssim 0.02$ [19]. The fact that in the SM $h \to Z\gamma$ arises at the one-loop level, and therefore has a small branching fraction $BR(h \to Z\gamma) \sim 0.15\%$, makes this BR very sensitive to new-physics; it probably provides the last chance to find large BSM effects in SM Higgs couplings.

Among the remaining primary Higgs couplings to be measured we have g_{3h}. Its determination however will be very difficult since it requires to search for double-Higgs production $pp \to hh$ that has small rates [30]. Also Higgs couplings to light fermions g_{ff}^h (beyond the 3rd family) are going to be difficult to measure since we expect these couplings to be proportional to m_f/m_W (see Eq. (14) and Eq. (30)), giving then very small BR. For example, for the case of the muon, that is probably the most accessible, we have in the SM $BR(h \to \mu\mu) \sim 0.02\%$. Therefore a high luminosity at the LHC run 2 will be needed to measure this coupling. Flavour-violating Higgs couplings in g_{ff}^h can also be accessible through Higgs decays. This is particularly interesting for theories of flavour in which Yukawas are generated from the mixing of the SM fermions with heavy BSM states. The strength of these mixings are expected to be $\sim \sqrt{m_{f_i}/v}$, and therefore predicting $g_{f_i f_j}^h \sim \sqrt{m_{f_i} m_{f_j}}/v$ that can lead to sizeable flavour-violating Higgs decays. In particular, one has $BR(h \to \tau\mu) \sim m_\mu/m_\tau \times BR(h \to \tau\tau) \sim 0.4\%$ that is quite close to the present experimental bound $BR(h \to \tau\mu) < 1.57\%$ [31]. Finally, most of the CP-violating Higgs couplings are poorly measured since they appear quadratically in production rates and BR since the interference terms with the SM contributions vanish. [8] Kinematical differential distributions can be used to measure these couplings [32], and alternative methods have been recently proposed in [33]. Nevertheless, indirect bounds on most of these couplings are very strong (see for example [34] for bounds on $\widetilde{\kappa}_{\gamma\gamma}$ from EDMs), making difficult to believe that Higgs CP-violating couplings are sizeable. The exception is probably $\delta\widetilde{g}_{\tau\tau}^h$ whose bounds are not so strong and could have possible impact in CP-violating Higgs decays.

The experimental full extraction of all Higgs couplings, including the non-primary ones, Eq. (3) and Eq. (5), is a difficult task. The best way to disentangle the effects of δg_{ZZ}^h, $\kappa_{ZZ,WW}$ and g_{Vff}^h ($V = Z, W$), as well as their CP-violating counterparts, is by looking for modifications in differential

---

[8]Since in the SM the hGG, $h\gamma\gamma$ and $hZ\gamma$ couplings are small (as they arise at the one-loop level), the interference terms are also small, and the corresponding bounds on CP-conserving and CP-violating couplings, κ_i and $\widetilde{\kappa}_i$, are comparable.
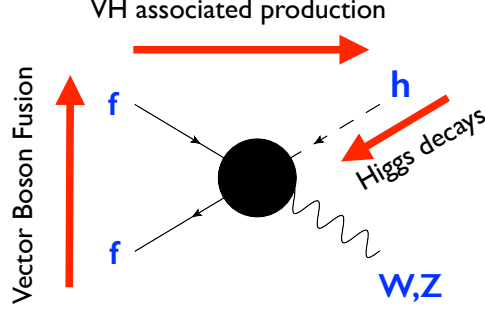
Fig. 4: The form-factor $hVff$, that as a function of the effective Higgs couplings is given in Eq. (39), can be tested in three different Higgs processes at the LHC: either in Higgs decays $h \to Vff$, in Vh-associated production or in the VBF-like process $pp \to qqV/qqVV^* \to qqh$.

distributions in Higgs processes. The most relevant ones are the Higgs decays $h \to Vff$, the Vh-associated production and the VBF-like process $pp \to qqV/qqVV^* \to qqh$. All of them arise from the $hVff$ amplitude (see Fig. 4) given by (neglecting fermion masses)

$$\mathcal{M}_{hVff}(q,p) = \frac{1}{v}\epsilon^{*\mu}(q)\,J_V^\nu(p)\left[A^V\,\eta_{\mu\nu} + B^V\,(p\cdot q\,\eta_{\mu\nu} - p_\mu\,q_\nu) + C^V\,\epsilon_{\mu\nu\rho\sigma}p^\rho q^\sigma\right], \tag{39}$$

where q and p are respectively the total 4-momentum of V and the fermion pair in $J_V^\mu = J_N^\mu, J_C^\mu$ for $V = Z, W$, and ϵ^μ is the polarization 4-vector of V. We have defined

$$A^V = a^V + \hat{a}^V\,\frac{m_V^2}{p^2 - m_V^2}\,, \qquad B^V = b^V\,\frac{1}{p^2 - m_V^2} + \hat{b}^V\,\frac{1}{p^2}\,, \qquad C^V = c^V\,\frac{1}{p^2 - m_V^2} + \hat{c}^V\,\frac{1}{p^2}\,, \tag{40}$$

with $\hat{b}^W, \hat{c}^W = 0$, and where

$$a^Z = \delta g_{Zff}^h + i\delta\tilde{g}_{Zff}^h\,, \qquad\qquad a^W = \delta g_{Wff'}^h + i\delta\tilde{g}_{Wff'}^h\,,$$

$$\hat{a}^Z = 2g_{ff}^Z\left(1 + \frac{\delta g_{VV}^h + \delta g_{ZZ}^h}{gm_W}\right)\,, \qquad \hat{a}^W = 2g_{ff'}^W\left(1 + \frac{\delta g_{VV}^h}{gm_W}\right)\,,$$

$$b^Z = -2g_{ff}^Z\kappa_{ZZ}\,, \qquad\qquad b^W = -2g_{ff'}^W\kappa_{WW}\,,$$

$$\hat{b}^Z = -2eQ_f\kappa_{Z\gamma}\,,$$

$$c^Z = -2g_{ff}^Z\tilde{\kappa}_{ZZ}\,, \qquad\qquad c^W = -2g_{ff'}^W\tilde{\kappa}_{WW}\,,$$

$$\hat{c}^Z = -2eQ_f\tilde{\kappa}_{Z\gamma}\,. \tag{41}$$

From the differential distributions of the decay products in $h \to Vff$, one can put bounds on the coefficients of Eq. (40) and, consequently, on non-primary Higgs couplings. Nevertheless, we still have poor statistics and bounds on Higgs couplings are almost irrelevant unless we turn on one by one [32]. At present, the most promising way to obtain significant bounds in some of the Higgs couplings of Eq. (3) is, as we will discuss below, by measuring them at the LHC high-energy regime, for example in the Vh-associated Higgs production where the effects of some of these couplings are enhanced.

Since primary Higgs couplings predict equal deviations in the $hZff$ and $hWff$ physical amplitudes (normalized to their SM values), measuring a relative deviation between these two would provide evidence for non-primary Higgs couplings. At the LHC this relative deviation is parametrized by $\lambda_{WZ} - 1$ [2,3] that at present does not show any evidence of being different from zero; from the experimental data we have $-0.35 < \lambda_{WZ} - 1 < 0.08$ [3]. This quantity is predicted in the SM EFT of Eq. (15) to be [19]

$$\lambda_{WZ}^2 - 1 \simeq 0.6\delta g_1^Z - 0.5\delta\kappa_\gamma - 0.7\kappa_{Z\gamma}\,, \tag{42}$$

where we have used Eqs. (18)-(19), neglecting $\kappa_{\gamma\gamma}$ and $\delta g_{ff}^{Z,W}$, since they are experimentally constrained to be less than $10^{-2} - 10^{-3}$.

5.1 Towards the high-energy regime

One of the most interesting perspectives at the LHC run 2 is the access to physical processes at much higher energies. This can be used to probe Higgs production mechanism or off-sell Higgs mediated processes in a regime in which the effects of some anomalous Higgs couplings can be enhanced by factors E^2/Λ^2. As an example, let us consider the associated Higgs production, $pp \to Vh$. As it is clear from Eq. (40), at high-energies, $E \gg m_V$, the coefficient a^V dominates the amplitude. Thanks to our parametrization for Higgs couplings, this coefficient is in one-to-one correspondence with the contact-interaction g_{Vff}^h. Indeed, at the partonic level, we have

$$\sigma(qq \to hV)\Big|_{\hat{s} \gg m_h^2} = \sigma(qq \to hV_L)_{\rm SM} \left(1 + \frac{g_{Vff}^h}{g_{ff}^V} \frac{\hat{s}}{m_V^2} + \dots \right) . \tag{43}$$

By looking at high invariant-masses for hV, it is possible to put important bounds on g_{Vff}^h [35, 36]. Nevertheless, one has to be careful that one is not probing these couplings at energies above Λ where an expansion in $\hat{s}/\Lambda^2$ would not be valid. To address this issue, the power-counting of section 4.3 is crucial. Using Eq. (35), we can write $g_{Vff}^h \equiv gc_{Vff}^h g_*^2 v^2/\Lambda^2$ where c_{Vff}^h is a coefficient $O(1)$. Now, experimentally, due to the lack of experimental accuracy in the measurement of $pp \to Vh$ at the LHC, we can only bound at present high-energy deviations from the SM to be less than $O(1)$ [35, 36], that is equivalent to say, using Eq. (43),

$$\frac{g_{Vff}^h}{g_{ff}^V} \frac{\hat{s}}{m_V^2} < O(1) \quad \to \quad c_{Vff}^h \lesssim \frac{\Lambda^2}{\hat{s}} \frac{g^2}{g_*^2} . \tag{44}$$

To guarantee the validity of the expansion in $\mathcal{L}_h$, we must stay in the regime $\Lambda^2/\hat{s} \gg 1$. Therefore the experimental bound Eq. (44) can only be restrictive (and useful) for strongly-interacting BSMs in which $g_* \gg g$. In these scenarios we can safely use the hV-production high-energy data to obtain bounds on g_{Vff}^h at the per-cent level [36]. In models in which, in addition, the expansion of Eq. (15) is valid, bounds on g_{Vff}^h can be translated into bounds on δg_1^Z. Indeed, we have from Eq. (18), after neglecting δg_{ff}^Z due to the strong constraints from LEP, and neglecting $\delta\kappa_\gamma$ since this does not grow with g_*^2 [13],

$$\delta g_1^Z \simeq -\frac{gc_{Zff}^h}{2(g_{ff}^Z c_{2\theta_W} + eQ_f s_{2\theta_W})} \frac{g_*^2 v^2}{\Lambda^2} \simeq -\frac{gc_{Wff'}^h}{2g_{ff'}^W c_{\theta_W}^2} \frac{g_*^2 v^2}{\Lambda^2} . \tag{45}$$

From the experimental data at the high-energy regime of the hV-associated production we obtain [36]

$$-0.01 < \delta g_1^Z < 0.04 \quad (95\% \text{ CL}) . \tag{46}$$

This is as competitive as the one obtained from anomalous TGC at LEP [21] and at the LHC [37].

5.2 Invisible Higgs decay

We have assumed so far that there are no more light particles than those of the SM. If there were new light states to which the Higgs could decay to, all the Higgs BRs would be reduced, changing the fit of the Higgs couplings [38]. There are well-motivated BSMs where the Higgs can decay invisibly. An example is given in [39] where the Higgs can decay to a gravitino and neutrino that interact so weakly that escape from detection. Also in certain models the Higgs can decay to dark matter that, being stable and EM neutral, also escape from detection. [9] There are direct searches for Higgs decaying invisibly based on looking for missing energy plus a $Z/W/\gamma/jet$. The CMS bound is given in Fig. 3.

---

[9]Alternative effects from new light physics can be found in [40].

6 Predictions for the Higgs couplings from BSM solutions to the hierarchy problem

The simplicity of the SM Higgs-mechanism is at odds with its quantum stability. The fact that the Higgs is a scalar, a spin zero state, makes it difficult to keep it light ($m_h \ll M_P$). This problematic can be easily understood just by looking at the degrees of freedom (DOF) of a massless and massive state of spin 0, and compare them with those of a state of spin 1/2, 1, or higher. Indeed, a massless vector, as the photon, has two polarizations (2 DOF), while a massive vector has 3 polarizations. The $2 \neq 3$ guarantees that a massless vector can never get a mass by continuous variations of parameters (or quantum fluctuations); only a discrete change in the theory, increasing the DOF, can make vector massive. Similarly for fermions, we have that a charged massless fermion has 2 DOF, while a massive one has the double (left- and right-handed states), and therefore, for the same reason, massless fermions are safe from getting masses under fluctuations. [10] Now, massless scalars have the same DOF as massive scalars: 1 DOF for neutral ones. Even if we start with a massless scalar at tree-level, it is not guaranteed that quantum corrections will not give it a mass.

A possible solution to keep the Higgs stable from getting a large mass is to upgrade the SM to include a symmetry relating the Higgs, a scalar, to a fermion whose mass can be stable, as we explained above. This is the case of supersymmetry. An alternative option is to assume that the Higgs is not an elementary state but a state made of elementary fermions, as pions in QCD. In this case, the Higgs arises as a composite state from a new strong-sector at the TeV. It is interesting to point out that both scenarios predicted a light Higgs. While in minimal supersymmetric versions of the SM (MSSM) the lightest-Higgs mass was expected to be in the range $m_h \lesssim 135$ GeV [41], minimal versions of composite Higgs (MCHM) predicted 115 GeV $\lesssim m_h \lesssim 185$ GeV [42]. The connection between the Higgs mass and the mass spectrum of resonances is of crucial phenomenological interest, since allows to obtain predictions, from the present experimental value $m_h \simeq 125$ GeV, for the heavy spectrum, either stops for the MSSM [43] or fermionic resonances for the MCHM [44, 45].

In the following, we will centre in the predictions of these models to Higgs couplings. As we emphasized in the introduction, the Higgs is usually the SM particle whose couplings are most sensitive to BSM corrections. Indeed, as we will see below, in supersymmetric theories Higgs couplings can be affected at tree-level [46], while other SM couplings are affected at the loop level. Similarly, in strongly-interacting theories in which the Higgs is composite, effects on Higgs couplings can be enhanced by a factor g_*^2 [4], that can be as large as $\sim 16\pi^2$, with respect to effects in other couplings. It is also important to remark that in BSMs trying to solve the hierarchy problem the main BSM effects in Higgs physics are captured by the primary Higgs couplings, as contributions to non-primary Higgs couplings are usually negligible. This shows once more the importance of the primaries.

6.1 The Minmal Supersymmetric SM (MSSM)

We will work in the limit in which the supersymmetric spectrum is heavier than m_h. This covers *most* of the parameter space of the MSSM, after LHC searches have pushed the superpartner masses towards the TeV regime, and none deviation from the SM has been observed. Also to accommodate $m_h \simeq 125$ GeV requires large stop masses in the MSSM [43].

The only tree-level corrections to the lightest-Higgs couplings come from the extra heavy Higgs doublet of the MSSM H'. This is due to the R-parity of the MSSM that only allow R-even field tree-level corrections. At order $v^2/M_{H'}^2$ (*i.e.*, keeping only $1/\Lambda^2$-suppressed effects where now $\Lambda = M_{H'}$), only the Higgs couplings to fermions are affected, since corrections to hVV appear at order $v^4/M_{H'}^4$ as can be easily understood from Feynman diagrams –see Fig. 5. Deviations from the SM values for the hff

---

[10] If a fermion has no charge, it can get a Majorana-type mass without increasing the DOF, as probably is the case for the SM neutrinos. For this reason, to keep naturally massless fermions, we must assume that the fermion has some type of charge.
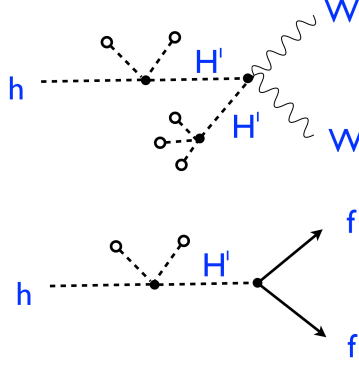
Fig. 5: Feynman diagrams contributing to g^h_{VV} and g^h_{ff} from integrating the heavy MSSM Higgs H'.
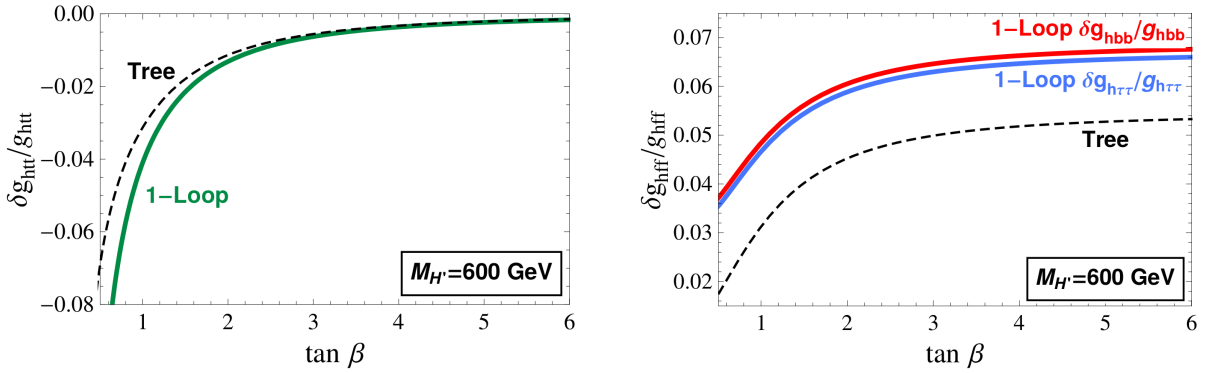

Fig. 6: Relative modifications of the Higgs couplings to fermions with respect to their SM values at tree-level (dashed line), and after including RGE effects from Λ to the electroweak scale (solid lines), as a function of $\tan\beta$ in a MSSM scenario with $\Lambda = M_{H'} = 600$ GeV and unmixed stops heavy enough to reproduce $m_h = 125$ GeV. Left plot: Higgs coupling to tops. Right plot: Higgs coupling to bottoms (upper solid line) and taus (lower solid line) [9].

couplings, including also one-loop RGE effects coming from the top, are given by [9]

$$
\frac{\delta g^h_{tt}}{g^{h\,\mathrm{SM}}_{tt}} = \frac{v^2}{M_{H'}^2}\left(\frac{\lambda'}{t_\beta}\left[1 - \frac{21 y_t^2}{16\pi^2}\log\frac{M_{H'}}{m_h}\right] + \frac{3 y_t^4}{4\pi^2 t_\beta^2}\log\frac{M_{H'}}{m_h}\right) ,
$$

$$
\frac{\delta g^h_{bb}}{g^{h\,\mathrm{SM}}_{bb}} = -\frac{v^2}{M_{H'}^2}\left(\lambda' t_\beta\left[1 - \frac{y_t^2}{2\pi^2}\log\frac{M_{H'}}{m_h}\right] + \frac{y_t^2}{16\pi^2}\left[5\frac{\lambda'}{t_\beta} - 14 y_t^2\right]\log\frac{M_{H'}}{m_h}\right) ,
$$

$$
\frac{\delta g^h_{\tau\tau}}{g^{h\,\mathrm{SM}}_{\tau\tau}} = -\frac{v^2}{M_{H'}^2}\left(\lambda' t_\beta\left[1 - \frac{3 y_t^2}{8\pi^2}\log\frac{M_{H'}}{m_h}\right] + \frac{3 y_t^2}{8\pi^2}\left[\frac{\lambda'}{t_\beta} - 2 y_t^2\right]\log\frac{M_{H'}}{m_h}\right) , \tag{47}
$$

with $t_\beta \equiv \tan\beta$ and [11]

$$
\lambda' = \frac{1}{8}(g^2 + g'^2)\sin 4\beta - \frac{3 y_t^4}{8\pi^2 t_\beta}\log\frac{M_{\tilde{t}}^2}{M_{H'}^2}, \tag{48}
$$

where $M_{\tilde{t}}$ is the value of the stop masses taking, for simplicity, zero stop left-right mixing. To illustrate the impact of these corrections, let us take $M_{\tilde{t}}$ large enough to get $m_h \simeq 125$ GeV through the well-known loop corrections to the Higgs quartic coupling, which at one-loop and neglecting stop left-right mixings read: $\lambda = \frac{1}{8}(g^2 + g'^2)\cos^2 2\beta + \frac{3 y_t^4}{16\pi^2}\log\frac{M_{\tilde{t}}^2}{M_t^2}$. This gives the value of λ' as a function of t_β

[11]In Eq. (48) we are also including RGE effects from $M_{\tilde{t}}$ to $M_{H'}$ proportional to the top-Yukawa y_t.
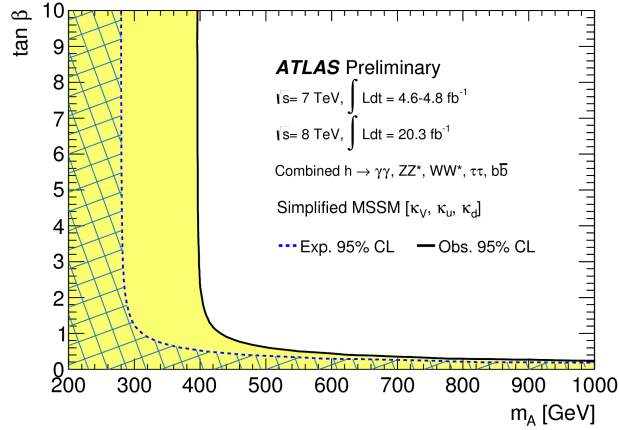
Fig. 7: Regions of the $m_A - \tan\beta$ plane excluded by Higgs physics in a MSSM with heavy partners [47].

and $M_{H'}$ that we can then plug in Eq. (47) to obtain the RGE-improved corrections for g_{ff}^h induced by integrating out the heavy Higgs. The results are shown in Fig. 6. The experimental bounds on the Higgs couplings can be translated into a bound on $M_{H'}$ as a function of t_β. This is given in Fig. 7 where m_A is the mass of the heavy MSSM CP-odd scalar that, at the order we are working at, is equal to $M_{H'}$. [12] Stop left-right mixing effects or extra D-term effects can be easily included along the lines of [48]. Corrections to g_{3h} can also arise at order $O(v^2/M_{H'}^2)$, but we already said that this coupling is difficult to measure as it requires double Higgs production.

6.2 The Minimal Composite Higgs Model (MCHM)

For models in which the Higgs is a pseudo Goldstone boson (PGB) arising from a new strong-sector at the TeV [49], similar to a pion in QCD, the Higgs couplings must depart from their SM value. This was studied in generality in [4]. The main effects are expected to arise in the Higgs coupling to Z/W and fermions. The minimal model is the MCHM [50], where the global symmetry-breaking pattern is $SO(5) \to SO(4)$ with an "order parameter" f, that give the following predictions [4]:

$$
\begin{aligned}
\frac{g_{VV}^h}{g_{VV}^{h\,\mathrm{SM}}} &= \sqrt{1 - \frac{v^2}{f^2}}\,, \\
\frac{g_{ff}^h}{g_{ff}^{h\,\mathrm{SM}}} &= \frac{1 - (1+n)v^2/f^2}{\sqrt{1 - v^2/f^2}}\,,
\end{aligned}
\tag{49}
$$

where $n = 0, 1, 2, \ldots$ depends on how fermions are implemented in the model. In particular, for the MCHM4 (MCHM5) we have $n = 0\,(1)$ [45]. From the minimization of the Higgs potential, we expect $f \gtrsim v$ [4], but constraints from the $\widehat{S}$ parameter give $v^2/f^2 \lesssim 0.1$ [49]. The Higgs coupling predictions of the MCHM are shown in Fig. 8 and compared with a fit of the ATLAS data. The fact that the experimental data does not favour smaller Higgs couplings than those of the SM, as predicted from Eq. (49), implies that we can derive an upper bound on $\xi \equiv v^2/f^2$, and consequently on the composite scale, $\Lambda \simeq g_* f$, where g_* is here the coupling among the resonances of the strong sector, expected to be in the range, $1 \ll g_* \lesssim 4\pi$. ATLAS [47] gives the observed (expected) 95% CL upper limit of $\xi < 0.12\ (0.29)$ for the MCHM4 and $\xi < 0.15\ (0.20)$ for the MCHM5 that start being as competitive as the ones coming from LEP [49].

---

[12]Mass splittings among the heavy Higgs-doublet components are $O(v^2/M_{H'}^2)$, and then their effects are of higher-order in our expansion.
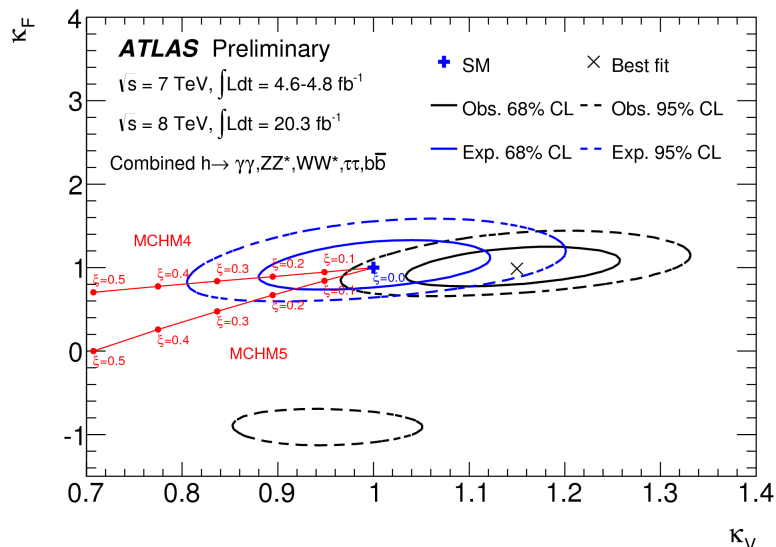
Fig. 8: Two-dimesional fit of the Higgs couplings $\kappa_V \equiv g^h_{VV}/g^{h\,\mathrm{SM}}_{VV}$ and $\kappa_F \equiv g^h_{ff}/g^{h\,\mathrm{SM}}_{ff}$ and predictions from the MCHM4 and MCHM5 as a function of $\xi \equiv v^2/f^2$ [47].

Contributions to $\kappa_{\gamma\gamma}$ and κ_{GG} are suppressed in the MCHM due to the PGB nature of the Higgs [4]. Nevertheless, this suppression is not present in $\kappa_{Z\gamma}$ that can receive significant contributions [51] that could be even larger than those of the SM, providing a strong motivation for searching for $h \to Z\gamma$.

7   Conclusions

With the Higgs discovery, the full SM has been experimentally established. Nevertheless, the presence of the Higgs, a zero-spin state, demands new physics at the TeV to make the SM a natural theory. The Higgs is the most sensitive SM particle to new physics, and for this reason an accurate measurement of its couplings provides an excellent way to indirectly discover new phenomena.

At the LHC (and in future colliders) we can have access to a large variety of Higgs couplings. We have argued that the most relevant Higgs couplings are the primary ones, given in Eq. (2) for CP-conservation. These couplings probe new directions in the parameter space of BSMs. We have showed the predictions for two of the most well-motivated BSMs, the MSSM and the MCHM. These analysis can be extended to other BSMs, such as the non-minimal MSSM (NMSSM), or other possibilities for composite Higgs, for example those in which the Higgs is lighter than the composite scale Λ not because of its PGB nature, as in the MCHM, but due to an "accidental" supersymmetry (SUSY Composite Higgs) or scale symmetry (Higgs as a dilaton) [49]. Supersymmetry can also allow for partly-composite Higgs where the TeV strong-sector could also break the electroweak symmetry (bosonic TC) [24]. A brief summary of the largest effects in the primary Higgs coupling arising from these scenarios is giving in Table 1. If in the future departures from the SM Higgs couplings are observed, the analysis of the pattern of these deviations will be extremely useful to discriminate between different BSM scenarios.

Acknowledgements

	g_{ff}^h	g_{VV}^h	κ_{GG}	$\kappa_{\gamma\gamma}$	$\kappa_{Z\gamma}$	g_{3h}
MSSM	✓					✓
NMSSM	✓	✓	✓	✓	✓	✓
MCHM	✓	✓			✓	✓
SUSY Composite Higgs	✓	✓	✓	✓	✓	✓
Higgs as a Dilaton			✓	✓	✓	✓
Partly-Composite Higgs			✓	✓	✓	✓
Bosonic TC						✓

Table 1: Largest contributions to Higgs couplings (relative to the SM one) expected from different BSM scenarios.

References

[1] G. Aad *et al.*, [ATLAS Collab.], Phys. Lett. B **716** (2012) 1; S. Chatrchyan *et al.*, [CMS Collab.], Phys. Lett. B **716** (2012) 30.

[2] A. David for the CMS Collaboration, Talk at ICHEP14 (Valencia); see also CMS-PAS-HIG-14-009.

[3] M. Kado for the ATLAS Collaboration, Talk at ICHEP14 (Valencia); see also ATLAS-CONF-2014-009, ATLAS-COM-CONF-2014-013.

[4] G. F. Giudice, C. Grojean, A. Pomarol and R. Rattazzi, JHEP **0706** (2007) 045 [hep-ph/0703164].

[5] S. Weinberg, Phys. Rev. D **19** (1979) 1277; L. Susskind, Phys. Rev. D **20** (1979) 2619; P. Sikivie, L. Susskind, M. B. Voloshin and V. I. Zakharov, Nucl. Phys. B **173** (1980) 189.

[6] Work in preparation.

[7] We follow the conventions of M. E. Peskin and D. V. Schroeder, "An Introduction to quantum field theory," Reading, USA: Addison-Wesley (1995) 842 p.

[8] R. Contino, M. Ghezzi, C. Grojean, M. Muhlleitner and M. Spira, JHEP **1307** (2013) 035 [arXiv:1303.3876 [hep-ph]].

[9] J. Elias-Miro, J. R. Espinosa, E. Masso and A. Pomarol, JHEP **1311** (2013) 066 [arXiv:1308.1879 [hep-ph]].

[10] J. F. Gunion, H. E. Haber, G. L. Kane and S. Dawson, Front. Phys. **80** (2000) 1.

[11] B. Grzadkowski, M. Iskrzynski, M. Misiak and J. Rosiek, JHEP **1010** (2010) 085 [arXiv:1008.4884 [hep-ph]].

[12] M. E. Peskin and T. Takeuchi, Phys. Rev. Lett. **65** (1990) 964.

[13] R. S. Gupta, A. Pomarol and F. Riva, arXiv:1405.0181 [hep-ph].

[14] E. Masso, arXiv:1406.6376 [hep-ph].

[15] M. B. Einhorn and J. Wudka, Nucl. Phys. B **876** (2013) 556 [arXiv:1307.0478 [hep-ph]].

[16] K. Hagiwara, S. Ishihara, R. Szalapski and D. Zeppenfeld, Phys. Lett. B **283** (1992) 353; Phys. Rev. D **48** (1993) 2182.

[17] J. Elias-Miro, J. R. Espinosa, E. Masso and A. Pomarol, JHEP **1308** (2013) 033 [arXiv:1302.5661 [hep-ph]].

[18] C. Grojean, E. E. Jenkins, A. V. Manohar and M. Trott, JHEP **1304** (2013) 016 [arXiv:1301.2588 [hep-ph]]; E. E. Jenkins, A. V. Manohar and M. Trott, JHEP **1310** (2013) 087 [arXiv:1308.2627 [hep-ph]]; JHEP **1401** (2014) 035 [arXiv:1310.4838 [hep-ph]]; J. Elias-Miro, C. Grojean, R. S. Gupta and D. Marzocca, JHEP **1405** (2014) 019 [arXiv:1312.2928 [hep-ph]].

[19] A. Pomarol and F. Riva, JHEP **1401** (2014) 151 [arXiv:1308.2803 [hep-ph]].

[20] S. Schael *et al.* [ALEPH and DELPHI and L3 and OPAL and SLD and LEP Electroweak Working Group and SLD Electroweak Group and SLD Heavy Flavour Group Collaborations], Phys. Rept. **427** (2006) 257 [hep-ex/0509008].

[21] The LEP collaborations ALEPH, DELPHI, L3, OPAL, and the LEP TGC Working Group, LEPEWWG/TGC/2003-01.

[22] Model-independent bounds were obtained for the first time in Z. Han and W. Skiba, Phys. Rev. D **71** (2005) 075009 [hep-ph/0412166], and, more recently, in [19]; J. Ellis, V. Sanz and T. You, arXiv:1410.7703 [hep-ph]; A. Falkowski and F. Riva, arXiv:1411.0669 [hep-ph]. See also M. Ciuchini, E. Franco, S. Mishima and L. Silvestrini, JHEP **1308** (2013) 106 [arXiv:1306.4644 [hep-ph]]; M. Ciuchini, E. Franco, S. Mishima, M. Pierini, L. Reina and L. Silvestrini, arXiv:1410.6940 [hep-ph], though the bounds derived there are not fully model-independent.

[23] R. Barbieri *et al.*, Nucl. Phys. B **703** (2004) 127 [hep-ph/0405040].

[24] For models with this property, see for example, M. Dine, A. Kagan and S. Samuel, Phys. Lett. B **243** (1990) 250, and more recently, A. Azatov, J. Galloway and M. A. Luty, Phys. Rev. Lett. **108** (2012) 041802 [arXiv:1106.3346 [hep-ph]]; Phys. Rev. D **85** (2012) 015018 [arXiv:1106.4815 [hep-ph]]; T. Gherghetta and A. Pomarol, JHEP **1112** (2011) 069 [arXiv:1107.4697 [hep-ph]].

[25] A. Manohar and H. Georgi, Nucl. Phys. B **234** (1984) 189.

[26] See https://twiki.cern.ch/twiki/bin/view/LHCPhysics/LHCHXSWG.

[27] CMS Collaboration, arXiv:1307.5515 [hep-ex]; ATLAS Collaboration, ATLAS-CONF-2013-009.

[28] A. Falkowski, F. Riva and A. Urbano, JHEP **1311** (2013) 111 [arXiv:1303.1812 [hep-ph]].

[29] C. Englert, A. Freitas, M. M. Muhlleitner, T. Plehn, M. Rauch, M. Spira and K. Walz, J. Phys. G **41** (2014) 113001 [arXiv:1403.7191 [hep-ph]].

[30] R. Contino, C. Grojean, M. Moretti, F. Piccinini and R. Rattazzi, JHEP **1005** (2010) 089 [arXiv:1002.1011 [hep-ph]].

[31] CMS Collaboration, CMS-PAS-HIG-14-005 (2014).

[32] CMS Collaboration, CMS-PAS-HIG-13-002.

[33] C. Delaunay, G. Perez, H. de Sandes and W. Skiba, Phys. Rev. D **89** (2014) 035004 [arXiv:1308.4930 [hep-ph]]; F. Bishara, Y. Grossman, R. Harnik, D. J. Robinson, J. Shu and J. Zupan, JHEP **1404** (2014) 084 [arXiv:1312.2955 [hep-ph]].

[34] D. McKeen, M. Pospelov and A. Ritz, Phys. Rev. D **86** (2012) 113004 [arXiv:1208.4597 [hep-ph]].

[35] J. Ellis, V. Sanz and T. You, JHEP **1407** (2014) 036 [arXiv:1404.3667 [hep-ph]].

[36] A. Biekoetter, A. Knochel, M. Kraemer, D. Liu and F. Riva, arXiv:1406.7320 [hep-ph].

[37] G. Aad *et al.* [ATLAS Collaboration], Phys. Rev. D **87** (2013) 11, 112001 [Erratum-ibid. D **88** (2013) 7, 079906] [arXiv:1210.2979 [hep-ex]].

[38] See, for example, S. Chang, R. Dermisek, J. F. Gunion and N. Weiner, Ann. Rev. Nucl. Part. Sci. **58** (2008) 75 [arXiv:0801.4554 [hep-ph]].

[39] F. Riva, C. Biggio and A. Pomarol, JHEP **1302** (2013) 081 [arXiv:1211.4526 [hep-ph]].

[40] M. Gonzalez-Alonso and G. Isidori, Phys. Lett. B **733** (2014) 359 [arXiv:1403.2648 [hep-ph]]; A. Falkowski and R. Vega-Morales, arXiv:1405.1095 [hep-ph].

[41] See, for example, A. Djouadi, Phys. Rept. **459** (2008) 1 [hep-ph/0503173].

[42] R. Contino, L. Da Rold and A. Pomarol, Phys. Rev. D **75** (2007) 055014 [hep-ph/0612048].

[43] See, for example, L. J. Hall, D. Pinner and J. T. Ruderman, JHEP **1204** (2012) 131 [arXiv:1112.2703 [hep-ph]].

[44] O. Matsedonskyi, G. Panico and A. Wulzer, JHEP **1301** (2013) 164 [arXiv:1204.6333 [hep-ph]]. M. Redi and A. Tesi, JHEP **1210** (2012) 166 [arXiv:1205.0232 [hep-ph]]; D. Marzocca, M. Serone and J. Shu, JHEP **1208** (2012) 013 [arXiv:1205.0770 [hep-ph]].

[45] A. Pomarol and F. Riva, JHEP **1208** (2012) 135 [arXiv:1205.6434 [hep-ph]].

[46] See, for example, A. Arvanitaki and G. Villadoro, JHEP **1202** (2012) 144 [arXiv:1112.4835 [hep-ph]]; A. Azatov, S. Chang, N. Craig and J. Galloway, Phys. Rev. D **86** (2012) 075033 [arXiv:1206.1058 [hep-ph]].

[47] ATLAS Collaboration, ATLAS-CONF-2014-010.

[48] R. S. Gupta, M. Montull and F. Riva, JHEP **1304** (2013) 132 [arXiv:1212.5240 [hep-ph]].

[49] For a review, see for example, R. Contino, arXiv:1005.4269 [hep-ph]; B. Bellazzini, C. Csáki and J. Serra, Eur. Phys. J. C **74** (2014) 2766 [arXiv:1401.2457 [hep-ph]].

[50] K. Agashe, R. Contino and A. Pomarol, Nucl. Phys. B **719** (2005) 165 [hep-ph/0412089].

[51] A. Azatov, R. Contino, A. Di Iura and J. Galloway, Phys. Rev. D **88** (2013) 7, 075019 [arXiv:1308.2676 [hep-ph]].

Flavour Physics and CP Violation

J. F. Kamenik
J. Stefan Institute, Ljubljana, Slovenia
Department of Physics, University of Ljubljana, Ljubljana, Slovenia

Abstract
These notes represent a summary of three lectures on flavour and CP violation, given at the CERN's European School of High Energy Physics in 2014. They cover flavour physics within the standard model, phenomenology of CP violation in meson mixing and decays, as well as constraints of flavour observables on physics beyond the standard model. In preparing the lectures (and consequently this summary) I drew heavily from several existing excellent and exhaustive sets of lecture notes and reviews on flavour physics and CP violation [1]. The reader is encouraged to consult those as well as the original literature for a more detailed study.

1 What is flavour?

In the standard model (SM) the basic constituents of matter are excitations of fermionic fields with spin $1/2$. In this context *matter flavours* refers to several copies of the same gauge representation. Under the unbroken SM gauge group $SU(3)_c \times U(1)_{\rm EM}$ these are

- up-type quarks: $(3)_{2/3} : u, c, t$,
- down-type quarks: $(3)_{-1/3} : d, s, b$,
- chrged leptons: $(1)_{-1} : e, \mu, \tau$,
- neutrinos: $(1)_0 : \nu_1, \nu_2, \nu_3$,

where the colour representations are given in the brackets, while the electric charges are written as subscripts. The different flavours of the same gauge representation differ only in their masses.

Ordinary matter is essentially made up of the first generation: u and d quarks are bound within protons and neutrons, while the electrons form atoms; finally "electron neutrinos", which are an admixture of $\nu_{1,2,3}$, are produced in reactions inside stars. Second and third generation families are produced only in high-energy particle collisions. They all decay via weak interactions into first generation particles. One of the big open questions in fundamental physics is why there are thee almost identical replicas of quarks and leptons and which is the origin of their different masses?

Flavour physics refers to interactions that distinguish between flavours. Within the SM these are weak and Yukawa (Higgs boson) interactions.

Flavour parameters are those that carry flavour indices. Within the SM these are the nine masses of charged fermions and four mixing parameters (three angles and one complex CP violating phase).[1]

Flavour universal interactions are those with couplings proportional to the identity in flavour space. Within the SM these are strong and electromagnetic interactions (and also weak interactions in the so-called interactions basis, see below). Such interactions are sometimes also called *flavour blind*.

Flavour diagonal interactions are those whose couplings are diagonal (in the matter mass basis), but not necessarily universal. Within the SM these are the Yukawa interactions of the Higgs boson.

Flavour changing processes are those where the initial and final flavour-numbers are different (a flavour number is the number of particles with a certain flavour minus the number of anti-particles of

---

[1]Adding Majorana mass terms for neutrinos introduces three additional neutrino masses plus six mixing parameters (three mixing angles and three phases).

the same flavour). We can further specify *flavour changing charged currents* which involve both up- and down-type quark flavours or both charged lepton and neutrino flavours. Examples of such processes are the muon decay $\mu^- \to e^- \nu_i \bar{\nu}_j$ or the muonic charged kaon decay $K^- \to \mu^- \bar{\nu}_i$ (which corresponds to the quark-level transition $s\bar{u} \to \mu^- \bar{\nu}_i$). Within the SM such processes are mediated already by a single W exchange at the tree level (the amplitudes being proportional to the Fermi constant G_F). On the other hand, *flavour changing neutral currents* (FCNCs) involve either up- or down- type flavours but not both; and/or either charged lepton flavours or neutrino flavours but not both. Examples of such processes are the radiative muon decay $\mu^- \to e^- \gamma$ and the muonic decays of the neutral kaons, $K_L \to \mu^+ \mu^-$ ($s\bar{d} \to \mu^+ \mu^-$ at the quark level). Within the SM these processes occur at higher orders in the weak expansion (i.e. via loops) and are often *highly suppressed*. In connection with flavour changing interactions, one often speaks also of *flavour violation*.

1.1 Why is flavour interesting?

Flavour physics can discover new physics (NP) or probe it before it is directly observed in high-energy experiments. Historical examples of this include:

- The smallness of the ratio $\Gamma(K_L \to \mu^+ \mu^-)/\Gamma(K^- \to \mu^- \bar{\nu}_i)$ lead to the prediction of the charmed quark.
- Furthermore, the measurement of the mass difference between the two neutral kaons $\Delta m_K \equiv m_{K_L} - m_{K_S}$ lead to the prediction of the charm quark mass.
- Similarly, the mass difference between the two neutral B mesons $\Delta m_B \equiv m_{B_H^0} - m_{B_L^0}$ inferred a prediction of the top quark mass almost two decades before top quarks (or more precisely, their decay products) were directly observed in experiments.
- Finally, the observation of the CP violating decay $K_L \to \pi^+ \pi^-$ (i.e the measurement of ϵ_K) lead to the prediction of the third generation of matter.

CP violation: Within the SM there is a single CP violating parameter determining the amount of CP violation in all flavour changing processes. Successful baryogenesis would require new CP violating sources.

Solutions of the electroweak (EW) hierarchy problem (in the form of a quadratic sensitivity of the EW scale to UV physics) require NP to appear at or below the TeV scale. On the other hand, such NP with a generic flavour structure would predict FCNCs orders of magnitude above the observed rates. Conversely, flavour physics can probe NP scales up to $\mathcal{O}(10^5 \text{ TeV})$. The resulting *NP flavour puzzle* refers to the fact that NP at the TeV scale needs to exhibit approximate flavour symmetries.

The SM flavour parameters are both hierarchical (i.e. $m_u \ll m_c \ll m_t$) and mostly very small ($m_{f \neq t} \ll m_{W,Z,h}$). The question whether this points to some unknown underlying flavour dynamics is sometimes called the *SM flavour puzzle*.

2 Flavour in the standard model

Any (local) quantum field theory model is specified by both (i) symmetries and the pattern of their spontaneous breaking; as well as (ii) representations of fermions and scalars. The SM Lagrangian ($\mathcal{L}_{\text{SM}}$) is thus completely determined by specifying the local (gauge) symmetry $\mathcal{G}_{\text{local}}^{\text{SM}} = SU(3)_c \times SU(2)_L \times U(1)_Y$ which is spontaneously broken to $\mathcal{G}_{\text{local}}^{\text{SM}} \to SU(3)_c \times U(1)_{\text{EM}}$; plus the relevant fermionic

$$Q_L^i \sim (3,2)_{1/6}\,, \qquad U_R^i \sim (3,1)_{2/3}\,, \qquad D_R^i \sim (3,1)_{-1/3}\,, \qquad L_L^i \sim (1,2)_{-1/2}\,, \qquad (1)$$

(where $i = 1,2,3$) and scalar

$$\phi \sim (1,2)_{1/2}\,, \qquad\qquad \langle \phi^0 \rangle \equiv \frac{v}{\sqrt{2}} \simeq 174 \text{GeV}\,, \qquad (2)$$

representations. Above, the first (second) entries in the brackets denote the $SU(3)_c$ $(SU(2)_L)$ representations, while the $U(1)_Y$ charges are given in the subscripts. Also, $\langle \ldots \rangle$ denotes a vacuum condensate value. $\mathcal{L}_{\text{SM}}$ can be conveniently split into three parts

$$\mathcal{L}_{\text{SM}} = \mathcal{L}_{\text{kinetic}}^{\text{SM}} + \mathcal{L}_{\text{EWSB}}^{\text{SM}} + \mathcal{L}_{\text{Yukawa}}^{\text{SM}} \,. \tag{3}$$

The sum of the gauge-kinetic terms $\mathcal{L}_{\text{kinetic}}^{\text{SM}}$ is simple and symmetric. It is completely specified by the SM local symmetry and its matter representations. The three physical parameters associated with this part of the theory are conventionally chosen to be the three gauge couplings $(g_s, g$ and $g')$. The EW symmetry breaking (EWSB) part $\mathcal{L}_{\text{EWSB}}^{\text{SM}}$ contains two additional parameters. They can be chosen to correspond to v and the physical Higgs boson mass m_h. Finally, all flavour dynamics is contained in $\mathcal{L}_{\text{Yukawa}}^{\text{SM}}$ which also involves all the SM flavour parameters.

2.1 Interaction basis

It is convenient to start our discussion in a flavour basis where all the gauge-kinetic terms are diagonal. This can always be achieved by applying suitable unitary rotations on the matter fields. In this basis

$$\mathcal{L}_{\text{kinetic}}^{\text{SM}} = (D_\mu \phi)^\dagger (D^\mu \phi) + \sum_{i,j=1,2,3} \sum_{\psi = Q_L, \ldots, E_R} \bar{\psi}^i i \slashed{D} \delta^{ij} \psi^j$$
$$- \frac{1}{4} \sum_{a=1,\ldots,8} G_{\mu\nu}^a G^{a,\mu\nu} - \frac{1}{4} \sum_{a=1,2,3} W_{\mu\nu}^a W^{a,\mu\nu} - \frac{1}{4} B_{\mu\nu} B^{\mu\nu} \,, \tag{4}$$

where G, W, and B denote the field strengths of the $SU(3)_c$, $SU(2)_L$ and $U(1)_Y$ gauge interactions, respectively. The covariant derivatives D_μ are defined as $D_\mu = \partial_\mu + i g_s G_\mu^a L^a + i g W_\mu^b T^b + i g' B_\mu Y$, where L^a, T^a and Y denote the $SU(3)_c$, $SU(2)_L$ generators and the $U(1)_Y$ charges, respectively. Note that in this basis, $\mathcal{L}_{\text{kinetic}}^{\text{SM}}$ is manifestly flavour universal and CP conserving. Similarly

$$\mathcal{L}_{\text{EWSB}}^{\text{SM}} = \mu^2 \phi^\dagger \phi - \lambda (\phi^\dagger \phi)^2 \,, \tag{5}$$

is also CP and flavour conserving.[2] Thus both $\mathcal{L}_{\text{kinetic}}^{\text{SM}}$ and trivially $\mathcal{L}_{\text{EWSB}}^{\text{SM}}$ have a large flavour symmetry corresponding to the independent unitary rotations in the flavour space of the five fermionic fields

$$\mathcal{G}_{\text{flavour}}^{\text{SM}} = U(3)^5 = SU(3)_q^3 \times SU(3)_\ell^2 \times U(1)^5 \,,$$
$$SU(3)_q^3 = SU(3)_Q \times SU(3)_U \times SU(3)_D \,,$$
$$SU(3)_\ell^2 = SU(3)_L \times SU(3)_E \,,$$
$$U(1)^5 = U(1)_B \times U(1)_L \times U(1)_Y \times U(1)_{\text{PQ}} \times U(1)_E \,. \tag{6}$$

Among the $U(1)$ factors, $U(1)_{B,L}$ are the baryon and lepton number, respectively. $U(1)_Y$ is gauged and broken spontanouesly by $\langle \phi^0 \rangle$. On the other hand $U(1)_{\text{PQ}}$ can be defined such that only the Higgs and D_R^i, E_R^i are charged under it and with opposite charges. It is thus broken only by the up-quark Yukawas. Finally $U(1)_E$ refers to flavour universal phase rotations of E_R^i alone and is thus broken by the charged lepton Yukawas.

The Yukawa Lagrangian of the SM

$$-\mathcal{L}_{\text{Yukawa}}^{\text{SM}} = Y_d^{ij} \bar{Q}_L^i \phi D_R^j + Y_u^{ij} \bar{Q}_L^i \tilde{\phi} U_R^j + Y_e^{ij} \bar{L}^i \phi E_R^j + \text{h.c.} \,, \tag{7}$$

where $\tilde{\phi} = i\sigma_2 \phi$, is in general flavour dependent (if $Y_f \not\propto \mathbb{I}$) and CP violating. The pattern of explicit $\mathcal{G}_{\text{flavour}}^{\text{SM}}$ breaking by $Y_f \neq 0$ is as follows:

---

[2]It is also symmetric under $SO(4)$ rotations of the four real scalar fields $\phi_{1,2,3,4}$ contained in $\phi = (\phi_1 + i\phi_2, \phi_3 + i\phi_4)^T$. This approximate symmetry of the SM is sometimes called the *custodial symmetry*.

– $U(1)_E$ is broken by $Y_e \neq 0$,
– $U(1)_{\mathrm{PQ}}$ is broken by $Y_u \cdot Y_d \neq 0$ and $Y_u \cdot Y_e \neq 0$,
– $SU(3)_Q \times SU(3)_U \to U(1)_u \times U(1)_c \times U(1)_t$ is due to $Y_u \not\propto \mathrm{I}$,
– $SU(3)_Q \times SU(3)_D \to U(1)_d \times U(1)_s \times U(1)_b$ is due to $Y_d \not\propto \mathrm{I}$,
– the remaining $U(1)$ factors in the quark sector are broken by the fact that $[Y_u, Y_d] \neq 0$ down to $U(1)_B$,
– finally, $SU(3)_L \times SU(3)_E \to U(1)_e \times U(1)_\mu \times U(1)_\tau$ due to $Y_e \not\propto \mathrm{I}$. The remaining factor group also contains the global $U(1)_L$.

Thus, the global symmetry of the SM in presence of the Yukawas is $\mathcal{G}_{\mathrm{global}}^{\mathrm{SM}}(Y_f \neq 0) = U(1)_B \times U(1)_e \times U(1)_\mu \times U(1)_\tau$. In this language, *flavour physics* refers to interactions which break the $SU(3)_q^3 \times SU(3)_\ell^2$ and are thus *flavour violating*.

Commonly, a spurion analysis is useful for parameter counting, identification of suppression factors, and for the idea of minimal flavour violation (MFV) [2]. In this approach we promote the SM Yukawas to non-dynamical fields with well-defined transformation properties under $\mathcal{G}_{\mathrm{flavour}}^{\mathrm{SM}}$

$$Y_u \sim (3, \bar{3}, 1)_{SU(3)_q^3}, \qquad Y_d \sim (3, 1, \bar{3})_{SU(3)_q^3}, \qquad Y_e \sim (3, \bar{3})_{SU(3)_\ell^2}. \tag{8}$$

In the following we will focus on the quark sector.

2.2 Counting the standard model quark flavour parameters

The flavour symmetry breaking pattern described above is useful in counting the number of physical flavour parameters in the theory. In particular:

1. Consider a theory with a global symmetry group $\mathcal{G}_f$ with N_{total} generators.
2. Add interactions with N_{general} parameters, breaking $\mathcal{G}_f \to \mathcal{H}_f$ with $N_{\mathrm{total}} - N_{\mathrm{broken}}$ generators.
3. Then the N_{broken} generators can be used to rotate away N_{broken} number of symmetry breaking parameters.
4. The number of remaining physical parameters is thus $N_{\mathrm{physical}} = N_{\mathrm{general}} - N_{\mathrm{broken}}$.

We can apply this recipe to the SM breaking of $U(3)_Q \times U(3)_U \times U(3)_D \to U(1)_B$. In this case the three $U(3)$ group rotations are described by unitary 3×3 matrices containing three real angles and six phases each. Thus schematically $N_{\mathrm{total}} = 3 \times (3 + 6i)$. Consequently $N_{\mathrm{broken}} = N_{\mathrm{total}} - 1i = 9 + 17i$. The two quark Yukawas are general 3×3 matrices containing nine complex parameters ($N_{\mathrm{general}} = 2 \times (9 + 9i)$). Finally, the number of physical parameters is $N_{\mathrm{physical}} = N_{\mathrm{general}} - N_{\mathrm{broken}} = 9 + 1i$, representing six quark masses, three mixing angles and a single CP violating phase.

2.3 Discrete symmetries of the standard model

Any local Lorentz invariant quantum field theory conserves CPT [3]. It follows that in these theories (including the SM) T violation equals CP violation. There is no reason, a priori, for C, P and CP to be related to flavour physics. However, in the SM (and apparently in Nature) this is so. In the SM C and P are violated maximally: left-handed and right-handed fermion fields furnish different gauge representations, while C and P both change the chirality of fermion fields. This maximal C and P violation within the SM is also independent of the values of the SM parameters. On the other hand, the CP violation within the SM does depend on the (Yukawa) parameters. The hermiticity of the Lagrangian namely implies

$$Y_{ij} \bar{\psi}_L^i \phi \psi_R^j + Y_{ij}^* \bar{\psi}_R^j \phi^\dagger \psi_L^i \overset{\mathrm{CP}}{\to} Y_{ij} \bar{\psi}_R^j \phi^\dagger \psi_L^i + Y_{ij}^* \bar{\psi}_L^i \phi \psi_R^j. \tag{9}$$

Thus, the Yukawa Lagrangian will be CP symmetric if $Y_{ij} = Y_{ij}^*$. More precisely, the requirement for CP conservation can be written in terms of the Jarlskog invariant (J) [4] as

$$J \equiv \mathrm{Im}[\det(Y_d Y_d^\dagger, Y_u Y_u^\dagger)] = 0. \tag{10}$$

2.4 Mass basis

Upon replacing $\mathrm{Re}(\phi^0) \to (v+h)/\sqrt{2}$, Yukawa interactions give rise to fermion mass matrices

$$M_q = \frac{v}{\sqrt{2}} Y_q \,. \tag{11}$$

The *mass bassis* corresponds, by definition, to diagonal mass matrices. The unitary transformations between any two bases which leave the gauge-kinetic terms invariant are

$$Q_L \to V_Q Q_L \,, \qquad\qquad U_R \to V_U U_R \,, \qquad\qquad D_R \to V_D D_R \,. \tag{12}$$

The Yukawa matrices on the other hand transform as

$$Y_u \to V_Q Y_u V_U^\dagger \,, \qquad\qquad Y_d \to V_Q Y_d V_D^\dagger \,. \tag{13}$$

The diagonalization of M_Q requires bi-unitary transformations

$$
\begin{aligned}
V_Q^u M_u V_U^\dagger = M_u^{\mathrm{diag}} = \frac{v}{\sqrt{2}} \lambda_u \,; &\qquad\qquad \lambda_u = \mathrm{diag}(y_u, y_c, y_t) \,, \\
V_Q^d M_d V_D^\dagger = M_d^{\mathrm{diag}} = \frac{v}{\sqrt{2}} \lambda_d \,; &\qquad\qquad \lambda_d = \mathrm{diag}(y_d, y_s, y_b) \,.
\end{aligned}
\tag{14}
$$

While $V_{U,D}$ are unphysical (they leave the gauge-kinetic terms invariant), $V_Q^{u,d}$ produce a physical effect. In particular, since $[M_u, M_d] \neq 0$, a nontrivial mixing matrix $V_Q^u V_Q^{d\dagger} \equiv V_{\mathrm{CKM}} \neq 1$ (due to Cabibbo, Kobayashi and Maskawa [5]) modifies the charged weak gauge interactions. The resulting SM flavour Lagrangian in the mass basis is thus

$$\mathcal{L}_m^F = \left(\bar{q}_i \slashed{D} q^j \delta_{ij}\right)_{\mathrm{NC}} + \frac{g}{\sqrt{2}} \bar{u}_L^i \slashed{W}^+ V_{\mathrm{CKM}}^{ij} d_L^j + \bar{u}_L^i \lambda_u^{ij} u_R^j \left(\frac{v+h}{\sqrt{2}}\right) + \bar{d}_L^i \lambda_d^{ij} d_R^j \left(\frac{v+h}{\sqrt{2}}\right) + \mathrm{h.c.} \,, \tag{15}$$

where $(u_L^i, d_L^i) \equiv Q_L^T$ and NC refers to neutral currents (interactions with gluons, the photon and the Z boson).

3 Testing the CKM description of flavour

Let us recap the main features of quark flavour conversion in the SM: (i) it only proceeds via the three CKM angles; (ii) is mediated by charged current electroweak interactions; and (iii) these charged current interactions involve exclusively left-handed fermion fields.

3.1 Parametrisation of the CKM matrix

We start by fixing the permutation of quark generations via mass ordering. The resulting CKM matrix has the form

$$V_{\mathrm{CKM}} = \begin{pmatrix} V_{ud} & V_{us} & V_{ub} \\ V_{cd} & V_{cs} & V_{cb} \\ V_{td} & V_{ts} & V_{tb} \end{pmatrix} \,. \tag{16}$$

Experimentally, V_{CKM} exhbits a strong hierarchical pattern in off-diagonal elements [6]

$$
\begin{aligned}
|V_{ud}| \simeq |V_{cs}| \simeq |V_{tb}| \simeq 1 \,, &\qquad\qquad |V_{us}| \simeq |V_{cd}| \simeq 0.22 \,, \\
|V_{cb}| \simeq |V_{ts}| \simeq 4 \times 10^{-2} \,, &\qquad\qquad |V_{ub}| \simeq |V_{td}| \simeq 5 \times 10^{-3} \,.
\end{aligned}
\tag{17}
$$

Such structure can be made explicit in the *Wolfenstein expansion* [7] in $\lambda \equiv |V_{us}| \simeq 0.22$

$$V_{\mathrm{CKM}} = \begin{pmatrix} 1 - \frac{\lambda^2}{2} & \lambda & A\lambda^3(\rho - i\eta) \\ -\lambda & 1 - \frac{\lambda^2}{2} & A\lambda^2 \\ A\lambda^3(1 - \rho - i\eta) & -A\lambda^2 & 1 \end{pmatrix} + \mathcal{O}(\lambda^4) \,. \tag{18}$$

The four parameters in this parametrisation λ, A, ρ and η can be mapped exactly to the four physical CKM parameters at any order in the λ expansion. All are of the order $\mathcal{O}(0.1 - 1)$ and the CP violating phase is encoded in the imaginary contribution proportional to η. Current experimental precision already requires that in phenomenological applications, expansion at least to order $\mathcal{O}(\lambda^4)$ should be taken into account.

3.2 Unitarity of the CKM

Being a unitary matrix, one can derive unitarity conditions on the rows and columns of the CKM matrix, in particular

$$\sum_k V_{ik}^* V_{jk} = \delta_{ij} , \qquad\qquad \sum_k V_{ki}^* V_{kj} = \delta_{ij} . \qquad (19)$$

Phenomenologically, the most interesting condition applies for $i = 1$ and $j = 3$

$$V_{ud} V_{ub}^* + V_{cd} V_{cb}^* + V_{td} V_{tb}^* = 0 , \qquad (20)$$

simply because all the three terms on the left hand side are of the same order in λ. The equation defines a triangle in the complex plane. Normalizing one of the sides to unity

$$\frac{V_{ud} V_{ub}^*}{V_{cd} V_{cb}^*} + \frac{V_{td} V_{tb}^*}{V_{cd} V_{cb}^*} + 1 = 0 , \qquad (21)$$

one can re-express it in terms of the Wolfenstein parameters (up to $\mathcal{O}(\lambda^5)$)

$$[\bar{\rho} + i\bar{\eta}] + [(1 - \bar{\rho}) - i\bar{\eta}] + 1 = 0 , \qquad (22)$$

where $\bar{\rho} = \rho(1 - \lambda^2/2) + \mathcal{O}(\lambda^4)$ and $\bar{\eta} = \eta(1 - \lambda^2/2) + \mathcal{O}(\lambda^4)$. The angles (denoted by α, β and γ in Fig. 1) and sides of this triangle are invariant under phase transformations of quark fields and are observable quantities.

3.3 Self consistency of the CKM assumption

The CKM description of quark flavour conversion has been tested experimentally to great precision. In particular

- $|V_{us}|$ (λ) can be extracted from the semileptonic kaon decay $K \to \pi \ell \nu$ with a precision of three per-mille: $\lambda = 0.2253(9)$ [6].
- $|V_{cb}|$ (A) can be determined from semileptonic B meson decay width measurements $B \to X_c \ell \nu$ to a precision of two percent: $A = 0.822(12)$ [6, 8].
- Then, $|V_{ub}| \propto \sqrt{\bar{\rho}^2 + \bar{\eta}^2}$ can be extracted using charmless semileptonic decays of B mesons $B \to X_u \ell \nu$.
- The time-dependent CP asymmetry in the decay $B \to \psi K_S$ ($S_{\psi K_S} \simeq \sin 2\beta = 2\bar{\eta}(1 - \bar{\rho})/[(1 - \bar{\rho})^2 + \bar{\eta}^2]$) has been measured to great precision at the B factory experiments Belle and BaBar.
- The rates $B \to DK$ decays depend on the phase $\exp(i\gamma) = (\rho + i\eta)/(\rho^2 + \eta^2)$.
- Similarly, the rates of $B \to \pi\pi, \rho\pi, \rho\rho$ depend on the angle $\alpha = \pi - \beta - \gamma$.
- The ratio of neutral B and B_s meson mass diferences $\Delta m_d / \Delta m_s \propto |V_{td}/V_{ts}|^2 = \lambda^2 [(1 - \bar{\rho})^2 + \bar{\eta}^2]$ exhibits another non-trivial constraint in the $(\bar{\rho}, \bar{\eta})$ plane.
- Finally, CP violation in $K \to \pi\pi$ decays (ϵ_K) depends in a complicate way on $(\bar{\rho}, \bar{\eta})$.
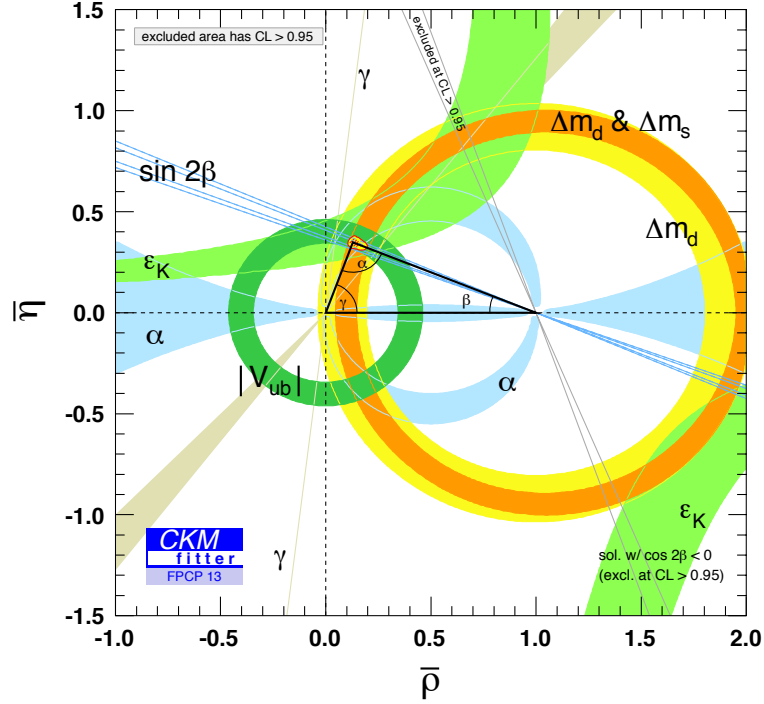
Fig. 1: Result of the SM CKM fit projected onto the $\bar{\rho} - \bar{\eta}$ plane, as obtained by the CKMfitter [8] collaboration. Shown shaded are the 95% C.L. regions selected by the given observables.

Combined, these measurements lead to an impressive agreement with the best fit ranges for ρ and η (see also Fig. 1 and Ref. [9]) [8]

$$\rho = 0.130 \pm 0.024 , \qquad\qquad \eta = 0.362 \pm 0.014 . \qquad (23)$$

Note that $|\eta| \gtrsim |\rho|$ implies that the CKM phase defined in this way is $\mathcal{O}(1)$. We can also conclude that, very likely, CP violation in flavour changing processes is dominated by the CKM phase and that the Kobayashi-Maskawa mechanism of CP violation is at work. Again one can define a reparametrisation invariant measure of CP violation

$$\mathrm{Im}[V_{ij}V_{kj}^*V_{kl}V_{il}^*] = J_{KM} \sum \epsilon_{ikm}\epsilon_{jln} , \qquad (24)$$

where $J_{KM} = \lambda^6 A^2 \eta = \mathcal{O}(10^{-5})$. Written in this form it is clear the CP violation in the SM is suppressed by small mixing among the quark generations. The Jarlskog determinant in the SM can then be written compactly as

$$J = J_{KM} \prod_{i>j} \frac{m_i^2 - m_j^2}{v^2} = \mathcal{O}(10^{-22}) . \qquad (25)$$

We see that compared to J_{KM}, J is further suppressed by the large quark mass hierarchies.

4 Closer look at CP violation in neutral meson mixing and decays

For simplicity, we will focus on the neutral B meson sistem with the flavour eigenstates $B^0 \sim \bar{b}d$ and $\bar{B}^0 \sim b\bar{d}$. Since in general, these are not CP eigenstates, we have

$$CP|B^0\rangle = e^{i\xi_B}|\bar{B}^0\rangle ,$$

$$CP|\bar{B}^0\rangle = e^{-i\xi_B}|B^0\rangle\,. \tag{26}$$

Stating from an initial superposition state at $t=0$ $|\psi(0)\rangle = a(0)|B^0\rangle + b(0)|\bar{B}^0\rangle$, the time evolution of such a system can in general be described as

$$|\psi(t)\rangle = a(t)|B^0\rangle + b(t)|\bar{B}^0\rangle + c_1(t)|f_1\rangle + c_2(t)|f_2\rangle + \ldots\,, \tag{27}$$

where $f_{1,2,\ldots}$ denote the B^0 and $\bar{B}^0$ decay products. If we are only interested in $a(t)$ and $b(t)$, we can construct an effective description of the time evolution in terms of a non-hermition Hamiltonian

$$\mathcal{H} = M + i\frac{\Gamma}{2}\,, \tag{28}$$

where M and Γ are time-independent, Hermitian 2×2 matrices, describing possible oscillations and decays, respectively. The dispersive part M recieves contributions from off-shell intermediate states, while Γ is the absorptive part and given by a sum over possible on-shell intermediate states. The time-evolution is then described by

$$i\frac{d}{dt}\begin{pmatrix}a(t)\\b(t)\end{pmatrix} = H\begin{pmatrix}a(t)\\b(t)\end{pmatrix}\,, \tag{29}$$

with the eigenvectors $|B_{L,H}\rangle = p_{L,H}|B^0\rangle \pm q_{L,H}|\bar{B}^0\rangle$, and where $|p_{L,H}|^2 + |q_{L,H}|^2 = 1$. Imposing CPT, one obtains $M_{11} = M_{22}$, $\Gamma_{11} = \Gamma_{22}$, and consequently $p_L = p_H \equiv p$ and $q_L = q_H \equiv q$. If CP is conserved one furthermore obtains that $\mathrm{Arg}(M_{12}) = \mathrm{Arg}(\Gamma_{12})$ and thus $|q/p| = 1$.

Conventionally, on defines the following CP conserving oscillation parameters

$$m \equiv \frac{M_L + M_H}{2}\,, \qquad\qquad \Gamma \equiv \frac{\Gamma_L + \Gamma_H}{2}\,,$$
$$\Delta m \equiv M_H - M_L\,, \qquad\qquad \Delta\Gamma \equiv \Gamma_H - \Gamma_L\,, \tag{30}$$

or equivalently $x \equiv \Delta m/\Gamma$ and $y \equiv \Delta\Gamma/2\Gamma$.

The time evolution of the neutral meson system can finally be parametrized in terms of states $|B^0(t)\rangle$ corresponding to $|B^0\rangle$ at initial time $t=0$, and $|\bar{B}^0(t)\rangle$ corresponding to $|\bar{B}^0\rangle$ at $t=0$

$$|B^0(t)\rangle = g_+(t)|B^0\rangle - \frac{q}{p}g_-(t)|\bar{B}^0\rangle\,,$$
$$|\bar{B}^0(t)\rangle = g_+(t)|\bar{B}^0\rangle - \frac{q}{p}g_-(t)|B^0\rangle\,, \tag{31}$$

where

$$g_\pm \equiv \frac{1}{2}\left(e^{-m_H t - \Gamma_H t/2} \pm e^{-m_L t - \Gamma_L t/2}\right)\,. \tag{32}$$

The decay of the two mass eigenstates to some some final state f after time t is described by the decay amplitudes

$$\langle f|\mathcal{H}|B^0\rangle \equiv A_f\,,$$
$$\langle \bar{f}|\mathcal{H}|B^0\rangle \equiv A_{\bar{f}}\,. \tag{33}$$

The time-dependent decay rates are then given by

$$\frac{d\Gamma(|B^0(0)\rangle) \to |f(t)\rangle}{dt} = \mathcal{N}_0 e^{-\Gamma t}|A_f|^2 \times \left\{\frac{1 + |\lambda_f|^2}{2}\cosh\frac{\Delta\Gamma t}{2} + \frac{1 - |\lambda_f|^2}{2}\cos\Delta m\,t\right.$$
$$\left. + \mathrm{Re}\lambda_f \sinh\frac{\Delta\Gamma t}{2} - \mathrm{Im}\lambda_f \sin\Delta m\,t\right\}\,,$$

$$\frac{d\Gamma(|\bar{B}^0(0)\rangle) \rightarrow |f(t)\rangle}{dt} = \mathcal{N}_0 e^{-\Gamma t} |\bar{A}_f|^2 \times \left\{ \frac{1 + |\bar{\lambda}_f|^2}{2} \cosh \frac{\Delta\Gamma t}{2} + \frac{1 - |\bar{\lambda}_f|^2}{2} \cos \Delta m\, t \right.$$
$$\left. + \mathrm{Re}\bar{\lambda}_f \sinh \frac{\Delta\Gamma t}{2} - \mathrm{Im}\bar{\lambda}_f \sin \Delta m\, t \right\}, \qquad (34)$$

where $\mathcal{N}_0$ is the overall flux normalization,

$$\lambda_f \equiv \frac{q}{p}\frac{\bar{A}_f}{A_f}, \qquad\qquad \bar{\lambda}_f \equiv \frac{p}{q}\frac{A_f}{\bar{A}_f} = \frac{1}{\lambda_f}, \qquad (35)$$

and analogously for decays to $\bar{f}$. The various terms in the above tiem-evolution can be understood as follwing

- Terms proportional to $|A_f|^2$, $|\bar{A}_f|^2$ describe a decay without net oscillation.
- Terms proportional to $|\lambda_f|^2$, $|\bar{\lambda}_f|^2$ describe a decays following net oscillations.
- Terms proportional to $\sin\Delta mt$, $\sinh\Delta\Gamma t/2$ describe interference between the above two cases.
- CP violation in interference is possible only if $\mathrm{Im}(\lambda_f) \neq 0$.

Such effects can be observed in neutral B meson decays to CP eigenstates via a time-dependent CP asymmetry

$$A_{f_{CP}}(t) \equiv \frac{\frac{d\Gamma}{dt}\left[\bar{B}^0(0) \rightarrow f_{CP}(t)\right] - \frac{d\Gamma}{dt}\left[B^0(0) \rightarrow f_{CP}(t)\right]}{\frac{d\Gamma}{dt}\left[\bar{B}^0(0) \rightarrow f_{CP}(t)\right] + \frac{d\Gamma}{dt}\left[B^0(0) \rightarrow f_{CP}(t)\right]}. \qquad (36)$$

In the B (and also B_s) system experimentally $\Delta\Gamma \ll \Delta m$ and so $|q/p| \simeq 1$. In this limit, the full expression for A_f greatly simplifies and can be written as

$$A_f(t) = S_f \sin(\Delta m\, t) - C_f \cos(\Delta m\, t), \qquad (37)$$

where

$$S_f \equiv \frac{2\,\mathrm{Im}(\lambda_f)}{1 + |\lambda_f|^2}, \qquad\qquad C_f \equiv \frac{1 - |\lambda_f|^2}{1 + |\lambda_f|^2}. \qquad (38)$$

4.1 Phases in decay amplitudes

Consider the decay $B \rightarrow f$ described by the amplitude A_f and its CP conjugate process $\bar{B} \rightarrow \bar{f}$ associated with the amplitude $\bar{A}_{\bar{f}}$. Any complex parameter in the theory Lagrangian entering the two amplitudes will appear complex conjugated after CP and will thus appear with opposite signs in A_f and $\bar{A}_{\bar{f}}$. The associated CP odd phases are conventionally called *weak phases*. In the SM they are induced via W exchanges. Note that single amplitude phases are convention dependent and thus not physical. Only differences between phases of different amplitudes are physical.

On the other hand, on-shell intermediate states in scattering or decay ampitudes can produce phase changes even if the relevant Lagrangian is real. These are thus independent of CP. They will appear with same signs in both A_f and $\bar{A}_{\bar{f}}$. These CP even phases are often reffered to as *strong phases*. In the SM they are due to strong interaction induced re-scattering. Again, only relative phases between amplitudes are physical.

In general, one can thus write both decay amplitudes as

$$A_f = |a_1|e^{i(\delta_1 + \phi_1)} + |a_2|e^{i(\delta_2 + \phi_2)} + \ldots,$$
$$\bar{A}_{\bar{f}} = |a_1|e^{i(\delta_1 - \phi_1)} + |a_2|e^{i(\delta_2 - \phi_2)} + \ldots, \qquad (39)$$

where $a_{1,2,\ldots}$ are contributions to the amplitude with different phases, $\delta_{1,2\ldots}$ are the strong phases and $\phi_{1,2\ldots}$ are the weak phases.

4.2 CP violation in $B \to \psi K_S$

To a good approximation, the $B \to \psi K_S$ decays are described by a just single weak decay amplitude to a CP eigenstate (with CP eigenvalue η_f)

$$A_f = |a_f|e^{i(\delta_f + \phi_f)} \,,$$
$$\bar{A}_f = |a_f|e^{i(\delta_f - \phi_f)}\eta_f \,, \tag{40}$$

so that $\lambda_f = \eta_f (q/p) \exp(-2i\phi_f)$. In the neutral B system $|\Gamma_{12}| \ll |M_{12}|$, since it is due to $\mathcal{O}(G_F^2)$ long distance effects, which are suppressed by small CKM elements (a fact also verified experimentally since $\Delta\Gamma \ll \Delta m$). Then one can write

$$\left(\frac{q}{p}\right)^2 = \frac{M_{12}^* - \frac{i}{2}\Gamma_{12}^*}{M_{12} - \frac{i}{2}\Gamma_{12}} \simeq e^{2i\xi_B} \,, \tag{41}$$

and thus $\lambda_f \simeq \eta_f \exp[i(\xi_B - 2\phi_f)]$, leading to a simple expression for the time-dependent CP asymmetry $A_f(t)$, in particular

$$S_{f_{CP}} \simeq \eta_f \sin(\xi_B - 2\phi_f) \,. \tag{42}$$

In the SM, ξ_B and ϕ_f are exactly computable in terms of the CKM elements. In particular

$$\xi_B = -\mathrm{Arg}(M_{12}) \simeq -\mathrm{Arg}[(V_{tb}^* V_{td})^2] = -\mathrm{Arg}\left(\frac{V_{tb}^* V_{td}}{V_{tb} V_{td}^*}\right) \,, \tag{43}$$

while

$$-e^{-2i\phi_f} = \frac{\bar{A}_{\psi K_S}^{(B)}}{A_{\psi K_S}^{(B)}} = -\frac{V_{cb} V_{cs}^* a_T + \dots}{V_{cb}^* V_{cs} a_T + \dots}e^{i\xi_K} \simeq -\frac{V_{cb} V_{cs}^*}{V_{cb}^* V_{cs}}\frac{V_{cd}^* V_{cs}}{V_{cd} V_{cs}^*} \,. \tag{44}$$

In the above equation, the dots denote additional amplitudes suppressed by small coefficients and CKM elements. Also, in the second step we have taken into account the phase projection of the neutral kaon flavour eigenstates onto the mass eigenstate K_S due to $K - \bar{K}$ oscillations (analogous to Eq. (43)). Combining Eqs. (43) and (44) we thus obtain

$$\lambda_{\psi K_S}^{(B)} \simeq \frac{V_{tb}^* V_{td}}{V_{tb} V_{td}^*}\frac{V_{cb} V_{cd}^*}{V_{cb}^* V_{cd}} = -e^{-2i\beta} \,. \tag{45}$$

The observable $S_{\psi K_S}^{(B)} \simeq \sin 2\beta$ (note that $C_{\psi K_S}^{(B)} \simeq 0$) demonstrates *CP violation in interference between the mixing and decay* amplitudes. Experimentally, it has been measured to an accuracy of $\sim 1\%$ at the B factories [6].

4.3 CP violation in B_s mixing

Establishing CP violation in the B_s system is considerably more challenging. The golden channel is the decay $B_s \to \psi\phi$. Since it is an admixture of different CP eigenestates (represented by the different polarizations of the two vector mesons in the final state), an angular analysis is required for the extraction of the CP violating phase. In addition, B_s oscillations are much faster than those of B_d, namely

$$\frac{\Delta m_s}{\Delta m_d} \sim \frac{|M_{12}^s|}{|M_{12}^d|} \propto \left|\frac{V_{ts}}{V_{td}}\right|^2 \sim 30 \,. \tag{46}$$

Finally, $\Delta\Gamma_s$ effects in the time evolution cannot be neglected compared to Δm_s. In the SM $\lambda_{\psi\phi}^{(B_s)} = -\exp[i(\xi_{B_s} - 2\phi_{\psi\phi})]$ evaluates to [10]

$$\left[S_{\psi\phi}^{(B_s)}\right]_{\mathrm{SM}} = 2\mathrm{Arg}\frac{V_{tb}^* V_{ts}}{V_{cb}^* V_{cs}} = 0.036(1) \,, \tag{47}$$

which is still small compared to the currently attainable experimental precision of $S_{\psi\phi}^{(B_s)} = -0.02(4)$ [11].

4.4 CP violation in B decays to CP conjugate states

This form of measurements is interesting if $B^0 \to \bar{f}$ and $\bar{B}^0 \to f$ transitions are forbidden. In this case $|A_f| = |\bar{A}_{\bar{f}}|$ and $|A_{\bar{f}}| = |\bar{A}_f| = 0$ and one can define a CP asymmetry

$$\frac{\frac{d\Gamma}{dt}\left[\bar{B}^0(0) \to f(t)\right] - \frac{d\Gamma}{dt}\left[B^0(0) \to \bar{f}(t)\right]}{\frac{d\Gamma}{dt}\left[\bar{B}^0(0) \to f(t)\right] + \frac{d\Gamma}{dt}\left[B^0(0) \to \bar{f}(t)\right]} = \frac{\left|\frac{p}{q}\right|^2 - \left|\frac{q}{p}\right|^2}{\left|\frac{p}{q}\right|^2 + \left|\frac{q}{p}\right|^2} \simeq \text{Im}\left(\frac{\Gamma_{12}}{M_{12}}\right) + \mathcal{O}\left(\left|\frac{\Gamma_{12}}{M_{12}}\right|^2\right), \quad (48)$$

where in the last step we have again used the fact the $|\Gamma_{12}| \ll |M_{12}|$ in the B system. Note that the above asymmetry is accessible with a time-independent measurement. It also represents *CP violation in mixing*, simetimes termed *indirect CP violation*. An illustrative example is the wrong sign semileptonic decay asymmetry

$$a_{SL}^{(d)} = \frac{\Gamma(\bar{B}^0 \to X\ell^+\nu) - \Gamma(B^0 \to X\ell^-\bar{\nu})}{\Gamma(\bar{B}^0 \to X\ell^+\nu) + \Gamma(B^0 \to X\ell^-\bar{\nu})}, \quad (49)$$

with the SM expectation of $a_{SL}^{(d)} = -8(2) \times 10^{-4}$ [10].

4.5 CP violation in charged B decays

The possibility of CP violation in charged B decays is of special interest in the case of $B^\pm \to DK^\pm$, since $D - \bar{D}$ oscillations allow for interference of two tree-level dominated decay amplitudes, in particular

$$B^- \to D^0 K^- : \; b \to c\bar{u}s,$$
$$B^- \to \bar{D}^0 K^- : \; b \to \bar{c}us. \quad (50)$$

The resulting phenomenology is particularly transparent by focusing on subsequent D decays to CP eigenstates [12]

$$D^0 \to f_{CP} : \; c \to d\bar{d}u, s\bar{s}u,$$
$$\bar{D}^0 \to f_{CP} : \; \bar{c} \to d\bar{d}\bar{u}, s\bar{s}\bar{u}. \quad (51)$$

In the SM the ratio of the two decay amplitudes is then

$$\frac{A^B_{(D\to f)K}}{A^B_{(\bar{D}\to f)K}} = \frac{V^*_{cb}V_{us}a^B_{DK}}{V^*_{ub}V_{cs}a^B_{\bar{D}K}}e^{i(\delta^B_{DK}-\delta^B_{\bar{D}K})}\eta_f\frac{V_{cd}V^*_{ud}}{V^*_{cd}V_{ud}}\frac{a^D_f}{a^{\bar{D}}_f}e^{i(\delta^D_f-\delta^{\bar{D}}_f)} \simeq \eta_f r_B e^{i(\delta_B-\gamma)}, \quad (52)$$

where we have used the definition of the angle $\gamma \equiv \text{Arg}(-V_{ud}V^*_{ub}/V_{cd}V^*_{cb}) \simeq 70°$ [6] and have collected the hadronic amplitude ratios into r_B and the associated strong phases in δ_B.

The virtue of these modes is that in principle all unknown parameters can be determined by measuring several available decay rates only, which are CP even quantities. In particular

$$A(B^- \to f_+ K^-) = A_0\left[1 + r_B e^{i(\delta_B-\gamma)}\right],$$
$$A(B^- \to f_- K^-) = A_0\left[1 - r_B e^{i(\delta_B-\gamma)}\right],$$
$$A(B^+ \to f_+ K^-) = A_0\left[1 + r_B e^{i(\delta_B+\gamma)}\right],$$
$$A(B^+ \to f_- K^-) = A_0\left[1 - r_B e^{i(\delta_B+\gamma)}\right]. \quad (53)$$

can be used to extract the three hadronic parameters (A_0, r_B and δ_B) as well as γ. Since no B mixing is involved, these measurements are sensitive to *CP violation in decay* also termed *direct CP violation*. The determination of γ in this way is theoretically extremely clean, in particular, since CP violation in $D - \bar{D}$ mixing is negligible. Experimentally, it is advantageous to have both a large r_B and large δ_B. Therefore, it is welcome that such approach can be adapted also for D-decay products, which are non CP eigenstates [13].

5 Flavour and New Physics

Let us first consider how much NP can still contribute to flavour observables, given the current experimental and theoretical precision. For example, given the good agreement of SM tree-level mediated processes with experiment, one can perform basic tests of CKM unitarity. Taking only the moduli of the first row CKM elements:

- $|V_{ud}|$ which can be extracted from $0^+ \to 0^+ e\nu$ super-allowed nuclear β decays, yielding $|V_{ud}| = 0.97425(22)$ [6];
- $|V_{us}|$ which is determined from the semileptonic kaon decays $K^+ \to \pi^+ \ell\nu$, yielding $|V_{us}| = 0.2237(13)$ [6];
- finally, $|V_{ub}|$ which is measured using charmless semileptonic B decays $B \to X_u \ell\nu$, yelding $|V_{ub}| = 4.2(5) \times 10^{-3}$ [6];

one can form the following CKM unitarity constraint [14]

$$|V_{ud}|^2 + |V_{us}|^2 + |V_{ub}|^2 - 1 = -0.0008(7) \,. \tag{54}$$

Using the measurements of the Fermi constant from the muon life-time, one can further reinterpret these constraints as tests of the charged current universality between leptonic and semileptonic weak processes at the per-mille level. In light of this, it is reasonable to consider NP contributions to observables which are (loop, CKM) suppressed in the SM. Then one can use the CKM determination from tree-level observables, in particular $|V_{ud}|$, $|V_{us}|$, $|V_{cb}|$ and $|V_{ub}|$ as well as γ from $B \to DK$ decays (and/or α from tree-level dominated $B \to \pi\pi$ decays). This finally allows to predict SM contributions also to loop suppressed observables, greatly enhancing their sensitivity to NP.

5.1 New physics in $B - \bar{B}$ mixing

In the following we will assume a presence of heavy NP – such that it would only contribute to dispersive $B - \bar{B}$ amplitudes. In that case, the most general modification of M_{12} can be parametrised as

$$M_{12} = M_{12}^{\mathrm{SM}} r_d^2 e^{2i\theta_d} \tag{55}$$

where the NP parameters r_d and θ_d signify a change of the magnitude and phase with respect to the SM prediction, respectively. Such effects of NP can then be easily translated to all relevant B mixing observables as

$$\begin{aligned}
\Delta m_B &= r_d^2 \left(\Delta m_B\right)^{\mathrm{SM}} , \\
S_{\psi K_S}^{(B)} &\simeq \sin(2\beta + 2\theta_d) , \\
a_{SL}^{(d)} &= -\mathrm{Re}\left(\frac{\Gamma_{12}}{M_{12}}\right)^{\mathrm{SM}} \frac{\sin 2\theta_d}{r_d^2} + \mathrm{Im}\left(\frac{\Gamma_{12}}{M_{12}}\right)^{\mathrm{SM}} \frac{\cos 2\theta_d}{r_d^2} \,.
\end{aligned} \tag{56}$$

One can compare these expectations to the current experimental measurements of [6]

$$\Delta m_B = 51.0(4) \times 10^{10}/s \,, \qquad S_{\psi K_S}^{(B)} = 0.671(24) \,, \qquad a_{SL}^{(d)} = -0.2(7) \times 10^{-3} \,, \tag{57}$$

where the SM expectation with tree-level CKM inputs for $[S_{\Psi K_S}^{(B)}]_{\mathrm{tree}}^{\mathrm{SM}} = 0.76(4)$ [8]. We can immediately draw the following conclusions

- NP in M_{12} with a large phase relative to β is constrained to $20\% - 30\%$ of the SM contribution. Thus, CKM clearly dominates CP violation in $B - \bar{B}$ mixing. (A similar conclusion can be made for the case of $K^0 - \bar{K}^0$ system: the measured value of $\epsilon_K = 1.596(13) \times 10^{-3}$ constrains CP violating NP in kaon mixing amplitudes to be subdominant. The power of this constraint is however presently limited by theory uncertainties.)

– NP in M_{12} with a phase that is aligned to β is constrained to be at most comparable to the SM contribution. (Again a similar conclusion can be made for the case of $K^0 - \bar{K}^0$ system: the measured value of $\Delta m_K = 52.93(9) \times 10^8/s$ constrains CP conserving NP in kaon mixing amplitudes to be comparable to SM estimates, which however contrary to the B case carry sizable theory uncertainties.)

As a comparison, in the case of B_s mixing, NP can be at most comparable to the SM contribution regardless of the phase since $S_{\psi\phi}^{\mathrm{SM}} \lesssim \delta S_{\psi\phi}^{\mathrm{exp}}$.

5.2 The new physics flavour puzzle

The SM is not a complete theory of Nature.

1. It does not include a (quantum) description of gravity. Thus its validity is limited below the Planck scale $m_{\mathrm{Planck}} \simeq 10^{19}$ GeV.

2. It does not include neutrino masses. This further limits its validity down to below the maximal scale at which new degrees of freedom can accommodate at least two massive neutrinos $m_{\mathrm{see-saw}} \lesssim 10^{15}$ GeV.

3. The fine-tuning of the EW symmetry breaking scale compared to the large scales in the above points 1. and 2. suggests NP already at scales of the order $4\pi v \sim 1$ TeV .[3]

Given the SM is merely an effective field theory valid below a cut-off energy scale Λ, one needs to consider additional terms in the theory Lagrangian consisting of SM field operators with canonical dimensions $d > 4$:

$$\mathcal{L} = \mathcal{L}_{\mathrm{SM}} + \sum_{d>4} \sum_n \frac{c_n^{(d)}}{\Lambda^{d-4}} \mathcal{O}_n^{(d)} . \tag{58}$$

In a natural theory one expects $c_n^{(d)} \sim \mathcal{O}(1)$ unless the relevant operators are forbidden or suppressed by symmetries. For $\Lambda \sim$ TeV and without imposing additional symmetries beyond the gauged SM ones, the above condition is severely violated for several $\mathcal{O}_n^{(6)}$, which contribute to flavour changing processes. This constitutes the so-called *NP flavour puzzle*, which can be articulated through the following question: If there is NP at the TeV scale, why haven't we seen its effects in flavour observables? Naively, one could argue, that the same it true for NP violating baryon and lepton numbers. However, B and L are (classically) exact accidental symmetries of the SM, while in the SM the flavour symmetry is already broken explicitly.

5.3 Bounds on new physics from $\Delta F = 2$ processes

The NP flavour puzzle can be demonstrated perhaps most dramatically in the case $\Delta F = 2$ FCNCs. In the SM the dispersive contributions to $\Delta F = 2$ processes of down-quarks are typically dominated by box diagrams with the top quarks appearing in the loop. These contributions can be schematically written as

$$M_{12}^{\mathrm{SM}} = \frac{G_F^2 m_t^2}{16\pi^2} (V_{ti}^* V_{tj})^2 \langle \bar{M} | (\bar{d}_L^i \gamma_\mu d_L^j)^2 | M \rangle F\left(\frac{m_t^2}{m_W^2}\right) + \dots , \tag{59}$$

where $M = K^0$, B^0, B_s, $d^{i,j}$ denote meson valence quarks, $F(x) \sim \mathcal{O}(1)$ is the relevant loop function normalized to $F(\infty) = 1$, while the dots denote corrections due to charm quark contributions, which are numerically relevant only in the case of $K - \bar{K}$ mixing. Note that the prefactor can be rewritten completely in terms of the fundamental flavour parameters (Yukawas) in the unbroken theory

$$\frac{G_F^2 m_t^2}{16\pi^2} (V_{ti}^* V_{tj})^2 = \frac{(Y_u Y_u^*)_{ij}}{128\pi^2 m_t^2} , \tag{60}$$

---

[3]Incidentally, the TeV mass scale can also be associated with the explanation of the cosmological dark matter, if the later is in the form of a thermal particle relic.

which can be interpreted as due to Goldstone Higgs exchanges in the gaugeless ($g \to 0$) limit of the SM.

The relevant hadronic matrix elements between the external M and $\bar{M}$ mesons can be written as

$$\langle \bar{M} | (\bar{d}_L^i \gamma_\mu d_L^j)(\bar{d}_L^i \gamma^\mu d_L^j) | M \rangle = \frac{2}{3} f_M^2 m_M^2 \hat{B}_M \,, \tag{61}$$

where the relevant meson decay constant f_M is defined via $\langle 0 | d^i \gamma_\mu \gamma_5 d^j | M(p) \rangle \equiv i p_\mu f_M$, while $\hat{B}_M \sim \mathcal{O}(1)$ is called the bag parameter. These two hadronic quantities can be computed numerically using lattice QCD methods. The tremendous progress in these calculations over the past 30 years is reflected in the precise values of [15]

$$
\begin{aligned}
f_B &= 0.186(4) \text{ GeV} \,, & \hat{B}_B &= 1.27(10) \,, \\
f_{B_s} &= 0.224(5) \text{ GeV} \,, & \hat{B}_{B_s} &= 1.33(6) \,, \\
f_K &= 0.1563(9) \text{ GeV} \,, & \hat{B}_K &= 0.7661(99) \,.
\end{aligned}
\tag{62}
$$

With these inputs we can use the experimental measurements of neutral meson mixing observables to constrain possible NP contributions of the form

$$
\begin{aligned}
\mathcal{L}_{\text{NP}}^{\Delta F=2} ={}& \frac{c_{sd}}{\Lambda^2} \left(\bar{d}_L \gamma^\mu s_L \right)^2 + \frac{c_{bd}}{\Lambda^2} \left(\bar{b}_L \gamma^\mu s_L \right)^2 + \frac{c_{bs}}{\Lambda^2} \left(\bar{s}_L \gamma^\mu b_L \right)^2 \\
&+ \frac{c_{cu}}{\Lambda^2} \left(\bar{u}_L \gamma^\mu c_L \right)^2 + \frac{c_{tu}}{\Lambda^2} \left(\bar{u}_L \gamma^\mu t_L \right)^2 + \frac{c_{tc}}{\Lambda^2} \left(\bar{c}_L \gamma^\mu t_L \right)^2 \,.
\end{aligned}
\tag{63}
$$

The effects of such NP on neutral meson oscillations can namely be completely encoded into

$$\frac{M_{12}^M}{m_M} \sim c_{ij} \left(\frac{f_M}{\Lambda} \right)^2 \,, \tag{64}$$

which leads to the following set of current experimental constraints [9, 16]

$$
\begin{aligned}
\frac{\Delta m_K}{m_K} &\sim 7 \times 10^{-15} &\Rightarrow& \quad \frac{\Lambda}{\sqrt{|c_{sd}|}} \gtrsim 10^3 \text{ TeV} &\text{or}& \quad |c_{sd}| \lesssim 10^{-6} \left(\frac{\Lambda}{\text{TeV}} \right)^2 \,, \\
\frac{\Delta m_D}{m_D} &\sim 9 \times 10^{-15} &\Rightarrow& \quad \frac{\Lambda}{\sqrt{|c_{cu}|}} \gtrsim 10^3 \text{ TeV} &\text{or}& \quad |c_{cu}| \lesssim 10^{-6} \left(\frac{\Lambda}{\text{TeV}} \right)^2 \,, \\
\frac{\Delta m_B}{m_B} &\sim 6 \times 10^{-14} &\Rightarrow& \quad \frac{\Lambda}{\sqrt{|c_{bd}|}} \gtrsim 4 \times 10^2 \text{ TeV} &\text{or}& \quad |c_{bd}| \lesssim 5 \times 10^{-6} \left(\frac{\Lambda}{\text{TeV}} \right)^2 \,, \\
\frac{\Delta m_{B_s}}{m_{B_s}} &\sim 2 \times 10^{-12} &\Rightarrow& \quad \frac{\Lambda}{\sqrt{|c_{bs}|}} \gtrsim 70 \text{ TeV} &\text{or}& \quad |c_{bs}| \lesssim 2 \times 10^{-4} \left(\frac{\Lambda}{\text{TeV}} \right)^2 \,.
\end{aligned}
\tag{65}
$$

Furthermore, in case of maximal CP violating phases in c_{ij}, one obtains even stronger constraints

$$
\begin{aligned}
\epsilon_K &\sim 0.0023 &\Rightarrow& \quad \frac{\Lambda}{\sqrt{|\text{Im}(c_{sd})|}} \gtrsim 2 \times 10^4 \text{ TeV} &\text{or}& \quad |\text{Im}(c_{sd})| \lesssim 6 \times 10^{-10} \left(\frac{\Lambda}{\text{TeV}} \right)^2 \,, \\
\frac{A_\Gamma}{y_{CP}} &\lesssim 0.2 &\Rightarrow& \quad \frac{\Lambda}{\sqrt{|\text{Im}(c_{cu})|}} \gtrsim 3 \times 10^3 \text{ TeV} &\text{or}& \quad |\text{Im}(c_{cu})| \lesssim 10^{-7} \left(\frac{\Lambda}{\text{TeV}} \right)^2 \,, \\
S_{\psi K_S} &\sim 0.67 &\Rightarrow& \quad \frac{\Lambda}{\sqrt{|\text{Im}(c_{bd})|}} \gtrsim 8 \times 10^2 \text{ TeV} &\text{or}& \quad |\text{Im}(c_{bd})| \lesssim 10^{-6} \left(\frac{\Lambda}{\text{TeV}} \right)^2 \,, \\
S_{\psi\phi} &\sim 0.1 &\Rightarrow& \quad \frac{\Lambda}{\sqrt{|\text{Im}(c_{bs})|}} \gtrsim 70 \text{ TeV} &\text{or}& \quad |\text{Im}(c_{bs})| \lesssim 2 \times 10^{-4} \left(\frac{\Lambda}{\text{TeV}} \right)^2 \,.
\end{aligned}
\tag{66}
$$

The two main messages one can draw from such an analysis are that (1) NP with a generic flavour structure is irrelevant for EW hierarchy, since flavour measurements in this case require $\Lambda \gg$ TeV; and (2) in case of TeV NP, its flavour structure needs to be far from generic.

6 Conclusions

The absence of significant deviations from the SM in quark flavour physics is a key constraint on any extension of the SM. At the same time there are still various open questions regarding the flavour structure of the standard model itself that can be possibly addressed only at low energies, using flavour phyiscs measurements. The set of flavour observables to be measured with higher precision in the search for indirect hints of NP is limited, but not necessarily small. For example, we still have only limited knowledge about CP violation in the B_s and D systems. In addition, despite significant recent progress, new-physics effects could still be hidden in certain rare kaon, D and B decays [17]. The experimental progress on these, as expected from the LHCb [18] in LHC run II, Belle II [19] and other upcoming flavour experiments will thus be invaluable.

Acknowledgements

References

[1] A. J. Buras, hep-ph/9806471; G. C. Branco, L. Lavoura and J. P. Silva, Int. Ser. Monogr. Phys. **103** (1999) 1; U. Nierste, arXiv:0904.1869 [hep-ph]; O. Gedalia and G. Perez, arXiv:1005.3106 [hep-ph]; Y. Grossman, CERN Yellow Report CERN-2010-002, 111-144 [arXiv:1006.3534 [hep-ph]]; Y. Nir, CERN Yellow Report CERN-2010-001, 279-314 [arXiv:1010.2666 [hep-ph]]; G. Isidori, arXiv:1302.0661 [hep-ph].

[2] R. S. Chivukula and H. Georgi, *Phys. Lett. B* **188**, 99 (1987); A. J. Buras, *Acta Phys. Polon. B* **34**, 5615 (2003); G. D'Ambrosio, G. F. Giudice, G. Isidori and A. Strumia, *Nucl. Phys. B* **645**, 155 (2002).

[3] R. F. Streater and A. S. Wightman, Princeton, USA: Princeton Univ. Pr. (2000) 207 p.

[4] C. Jarlskog, Phys. Rev. Lett. **55** (1985) 1039.

[5] N. Cabibbo, Phys. Rev. Lett. **10** (1963) 531; M. Kobayashi and T. Maskawa, Prog. Theor. Phys. **49**, 652 (1973).

[6] J. Beringer *et al.* [Particle Data Group Collaboration], Phys. Rev. D **86** (2012) 010001.

[7] L. Wolfenstein, Phys. Rev. Lett. **51** (1983) 1945.

[8] J. Charles et al. [CKMfitter Group], Eur. Phys. J. C **41**, 1-131 (2005), updated results and plots available at: http://ckmfitter.in2p3.fr

[9] M. Bona *et al.* [UTfit Collaboration], JHEP **0803** (2008) 049 [arXiv:0707.0636 [hep-ph]].

[10] A. Lenz, U. Nierste, J. Charles, S. Descotes-Genon, A. Jantsch, C. Kaufhold, H. Lacker and S. Monteil *et al.*, Phys. Rev. D **83** (2011) 036004 [arXiv:1008.1593 [hep-ph]].

[11] D. Martinez Santos [LHCb Collaboration], LHCb-TALK-2014-337, Cern, Switzerland, 15 - 17 Oct 2014.

[12] M. Gronau and D. London, Phys. Lett. B **253** (1991) 483; M. Gronau and D. Wyler, Phys. Lett. B **265** (1991) 172.

[13] D. Atwood, I. Dunietz and A. Soni, Phys. Rev. Lett. **78** (1997) 3257 [hep-ph/9612433]; A. Giri, Y. Grossman, A. Soffer and J. Zupan, Phys. Rev. D **68** (2003) 054018 [hep-ph/0303187].

[14] P. A. Boyle, J. M. Flynn, N. Garron, A. Jï£¡ttner, C. T. Sachrajda, K. Sivalingam and J. M. Zanotti, JHEP **1308** (2013) 132 [arXiv:1305.7217, arXiv:1305.7217 [hep-lat]].

[15] S. Aoki, Y. Aoki, C. Bernard, T. Blum, G. Colangelo, M. Della Morte, S. Dï£¡rr and A. X. El Khadra *et al.*, Eur. Phys. J. C **74** (2014) 9, 2890 [arXiv:1310.8555 [hep-lat]].

[16] G. Isidori, Y. Nir and G. Perez, Ann. Rev. Nucl. Part. Sci. **60** (2010) 355 [arXiv:1002.0900 [hep-ph]]; A. Lenz, U. Nierste, J. Charles, S. Descotes-Genon, H. Lacker, S. Monteil, V. Niess and S. T'Jampens, Phys. Rev. D **86** (2012) 033008 [arXiv:1203.0238 [hep-ph]]; V. Bertone *et al.* [ETM Collaboration], JHEP **1303** (2013) 089 [Erratum-ibid. **1307** (2013) 143] [arXiv:1207.1287 [hep-lat]]; N. Carrasco *et al.* [ETM Collaboration], JHEP **1403** (2014) 016 [arXiv:1308.1851 [hep-lat]]; N. Carrasco, M. Ciuchini, P. Dimopoulos, R. Frezzotti, V. Gimenez, V. Lubicz, G. C. Rossi and F. Sanfilippo *et al.*, Phys. Rev. D **90** (2014) 014502 [arXiv:1403.7302 [hep-lat]].

[17] M. Artuso, D. M. Asner, P. Ball, E. Baracchini, G. Bell, M. Beneke, J. Berryhill and A. Bevan *et al.*, Eur. Phys. J. C **57** (2008) 309 [arXiv:0801.1833 [hep-ph]]; J. F. Kamenik, Mod. Phys. Lett. A **29** (2014) 22, 1430021.

[18] R. Aaij *et al.* [LHCb Collaboration], Eur. Phys. J. C **73** (2013) 2373 [arXiv:1208.3355 [hep-ex]].

[19] T. Aushev, W. Bartel, A. Bondar, J. Brodzicka, T. E. Browder, P. Chang, Y. Chao and K. F. Chen *et al.*, arXiv:1002.5012 [hep-ex].

Introduction to Supersymmetry

Y. Shadmi
Technion—Israel Institute of Technology, Haifa 32100, Israel

Abstract
These lectures are a brief introduction to supersymmetry.

1 Introduction

You have probably heard in the past about the motivation for supersymmetry. Through these lectures, this will (hopefully) become clear and more concrete. But it's important to state at the outset: There is no experimental evidence for supersymmetry. The amount of effort that has been invested in supersymmetry, in both theory and experiment, may thus be somewhat surprising. In this respect, supersymmetry is no different from any other "new physics" scenario. There is no experimental evidence for *any* underlying theory of electroweak symmetry breaking, which would give rise to the (fundamental scalar) Higgs mechanism as an effective description. There is of course experimental evidence for physics beyond the standard model (SM): dark matter, the baryon asymmetry—CP violation.

Why so much effort on supersymmetry? It is a very beautiful and exciting idea because it's conceptually different from anything we know in Nature. It's a symmetry that relates particles of *different spins*—bosons and fermions. In fact, we are now in a very special era from the point of view of spin: The Higgs was discovered. As far as we know, it is a fundamental particle. So for the first time, we have a spin-0 fundamental particle. It would be satisfying to have some unified understanding of the spins we observe. Supersymmetry would be a step in this direction. Given the SM fermions, it predicts spin-0 particles. Beyond this purely theoretical motivation, the fact that the Higgs is a scalar poses a more concrete (yet purely theoretical) puzzle. Scalar fields (unlike vector bosons or fermions) have quadratic divergences. This leads to the fine-tuning problem, as we will review in the next Section. Supersymmetry removes these divergences. We will see that in some sense **Supersymmetry makes a scalar behave like a fermion.**

Supersymmetry is not a specific model. Rather, there is a wide variety of supersymmetric extensions of the SM. These involve different superpartner spectra, and therefore different experimental signatures. In thinking about these, we have developed a whole toolbox for collider searches, including different triggers and analyses. In particular, supersymmetry supplies many concrete examples with new scalars (same charges as SM fermions), new fermions (same charges as SM gauge bosons), potentially leading to missing energy, displaced vertices, long lived charged particles, or disappearing tracks, to name just some of the possible signatures.. For discovery, spin is a secondary consideration. So even if we are misguided in thinking about supersymmetry, and Nature is not supersymmetric, the work invested in supersymmetry searches may help us discover something else.

1.1 Plan

In Section 2 of these lectures we will see the basics of supersymmetry through a few simple toy models. These toy models can be thought of as "modules" for building the supersymmetrized standard model. In the process, we will try to de-mystify supersymmetry and understand the following questions about it:

- In what sense is it a space-time symmetry (extending translations, rotations and boosts)?
- Why does it remove UV divergences (thus solving the fine-tuning, or Naturalness problem)?
- Why do we care about it even though it's clearly broken?
- Why is the gravitino relevant for LHC experiments?

In Section 3 we will describe the Minimal Supersymmetric Standard Model (MSSM). Here we will put to use what we learned in Section 2. We will discuss:

- Motivation (now that you can appreciate it)
- The field content
- The interactions: we will see that there is (almost) no freedom in these
- The supersymmetry-breaking terms: this is where we have freedom, and these determine experimental signatures.
- EWSB and the Higgs mass
- Spectra (the general structure of superpartner masses)

We will conclude in Section 5 with general considerations for LHC searches.

The aim of these lectures is to provide a conceptual understanding of supersymmetry and the supersymmetrized standard model. Therefore, we will start with a pretty technical review of what symmetries are and their derivation from Lagrangians. This is necessary so that you get a clear idea of what supersymmetry is. As we go on however, we will take a more qualitative approach. For more details, I refer you to the many excellent books and reviews of the subject, including, for example [1–3]. I cannot do justice to the vast literature on the subject in these short lectures. For original references, I refer you again to the books and reviews above.

2 Supersymmetry basics

2.1 Spacetime symmetry

The symmetry we are most familiar with is Poincare symmetry. It contains

- Translations: $x^\mu \to x^\mu + a^\mu$ (generators: P^μ)
- Lorentz transformations: $x^\mu \to x^\mu + w^\mu_\nu x^\nu$, where $w^{\mu\nu}$ is antisymmetric (generators: $J^{\mu\nu}$)

Throughout we will only consider global, infinitesimal transformations, so a^μ and $w^{\mu\nu}$ are small, coordinate-independent numbers.

These transformations contain rotations. For a rotation around the axis x^k (with angle θ^k): $w^{ij} = \epsilon^{ijk}\theta^k$. Thus for example for rotations around z:

$$x^0 \to x^0 ; \quad x^1 \to x^1 - \theta x^2 ; \quad x^2 \to x^2 + \theta x^1 ; \quad x^3 \to x^3$$

The Lorentz transformations also contain boosts. For a boost along the axis x^k (with speed β^k): $-w^{0k} = w^{k0} = \beta^k$. Thus for example for a boost along z,

$$x^0 \to x^0 + \beta x^3 ; \quad ; \quad x^1 \to x^1 ; \quad x^2 \to x^2 ; \quad x^3 \to x^3 + \beta x^0 .$$

The Lorentz algebra is:

$$[P^\mu, P^\nu] = 0$$
$$[P^\mu, J^{\rho\sigma}] = 0 \tag{1}$$
$$[J^{\mu\nu}, J^{\rho\sigma}] = i(g^{\nu\rho}J^{\mu\sigma} - g^{\mu\rho}J^{\nu\sigma} - g^{\nu\sigma}J^{\mu\rho} + g^{\mu\sigma}J^{\nu\rho}) .$$

Here P^μ are the momenta—the generators of translations, $J^{\mu\nu}$ contain the angular momenta, which generate rotations (with $\mu, \nu = 1, 2, 3$) and the generators of boosts (with $\mu = 0, \nu = 1, 2, 3$).

Let's recall where all this is coming from. To do that, let's "discover" all the above in a simple field theory, namely a field theory of a single free complex scalar field. The Lagrangian is,

$$\mathcal{L} = \partial^\mu \phi^* \, \partial_\mu \phi - m^2 \, |\phi|^2 . \tag{2}$$

What's a symmetry? It's a transformation of the fields which leaves the Equations of Motion (EOMs) invariant. The EOMs follow from the action, so this tells us that the action is invariant under the symmetry transformation. Since the action is the integral of the Lagrangian, it follows that the Lagrangian can change by a total derivative,

$$\mathcal{L} \to \mathcal{L} + \alpha \partial_\mu \mathcal{J}^\mu, \tag{3}$$

where α is the (small) parameter of the transformation.

What's the symmetry of our toy theory? First, there's a U(1) symmetry:

$$\phi(x) \to e^{i\alpha} \phi(x). \tag{4}$$

Under this transformation, $\mathcal{L}$ is invariant. This is an example of an *internal symmetry*, that is, a symmetry which is *not* a space-time symmetry (it does not do anything to the coordinates).

But our toy theory also has *spacetime symmetries*:

Translations:

$$x^\mu \quad \to \quad x^\mu + a^\mu \tag{5}$$

$$\phi(x) \to \phi(x-a) \quad = \quad \phi(x) - a^\mu \partial_\mu \phi(x) \tag{6}$$

or

$$\delta_a \phi(x) = a^\mu \partial_\mu \phi(x) \tag{7}$$

and **Lorentz transformations:**

$$x^\mu \quad \to \quad x^\mu + w^{\mu\nu} x_\nu \tag{8}$$

$$\phi(x^\mu) \quad \to \quad \phi(x^\mu - w^{\mu\nu} x_\nu) \tag{9}$$

so

$$\delta_w \phi(x) = w^{\mu\nu} x_\mu \partial_\nu \phi(x) = \frac{1}{2} w^{\mu\nu} (x_\mu \partial_\nu - x_\nu \partial_\mu) \phi(x) \tag{10}$$

The Lagrangian only changes by a total derivative under these, so the action is invariant.

Now let's see how the algebra arises. Consider performing two translations. First we do a translation with $x^\mu \to x^\mu + a^\mu$. Then we do a translation with $x^\mu \to x^\mu + b^\mu$. Alternatively, we could first perform the translation with b^μ and then the one with a^μ. Obviously, this should not make any difference. Mathematically, this translates to the fact that the commutator of two translations vanishes. Indeed,

$$[\delta_a, \delta_b] \phi \equiv \delta_a(\delta_b \phi) - \delta_b(\delta_a \phi) = 0. \tag{11}$$

With rotations and boosts, the order does matter. Consider the commutator of two Lorentz transformations with parameters $w^{\mu\nu}$ and $\lambda^{\rho\sigma}$:

$$[\delta_{w^{\mu\nu}}, \delta_{\lambda^{\rho\sigma}}] \phi = i w_{\mu\nu} \lambda_{\rho\sigma} \cdot i \left\{ g^{\nu\rho} (x_\mu \partial_\sigma - x_\mu \partial_\sigma) + \text{ permutations} \right\} \tag{12}$$

So we derived the algebra of spacetime symmetry transformations (=the Poincare algebra) in this toy example. Now let's do the same in a supersymmetric theory.

2.2 A simple supersymmetric field theory

Our example will be a free theory with one massive (Dirac) fermion of mass m, which we will denote by $\psi(x)$, and two complex scalars of mass m which we will denote by $\phi_+(x)$ and $\phi_-(x)$. The Lagrangian is,

$$\mathcal{L} = \partial^\mu \phi_+^* \, \partial_\mu \phi_+ - m^2 \, |\phi_+|^2 + \partial^\mu \phi_-^* \, \partial_\mu \phi_- - m^2 \, |\phi_-|^2 + \bar{\psi}(i\slashed{\partial} - m)\psi \tag{13}$$

The labels $+$, $-$ are just names, we'll see the reason for this choice soon. This isn't the most minimal supersymmetric 4d field theory. "Half of it" is: a 2-component (Weyl) fermion plus one complex scalar. But Dirac spinors are more familiar so we start with this example.

Just as in the previous example, this theory has spacetime symmetry, including translations, rotations, and boosts. The only difference is that $\psi(x)$ itself is a spinor, so it transforms nontrivially,

$$\psi(x) \to \psi'(x') . \tag{14}$$

Actually, the L-handed and R-handed parts of the spinor transform differently under Lorentz. Write

$$\begin{pmatrix} \psi_L \\ \psi_R \end{pmatrix} \tag{15}$$

where ψ_L and ψ_R are 2-component spinors. Then under Lorentz transformations,

$$\psi_L \quad \to \quad \psi'_L = (1 - i\theta^i \frac{\sigma^i}{2} - \beta^i \frac{\sigma^i}{2}) \tag{16}$$

$$\psi_R \quad \to \quad \psi'_R = (1 - i\theta^i \frac{\sigma^i}{2} + \beta^i \frac{\sigma^i}{2}) \tag{17}$$

so it will be useful to write everything in terms of 2-component spinors.

Recall that we can write any R-handed spinor in terms of a L-handed one:

$$\psi_R = -\varepsilon \chi_L^* \tag{18}$$

where

$$\varepsilon \equiv -i\sigma^2 = \begin{pmatrix} 0 & -1 \\ 1 & 0 \end{pmatrix} \tag{19}$$

Exercise: prove eq. (18)

We can then write our Dirac spinor in terms of two **L-handed spinors** ψ_+ and ψ_-: $\psi_L = \psi_+$, $\psi_R = -\varepsilon\psi_-^*$ so that,

$$\psi = \begin{pmatrix} \psi_- \\ -\varepsilon\psi_+^* \end{pmatrix} \tag{20}$$

Let's write the Lagrangian in terms of these 2-component spinors,

$$\begin{aligned} \mathcal{L} &= \partial^\mu \phi_+^* \, \partial_\mu \phi_+ + \psi_+^\dagger i\bar{\sigma}^\mu \partial_\mu \psi_+ \\ &+ \partial^\mu \phi_-^* \, \partial_\mu \phi_- + \psi_-^\dagger i\bar{\sigma}^\mu \partial_\mu \psi_- \\ &- m^2 |\phi_-|^2 - m^2 |\phi_+|^2 - m(\psi_+^T \varepsilon \psi_- + \mathrm{hc}) \end{aligned} \tag{21}$$

Exercise: Derive this. Show also that $\psi_+^T \varepsilon \psi_- = \psi_-^T \varepsilon \psi_+$, where $\psi_\pm$ are any 2-component spinors.

All we've done so far is to re-discover spacetime symmetry in this simple field theory. Now comes the big question: **Can this spacetime symmetry be extended?**

The answer is YES: there's more symmetry hiding in our theory! Take a constant (anti-commuting) 2-component L-spinor ξ. Consider the following transformations,

$$\begin{aligned} \delta_\xi \phi_+ &= \sqrt{2}\, \xi^T \varepsilon \psi_+ \\ \delta_\xi \psi_+ &= \sqrt{2}\, i\sigma^\mu \varepsilon \xi^* \partial_\mu \phi_+ \end{aligned} \tag{22}$$

98

and similarly for $+ \to -$.

Exercise: Check that this is a symmetry of our theory: 1. Show that the massless part of the Lagrangian is invariant. 2. Show that the rest of the Lagrangian is invariant too *if* the masses of the fermion and scalars are the same. Here you will have to use the EOMs.

We see that *the symmetry transformations take a boson into a fermion and vice versa.* THIS IS SUPERSYMMETRY.

As an (important) aside, we note that the symmetry *separately* relates $\phi_- - \psi_-$ and $\phi_+ - \chi_+$. Thus, if $m = 0$, the two halves of the theory decouple, and each one is symmetric separately. Therefore, as mentioned above, this theory is not the most minimal supersymmetric theory, but half of it is. This is very handy if we're to implement supersymmetry in the SM, because the SM is a *chiral theory*.

Is the symmetry we found indeed an extension of Poincare? It's surely a spacetime symmetry since it takes a fermion into a boson (the transformation parameters carry spinor indices). Furthermore, let's consider the algebra. Take the commutator of two new transformations with parameters ξ, η:

$$[\delta_\xi, \delta_\eta]\phi_L = a^\mu \partial_\mu \phi_L \qquad with \quad a^\mu = 2i \left(\xi^\dagger \bar\sigma^\mu \eta - \eta^\dagger \bar\sigma^\mu \xi \right) \tag{23}$$

This is a translation! We see that the commutator of two new transformations gives a translation. So indeed, the new symmetry is an extension of the "usual" spacetime symmetry.

Exercise: Check eq. (23). You will have to use the EOMs.

Let's summarize: Our simple theory is supersymmetric. We have an extension of spacetime symmetry that involves anti-commuting generators. The supersymmetry transformations relate bosons and fermions.

There are a couple of features of this simple example that are worth stressing because they hold quite generally: (i) If the bosons and fermions had different masses, we would not have this symmetry. That is, the theory would not be supersymmetric. (ii) Let's count the physical degrees of freedom (dof's): on-shell we have $2 + 2 = 4$ fermions, $2 + 2 = 4$ bosons. Thus we have equal numbers of fermionic and bosonic dof's. (Off shell, the bosons are the same, but the fermions have 2×4.)

2.3 The vacuum energy

Recall that global symmetries lead to Noether currents. For each global symmetry there is a current j^μ, with $\partial_\mu j^\mu = 0$, so that there is a conserved charge:

$$Q = \int d^3x \, j^0(x) \quad \text{with} \quad \frac{d}{dt} Q = 0 \,. \tag{24}$$

For translations in time, the conserved charge is the Hamiltonian H.

Thus, what we found above in eqn. (23) means that the anti-commutator of two supersymmetry transformations gives the Hamiltonian. Schematically,

$$\{\text{SUSY}, \text{SUSY}\} \propto H \,, \tag{25}$$

where SUSY stands for the generator of a supersymmetry transformation.

Now consider the vacuum expectation value (VEV) of this last relation,

$$\langle 0| \{\text{SUSY}, \text{SUSY}\} |0\rangle \propto \langle 0|H|0\rangle \,. \tag{26}$$

If supersymmetry is unbroken, the ground state is supersymmetric. Therefore it is annihilated by the SUSY generator,

$$\text{SUSY}|0\rangle = 0 \,. \tag{27}$$

Using eqn (26) we find

$$\langle 0|H|0\rangle = 0\,. \tag{28}$$

In a supersymmetric theory, the ground state energy is zero.

As you probably heard many times (and as we will review soon), one of the chief motivations for supersymmetry is the fine-tuning problem, that is, the fact that supersymmetry removes the quadratic divergence in the Higgs mass. Here you can already see the power of supersymmetry in removing UV divergences. The vacuum energy usually diverges. (This should remind you of your first quantum mechanics class, where you saw that there's an infinite constant in the energy of the harmonic oscillator. In QM, we just set this infinite constant to zero, by choosing the zero of the energy.) This is in fact the worst divergence we encounter in field theory, a quartic divergence. Now we see that supersymmetry completely removes this divergence: in a supersymmetric theory, the ground state energy is zero. This gives us hope that supersymmetry can help with other UV divergences.

The next worst divergence you can have in field theory is a quadratic divergence. Where does it show up? In the mass-squared of scalar fields:

$$\delta m^2 \propto \Lambda^2 \tag{29}$$

where Λ is the cutoff. This is why we are worried about fine tuning in the Higgs mass. You could ask yourself why no one ever worries about the electron mass. It too is much smaller than the Planck scale. The reason this is not a problem, is that fermion masses have no quadratic divergences, only logarithmic divergences. This is a very important result so we will see it in three ways.

(1) Consider a fermion Lagrangian with a mass term m_0,

$$\mathcal{L} = \bar{\psi}(i\partial\!\!\!/ - m_0)\psi \ = \ \bar{\psi}(i\partial\!\!\!/)\psi - m_0(\psi_L^\dagger \psi_R + \psi_R^\dagger \psi_L) \tag{30}$$

Note that the mass term is the only term that couples ψ_L and ψ_R. So if $m_0 = 0$, ψ_L, ψ_R don't talk to each other. A mass term (L-R coupling) is never generated. Therefore, even if we include quantum corrections,

$$\delta m \propto m_0\,, \tag{31}$$

(Here m is the full, physical mass including quantum corrections.) We see that with $m_0 = 0$ we have two different species: ψ_L—call it,say, a "blue" fermion, and ψ_R, a "red fermion", and they don't interact at all.

(2) Consider $m_0 \neq 0$. Take a L-fermion (spin along $\hat{p}$). This is our "blue fermion". We can run very fast alongside. If our speed is greater than the fermion's speed, $\hat{p} \to -\hat{p}$, but the spin stays the same. Thus the fermion helicity (which is the projection of the spin along the direction of motion) changes. L becomes R. The "blue" fermion turns into a "red" fermion. (We see that helicity is not a good quantum number for a massive fermion.) But if $m_0 = 0$, the "blue" fermion is massless. It travels at the speed of light—we can never run fast enough. The blue fermion does not change into a red fermion. Thus, L and R are distinct in this case, and the blue fermion and the red fermion are decoupled. We thus learn that any correction to the bare mass m_0 must be proportional to m_0,

$$\delta m \equiv m - m_0 \propto m_0 \tag{32}$$

How can the UV cutoff Λ enter? On dimensional grounds,

$$\delta m \propto m_0 \, \log \frac{m_0}{\Lambda}\,, \tag{33}$$

so

$$\delta m = 0 \cdot \Lambda + \# \, m_0 \, \log \frac{m_0}{\Lambda}\,. \tag{34}$$

Indeed, there is no quadratic divergence in the fermion mass. The worst divergence that can appear is a logarithmic divergence. This is why no one ever worries about fine-tuning in the electron mass.

(3) Again, the question we're asking is: why is there no quadratic divergence in the fermion mass? We'll now see this using a global symmetry—the chiral symmetry. Let's consider the fermion Lagrangian again,

$$\mathcal{L} = \bar{\psi}(i\slashed{\partial})\psi - m_0(\psi_L^\dagger \psi_R + \psi_R^\dagger \psi_L) \tag{35}$$

if $m_0 = 0$, we have two independent U(1) symmetries, $\mathrm{U}(1)_L \times \mathrm{U}(1)_R$. This symmetry forbids the mass term. We again conclude (33).

We saw that supersymmetry implies that the boson mass equals the fermion mass. We also saw that chiral symmetry implies that there is no quadratic divergence in the fermion mass. Putting these together we conclude that **in a supersymmetric theory: there is no quadratic divergence in the boson mass.** This is how supersymmetry solves the fine-tuning problem.

But there's more that we can learn just based on dimensional analysis. We know there is no supersymmetry in Nature. We know for example that there is no spin-0 particle whose mass equals the electron mass. So why should we care about supersymmetry? The reason is that supersymmetry is so powerful that even when it's broken *by mass terms*, the quadratic divergence does not reappear! All we need in order to see this is dimensional analysis. Suppose we take a supersymmetric theory and change the scalar mass (squared) [1]

$$m_{0\,scalar}^2 = m_{0\,fermion}^2 + \tilde{m}^2 \tag{36}$$

where $\tilde{m}^2$ is some constant. Will there be a quadratic divergence in the scalar mass?

$$\delta m_{scalar}^2 = \#\Lambda^2 + \# m_{0\,scalar}^2 \log \frac{m_{0\,scalar}^2}{\Lambda^2} \quad ?? \tag{37}$$

No. For $\tilde{m}^2 = 0$, supersymmetry is restored, and therefore there shouldn't be a quadratic divergence. So the Λ^2 term (which is the quadratic divergence) must be proportional to $\tilde{m}^2$. But there's nothing we can write in perturbation theory that would have the correct dimension.

We conclude that, if supersymmetry is broken by

$$m_{0\,scalar}^2 \neq m_{0\,fermion}^2 \tag{38}$$

the scalar mass-squared has only log divergences. In other words, the supersymmetry breaking (given by the fact that the scalar mass is different from the fermion mass) does not spoil the cancellation of the quadratic divergence. This type of breaking is called **soft**-supersymmetry breaking. (This is what we have in the Minimal Supersymmetric Standard Model (MSSM).)

Parenthetically, we note that one can also have **hard** supersymmetry breaking. Take a supersymmetric theory, and change some dimension-*less* number, eg, the coupling of the boson compared to the coupling of the fermion. This will reintroduce the quadratic divergences.

We derived all these results based on dimensional analysis. Now let's see them concretely. To get something non-trivial we must add interactions. Let's go back to our simple theory,

$$\mathcal{L} = \partial^\mu \phi_+^* \, \partial_\mu \phi_+ + \psi_+^\dagger i \bar{\sigma}^\mu \partial_\mu \psi_+ \tag{39}$$
$$+ \quad \partial^\mu \phi_-^* \, \partial_\mu \phi_- + \psi_-^\dagger i \bar{\sigma}^\mu \partial_\mu \psi_- \tag{40}$$
$$- \quad m^2 \, |\phi_-|^2 - m^2 \, |\phi_+|^2 - m(\psi_+^T \varepsilon \psi_- + \mathrm{hc}) \tag{41}$$

Our two fermions look like the two pieces of an electron or a quark. For example, you can think of ψ_- as the SM SU(2)-doublet quark, and of the ψ_+ as the SM SU(2)-singlet quark. To get interactions, let's add a complex scalar h, with the "Yukawa" interaction:

$$\delta\mathcal{L} = -y \, h \, \psi_+^T \varepsilon \psi_- + \mathrm{hc} \tag{42}$$

---

[1] For scalar fields, the physical parameter is the mass-squared. This is what appears in the Lagrangian.

here y is a coupling. To make a supersymmetric theory we also need a (L) fermion $\tilde{h}$ (their supersymmetry transformations are just like ϕ_+ and ψ_+) [2]. Finally, just for simplicity, let's set $m = 0$.

It's easy to see that if we just add this Yukawa interaction, the Lagrangian is not invariant under supersymmetry. So we must add more interactions,

$$
\begin{aligned}
\mathcal{L} &= \partial^\mu \phi_+^* \, \partial_\mu \phi_+ + \partial^\mu \phi_-^* \, \partial_\mu \phi_- + \partial^\mu h^* \, \partial_\mu h \\
&+ \psi_+^\dagger i \bar{\sigma}^\mu \partial_\mu \psi_+ + \psi_-^\dagger i \bar{\sigma}^\mu \partial_\mu \psi_- + \tilde{h}^\dagger i \bar{\sigma}^\mu \partial_\mu \tilde{h} \\
&+ \mathcal{L}_{int} \,,
\end{aligned}
\tag{43}
$$

with

$$
\begin{aligned}
\mathcal{L}_{int} = &- y \left(h \psi_+^T \varepsilon \psi_- + \phi_+ \tilde{h}^T \varepsilon \psi_- + \phi_- \tilde{h}^T \varepsilon \psi_+ + \text{hc} \right) \\
&- |y|^2 \left[|\phi_+|^2 \, |\phi_-|^2 + |h|^2 \, |\phi_-|^2 + |h|^2 \, |\phi_+|^2 \right] .
\end{aligned}
\tag{44}
$$

Now that we have an interacting supersymmetric theory, we are ready to consider the UV divergence in the scalar mass-squared. Consider δm_h^2. It gets contributions from a ϕ_+ loop, a ϕ_- loop and a fermion loop.

To calculate the fermion loop, let's convert to Dirac fermion language,

$$
y \, h \psi_+^T \varepsilon \psi_- + \text{hc} = y h \bar{\psi} P_L \psi + \text{hc} \,.
\tag{45}
$$

So the fermion loop is

$$
-|y|^2 \int \frac{d^4 p}{(2\pi)^4} \text{Tr} P_L \frac{i}{\not{p}} P_R \frac{i}{\not{p}} = 2|y|^2 \int \frac{d^4 p}{(2\pi)^4} \frac{1}{p^2} \,.
\tag{46}
$$

(In the MSSM, the analog of this is the top contribution to the Higgs mass).

The boson loop is,

$$
2 \times i|y|^2 \int \frac{d^4 p}{(2\pi)^4} \frac{i}{p^2} = -2|y|^2 \int \frac{d^4 p}{(2\pi)^4} \frac{1}{p^2} \,,
\tag{47}
$$

(in the MSSM, the analog of this is the stop contribution to the Higgs mass).

Before we argued that the cancellation is not spoiled by soft supersymmetry breaking. Let's see this in this example. Suppose we change the $\phi_\pm$ masses-squared to $\tilde{m}_\pm^2$. Indeed there is no quadratic divergence,

$$
\begin{aligned}
\delta m_h^2 &\propto |y|^2 \int \frac{d^4 p}{(2\pi)^4} \left[\frac{2}{p^2} - \frac{1}{p^2 - \tilde{m}_+^2} - \frac{1}{p^2 - \tilde{m}_-^2} \right] \\
&= |y|^2 \, \tilde{m}_1^2 \int \frac{d^4 p}{(2\pi)^4} \frac{1}{p^2 (p^2 - \tilde{m}_+^2)} + (\tilde{m}_+^2 \to \tilde{m}_-^2) \,.
\end{aligned}
\tag{48}
$$

We see that when supersymmetry is softly broken, the scalar mass squared is log divergent, and the divergence is proportional to the supersymmetry breaking $\tilde{m}^2$. In contrast to "hard" supersymmetry breaking: if we change one of the 4-scalar couplings from $|y|^2$, the quadratic divergence is not cancelled.

We now know a lot of supersymmetry basics. Let's recap and add some language:

– Supersymmetry is an extension of the Poincare symmetry: it's a spacetime symmetry.

---

[2] If h and $\tilde{h}$ remind you of the Higgs and Higgsino that's great, but here they have nothing to do with generating mass, we are just interested in the interactions.

- The basic supersymmetry "module" we know is a complex scalar + a 2-component spinor *of the same mass.* eg,

$$(\phi_+, \psi_+) \tag{49}$$

These transform into each other under supersymmetry. Together they form a representation, or a multiplet of supersymmetry. For obvious reasons, we call this the "chiral supermultiplet".

- The number of fermionic dof's equals the number of bosonic dof's. (This is true generally.)

- Supersymmetry dictates not just the field content but also the interactions. The couplings of fermions, bosons of the same supermultiplets are related. (Again, this is true generally.) Starting from a scalar1–fermion2–fermion3 vertex, supersymmetry requires also a fermion1–scalar2–fermion3 vertex and a fermion1–fermion2–scalar3 vertex all with same coupling, as well as 4-scalar vertices (with the **same** coupling squared).

You see that the structure of supersymmetric theories is very constrained, and that as a result it's less divergent. (This is the *real* reason theorists like supersymmetry, it's easier.. In fact, the more supersymmetry, the easier it gets. There are less divergences, more constraints, one can calculate many things, even at strong coupling. By the time you get to maximal supersymmetry in 4d you have a finite, scale invariant theory.)

We also know a great deal about supersymmetry breaking, so let's summarize that too.

- With unbroken supersymmetry the vacuum energy is zero. Thus the vacuum energy is an order parameter for supersymmetry breaking, and supersymmetry breaking always involves a scale E_{vac}.

- Supersymmetry (breaking) and UV divergences: With unbroken supersymmetry we have only log divergences. Even in the presence of soft supersymmetry breaking (ie, supersymmetry is broken by dimensionful quantities only), there are only log divergences. In contrast, hard supersymmetry breaking (ie when pure numbers, such as couplings, break supersymmetry) reintroduces quadratic divergences, so it's not that interesting from the point of view of the fine-tuning problem.

Let's pause and talk about language. This will be useful when we supersymmetrize the SM. Our simple example of eqn (21) has two chiral supermultiplets, each contains one complex scalar and one L-handed fermion,

$$(\phi_+ \quad \psi_+), \quad (\phi_- \quad \psi_-) \tag{50}$$

In the SM each fermion, eg the top quark, comes from a fusion of 2 Weyl fermions: one originating from an SU(2) doublet and the other from an SU(2) singlet. These are the analogs of ψ_+, ψ_-. When we supersymmetrize the SM we must add two scalars (the stops, or top squarks) these are the analogs of ϕ_+, ϕ_-. One often refers to the doublet and singlet fermions as "L-handed" and "R-handed". This is bad language (remember we can always write a left handed spinor using a right-handed spinor). If we used this bad language anyway, we could call our fermions ψ_L, ψ_R, and the accompanying scalars: ϕ_L, ϕ_R. This is why you hear people talk about the stop-left and stop-right, or left squarks and right squarks. Of course the stops are scalars, and have no chirality, but the names just refer to their fermionic partners.

2.4 Spontaneous supersymmetry breaking: the vacuum energy, UV divergences

If supersymmetry is realized in Nature it's realized as a broken symmetry. We already saw that even explicit (soft) supersymmetry breaking can be powerful. But the picture we had is not very satisfying: we don't want to put in the parameter $\tilde{m}^2$ by hand. We want it to be generated by the theory itself: we want the theory to break supersymmetry *spontaneously*.

We also saw that with unbroken supersymmetry the vacuum energy vanishes, and the potential $V \geq 0$. Thus, supersymmetry is unbroken if there are solution(s) of the EOMs with $V = 0$. Recall that this followed from

$$\langle 0 | \{\text{SUSY}, \text{SUSY}\} | 0 \rangle \propto \langle 0 | H | 0 \rangle \tag{51}$$

and with unbroken SUSY,

$$\text{SUSY}|0\rangle = 0 \tag{52}$$

However, if supersymmetry is *spontaneously* broken:

$$\text{SUSY}|0\rangle \neq 0 \tag{53}$$

and the ground state has nonzero (positive) energy!

In the SM, the only scalar is the Higgs, so the only potential is the Higgs potential, and we're not that used to thinking about scalar potentials. But in supersymmetric theories, fermions are always accompanied by scalars and any fermion interaction results in a scalar potential, eg

$$V(\phi_+, \phi_-, h) = |y|^2 \left[|\phi_+|^2 |\phi_-|^2 + |h|^2 |\phi_-|^2 + |h|^2 |\phi_+|^2 \right] \tag{54}$$

Note that indeed: $V \geq 0$—unbroken supersymmetry.

To break supersymmetry spontaneously all we need is to find a supersymmetric theory with a potential which is always *above* zero. So we need a scale. Classically, we can just put in scale by hand. This brings us to the simplest example of spontaneous supersymmetry breaking.

2.4.1 The O'Raifeartaigh model

The simplest supersymmetric theory with chiral supermultiplets that breaks supersymmetry spontaneously has three chiral supermultiplets,

$$(\phi, \psi), \quad (\phi_1, \psi_1), \quad (\phi_2, \psi_2) \tag{55}$$

and two mass parameters. We will only write the scalar potential[3],

$$V = |y\phi_1^2 - f|^2 + m^2|\phi_1|^2 + |2\phi_1\phi + m\phi_2|^2 \tag{56}$$

Here m is a mass, f has dimension mass^2, and y is a dimensionless coupling. It is easy to see that there is no supersymmetric minimum. The first two terms cannot vanish simultaneously. Supersymmetry is broken! Note that we need $f \neq 0$ for that (we must push some field away from the origin) as well as $m \neq 0$.

Finding the ground state requires more effort. Let's assume $f < m^2/(2y)$. The ground state is at $\phi_1 = \phi_2 = 0$ with ϕ arbitrary (ϕ is a flat direction of the potential),

$$V_0 = |f|^2 \tag{57}$$

Expanding around the VEVs, one finds the following spectrum: One massless Weyl fermion, one Dirac fermion of mass m, and several real bosons of which two are massless, two have mass m, one has mass $\sqrt{m^2 + 2yf}$, and one $\sqrt{m^2 - 2yf}$. Indeed, for $f = 0$ supersymmetry is restored, and the fermions and bosons become degenerate.

Why are there massless bosons in the spectrum? Recall that ϕ is arbitrary, it's a flat direction (2 real dof's). Why is there a massless Weyl fermion? Normally a spontaneously broken global symmetry implies the existence of a massless Goldstone boson (or pion). Here we have spontaneously broken *super*symmetry, which is a "fermionic" symmetry, so we have a massless Goldstone *fermion*. Since supersymmetry is broken spontaneously, the supersymmetry generator does not annihilate the vacuum,

$$\text{SUSY}|0\rangle \neq 0 \tag{58}$$

---

[3]The kinetic terms and fermion-fermion-scalar interactions are there too, but there's nothing instructive in them at this point.

where SUSY stands for the supersymmetry generator. Since this generator carries a spinor index, this state is a fermion state, which is precisely the Golsdtone fermion (sometimes called a Goldstino).

Recall that we needed a scale, or a dimensionful parameter in order to break supersymmetry. Above we simply put it in by hand. But suppose we started with no scale in the Lagrangian. Then classically, supersymmetry would remain unbroken. This suggest that, since no scale can be generated perturbatively, if supersymmetry is unbroken at the tree-level, it remains unbroken to all orders in perturbation theory. This is actually true, and it is a very powerful result. It's a consequence of the constrained structure of supersymmetry. So if supersymmetry is unbroken at tree level, it can only be broken by non-perturbative effects, with a scale that's generated dynamically, just like the QCD scale,

$$\Lambda = M_{UV} \, \exp\left(\frac{-8\pi^2}{bg^2}\right) \tag{59}$$

which is exponentially suppressed compared to the cutoff scale.

This type of supersymmetry breaking is called, for obvious reasons, *dynamical* supersymmetry breaking. We will come back to this when we discuss the standard model. It leads to a beautiful scenario: The supersymmetry breaking scale can naturally be 16 or so orders of magnitude below the Planck scale.

2.5 The chiral and vector multiplets

We have the chiral supermultiplet:

$$(\phi, \psi) \tag{60}$$

with ϕ a complex scalar, ψ a 2-component fermion. In the real world we also have spin-1 gauge bosons, A_μ^a, where a denotes the gauge group index. So in order to supersymmetrize the SM we also need vector supermultiplets,

$$(A_\mu^a, \lambda^a) \tag{61}$$

namely, a gauge field + a "gaugino". On-shell A_μ^a has 2 dof's (2 physical transverse polarizations), so λ^a is a 2-component spinor. A_μ^a is real, so if we want to write λ^a as a 4-component spinor it must be a Majorana spinor[4],

$$\begin{pmatrix} \lambda \\ -\varepsilon\lambda^* \end{pmatrix} \tag{63}$$

Under a supersymmetry transformation, A_μ^a λ^a transform into each other, and we can construct supersymmetric Lagrangians for them as we did for the chiral supermultiplet.

2.6 Supersymmetric Lagrangians

We now have the gauge module (gauge field + gaugino) and the chiral module (scalar + fermion). What are the Lagrangians we can write down? With a theory of such a constrained structure, you expect to have many limitations. Indeed, all the theories we can write down are encoded by two functions, the Kähler potential (K), which gives the kinetic and gauge interactions[5], and the superpotential (W), which gives the non-gauge (Yukawa like) interactions of chiral fields.

Let's start with the gauge part: after all, gauge interactions are almost all we measure.

---

[4]As opposed to the Dirac fermion which consists of two distinct 2-component fermions,

$$\psi = \begin{pmatrix} \psi_- \\ -\varepsilon\psi_+^* \end{pmatrix} \tag{62}$$

.

[5]As we will see, there is no freedom there at the level of 4d terms so we won't even write it down.

2.7 A pure supersymmetric gauge theory

We want a gauge-invariant supersymmetric Lagrangian for

$$(A_\mu^a, \lambda^a) \tag{64}$$

Gauge symmetry (and supersymmetry) determine it completely up to higher-dimension terms. It is

$$\mathcal{L}_{gauge} = -\frac{1}{4} F^{a\mu\nu} F_{\mu\nu}^a + \lambda^{a\dagger} i\bar\sigma \cdot \mathcal{D} \lambda^a \tag{65}$$

Exercise: Check that this Lagrangian is supersymmetric.

2.8 A supersymmetric theory with matter fields and only gauge interactions

We also want to couple "matter fields" to the gauge field. So we add our chiral modules (ϕ_i, ψ_i). Here too, there is no freedom because of gauge symmetry plus supersymmetry,

$$\begin{aligned}
\mathcal{L} &= \mathcal{L}_{gauge} + \mathcal{D}^\mu \phi_i^* \mathcal{D}_\mu \phi_i + \psi_i^\dagger i\bar\sigma^\mu \mathcal{D}_\mu \psi_i \\
&\quad - \sqrt{2} g \left(\phi_i^* \lambda^{aT} T^a \varepsilon \psi_i - \psi_i^\dagger \varepsilon \lambda^{a*} T^a \phi_i \right) - \frac{1}{2} D^a D^a
\end{aligned} \tag{66}$$

where

$$D^a = -g \phi_i^\dagger T^a \phi_i \tag{67}$$

As in the chiral theory, supersymmetry dictates a "new" coupling. In non-supersymmetric theories we have a coupling

$$\text{gauge field—fermion—fermion}$$

Now we also have,

$$\text{gaugino—fermion—scalar,}$$

and of course there's also

$$\text{gauge field—scalar—scalar.}$$

In addition, there is a scalar potential with a 4-scalar interaction,

$$V = \frac{1}{2} D^a D^a \tag{68}$$

with

$$D^a = -g \phi_i^\dagger T^a \phi_i \tag{69}$$

This is a quartic scalar potential, but the quartic coupling isn't arbitrary, it's the gauge coupling. This will be very important when we discuss the Higgs!

Note what happened here. Starting from a non-supersymmetric gauge theory with a gauge field A_μ^a and a fermion ψ, and an interaction $g A_\mu - \psi - \psi$, when we supersymmetrize the theory, the field content is gauge field + gaugino, fermion + scalar. The interactions are $A_\mu - \phi - \phi$ (nothing new, ϕ is charged), but also, $\lambda - \phi - \psi$ (gaugino-scalar-fermion) all with same coupling g. In addition there is a 4-scalar interaction, with coupling g^2. We had no freedom in the process. The field content and couplings of the supersymmetric theory were dictated by (i) the original non-supersymmetric theory we started from (ii) the gauge symmetry (iii) supersymmetry.

2.9 Yukawa like interactions

We also want Yukawa-like interactions of just the chiral scalars and fermions (ϕ_i, ψ_i). There is a simple recipe for writing down the most general supersymmetric interaction Lagrangian. Choose an analytic

function $W(\phi_1, \ldots, \phi_n)$—the "superpotential". Analytic means that W is not a function of the conjugate fields (no daggers!). All the allowed interactions are given by

$$\mathcal{L}_{\text{int}} = -\frac{1}{2} \frac{\partial^2 W}{\partial \phi_i \partial \phi_j} \psi_i^T \varepsilon \psi_j + \text{hc} - \sum_i |F_i|^2 \tag{70}$$

where

$$F_i^* = -\frac{\partial W}{\partial \phi_i} \tag{71}$$

This Lagrangian is guaranteed to be supersymmetric! (There is an elegant way to see this.)

Let's write our previous examples in this language. Start with the theory containing h, ϕ_+, ϕ_-: Take

$$W = y\, h\, \phi_+ \,\phi_- \tag{72}$$

so

$$\begin{aligned} F_h^* &= -\frac{\partial W}{\partial h} = y\phi_+\phi_- \\ \frac{\partial^2 W}{\partial h\, \partial \phi_+} &= y\phi_- \end{aligned} \tag{73}$$

and similarly for the remaining fields. We indeed recover

$$\begin{aligned} \mathcal{L}_{int} = &- y\,(h\,\psi_+^T \varepsilon \psi_- + \phi_+\, \tilde{h}^T \varepsilon \psi_- + \phi_-\, \tilde{h}^T \varepsilon \psi_+ + \text{hc}) \\ &- |y|^2 (|\phi_+|^2\, |\phi_-|^2 + |h|^2\, |\phi_-|^2 + |h|^2\, |\phi_+|^2) \end{aligned} \tag{74}$$

Exercise: Check that the massive theory with $\phi_\pm$ is obtained from

$$W = m\phi_+\phi_- \tag{75}$$

Exercise: Check that the O'Raifeartaigh model is obtained from

$$W = \phi\,(y\phi_1^2 - f) + m\phi_1\phi_2 \tag{76}$$

2.10 R-symmetry

We now know how to write the most general supersymmetric theory in 4d (with minimal supersymmetry). Note that the theory has a global U(1) symmetry. Under this U(1), the gauge boson has charge 0, the gaugino has charge +1, the chiral fermion has charge 0 and the scalar -1. Alternatively we could take the fermion to have charge -1 and the scalar to be 0. This is called a U(1)$_R$ symmetry. It does not commute with supersymmetry: members of the same supermultiplet have different charges.

This symmetry (or its remanent) is crucial in LHC supersymmetry searches!

2.11 F-terms and D-terms

In writing the theory, we defined F-terms and D-terms. For each vector multiplet (λ^a, A_μ^a) we have

$$D^a = -g\phi_i^\dagger T^a \phi_i \qquad (\dim - 2) \tag{77}$$

(to which all the charged scalars contribute).

For each chiral multiplet (ϕ_i, ψ_i) we have a

$$F_i^* = -\frac{\partial W}{\partial \phi_i} \qquad (\dim - 2) \tag{78}$$

and the scalar potential is

$$V = F_i^* F_i + \frac{1}{2} D^a D^a \tag{79}$$

With this language, we can revisit supersymmetry breaking. First we immediately see that indeed $V \geq 0$. Second, supersymmetry is broken if some $F_i \neq$ or $D^a \neq 0$. So the F_i's and D^a's are order parameters for supersymmetry breaking.

2.12 Local supersymmetry: the gravitino mass and couplings

So far we thought about supersymmetry as a global symmetry. Translations and Lorentz transformations are however *local* symmetries. The "gauge theory" of local spacetime symmetry is gravity. We therefore have no choice: supersymmetry is a local symmetry too. The theory of local (spacetime and) supersymmetry is called supergravity. The spin-2 graviton must have a supersymmetric partner, the gravitino, which has spin-3/2. Since supersymmetry is broken the gravitino should get mass.

If you're only interested in collider experiments, should you care about this? Normally, the effects of gravity are suppressed by the Planck scale and we can forget about them when discussing HEP experiments. However, the gravitino mass is related to a broken local symmetry (supersymmetry), so just as in the usual Higgs mechanism of electroweak symmetry breaking, it gets mass by "eating" the Goldstone fermion. Thus, a piece of the gravitino (the longitudinal piece), is some "ordinary" field (which participates in supersymmetry breaking), and the gravitino couplings to matter are not entirely negligible. Furthermore, they are dictated by the supersymmetry breaking. If supersymmetry is broken by some non-zero F term, the gravitino mass is

$$m_{3/2} = \# \frac{F}{M_P} \tag{80}$$

3 The Supersymmetrized Standard Model

3.1 The Supersymmetrized SM: motivation and structure

Now that we understand what supersymmetry is, we can supersymmetrize the SM. Let's review first the motivations for doing that. Before 2012, all fundamental particles we knew had spin-1 or spin-1/2. We now have the Higgs, which is spin 0. This is the source of the fine-tuning problem, or the naturalness problem. Since the Higgs is spin-0, its mass is quadratically divergent

$$\delta m^2 \propto \Lambda_{UV}^2 \,, \tag{81}$$

unlike fermions, whose masses are protected by the chiral symmetry as we saw, or gauge bosons, whose masses are protected by gauge symmetry.

In the case of the Higgs mass, there are one loop corrections that are quadratically divergent. The dominant one is from the top quark. This is not a practical problem. We can calculate any physical observable by including a counter term that cancels this divergent contribution. Rather, the problem is of a theoretical nature. We believe that Λ_{UV} is a concrete physical scale, such as the mass scale of new fields, or the scale of new strong interactions. Then at the low-scale μ

$$m^2(\mu) = m^2(\Lambda_{UV}) + \# \Lambda_{UV}^2 \tag{82}$$

$m^2(\Lambda_{UV})$ determined by the full UV theory, and the number is $\#$ determined by the SM. We know the LHS of eqn. (82): $m^2 \sim 100 \text{ GeV}^2$. So if Λ_{UV} is the Planck scale $\sim 10^{18}$ GeV we need $m^2(\Lambda_{UV}) \sim 10^{36}$ GeV^2 and the two terms on the RHS must be tuned to 32 orders of magnitude.. Such dramatic tunings do not seem natural. In general, for a cutoff scale Λ_{UV}, the parameters of the two theories must be tuned to $\text{TeV}^2/\Lambda_{UV}^2$.

As we saw above, with supersymmetry (even softly broken), scalar masses-squared have only log divergences:

$$m^2(\mu) = m^2(\Lambda_{UV}) \left[1 + \# \log \left(\frac{m^2(\Lambda_{UV})}{\Lambda_{UV}^2} \right) \right] \tag{83}$$

just as for fermions! The reason is that supersymmetry ties the scalar mass to the fermion mass.

The way this happens in practice is that the quadratic divergence from fermion loops is cancelled by the quadratic divergence from scalar loops. The cutoff scale then only enters in the log, and $m^2(\Lambda_{UV})$ can be order $(100 \text{ GeV})^2$. This is the main motivation for supersymmetric extensions of the SM. There are further motivations too. Supersymmetric extensions of the SM often supply dark matter candidates, new sources of CP violation etc. Finally, extending space time symmetry is theoretically appealing.

So let's supersymmetrize the SM. Each gauge field is now part of a vector supermultiplet: for the gluon we have,

$$G_\mu^a \to (\tilde{g}^a, G_\mu^a) + D^a \,, \tag{84}$$

where the physical fields are the gluon and the spin-1/2 gluino. Similarly for the W,

$$W_\mu^I \to (\tilde{w}^I, W_\mu^I) + D^I \tag{85}$$

where the physical fields are the W and the wino, and for B

$$B_\mu \to (\tilde{b}, B_\mu) + D_Y \,, \tag{86}$$

where the physical fields are the B and the bino.

Each fermion is now part of a chiral supermultiplet of the form

$$(\phi, \psi) + F \,. \tag{87}$$

Taking all the SM fermions q, u^c, d^c, l, e^c to be L-fermions, we have

$$q \to (\tilde{q}, q) + F_q \quad \text{all transforming as } (3, 2)_{1/6} \tag{88}$$

with the physical fields being the (doublet) quark q and a spin-0 squark $\tilde{q}$. Similarly,

$$u^c \to (\tilde{u}^c, u^c) + F_u \quad \text{all transforming as } (\bar{3}, 1)_{-2/3} \tag{89}$$

with the physical fields being the (singlet) up-quark u^c + up squark $\tilde{u}^c$,

$$d^c \to (\tilde{d}^c, d^c) + F_d \quad \text{all transforming as } (\bar{3}, 1)_{1/3} \tag{90}$$

with the physical fields being the (singlet) down-quark d^c + down squark $\tilde{d}^c$,

$$l \to (\tilde{l}, l) + F_l \quad \text{all transforming as } (1, 2)_{-1/2} \tag{91}$$

with the physical fields being the (doublet) lepton l + a slepton $\tilde{l}$, and finally

$$e^c \to (\tilde{e}^c, e^c) + F_e \quad \text{all transforming as } (1, 1)_1 \tag{92}$$

with the physical fields being the (singlet) lepton e^c + a slepton $\tilde{e}^c$.

Once electroweak symmetry is broken the doublets split:

$$q = \begin{pmatrix} u \\ d \end{pmatrix} \quad \tilde{q} = \begin{pmatrix} \tilde{u} \\ \tilde{d} \end{pmatrix} \tag{93}$$

and

$$l = \begin{pmatrix} \nu \\ l \end{pmatrix} \quad \tilde{l} = \begin{pmatrix} \tilde{\nu} \\ \tilde{l} \end{pmatrix} \tag{94}$$

Now let's move on to the interactions, staring with the gauge interactions. There is nothing we have to do here. As we saw above, these interactions are completely dictated by supersymmetry and the gauge symmetry. We wrote the Lagrangian for a general gauge theory in the previous lecture:

$$\begin{aligned} \mathcal{L} &= \mathcal{L}_{gauge} + \mathcal{D}^\mu \phi_i^* \mathcal{D}_\mu \phi_i + \psi_i^\dagger i \bar{\sigma}^\mu \mathcal{D}_\mu \psi_i \\ &- \sqrt{2} g \left(\phi_i^* \lambda^{aT} T^a \varepsilon \psi_i - \psi_i^\dagger \varepsilon \lambda^{a*} T^a \phi_i \right) - \frac{1}{2} D^a D^a \end{aligned} \tag{95}$$

where

$$D^a = -g \phi_i^\dagger T^a \phi_i \tag{96}$$

Applying this to the SM,

$$\psi_i = q_i, u_i^c, d_i^c, l_i, e_i^c \quad \phi_i = \tilde{q}_i, \tilde{u}_i^c, \tilde{d}_i^c, \tilde{l}_i, \tilde{e}_i^c \tag{97}$$

The covariant derivatives now contain the SU(3), SU(2) and U(1) gauge fields, λ^a sums over the SU(3), SU(2), U(1) gauginos

$$\lambda^a \to \tilde{g}^a, \tilde{w}^I, \tilde{b} \tag{98}$$

and there are D terms for SU(3), SU(2), U(1)

$$D^a \to D^a, D^I, D_Y \tag{99}$$

In addition there is of course the pure gauge Lagrangian that I didn't write (we saw it in the previous lecture).

The Lagrangian above contains the scalar potential,

$$V = \frac{1}{2} D^a D^a + \frac{1}{2} D^I D^I + \frac{1}{2} D_Y D_Y \tag{100}$$

where for SU(3): (recall $T_{\bar{3}} = -T_3^*$ and we will write things in terms of the fundamental generators)

$$D^a = g_3 \left(\tilde{q}^\dagger T^a \tilde{q} - \tilde{u}^{c\dagger} T^{a*} u^c - \tilde{d}^{c\dagger} T^{a*} u^c \right) \tag{101}$$

similarly for the SU(2) and

$$D_Y = g_Y \sum_i Y_i \tilde{f}_i^\dagger \tilde{f}_i \tag{102}$$

We see that we get 4-scalar interactions with the quartic couplings equal to the gauge couplings.

Again we emphasize that there was no freedom so far, and no new parameters. We also didn't put in the Higgs field yet, so let's do this now. The SM Higgs is a complex scalar, so it must be part of a chiral module

$$H \to (H, \tilde{H}) + F_H \quad \text{all transforming as } (1, 2)_{-1/2} \tag{103}$$

We immediately see a problem (in fact, many problems, which are all related): First, there is a problem with having a single Higgs *scalar*. We want the Higgs (and **only** the Higgs) to get a VEV. However, the Higgs is charged under SU(2), U(1), so its VEV gives rise to nonzero D terms:

$$V \sim D^I D^I + D_Y^2 \tag{104}$$

where

$$D^I = g_2 \langle H^\dagger \rangle T^I \langle H \rangle \quad D_Y = g_1 \frac{1}{2} \langle H \rangle^\dagger \langle H \rangle \tag{105}$$

that is, EWSB implies supersymmetry breaking! You might think this is good, but it's not (for many reasons). For one, the non-zero D-terms would generate masses for the squarks and sleptons. Consider D_Y for example:

$$D_Y = \frac{1}{2}v^2 + \sum_i Y_i |\tilde{f}_i|^2 \tag{106}$$

where $\tilde{f}$ sums over all squarks, sleptons and Y_i is their hypercharge. Recall the scalar potential $V \sim D^2$. Therefore some of the squarks will get *negative* masses-squared of order v^2. This is a disaster: SU(3) and EM are broken at v! The solution is to add a second Higgs scalar, *with opposite charges*. The two Higgs scalars can then get equal VEVs with all $<D> = 0$.

A second problem is that $\tilde{H}$ is a Weyl fermion. If this is all there is, we will have a massless fermion around—the Higgsino. In the presence of massless fermions, gauge symmetries can become anomalous, that is, the gauge symmetry can be broken at the loop level. In the SM, the fermion representations and charges are such that there are no anomalies. Before discussing the Higgs, we only added scalars to the SM (squarks and sleptons, known collectively as sfermions). These are harmless from the point of view of anomalies. We also added gauginos. These are fermions, but they are adjoint fermions, which don't generate any anomalies (essentially because the adjoint is a real representation). In contrast, the Higgsino $\tilde{H}$ is a massless fermion which is a doublet of SU(2) and charged under U(1)$_Y$. The simplest way to cancel the anomaly is to add a second Higgsino in the conjugate representation. So we must add a second Higgs field with conjugate quantum numbers. When we consider interactions, we will see other reasons why we must do this.

We will call the SM Higgs H_D and the new Higgs H_U. Thus,

$$H_D \rightarrow (H_D, \tilde{H}_D) + F_{HD} \quad \text{all transforming as } (1,2)_{-1/2}, \tag{107}$$

and we also add,

$$H_U \rightarrow (H_U, \tilde{H}_U) + F_{HU} \quad \text{all transforming as } (1,2)_{1/2}, \tag{108}$$

and in the limit of unbroken supersymmetry,

$$\langle H_U \rangle = \langle H_D \rangle. \tag{109}$$

In the SM we add a quartic potential for the Higgs field,

$$\lambda(H^\dagger H)^2. \tag{110}$$

Here there is quartic potential built in, coming from the D terms. This potential will not necessarily give mass to the physical Higgs.

We now turn to the Yukawa couplings. In the SM we have Higgs-fermion-fermion Yukawa couplings. Consider the down-quark Yukawa first

$$y_D H_D q^T \varepsilon d^c \quad (\text{Higgs} - \text{quark} - \text{quark}), \tag{111}$$

as we saw above, with supersymmetry, this must be accompanied by

$$+y_D \left(\tilde{q}\tilde{H}_D^T \varepsilon d^c + \tilde{d}^c \tilde{H}_D^T \varepsilon q\right) \quad (\text{squark} - \text{Higgsino} - \text{quark})$$

all coming from the superpotential

$$W_D = y_D H_D q d^c. \tag{112}$$

Similarly for the lepton Yukawa,

$$W_l = y_l H_D l e^c \rightarrow \tag{113}$$

$$\mathcal{L}_l = y_l(H_D l^T \varepsilon e^c + \tilde{l}\tilde{H}_D^T \varepsilon e^c + \tilde{e}^c \tilde{H}_D^T \varepsilon l + \mathrm{hc}) \tag{114}$$

$$\mathrm{Higgs} - \mathrm{lepton} - \mathrm{lepton}$$

$$+ \quad \mathrm{slepton} - \mathrm{Higgsino} - \mathrm{lepton} \tag{115}$$

What about the up Yukawa? We need,

$$(\mathrm{Higgs})q^T \varepsilon u^c \tag{116}$$

This coupling must come from a superpotential,

$$(\mathrm{Higgs})q u^c \tag{117}$$

In the SM (Higgs)$= H_D^\dagger$. But the superpotential is **holomorphic**, no daggers are allowed.

This is the 4th reason why we needed a second Higgs field with the conjugate charges[6],

$$W_U = y_U H_U q u^c \rightarrow \tag{118}$$

$$\mathcal{L}_U = y_U(H_U q^T \varepsilon u^c + \tilde{q}\tilde{H}_U^T \varepsilon u^c + \tilde{u}^c \tilde{H}_U^T \varepsilon q) + \mathrm{hc} \tag{119}$$

You can now see what's going on. In some sense, holomorphy makes a scalar field "behave like a fermion". In a supersymmetric theory, the interactions of scalar fields are controlled by the superpotential, which is holomorphic. For a fermion to get mass you need an LR coupling. So starting from a L-fermion you need a R-fermion, or another L-fermion with the opposite charge(s). For a scalar ϕ to get mass in a non-supersymmetric theory: you don't need anything else (you can just use ϕ^* to write a charge neutral mass term). Not so in a supersymmetry theory: because you cannot use ϕ^*, you must have another scalar with the opposite charge(s), just as for fermions.

To summarize, we have 2 Higgs fields H_U and H_D. The SM Yukawa couplings come from the superpotential

$$W = y_U H_U q u^c + y_D H_D q d^c + y_l H_D l e^c \,. \tag{120}$$

Note again that there was no freedom here, and no new parameter.

3.2 R-symmetry

Our supersymmetric Lagrangian also has a U(1)$_R$ symmetry. Here is one possible choice of charges: gaugino (-1), sfermions (1), Higgsinos (1), with all other fields, namely the SM fields, neutral. You can easily check that the Lagrangian is invariant.

To recap, we wrote down the Supersymmetric Standard Model. It contains

- gauge bosons + (spin 1/2) gauginos,
- fermions + (spin 0) sfermions,
- 2 Higgses + 2 (spin 1/2) Higgsinos

The interactions are all dictated by the SM interactions + supersymmetry: The new interactions are

- gauge-boson—scalar—scalar
- gauge-boson—gauge-boson—scalar—scalar
- gaugino-sfermion-fermion
- gauge-boson—Higgsino—Higgsino
- 4-scalar (all gauge invariant contributions)

---

[6]All these are actually different aspects of the same problem.

All the couplings are determined by the SM gauge couplings. In particular, there is a quartic Higgs coupling which is proportional to the gauge-coupling squared.

Furthermore, there is the Yukawa part, which now contains
Higgsino—fermion—sfermion
with a coupling equal to the SM Yukawa coupling.

The Lagrangian is invariant under a $U(1)_R$ symmetry: in each of the interactions, the new superpartners appear in pairs! This is important both for LHC production and for DM.

There is now no quadratic divergence in the Higgs mass. Each quark contribution is canceled by the corresponding squark contribution. In particular the top loop is canceled by the L, R stops. Similarly, the contribution from the Higgs self coupling (from the D term) is canceled by the Higgsinos, and each gauge boson contribution is canceled by the gaugino contribution.

But we now have, a wino degenerate with the W, a selectron degenerate with the electron, etc. Supersymmetry must be broken. Somehow the wino, selectron, and all the new particles should get mass. It would be nice if the supersymmetrized SM broke supersymmetry spontaneously (after all we have lots of scalars with a complicated potential). But it does not, and so we must add more fields and interactions that break supersymmetry. These new fields must couple to the SM fields in order to generate masses for the superpartners.

3.3 The supersymmetrized standard model with supersymmetry-breaking superpartner masses

3.3.1 General structure

The general structure is then

$$\text{SB} \longrightarrow \text{SSM}$$

Here SSM is the Supersymmetrized SM. SB is a set of new fields and interactions such that supersymmetry is spontaneously broken. As a result there are mass splittings between the bosons and fermions of the same SB multiplet.

Finally, —— stands for some coupling(s) between the SSM fields and the SB fields. Since there are supersymmetry-breaking mass-splittings among the SB fields, this coupling will generate mass splitting between the SM fields and their superpartners, mediating the supersymmetry breaking to the MSSM. The mediation mechanism determines the supersymmetry-breaking terms in the MSSM, which in turn determine the experimental signatures of supersymmetry.

3.3.2 The supersymmetry-breaking terms: what do we expect?

Any term is allowed in the Lagrangian unless a symmetry prevents it. Now that we broke supersymmetry, supersymmetry breaking terms are allowed. In the matter sector, sfermions get mass. However, the fermions don't: they are protected by chiral symmetry. In the gauge sector, gauginos get mass. However, gauge bosons don't: they are protected by gauge symmetry. In the Higgs sector, the Higgses get mass. Higgsinos don't, they are protected by chiral symmetry. This is a problem. We would like the gauginos to get mass, so we will have to solve this problem.

In addition, there are trilinear scalar terms that can appear, such as a Higgs—squark—squark coupling, or a Higgs—slepton—slepton coupling. These are allowed by gauge symmetry, and supersymmetry is no longer there to forbid them. These terms are called A-terms.

Thus the supersymmetry-breaking part of the SSM Lagrangian is:

$$
\begin{aligned}
\mathcal{L}_{soft} &= -\frac{1}{2}[\tilde{m}_3 \tilde{g}^T \varepsilon \tilde{g} + \tilde{m}_2 \tilde{w}^T \varepsilon \tilde{w} + \tilde{m}_1 \tilde{b}^T \varepsilon \tilde{b}] \\
&- \tilde{q}^* \tilde{m}_q^2 \tilde{q} - \tilde{u}^{c*} \tilde{m}_{uR}^2 \tilde{u}^c - \tilde{d}^{c*} \tilde{m}_{dR}^2 \tilde{d}^c
\end{aligned}
$$

$$-\quad \tilde{l}^* \tilde{m}_l^2 \tilde{l} - \tilde{e}^{c*} \tilde{m}_{eR}^2 \tilde{e}^c \tag{121}$$
$$-\quad H_U^* m_{H_U}^2 H_U - H_D^* m_{H_D}^2 H_U$$
$$-\quad H_U \tilde{q}^* A_U \tilde{u}^c - H_D \tilde{q}^* A_U \tilde{d}^c - H_D \tilde{l}^* A_l \tilde{e}^c$$
$$-\quad B\mu H_U H_D$$

The last line is a quadratic term for the Higgs scalars. The line before last is the new trilinear scalar interactions, or A-terms. When the Higgses get VEVs, these too will induce sfermion mass terms (mixing L and R scalars). Finally, m_q^2 etc are 3×3 matrices in generation space. So are the A-terms (A_U etc).

The values of the supersymmetry-breaking parameters are determined by the SB theory and *mainly* by the mediation. You sometimes hear people criticize supersymmetric extensions of the SM for having a hundred or so new parameters (the parameters of $\mathcal{L}_{soft}$). These are all determined however by the SB and the mediation scheme. Often, these involve very few new parameters (only one in anomaly mediation and two in minimal gauge mediation).

Note too that the parameters of $\mathcal{L}_{soft}$ are the only freedom we have, and where all the interesting physics lies. These parameters determine the spectrum of squarks, sleptons, gauginos, and therefore the way supersymmetry manifests itself in Nature.

3.3.3 R-parity

The gaugino masses and A-terms break the U(1)$_R$ symmetry of the SSM Lagrangian. There is a discrete symmetry left however. This remanent symmetry is called R-parity. Under R-parity, the gauginos, sfermions, and Higgsinos are odd, and all SM fields are even. Thus, when we supersymmetrize the SM without adding any new interactions, we have a new parity symmetry. It follows that the the lightest superpartner (LSP) is stable!

3.3.4 The mu-term: a supersymmetric Higgs and Higgsino mass

Before we go on, let's discuss one remaining problem. We have two massless Higgsinos in the theory. As we saw above, these do not get mass from supersymmetry breaking. So we must also include a supersymmetric mass term for them,

$$W = \mu H_U H_D \,. \tag{122}$$

3.4 Mediating the breaking

What can mediate supersymmetry breaking? What can the coupling —— be? There are many possibilities. One is gauge interactions. This is the basis of Gauge Mediated Supersymmetry Breaking (GMSB). Another is gravity. This is the basis of Anomaly Mediated Supersymmetry Breaking (AMSB). Planck-suppressed interactions, which are also associated with gravity, are at the basis of "gravity mediated supersymmetry breaking"[7]. Even Yukawa-like interactions can do the job.

3.4.1 Gauge Mediated Supersymmetry Breaking

Gauge interactions are the ones we know best. Therefore gauge mediation gives full, concrete, and often fully calculable supersymmetric extensions of the SM.

We can start with a toy example to illustrate how things work. We saw the O'Raifeartaigh model,

$$W = \phi \left(\phi_1^2 - f \right) + m\phi_1\phi_2 \,. \tag{123}$$

Recall that this model breaks supersymmetry. The spectrum of the model contains a supermultiplet with supersymmetry-breaking mass splittings: a fermion of mass m, and scalars of masses-squared $m^2 + 2f$, $m^2 - 2f$.

---

[7]mSUGRA or the cMSSM are ansatze of gravity mediation with the assumption of flavor-blind soft terms.

Let's complicate the model slightly, by considering five fields, ϕ, $\phi_{1\pm}$, $\phi_{2\pm}$, with the superpotential,

$$W = \phi\left(\phi_{1+}\phi_{1-} - f\right) + m\phi_{1+}\phi_{2-} + m\phi_{1-}\phi_{2+} \tag{124}$$

now the model has a $U(1)$ symmetry, under which ϕ has charge zero, and $\phi_{i\pm}$ (with $i = 1, 2$) has charge ± 1. It is easy to see that supersymmetry is still broken. Again we have supermultiplets with supersymmetry breaking splittings between fermions and bosons. Now let's promote the $U(1)$ symmetry to a gauge symmetry, and identify it with hypercharge. Another way to think about this is the following. Add to the SM the fields ϕ, $\phi_{1\pm}$, $\phi_{2\pm}$ of hypercharges 0, ± 1, respectively, with the superpotential (124). Now consider a squark. It is charged under hypercharge, so it couples to these split supermultiplets. Therefore, a squark mass is generated!

Minimal Gauge Mediation Models are the simplest models of this type. Suppose we have a supersymmetry-breaking model with chiral supermultiplets Φ_i and $\bar{\Phi}_i$, $i = 1, 2, 3$ such that the fermions ψ_{Φ_i} and $\psi_{\bar{\Phi}_i}$ combine into a Dirac fermion of mass M, and the scalars have masses-squared $M^2 \pm F$ (with $F < M^2$). Now identify i as an SU(3) color index. Thus Φ is a 3 of SU(3), $\bar{\Phi}$ is a $\bar{3}$ of SU(3). These fields have supersymmetry-breaking masses. The gluino talks to the Φ's directly and therefore gets mass at one loop. The squarks talk to the gluino and therefore get mass at two loops. We have a gluino mass,

$$m_{\tilde{g}} = \#\frac{\alpha}{4\pi}\frac{F}{M} + \mathcal{O}(F^2/M^2) \tag{125}$$

and a squark mass-squared at two loops:

$$m_{\tilde{q}} = \#\frac{\alpha^2}{(4\pi)^2}\frac{F^2}{M^2} + \mathcal{O}(F^4/M^6) \tag{126}$$

where the numbers are group theory factors. We can infer this form very simply:

  – Since the masses arise at one or two loops there is the appropriate loop factor.
  – The masses should vanish as $F \to 0$.
  – The masses should vanish as $M \to \infty$.

Gauge mediation is very elegant:

  – The soft masses are determined by the gauge couplings.
  – The squark matrices are flavor-blind ($\propto 1_{3\times3}$ in flavor space).
  – The gluino masses $\sim$ squark masses.
  – The only new parameters are F and M, and the overall scale is F/M. If want soft masses around the TeV, $F/M \sim 100$ TeV.

The new fields Φ are the *messengers* of supersymmetry breaking. In order to give masses to all the MSSM fields we need messenger fields charged under SU(3), SU(2), U(1), eg, N_5 copies of $(3, 1)_{-1/3} + (\bar{3}, 1)_{1/3}$ and $(1, 2)_{-1/2} + (1, 2)_{1/2}$ (filling up a $5 + \bar{5}$ of SU(5)). This adds another parameter, namely the number of messengers, N_5.

The messenger scale M mainly enters through running. The soft masses are generated at the messenger scale. To calculate them at the TeV we need to include RGE effects.

The gravitino mass in these models is

$$m_{3/2} = F_{eff}/M_P \tag{127}$$

where F_{eff} is the the dominant F term. Therefore,

$$m_{3/2} \geq \frac{F}{M_P} \sim 100 \text{ TeV } \frac{M}{M_P} \tag{128}$$

and for low messenger scales, the gravitino can be very light ($\sim$eV).

Minimal gauge mediation is just a simple example. Gauge mediation can in principle have a very different structure. The only defining feature is that the soft masses are generated by the SM gauge interactions. Generically then,

- Colored superpartners (gluinos, squarks) are heavier than non-colored (EW gauginos, sleptons..) by a factor

$$\frac{\alpha_3}{\alpha_2} \quad \text{or} \quad \frac{\alpha_3}{\alpha_1} \tag{129}$$

- In particular, gaugino masses scale as

$$\alpha_3 : \alpha_2 : \alpha_1 \tag{130}$$

and the bino is the lightest gaugino.

- To leading order, the A terms vanish at M.
- The gravitino is light.

3.4.2 Gravity Mediation

With gauge mediation, we had to do some real work: add new fields, make sure they get supersymmetry-breaking masses, couple them to the MSSM. But supersymmetry breaking is one place where we can expect a free lunch. Imagine we have, in addition to the SM, some SB fields, eg, the O'Raifeartaigh model. Since supersymmetry is a space-time symmetry, the SM fields should know this automatically. We would expect soft terms to be generated, suppressed by M_P. This is known as "gravity mediation". We will discuss first the purest form of gravity mediation: anomaly mediation, and then what's commonly referred to as gravity mediation.

Anomaly mediation: We assume that supersymmetry is broken by some fields that have *no coupling* to the SM. These fields are called the "hidden sector". The gravitino gets mass $m_{3/2}$. Would the SSM "know" about supersymmetry breaking? Yes: at the quantum level, it's not scale-invariant: all the couplings (gauge, Yukawa) run—they are scale dependent. Therefore they are sensitive to the supersymmetry-breaking gravitino mass, and **all** the soft terms are generated. The gaugino masses are given by,

$$m_{1/2} = b \frac{\alpha}{4\pi} m_{3/2} \tag{131}$$

where α is the appropriate gauge coupling and b is the beta-function coefficient. Thus for SU(3) $b = 3$, for SU(2) $b = -1$ and for U(1) $b = -33/5$.

Sfermions get masses proportional to their anomalous dimensions:

$$m_0^2 \sim \frac{1}{16\pi^2}(y^4 - y^2 g^2 + b g^4)\, m_{3/2}^2 \tag{132}$$

For the first and second generation sfermions, we can neglect the Yukawas and,

$$m_0^2 \sim \frac{g^4}{16\pi^2}\, b\, m_{3/2}^2 \tag{133}$$

A terms are generated too, proportional to the beta functions of the appropriate Yukawa.

This is amazing: These contributions to the soft terms are **always there**. All the soft terms are determined by just the SM couplings with one new parameter, the gravitino mass. It seems too good to be true. Indeed, while SU(3) is asymptotically free and $b_3 > 0$, SU(2), U(1) are not, $b_2, b_1 < 0$. Therefore the sleptons are tachyonic. There are various solutions to this problem, but the gaugino masses are fairly robust,

$$m_{\tilde{w}} : m_{\tilde{b}} : m_{\tilde{g}} : m_{3/2} \sim 1 : 3.3 : 10 : 370 \tag{134}$$

In this scenario, the wino is the LSP. Note that the gravitino is roughly a loop factor heavier than the SM superpartners.

Gravity mediation: mediation by Planck suppressed operators: Let's return to our basic setup. The SSM is the supersymmetric standard model. SB contains new fields and interactions that break supersymmetry (the "hidden sector"). Generically, we expect to have higher-dimension operators, suppressed by M_P, that couple the SB fields and the SSM fields. Supersymmetry breaking leads to non-zero F terms (or D terms) for the SB fields, so the higher-dimension operators coupling the two sectors will generate supersymmetry-breaking terms in the SSM, with sfermion mass from

$$\frac{|F|^2}{M_P^2} \tilde{f}^\dagger \tilde{f} \tag{135}$$

and gaugino masses from

$$\frac{|F|}{M_P} \lambda^T \varepsilon \lambda \tag{136}$$

You can think of these as mediated by tree-level exchange of Planck-scale fields.

Unlike in the previous two schemes, here we don't know the order-one coefficients. Consider for example the doublet-squarks. Their mass terms are,

$$c_{ij} \frac{|F|^2}{M_P^2} \tilde{q}_i^\dagger \tilde{q}_j \tag{137}$$

where c_{ij} are order-one coefficients. Thus,

$$(m_{\tilde{q}}^2)_{ij} = c_{ij} m_0^2 \quad \text{where} \quad m_0 \equiv \frac{|F|}{M_P} \tag{138}$$

In "minimal sugra", or the cMSSM one **assumes**

$$c_{ij} = \delta_{ij} \,. \tag{139}$$

It is not easy to justify this: the Yukawas are presumably generated at this high scale, so there are flavor-dependent couplings in the theory.

Including the running to low scales,

$$\frac{d}{dt} m_{1/2} \propto \frac{\alpha}{4\pi} \, m_{1/2} \tag{140}$$

we find that starting from a common gaugino mass at the GUT scale, the gaugino masses scale as

$$\alpha_3 : \alpha_2 : \alpha_1 \tag{141}$$

just as in gauge mediation. Again the bino is the LSP. The gravitino mass is of order the superpartner masses in this case.

These are a few possibilities for mediating supersymmetry breaking but by no means an exhaustive list.

4 The MSSM spectrum

4.1 EWSB and the Higgs mass

In the MSSM we have two Higgses, H_U and H_D, which can get VEVs,

$$\langle H_U \rangle = \begin{pmatrix} v_U \\ 0 \end{pmatrix} \quad \langle H_D \rangle = \begin{pmatrix} 0 \\ v_D \end{pmatrix} \tag{142}$$

Let's start in the supersymmetry limit (with no mu term). The D term must vanish, so the VEVs must be equal,

$$D = 0 \quad \rightarrow \quad v_U = v_D \tag{143}$$

The two Higgs fields contain 8 real scalars. Of these, 3 are eaten by $W^\pm$, Z.

Consider the heavy Z supermultiplet. It contains a heavy gauge boson which has 3 physical polarizations, and therefore 3 bosonic dof's and a Dirac fermion (4 dof's). Therefore, in order to have the same number of fermion and boson dof's there must be one more real scalar. This scalar comes from the Higgs fields. The same holds for the $W^\pm$. Thus, 3 real scalars "join" the heavy $W^\pm$, Z supermultiplets. In the limit of unbroken supersymmetry which we are assuming now, all of these fields have masses M_W or M_Z.

Thus, of the 8 real scalars in H_U and H_D, 2 neutral fields remain. One is the SM physical Higgs, h. The other must be there because we have supersymmetry, and h must reside in a chiral supermultiplet. As we saw above, this multiplet contains a complex scalar field.

Note that so far there is no potential for h. This is not surprising. We haven't added any Higgs superpotential so the Higgs could only have a quartic from V_D. But along the D-flat direction, the physical Higgs is massless. Thus its mass must come from supersymmetry breaking !

Fortunately supersymmetry is broken—we have soft terms. The Higgs potential comes from the following sources:

- The mu term: $W = \mu H_U H_D$,

$$\delta V = |\mu|^2 |H_U|^2 + |\mu|^2 |H_D|^2 \tag{144}$$

- The Higgs soft masses:

$$\delta V = \tilde{m}_{H_U}^2 |H_U|^2 + \tilde{m}_{H_D}^2 |H_D|^2 \tag{145}$$

so we need $m_{H_U}^2 < 0$ and/or $m_{H_U}^2 < 0$

- The $B\mu$ term:

$$\delta V = B\mu H_U H_D + \text{hc} \tag{146}$$

These are all quadratic terms.

- Then we have quartic terms:

$$\delta V = \frac{1}{2} g_2^2 D^I D^I + \frac{1}{2} g_1^2 D_Y D_Y \tag{147}$$

where

$$D^I = H_U^\dagger \tau^I H_U - H_D^\dagger \tau^{I*} H_D \tag{148}$$

and

$$D_Y = \sum_i Y_i \tilde{f}_i^\dagger \tilde{f}_i + \frac{1}{2}(H_U^\dagger H_u - H_D^\dagger H_D) \tag{149}$$

Recall we had two parameters, the two Higgs VEVs. We can trade them for:

1. $\sqrt{v_U^2 + v_D^2}$: determined by W mass to be 246 GeV
2. $\tan\beta \equiv v_U/v_D$

Requiring a minimum of the potential determines:

$$B\mu = \frac{1}{2}(m_{H_U}^2 + m_{H_D}^2 + 2\mu^2)\sin 2\beta \tag{150}$$

118

$$\mu^2 \;=\; \frac{m_{H_D}^2 - m_{H_U}^2 \tan^2 \beta}{\tan^2 \beta - 1} - \frac{M_Z^2}{2} \tag{151}$$

Thus, for given $m_{H_U}^2$, $m_{H_D}^2$: $B\mu$ and μ are determined, and we have two free parameters, $\tan \beta$ and $\mathrm{sign}(\mu)$.

Expanding around the VEVs we find that the various scalars from H_U and H_D have the following masses (squared),

$$
\begin{aligned}
H^\pm \;\; &: \;\; M_W^2 + M_A^2 \qquad (\text{SUSY} : M_W^2) \\
H^0 \;\; &: \;\; \frac{1}{2}\left(M_Z^2 + M_A^2\right) + \frac{1}{2}\sqrt{(M_Z^2 + M_A^2)^2 - 4m_A^2 M_Z^2 \cos^2 2\beta} \\
& \qquad\qquad\qquad\qquad (\text{SUSY} : M_Z^2) \\
A^0 \;\; &: \;\; M_A^2 = B\mu(\cot \beta + \tan \beta) \quad (\text{SUSY} : 0)
\end{aligned}
\tag{152}
$$

and for the physical Higgs,

$$m_h^2 = \frac{1}{2}\left(M_Z^2 + M_A^2\right) - \frac{1}{2}\sqrt{(M_Z^2 + M_A^2)^2 - 4m_A^2 M_Z^2 \cos^2 2\beta} \tag{153}$$

This is a **PREDICTION:**

$$m_h \leq m_Z |\cos 2\beta| \leq M_Z \tag{154}$$

The measurement of the Higgs mass provides the first quantitative test of the Minimal Supersymmetric Standard Model. It fails. However, the result (153) is a tree-level result. There are large radiative corrections to this result, mainly from stop loops. In the decoupling limit

$$m_h^2 \sim m_Z^2 \cos^2 2\beta + \frac{3m_t^2}{4\pi^2 v^2}\left[\log \frac{M_S^2}{m_t^2} + \frac{X_t^2}{M_S^2}\right] \tag{155}$$

where

$$
\begin{aligned}
X_t \;\; &= \;\; A_t - \mu \cot \beta \quad \text{the LR stop mixing} \\
M_S \;\; &= \;\; \sqrt{m_{\tilde{t}_1} m_{\tilde{t}_2}} \quad \text{the average stop mass}
\end{aligned}
$$

This can raise Higgs mass to around 130–150 GeV. Thus for a 126 GeV Higgs we need heavy stops and/or large stop A terms. This is not very attractive. We wanted supersymmetry to solve the fine-tuning problem, for which we need light stops. So the large Higgs mass typically implies some fine-tuning.

In specific predictive models, like minimal GMSB, in which the stop mixing is small (because there no A-terms at messenger scale), one needs stops around 8 TeV, and because the other squarks and gluino masses are close by, all the colored superpartners are hopelessly heavy. Thus, the Higgs mass sets a much stronger constraint on this framework than direct supersymmetry searches.

There's another important caveat. So far we did not add in any Higgs potential on top of what the MSSM "gave us". Let's compare this to the SM. In the SM, we add (by hand) a quartic Higgs potential, with a quartic coupling λ, to get the Higgs mass. Here we didn't have to: D-terms give a quartic potential. As a result, there is no new parameter: $\lambda = g$. We could add a quartic interaction a la the SM. To do that, we must add at least one new field, a SM singlet S, with

$$W = \lambda S H_U H_D \;\; \rightarrow \;\; V = \lambda^2(|H_U|^2 |H_D|^2 + \dots) \tag{156}$$

This is called the Next to Minimal SSM (NMSSM).

We can pursue the comparison to the SM at a deeper level. In the SM, we put in EWSB by hand. We had to put in a negative mass-squared for the Higgs. In the MSSM, EWSB can have a dynamical

origin. Recall that we needed $\tilde{m}^2_{H_U} < 0$ or $\tilde{m}^2_{H_D} < 0$. This happens (almost) automatically in supersymmetric theories, since the RGEs drive the Higgs mass-squared negative! The crucial contribution is due to the large Yukawa coupling of the Higgs to stops.

Now let's see why this happens. Suppose we start with $\tilde{m}^2_{H_U} > 0$ at the supersymmetry breaking scale. The running gives

$$\frac{d}{dt} m^2_{H_U} \sim -\frac{g^2}{16\pi^2} m^2_{1/2} + \frac{y^2_t}{16\pi^2} \tilde{m}^2_t \, . \tag{157}$$

The negative Yukawa contribution wins because

1. The top Yukawa is large compared to the SU(2), U(1) gauge couplings.
2. The stop is colored, so the Yukawa contribution is enhanced by a color factor (=3).

Note that there are many scalars in the MSSM, so you could worry about their masses-squared driven negative by the RGE. However, the Higgs is special: it's an SU(3) singlet, so there is no large positive contribution from the gluino. Furthermore, it has an order-1 Yukawa to the colored stop. Thus only the Higgs develops a VEV.

Let's summarize our results so far. Putting aside the unpleasant 126 GeV Higgs mass (which can be accounted for), supersymmetry gives a very beautiful picture. The MSSM (SSM + soft terms) has only log divergences: the quadratic divergence in the Higgs mass-squared is cancelled by superpartners at $\tilde{m}$. The tuning is then $\sim M^2_Z/\tilde{m}^2$ and the hierarchy between the EWSB scale and the Planck/GUT scale is **stabilized**.

Furthermore: starting with $\tilde{m}^2_{H_U} > 0$ in the UV, the running (from stops) drives it negative, and electroweak symmetry is broken, with a scale proportional to $\tilde{m}$.

Finally, we remark that with a SB sector that breaks supersymmetry dynamically, the supersymmetry breaking scale is exponentially suppressed. $\tilde{m}$ can naturally be around the TeV. In this case, the correct hierarchy between the EWSB scale and the Planck/GUT scale is not only stabilized, but actually **generated**.

Returning to the Higgs mass, with $m_h = 126$ GeV the **Minimal** SSM is stretched: we often need heavy stops which implies some level of tuning. More practically, discovery becomes more of a challenge.

Now that we understand supersymmetry breaking and EWSB let's turn to the superpartner spectrum.

4.1.1 Neutralinos and charginos

We have 4 neutral 2-component spinors: two gauginos and two Higgsinos

$$\tilde{b}, \ \tilde{W}^0, \ \tilde{H}^0_D, \ \tilde{H}^0_U \tag{158}$$

with the mass matrix

$$\begin{pmatrix} M_1 & 0 & -g_1 v_D/\sqrt{2} & g_1 v_U/\sqrt{2} \\ 0 & M_2 & g_2 v_D/\sqrt{2} & -g_2 v_U/\sqrt{2} \\ -g_1 v_D/\sqrt{2} & g_2 v_D/\sqrt{2} & 0 & \mu \\ g_1 v_U/\sqrt{2} & -g_2 v_U/\sqrt{2} & \mu & 0 \end{pmatrix} \tag{159}$$

Diagonalizing this matrix we find 4 neutralino mass eigenstates: $\tilde{\chi}^0$ $i = 1, \ldots, 4$.

Similarly, there are two charginos mass eigenstates which are combinations of the charged Higgsino and wino, $\tilde{\chi}^\pm_i$ $i = 1, 2$.

4.1.2 Sfermion spectrum

Consider for example the up squarks. There are 6 complex scalars: $\tilde{u}_{Li}$ and $\tilde{u}_{Ra}$ with $i, a = 1, 2, 3$ labeling the three generations. The mass (squared) matrix is therefore a 6×6 matrix:

$$\begin{pmatrix} m_{LL}^2 & m_{LR}^2 \\ m_{LR}^{2\dagger} & m_{RR}^2 \end{pmatrix} \tag{160}$$

where each of the blocks is 3×3.

Consider $m_{U,LL}^2$. It gets contributions from:

1. the SSM Yukawa (supersymmetric)
2. the SUSY breaking mass-squared
3. the D-term (because $D \sim v_U^2 - v_D^2 + \tilde{q}^\dagger T q + \cdots$)

Thus,

$$m_{U,LL}^2 = m_u^\dagger m_u + \tilde{m}_q^2 + D_U 1_{3\times 3}\,, \tag{161}$$

and similarly for $m_{U,RR}^2$.

m_{LR}^2 gets contributions from:

1. the A term (supersymmetry breaking)
2. the μ term:

$$\left| \frac{\partial W}{\partial H_D} \right|^2 \quad \rightarrow \quad \frac{\partial W}{\partial H_D} = \mu H_U + y_U q u^c \tag{162}$$

so

$$m_{U,LR}^2 = v_U \left(A_U^* - y_U \mu \cot \beta \right). \tag{163}$$

The remaining sfermions (down-squarks, sleptons, sneutrinos) have a similar structure.

4.1.3 Flavor structure

Now let's consider the sfermion flavor structure, starting with the up squarks as before. Work in the quark mass basis (up, charm, top): the Lagrangian contains the following:

– gaugino—u_{Li}—$\tilde{u}_{Lj}$ couplings. Here the gaugino can be either a gluino, a wino or a bino. In our original Lagrangian, these are proportional to δij. We therefore say that the Lagrangian is given in the interaction basis. Note that since we are in the fermion mass basis, this defines the L up squark, charm squark and top squark (stop). For example, the L stop is the state that couples to a gluino and the doublet-top quark.
– gaugino—u_{Ra}—$\tilde{u}_{Rb}$ couplings. Again, in our original Lagrangian, these are proportional to δab.
– ...
– The up squark 6×6 mass matrix. This can in principle have an arbitrary structure. In particular, the various 3×3 blocks need not be diagonal.

Diagonalizing the squark mass matrix, we get 6 mass eigenstates, $\tilde{u}_I$, with $I = 1, \ldots, 6$. However, the gaugino—quark—squark couplings are no longer diagonal. Writing these in terms of the up-squark mass eigenstates we have in general

$$K_{iI} \tilde{g} u_{Li} - \tilde{u}_I\,, \tag{164}$$

These mix the different generations, and K_{iI} are the quark-squark mixing parameters. Each squark (mass state) is a composition of the different flavor states.

Are sfermions degenerate? Is $m_{U,LL}^2 \propto 1$? That depends on the mediation of supersymmetry. However, we don't understand the structure of fermion masses. In fact this structure is very strange, suggesting a fundamental theory of flavor. If there is such a theory, it will also control the structure of $m_{U,LL}^2$ and the other sfermion mass-matrices.

4.1.4 *R-parity violating couplings*

So far, we merely generalized the SM gauge and Yukawa interactions. In the SM, the Yukawa couplings were the only renormalizable couplings allowed. Now however, there are *new* renormalizable Yukawa-like interactions

$$W = \lambda_{ijk} L_i L_j e_k^c + \lambda'_{ijk} L_i Q_j d_k^c + \lambda''_{ijk} u_i^c d_j^c d_k^c \,. \tag{165}$$

These are the only terms we can add, nothing else is gauge invariant. These terms are problematic. The first two terms break lepton number, the third breaks baryon number. If they are all there we would get proton decay! Note also that all these new terms break R-parity. If we *impose* R-parity, these dangerous terms are forbidden, and proton decay can only arise from higher-dimension operators, much like in the SM. But this may be overly restrictive. Certain flavor patters of R-parity breaking operators are viable.

5   LHC searches: general considerations

As we saw, supersymmetry is not a single model. In the minimal supersymmetric extension of the standard model, the MSSM, in which we add no new fields to the SM apart from those required by supersymmetry, all the interactions are dictated by the SM and supersymmetry (with the exception of R-parity violating couplings), and the only freedom is in the soft supersymmetry breaking terms, which are determined by the mechanism for mediating supersymmetry breaking. Still, this allows for a wide variety of new and distinct signatures. Therefore, while searches for specific models are useful, it's also important to adopt a signature-based approach.

Here we will outline the main considerations to keep in mind.

1. Interactions: There are only two sources of model dependence here.
   – R-parity violating (RPV) couplings: If R-parity is conserved, superpartners are produced in pairs, and each superpartner decays to a lighter superpartner plus SM particles. Thus any decay chain ends with the stable LSP. In the presence of RPV couplings, a single superpartner can be produced. There are strong bounds on RPV couplings. Still, single superpartner production via a small RPV coupling may be competitive because of the kinematics. Most superpartners decay through the usual R-parity conserving couplings (gauge or Yukawa), with the exception of the LSP, which can only decay through RPV couplings.
   – Squark and/or slepton flavor mixing: For general sfermion mass matrices, the gaugino-sfermion-fermion couplings may mix different flavors. This could affect both production and decay.

2. Superpartner masses:
   – The hierarchy between colored and non-colored superpartners: In most mediation schemes, colored superpartners are heavier (roughly by factors of a few to 10). Unless there is a huge hierarchy between colored and non-colored superpartners, the production of squarks and gluinos dominates at the LHC. As the hierarchy increases, the production of EWK gauginos (ewkinos) and or sleptons becomes more competitive.
   – Flavor structure: superpartners of the same gauge charges may have generation dependent-masses. Thus for example, the L-handed up squark can have a different mass from the L-handed charm or top squarks. An arbitrary flavor structure leads to flavor changing processes which, especially when the 1st and 2nd generations are involved, are stringently constrained.

However, roughly speaking, the constrained quantities involve the products of the mass splittings and the flavor mixings K_{iI}, so models with some degree of mass degeneracy and some alignment of fermion and sfermion mass matrices are allowed. These would affect both the production of sfermions and their decay.

The (N)LSP plays a special role in determining the collider signatures of supersymmetry. Both the mass spectrum and its interactions are relevant here.

- The (N)LSP lifetime: The LSP is stable if R-parity is conserved. In the presence of RPV couplings, the LSP can decay to SM particles, but its lifetime may be long because the sizes of these couplings are constrained. Finally, the LSP may have only very weak couplings to the SM, as is the case of the gravitino. Superpartners produced at the LHC will decay to the lightest superpartner charged under the SM, which is called the NLSP (next to lightest superpartner), which in turn decays to the LSP. Clearly, since the latter is only weakly coupled to the SM, the NLSP can be long lived. Different models span the whole range from propmt NLSP decays to NLSPs which are long-lived on detector scales.
- The (N)LSP charge. The (N)LSP can be either neutral (eg a neutralino or sneutrino), charged (eg a slepton), or even colored (eg the gluino). Naturally, the precise identity of the (N)LSP plays an key role in determining the signatures of supersymmetry at the LHC. The signatures of a spectrum with a pure bino (N)LSP are very different from the signatures of a spectrum with a pure Higgsino (N)LSP even though both are neutral.

If the (N)LSP is neutral and long lived, superpartner production is accompanied by missing energy. If it's charged and long lived, it behaves like a heavy muon, and dE/dx and time-of-flight measurements must be used to distinguish it from a muon. If it's colored and long lived, it will hadronize in the detector, and subsequently either stop in the detector or traverse the entire detector. If it decays inside the detector, its charge and lifetime determine the specific signature, ranging from a disappearing track to a displaced vertex, with or without missing energy. Thus, supersymmetry has motivated a wide variety of ingenious approaches for searching for new physics. Whether supersymmetry is there or not, this net of searches will hopefully lead to new discoveries!

Acknowledgements

References

[1] H. Baer and X. Tata, "Weak scale supersymmetry: From superfields to scattering events," Cambridge, UK: Univ. Pr. (2006).

[2] M. Dine, "Supersymmetry and string theory: Beyond the Standard Model," Cambridge, UK: Univ. Pr. (2007).

[3] S. P. Martin, "A Supersymmetry primer," Adv. Ser. Direct. High Energy Phys. **21**, 1 (2010) [hep-ph/9709356].

Organizing Committee

T. Donskova (Schools Administrator, JINR)
N. Ellis (CERN)
M. Mulders (CERN)
A. Olchevsky (JINR)
G. Perez (CERN and Weizmann Institute, Israel)
K. Ross (Schools Administrator, CERN)

Local Organizing Committee

J. Berger (Nikhef, the Netherlands)
S. Caron (Radboud Univ., the Netherlands)
R. Fleischer (Nikhef & Vrije Univ., the Netherlands)
O. Igonkina (Nikhef, the Netherlands)
F. Linde (Nikhef & Univ. Amsterdam, the Netherlands)
V. Mexner (Nikhef, the Netherlands)
A. Mischke (Univ. Utrecht, the Netherlands)
P. Pani (Nikhef, the Netherlands)
D. Samtleben (Univ. Leiden, the Netherlands)
L. Wiggers (Nikhef, the Netherlands)

International Advisors

J. Engelen (NWO & Univ. Amsterdam, the Netherlands)
R. Heuer (CERN)
V. Matveev (JINR)
A. Skrinsky (BINP, Novosibirsk, Russia)
N. Tyurin (IHEP, Protvino, Russia)

Lecturers

J. L. Feng (UC Irvine, USA)
F. Gianotti (CERN)
G. 't Hooft (Univ. Utrecht, the Netherlands)
J. F. Kamenik (JSI and Univ. Ljubljana, Slovenia)
R. Kleiss (Radboud Univ., the Netherlands)
E. Laenen (Univ. Amsterdam, the Netherlands)
S. Petcov (SISSA, Italy)
A. Pomarol (UA Barcelona, Spain)
C. A. Salgado (Univ. Santiago de Compostela, Spain)
Y. Shadmi (Technion, Israel)
W. Verkerke (Nikhef, the Netherlands)
A. Weiler (CERN & DESY, Germany)

Discussion Leaders

P. Artoisenet (Nikhef, the Netherlands)
A. Bednyakov (JINR)
C. Delaunay (LAPTh, France)
A. Gladyshev (JINR)
C. Pisano (Nikhef, the Netherlands)
K. Schmidt-Hoberg (CERN)

Students

Antonios AGAPITOS

Alexey APARIN

Hannah Ruth ARNOLD

Alexandre AUBIN

Zuzana BARNOVSKA

Peter BERTA

Callie BERTSCHE

David BERTSCHE

Espen BOWEN

Kurt BRENDLINGER

Jacquelyn Kay BROSAMER

Elizabeth BROST

Ilia BUTOROV

Pierfrancesco BUTTI

Cecile Sarah CAILLOL

Alessandro CALANDRI

Jackson CLARKE

Fabio COLOMBO

Samuel COQUEREAU

Kristof DE BRUYN

Ingrid DEIGAARD

Giulia D'IMPERIO

Arne-Rasmus DRAEGER

Deborah DUCHARDT

Mateusz DYNDAL

Andrea FESTANTI

Linda FINCO

Alexey FINKEL

Sara FIORENDI

Anders FLODERUS

Silvia FRACCHIA

Laura FRANCONI

Jun GAO

Alex Edward GARABEDIAN

Jasone GARAY GARCIA

Geoffrey GILLES

Lavinia-Elena GIUBEGA

Giuliano GUSTAVINO

Stephan HAGEBOECK

Andrew HART

Oskar HARTBRICH

James HENDERSON

Miriam HESS

Christoph HOMBACH

Jan Hendrik HOSS

Walaa KANSO

Beata KRUPA

Rebecca LANE

Tobias LAPSIEN

Federico LASAGNI MANGHI

Maxime LEVILLAIN

Hans Martin LJUNGGREN

Riccardo MANZONI

Boyana MARINOVA

Mario MASCIOVECCHIO

Jimmy MCCARTHY

Daniel MEISTER

Mikhail MIKHASENKO

Gordana MILUTINOVIC-DUMBELOVIC

Marco MIRRA

Kazuya MOCHIZUKI

Naghmeh MOHAMMADI

Javier MONTEJO BERLINGEN

Alessandro MORDA

Tara NANUT

Francis NEWSON

Jennifer NGADIUBA

Tamsin NOONEY

Koen Pieter OUSSOREN

Klaas PADEKEN

Gabriel PALACINO

Rute PEDRO

Luis PESANTEZ

Olga PETROVA

Deborah PINNA

Lukas PLAZAK

Milena QUITTNAT

Bartlomiej RACHWAL

Christine Overgaard RASMUSSEN

Ferdos REZAEI HOSSEINABADI

Mehmet Ozgur SAHIN

Craig Anthony SAWYER

Ralph SCHAEFER

Steven Randolph SCHRAMM

Irina SHAKIRYANOVA

Yusufu SHEHU

Valérian SIBILLE

Marek SIRENDI

Philip SOMMER

Mario SOUSA

Simon SPANNAGEL

Rafael TEIXEIRA DE LIMA

Annemarie THEULINGS

Jui-Fa TSAI

Semen TURCHIKHIN

Alexis Roger Louis VALLIER

Bob VELGHE

Marco VENTURINI

Hartger WEITS

Lei ZHOU

Posters

Poster title	Presenter
Cumulative particle production and z-scaling	APARIN, A.
Search for top-squark pair production in the single-lepton final state at 8 TeV in the CMS experiment	AUBIN, A.
Search for narrow scalar diphoton resonances in the mass range 65-600 GeV with the ATLAS detector	BARNOVSKA, Z.
Top Quark Pole Mass Extraction With the ATLAS Detector at 7-8 TeV From the $t\bar{t}$ cross section using full NNLO+NNLL predictions	BERTSCHE, C.
Opto-Box: Mini-Crate for ATLAS Pixel and IBL Detector Modules	BERTSCHE, D.
VeloUT tracking in the Upgrade trigger of LHCb	BOWEN, E.
MPD/NICA - ECAL Development	BOYANA, M.
Search for FCNC in Top Pair Events at ATLAS	BROST, E.
Efficiency of hadronic tau identification in CMS	CAILLOL, C.
An O(1GeV) scalar right under our noses	CLARKE, J. D.
Module production for the Phase 1 Upgrade of the CMS Pixel Detector	COLOMBO, F.
Selection optimization for the updated $B^0 \rightarrow K^{*0}\mu^+\mu^-$ analysis by LHCb	COQUEREAU, S.
Hunting Penguins	DE BRUYN, K.
Differential cross section measurement of isolated photons at the center-of-mass energy of 8 TeV	D'IMPERIO, G.
AFP Detector Simulation	DYNDAL, M.
D^0 meson production measurement in p-Pb collisions at $\sqrt{s_{NN}} = 5.02$ TeV with ALICE	FESTANTI, A.

Poster title	Presenter
Calibration of Forward Calorimetry Using Z→ee Events	FINKEL, A.
Search for supersymmetric charginos, neutralinos and sleptons in final states with two leptons with ATLAS	FLODERUS, A.
Search for direct sbottom pair production in final states with missing transverse energy and two b-jets in pp collisions with the ATLAS detector at the LHC	FRACCHIA, S.
Jet Charge Studies for HiggsEvents when Produced in Association with Top-Quark Pairs	GARAY GARCIA, J.
A search for new charged heavy gauge W' bosons with the ATLAS detector at the LHC	GILLES, G.
CP-mixing and New Physics in the H→ZZ*→ 4ℓ channel in ATLAS	GUSTAVINO, G.
Search for displaced supersymmetry in dilepton final states	HART, A.
Measurement of the CP violating phase ϕ_s and penguin contributions in $B_s^0 \to J/\psi K^+K^-$ at LHCb	KANSO, W.
Improvement of top-tagging algorithms in CMS	LAPSIEN, T.
Search for the Higgs Boson in the Higgs→ $\tau\tau$ final state at CMS	LANE, R.
Evidence of the SM Higgs Boson in the Decay Channel into τ Leptons	MANZONI, R.
Search for SUSY in hadronic final states using M_{T2} with the CMS detector	MASCIOVECCHIO, M.
Partial wave analysis of $\pi^-\pi^0$ system with known background subtraction	MIKHASENKO, M.
SM-like Higgs decay into two muons at 1.4 TeV CLIC	MILUTINOVIC-DUMBELOVIC, G.
The CHarged ANTIcounter for the NA62 experiment at CERN	MIRRA, M.
Study of radiative $D^0 \to V\gamma$ decays at Belle	NANUT, T.
Angular Analysis of the decay $B_d^0 \to K^{0*}\mu^+\mu^-$	NOONEY, T.
Higgs Spin/CP Studies in the Collins-Soper Frame	OUSSOREN, K.

Poster title	Presenter
Higgs boson searches with ATLAS in the WH$\to l\nu bb$ channel	PEDRO, R.
Measurement of A_{CP} in $B \to X_{s+d}\gamma$ decays	PESANTEZ, L.
Search for Dark Matter associated top pair production in single-lepton channel with the CMS detector	PINNA, D.
FLUKA studies of hadron-irradiated scintillating crystals for calorimetry at the High Luminosity LHC	QUITTNAT, M.
Search for s-channel single top-quark production in pp collisions at 8 TeV	REZAEI, F.
ATLAS Sensitivity to WIMP Dark Matter in the Monojet Topology at $\sqrt{s} = 14$ TeV	SCHRAMM, S.
Multilepton Supersymmetric Signatures at ATLAS	SHEHU, Y.
Precision W measurements in the forward region and constraining PDFs	SIRENDI, M.
The global sequential jet calibration to improve $VH(b\bar{b})$ invariant mass resolution	SOUSA, M.
Test Beam Campaigns and Simulation for the CMS Pixel Detector Upgrade	SPANNAGEL, S.
CMS Electromagnetic Calorimeter Calibration and Performance	TEIXEIRA DE LIMA, R.
Study of $B_c^+ \to J/\psi D_s^{(*)+}$ decays with the ATLAS experiment	TURCHIKHIN, S.
Measurement of the CKM angle gamma in $B^0 \to D(K_s^0\pi^+\pi^-)K^{*0}$ decay at LHCb	VALLIER, A.
GigaTracker: a Fast and Low Mass Silicon Tracker	VELGHE, B.
The MEG-II Experiment	VENTURINI, M.